

## Table of contents

<b>Declaration</b> .....	<b>vii</b>
<b>Abstract</b> .....	<b>viii</b>
<b>Study outputs</b> .....	<b>xi</b>
<b>List of Figures</b> .....	<b>xiv</b>
<b>List of Tables</b> .....	<b>xx</b>
<b>List of abbreviations</b> .....	<b>xxiii</b>
<b>Chapter 1: Introduction to herbal remedy usage, and its relevance in hepatotoxicity and drug-herb interactions</b> .....	<b>1</b>
1.1. Literature review.....	1
1.1.1. Phytopharmacology and phytotoxicity .....	1
1.1.2. Highly-active retroviral therapy .....	2
1.1.3. Herb-induced liver injury .....	3
1.1.4. Herb-drug interactions .....	5
1.2. Aim of the study .....	7
1.3. Objectives .....	7
<b>Chapter 2: Extraction and crude phytochemical screening of herbal remedies</b> 8	
2.1. Literature review.....	8
2.1.1. Extraction of herbal remedies .....	8
2.1.2. Phytochemical matrices and allelochemicals.....	9
2.1.3. Phytochemical classes .....	9
2.1.4. Panel of herbal remedies chosen for this study .....	12
2.1.5. Aim of extraction and phytochemical screening.....	12
2.2. Materials and Methods.....	15
2.2.1. Preparation of crude extracts.....	15
2.2.2. Phytochemical screening.....	16
2.2.3. Statistics .....	18
2.3. Results .....	19
2.3.1. Extraction yields .....	19
2.3.2. Phytochemical screening.....	19
2.3.3. Antioxidant activity.....	20
2.4. Discussion.....	26

2.4.1. Amaryllidaceae .....	26
2.4.2. Anacardiaceae.....	28
2.4.3. Apocynaceae.....	28
2.4.4. Asteraceae .....	29
2.4.5. Combretaceae .....	30
2.4.6. Fabaceae.....	31
2.4.7. Lamiaceae .....	31
2.4.8. Moringaceae.....	32
2.4.9. Piperaceae .....	33
2.4.10. Rhamnaceae .....	33
2.4.11. Solanaceae .....	34
2.5. Conclusion .....	34
<b>Chapter 3: Preliminary phytotoxicological assessment of herbal remedies in the HepG2 hepatocarcinoma and Caco-2 colon carcinoma cell lines .....</b>	<b>35</b>
3.1. Literature review.....	35
3.1.1. Cytotoxic processes .....	35
3.1.2. Aim of phytotoxicological assessment .....	36
3.2. Materials and Methods.....	37
3.2.1. Cell culture, seeding and exposure of cells to crude extracts .....	37
3.2.2. Effect of crude extracts on cellular status .....	38
3.2.3. Statistics .....	40
3.3. Results .....	41
3.3.1. Comparison of cytotoxicity assays.....	41
3.3.2. Determination of cytotoxic effects of crude extracts .....	43
3.4. Discussion.....	48
3.4.1. The selection of cytotoxicity assay .....	48
3.4.2. Effects of crude extracts on the HepG2 and Caco-2 cell lines.....	49
3.4.3. Risk of cytotoxic effects in the intestinal and systemic compartments..	69
3.5. Conclusion .....	70
<b>Chapter 4: <i>In vitro</i> assessment of hepatotoxic potential of herbal remedies ...</b>	<b>71</b>
4.1. Literature review.....	71
4.1.1. Hepatotoxicity induced by xenobiotics .....	71
4.1.2. Mechanisms underlying hepatotoxicity .....	75
4.1.3. Plants selected for mechanistic evaluation of hepatotoxic potential .....	90

4.1.4.	Aim of hepatotoxicity assessment .....	91
4.2.	Materials and Methods .....	92
4.2.1.	Determination of hepatotoxicity using a single-plate method.....	92
4.2.2.	Determination of lipid peroxidation .....	96
4.2.3.	Determination of ATP levels .....	97
4.2.4.	Determination of cellular kinetics and mode of cell death .....	98
4.2.5.	Statistics .....	102
4.3.	Results .....	103
4.3.1.	Use of sulforhodamine B for normalization against protein content....	103
4.3.2.	Positive controls for the hepatotoxicity assays .....	103
4.3.3.	Selected plant extracts .....	107
4.4.	Discussion.....	144
4.4.1.	<i>Acokanthera oppositifolia</i> .....	144
4.4.2.	<i>Boophane disticha</i> .....	151
4.4.3.	<i>Moringa oleifera</i> .....	154
4.4.4.	<i>Solanum aculeastrum</i> .....	157
4.4.5.	<i>Tabernaemontana elegans</i> .....	160
4.4.6.	<i>Terminalia sericea</i> .....	167
4.4.7.	<i>Ziziphus mucronata</i> .....	172
4.5.	Conclusion .....	174
<b>Chapter 5: <i>In vitro</i> effect of herbal remedies on absorption and metabolism</b>		<b>175</b>
5.1.	Literature review.....	175
5.1.1.	Intestinal drug transport.....	175
5.1.2.	P-glycoprotein transporters.....	175
5.1.3.	Metabolism .....	179
5.1.4.	Nevirapine absorption and metabolism .....	184
5.1.5.	Aim of testing the crude extracts on pharmacokinetic parameters .....	185
5.2.	Materials and Methods.....	186
5.2.1.	Effect of herbal remedies on rhodamine-123 accumulation.....	186
5.2.2.	Effect of herbal remedies on transport of nevirapine .....	187
5.2.3.	Effect of herbal remedies on CYP450 enzyme systems .....	190
5.2.4.	Statistics .....	191
5.3.	Results .....	192

5.3.1. P-glycoprotein inhibitory activity .....	192
5.3.2. Alteration to nevirapine efflux in Caco-2 bidirectional assay.....	196
5.3.3. CYP450 inhibitory activity .....	197
5.4. Discussion.....	199
5.4.1. P-glycoprotein inhibitory activity and altered nevirapine permeation ..	199
5.4.2. Inhibition of CYP450 enzymes.....	204
5.5. Conclusion .....	213
<b>Chapter 6: Conclusion .....</b>	<b>214</b>
6.1. Concluding remarks .....	214
6.2. Executive summary.....	219
6.3. Limitations of the study and recommendations .....	219
<b>References.....</b>	<b>222</b>
<b>Appendix I: Publication .....</b>	<b>256</b>
<b>Appendix II: Ethical approval .....</b>	<b>257</b>
<b>Appendix III: Preparation of reagents.....</b>	<b>258</b>
<b>Appendix IV: Additional cellular experiments .....</b>	<b>275</b>

## Declaration

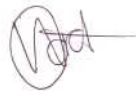
I: **Werner Cordier**

Student number: **25072499**

Thesis title: ***In vitro* hepatotoxicity and herb-drug interactions of selected African plant extracts**

1. Understand what plagiarism entails and am aware of the University's policy in this regard.
2. I declare that this thesis is of my own, original work. Where someone else's work was used (whether from a printed source, the internet or any other source) due acknowledgement was given and reference was made according to departmental requirements.
3. I did not make use of another student's previous work and submitted it as my own.
4. I did not allow and will not allow anyone to copy my work with the intention of presenting it as his or her own work.

Signature:



Date: 19 June 2016

## Abstract

Herbal remedies are an important and often-used commodity in developing countries, such as those in Africa. There is a long-standing belief that these medicinal preparations are more effective and safe than allopathic medications due to their natural origins. However, very little information is available to describe the toxicological nature of African herbal remedies, especially with regards to their hepatotoxic effects, or ability to alter the pharmacokinetic profiles of other compounds. The aim of this *in vitro* study was to assess the hepatotoxic potential of a panel of selected African herbal remedies, as well as their potential to induce drug-herb interactions.

Crude hot water and methanol extracts were prepared from seventeen African plants using brewing and ultrasonic maceration techniques, respectively. Phytochemical screening was done to determine the broad constituency of the extracts using thin layer chromatography, biochemical reactions and free radical scavenging. Cytotoxicity against the HepG2 hepatocarcinoma and Caco-2 colon carcinoma cell lines were determined using the sulforhodamine B staining assay. *Acokanthera oppositifolia*, *Boopane disticha*, *Moringa oleifera*, *Solanum aculeastrum*, *Tabernaemontana elegans*, *Terminalia sericea* and *Ziziphus mucronata* were selected for further hepatotoxic assessment using a mixture of spectrophotometric, fluorometric, chemiluminescent and flow cytometric assays. Oxidative stress (reactive oxygen species, glutathione and lipid peroxidation levels), mitochondrial membrane potential, fatty acid accumulation and caspase-3/7 activation was assessed using fluorometric assays, while adenosine triphosphate levels were assessed using a chemiluminescent assay. The effect of the extracts on cellular kinetics and mode of cell death was determined using flow cytometric techniques. Drug-herb interactions of the crude extracts were assessed by measuring their effect on P-glycoprotein activity, nevirapine permeability and cytochrome P450 (CYP2B6, CYP2D6 and CYP3A4) enzyme activity.

Phytochemical analyses successfully identified the broad constituency and antioxidant profiles of the crude extracts, which correlated well with that already described in literature. Phytochemical classes that were most prominent in the majority of extracts were the alkaloids, flavonoids, glycosides, phenolic acids and saponins. These results

were used to determine potential contributing factors during the hepatotoxicity and drug-herb interactions assays.

Thirteen extracts displayed activity against the HepG2 cell line, while twelve were active against the Caco-2 cell line. Cytotoxicity was in general more potent against the Caco-2 cell line, indicating a potential susceptibility of the intestinal tract towards these herbal remedies. A high risk of cytotoxicity was identified for extracts such as *A. oppositifolia*, *S. aculeastrum* and *T. elegans*. Further hepatotoxic assessment indicated that the majority of extracts depolarised the mitochondrial membrane, however oxidative stress was rarely induced. Steatotic changes were evident as shown by the increased retention of fatty acids. Cytotoxicity was mostly a mixture of antiproliferative effects, and worryingly, the induction of necrotic cell death. Although the methanol extracts tended to be more potent than the hot water extracts, the latter induced detrimental effects as well, albeit at a higher relative concentration. The most prominent hepatotoxic effects were observed after exposure to *T. elegans*, with a half-maximal inhibitory concentration of 3.07 µg/mL.

Only the methanol extract of *S. aculeastrum* displayed prominent P-glycoprotein inhibitory activity (HepG2 = 2.92-fold, Caco-2 = 1.29-fold). Five extracts (hot water extracts of *Burkea africana* and *Senecio latifolius*, and the methanol extracts of *Mundulea sericea*, *Rauvolfia caffra* and *Solanum aculeastrum*) were selected for assessment of their ability to modulate nevirapine transport across the Caco-2 cell line. All five extracts decreased nevirapine efflux, indicating a propensity for increasing its bioavailability. Due to the lack of P-glycoprotein inhibitory activity from the majority, it appears that this reduced efflux is not necessarily P-glycoprotein-dependent. Altered membrane fluidics and inhibition of other membrane transporters are suggested as potential contributing factors.

The majority of extracts displayed prominent CYP450 inhibitory activity (CYP3A4>CYP2B6>CYP2D6). Most extracts displayed a higher selectivity towards CYP3A4, which highlights the caution required. More than 50% of drugs currently used on the market are metabolised by the CYP3A4 isoform, and thus the risk is high when comparing it to the low concentrations required to elicit an effect. Both extracts of *B. africana*, the hot water extract of *T. sericea* and the methanol extract of *Z. mucronata* displayed non-selective inhibition across all three isoforms, indicating a possible

affinity for a structurally-conserved site across CYP450 enzymes. Due to the genetic makeup of the African populace, which has a significant proportion of CYP450 alleles displaying reduced or inactivated enzyme activity, risk is thus high for attenuating their metabolic functions. The methanol extract displayed the highest inhibitory activity against CYP3A4, with a half-maximal inhibitory concentration  $<1.2 \mu\text{g/mL}$ .

It is evident throughout the study that there is a high risk of hepatotoxicity or drug-herb interactions. This is specifically observed when taking into account the low amount of extract required to reach the inhibitory concentrations determined *in vitro*. Inhibition of intestinal P-glycoprotein transporters and CYP450 enzymes appear to be more at risk than that of the liver. This is one of the few studies delving into the toxicological natures of African herbal remedies, specifically in light of hepatotoxicity and herb-drug interactions, and thus serves as a foundation for further assessment.

## Study outputs

### Conference proceedings

#### *Poster presentations*

- Cordier W, Steenkamp V. The screening of African herbal remedies for their effect on P-glycoprotein activity. 3's Company Pharmacy Conference, Cape Town, SA, 4 – 6 Oct 2013.
- Cordier W, Steenkamp V. An evaluation of the hepatotoxic effects of an ethnomedicinal preparation of *Moringa oleifera* and *Terminalia sericea*. 3's Company Pharmacy Conference, Cape Town, SA, 4 – 6 Oct 2013.
- Cordier W, Steenkamp V. An *in vitro* mechanistic evaluation of the hepatotoxic properties of *Solanum aculeastrum*. 17<sup>th</sup> World Congress of Basic and Clinical Pharmacology, Cape Town, SA, 13 – 18 July 2014 **[IPASA Best Poster Presentation in Africa]**.
- Cordier W, Steenkamp V. The screening of African herbal remedies for their effect on P-glycoprotein activity. Health Sciences Faculty Day, University of Pretoria, SA, 19 Aug 2014.
- Cordier W, Steenkamp V. An evaluation of the hepatotoxic effects of an ethnomedicinal preparation of *Moringa oleifera* and *Terminalia sericea*. Health Sciences Faculty Day, University of Pretoria, SA, 19 Aug 2014.
- Cordier W, Steenkamp V. Cytostasis of HepG2 hepatocarcinoma cells after exposure to *Boophane disticha* bulb extracts. SASBCP & TOXSA 2015 Congress, The University of the Witwatersrand, Johannesburg, 31 Aug – 2 Sep 2015.
- Cordier W, Steenkamp V. Altered absorption of nevirapine during concomitant exposure to African herbal remedies: An *in vitro* evaluation. SASBCP & TOXSA 2015 Congress, The University of the Witwatersrand, Johannesburg, 31 Aug – 2 Sep 2015. **[1<sup>st</sup> place: Poster Presentation in Pharmacology]**.
- Cordier W, Steenkamp V. Cytostasis of HepG2 hepatocarcinoma cells after exposure to *Boophane disticha* bulb extracts. Health Sciences Faculty Day, University of Pretoria, SA, 18 – 19 Aug 2015.
- Cordier W, Steenkamp V. Altered absorption of nevirapine during concomitant exposure to African herbal remedies: An *in vitro* evaluation. Health Sciences Faculty Day, University of Pretoria, SA, 18 – 19 Aug 2015.
- Cordier W, Steenkamp V. Cytostasis of HepG2 hepatocarcinoma cells after exposure to *Boophane disticha* bulb extracts. The International Symposium on Methods for Studying Drug Metabolism and Transport, and African Traditional Medicines, Saint George's Hotel, SA, 23 – 25 Nov 2015.
- Cordier W, Steenkamp V. Altered absorption of nevirapine during concomitant exposure to African herbal remedies: An *in vitro* evaluation. The International Symposium on Methods for Studying Drug Metabolism and Transport, and African Traditional Medicines, Saint George's Hotel, SA, 23 – 25 Nov 2015.

### *Podium presentations*

- Cordier W, Steenkamp V. An *in vitro* multi-parametric assessment of the hepatotoxic effects of *Acokanthera oppositifolia* and *Tabernaemontana elegans*. 3's Company Pharmacy Conference, Cape Town, SA, 4 – 6 Oct 2013.
- Cordier W, Steenkamp V. Bepaling van *in vitro* hepatotoksisiteit van twee plante van die Apocynaceae familie. Die Suid Afrikaanse Akademie van Wetenskap en Kuns Konferensie, Pretoria, SA, 16 Oct 2013.
- Cordier W, Steenkamp V. An *in vitro* mechanistic evaluation of the hepatotoxic properties of *Solanum aculeastrum*. Health Sciences Faculty Day, University of Pretoria, SA, 20 Aug 2014. [**3<sup>rd</sup> place: Young Researcher Basic Podium Presentation**].
- Cordier W, Steenkamp V. Antiproliferative and pro-necrotic activity of *Solanum aculeastrum* fruits against HepG2 hepatocarcinoma cells. SASBCP & TOXSA 2015 Congress, The University of the Witwatersrand, Johannesburg, 31 Aug – 2 Sep 2015. [**1<sup>st</sup> place: Podium Presentation in Toxicology**].

### *Studentship poster presentations*

- Parkar H, Cordier W, Steenkamp V. Hepatotoxic effects of *Acokanthera oppositifolia* and *Boophane disticha*. Die Suid Afrikaanse Akademie van Wetenskap en Kuns Konferensie, Pretoria, SA, 16 Oct 2013.
- Burger TM, Steenkamp V, Cordier W. In-vitro anticancer potential of alkaloid-enriched fractions from *Solanum aculeastrum* fruits. Health Sciences Faculty Day, University of Pretoria, SA, 19 Aug 2014.
- Cordier W, Steenkamp V. Cytostasis of HepG2 hepatocarcinoma cells after exposure to *Boophane disticha* bulb extracts. Health Sciences Faculty Day, University of Pretoria, SA, 18 – 19 Aug 2015.

### *Studentship podium presentations*

- Parkar H, Cordier W, Steenkamp V. Hepatotoxic effects of *Acokanthera oppositifolia* and *Boophane disticha*. 17<sup>th</sup> World Congress of Basic and Clinical Pharmacology, Cape Town, SA, 13 – 18 July 2014.
- Burger TM, Steenkamp V, Cordier W. *In vitro* anticancer and P-glycoprotein inhibitory potential of alkaloid-enriched fractions from *Solanum aculeastrum* fruits. Health Sciences Faculty Day, University of Pretoria, SA, 18 – 19 Aug 2015.

### **Publications (provided in Appendix I)**

- Cordier W, Steenkamp V. Evaluation of four assays to determine cytotoxicity of selected crude medicinal plant extracts *in vitro*. *British Journal of Pharmaceutical Research* 2015;7:16 – 21.

### **Publications to be completed (titles subject to change)**

- Cordier W, Steenkamp V. Phytochemical and cytotoxicity screening of a selection of African herbal remedies.
- Cordier W, Steenkamp V. The cytostatic and cytotoxic properties of *Acokanthera oppositifolia* in a model of *in vitro* hepatotoxicity.
- Cordier W, Steenkamp V. Extracts of *Boophane disticha* induce cytostatic effects in a model of *in vitro* hepatotoxicity
- Cordier W, Steenkamp V. Negligible hepatotoxic effects of *Moringa oleifera* in an *in vitro* model.
- Cordier W, Steenkamp V. The pronecrotic and antiproliferative properties of *Solanum aculeastrum* in HepG2 hepatocarcinoma cells.
- Cordier W, Steenkamp V. The potent hepatotoxic properties of *Tabernaemontana elegans* methanol root extract.
- Cordier W, Steenkamp V. *In vitro* evaluation of the effect of *Terminalia sericea* on HepG2 hepatocarcinoma cells.
- Cordier W, Steenkamp V. Mechanisms contributing to *Ziziphus mucronata* cytotoxicity in HepG2 hepatocarcinoma cells.
- Cordier W, Steenkamp V. The risk of herb-drug interactions induced by selected African herbal remedies in an *in vitro* model.

## List of Figures

<b>Figure 1:</b> The effect that herb-drug interactions may elicit on drug efficacy and toxicity; ED <sub>50</sub> = dose that results in an effect in 50% of individuals; TD <sub>50</sub> = dose that results in toxicity in 50% of individuals.....	<b>5</b>
<b>Figure 2:</b> Phases of the pharmacokinetic profile where herbs are capable of inducing drug interactions (modified from Markovsky <i>et al.</i> <sup>39</sup> ). .....	<b>6</b>
<b>Figure 3:</b> Uses of extracts (adapated from Wink <sup>48</sup> ). .....	<b>10</b>
<b>Figure 4:</b> Plants investigated during the study. A) <i>A. oppositifolia</i> , <sup>66</sup> B) <i>B. disticha</i> , <sup>67</sup> C) <i>B. africana</i> , <sup>68</sup> D). <i>C. laureola</i> , <sup>69</sup> E) <i>C. bulbispermum</i> , <sup>70</sup> F) <i>L. leonurus</i> , <sup>71</sup> G) <i>M. olefeira</i> , <sup>72</sup> H) <i>M. sericea</i> , <sup>73</sup> I) <i>P. capense</i> , <sup>74</sup> J) <i>R. caffra</i> , <sup>75</sup> K) <i>R. lancea</i> , <sup>76</sup> L) <i>S. puniceus</i> , <sup>77</sup> M) <i>S. latifolius</i> , <sup>78</sup> N) <i>S. aculeastrum</i> , <sup>79</sup> O) <i>T. elegans</i> , <sup>80</sup> P) <i>T. sericea</i> <sup>81</sup> and Q) <i>Z. mucronata</i> <sup>82</sup> .....	<b>14</b>
<b>Figure 5:</b> Total flavonoid content of crude extracts, arranged by increasing relative abundance. HW – hot water extract; MeOH – methanol extract. ....	<b>23</b>
<b>Figure 6:</b> Total phenolic content of crude extracts, arranged by increasing relative abundance. HW – hot water extract; MeOH – methanol extract. ....	<b>23</b>
<b>Figure 7:</b> Total saponin content of crude extracts, arranged by increasing relative abundance. HW – hot water extract; MeOH – methanol extract. ....	<b>24</b>
<b>Figure 8:</b> Antioxidant activity, expressed as the IC <sub>50</sub> , of the crude extracts arranged from strongest to weakest activity (black dashed line represents the active threshold). Antioxidant activity at 100 µg/mL represents a value >100 µg/mL. HW – hot water extract; MeOH – methanol extract.....	<b>24</b>
<b>Figure 9:</b> Comparison of the effect of the methanol extract of <i>T. elegans</i> on metabolic activity and cell density using the A) resazurin and B) SRB assays, respectively. ...	<b>42</b>
<b>Figure 10:</b> The effects of crude extracts on resazurin conversion in absence of cells; HW – hot water, MeOH – methanol; NC – negative control; PC – positive control (1 mg/mL ascorbate) .....	<b>42</b>
<b>Figure 11:</b> The effect of tamoxifen on A) Caco-2 and B) HepG2 cells.....	<b>43</b>
<b>Figure 12:</b> The effect of crude extracts of A) <i>A. oppositifolia</i> , B) <i>B. disticha</i> , C) <i>B. africana</i> , D) <i>C. bulbispermum</i> , E) <i>M. sericea</i> , F) <i>S. puniceus</i> , G) <i>S. aculeastrum</i> , H) <i>T. elegans</i> and I) <i>Z. mucronata</i> on the cell density of HepG2 cells. ● hot water extracts, ○ methanol extracts.....	<b>45</b>
<b>Figure 13:</b> The effect of crude extracts of A) <i>A. oppositifolia</i> , B) <i>B. disticha</i> , C) <i>C. bulbispermum</i> , D) <i>M. sericea</i> , E) <i>P. capense</i> , F) <i>S. puniceus</i> , G) <i>S. aculeastrum</i> and H) <i>T. elegans</i> on the cell density of Caco-2 cells. ● hot water extracts, ○ methanol extracts.....	<b>45</b>
<b>Figure 14:</b> Cytotoxicity, expressed as the IC <sub>50</sub> , of the crude extracts arranged by reduction of cell density (black dashed line represents the active threshold) in the A) Caco-2 and B) HepG2 cell lines. Cytotoxicity at 100 µg/mL represents a value >100 µg/mL. HW – hot water extract; MeOH – methanol extract. ....	<b>47</b>

**Figure 15:** The effect of crude extracts of A) *B. africana*, B) *R. caffra* and C) *S. latifolius* on Caco-2 cells. ● hot water extracts, ○ methanol extracts. *S. latifolius* was the only crude extract that displayed an accurate dose-response fit using stimulatory non-linear regression. .... 47

**Figure 16:** Schematic representation of the mitochondrial fatty acid  $\beta$ -oxidation and oxidative phosphorylation pathways in liver mitochondria (reproduced from Begrich *et al.* with permission).<sup>247</sup>; ACS – acyl-CoA synthetases; acyl-CoA – acyl-conenzyme A; CPT – carnitine palmitoyltransferase; LCFA – long-chain fatty acids; MRC – mitochondrial respiratory chain; mtDNA – mitochondrial DNA ..... 77

**Figure 17:** The cell cycle (reproduced from Wikipedia with permission).<sup>288</sup> ..... 83

**Figure 18:** Differentiation between necrotic and apoptotic cell death (reproduced from Wikipedia<sup>297</sup> with permission). ..... 86

**Figure 19:** The intrinsic and extrinsic apoptotic pathways (reproduced from Wikipedia<sup>301</sup> with permission); Apaf - apoptotic protease activating factor 1; DISC – death inducing signal complex; FasL –Fas ligand; FasR – Fas receptor. .... 89

**Figure 20:** Plate template used for the determination of hepatotoxicity (CD – cell density, ROS – ROS concentration, GSH – GSH concentration, MMP –  $\Delta\Psi_m$ , FA – fatty acid concentration, CAS-3/7 – caspase-3/7) ..... 93

**Figure 21:** Interpretation of cell cycle kinetics using deconvolution software, where DNA content was determined through propidium iodide staining. .... 100

**Figure 22:** Interpretation of mode of cell death. .... 102

**Figure 23:** Correlation between the Bradford protein content and SRB assay. .... 103

**Figure 24:** The effect of positive controls on A) cell density (staurosporine), B)  $\Delta\Psi_m$  (rotenone), C) ROS concentration (potassium peroxodisulfate), D) GSH concentration (n-ethylmaleimide), E) fatty acid concentration (oleic acid). F) lipid peroxidation (AAPH), G) ATP levels (saponin) and F) caspase-3/7 activity (staurosporine) in HepG2 cells; significance was determined against the negative control. .... 105

**Figure 25:** The effect of positive controls on the cell cycle kinetics of HepG2 cells exposed to A) negative control for 24 h, B) negative control for 72 h, C) double thymidine block (synchronized cells), D) FCS-depleted EMEM (G1-block) for 24 h, E) methotrexate (S-block) for 14 h, and F) curcumin (G2/M-block) for 14 h. Significance determined relative to the 24 h negative control: ★★  $p < 0.01$ , ★★★  $p < 0.001$ ... 106

**Figure 26:** The effect of positive controls on the viability of HepG2 cells exposed to A) negative control for 24 h, B) negative control for 72 h, C) rotenone (apoptosis) for 24 h, and D) 70% ethanol sonication (necrosis) for 5 min. Significance determined relative to the 24 h negative control: ★★★  $p < 0.001$ . .... 106

**Figure 27:** The effect of the crude hot water extract of *A. oppositifolia* in HepG2 cells; A) cell density, B)  $\Delta\Psi_m$ , C) ROS concentration, D) GSH concentration, E) fatty acid concentration, F) lipid peroxidation, G) ATP levels and H) caspase-3/7 activity. ... 108

**Figure 28:** The effect of the crude methanol extract of *A. oppositifolia* in HepG2 cells; A) cell density, B)  $\Delta\Psi_m$ , C) ROS concentration, D) GSH concentration, E) fatty acid concentration, F) lipid peroxidation, G) ATP levels and H) caspase-3/7 activity. ... 109

- Figure 29:** The effect of the IC<sub>50</sub> of *A. oppositifolia* on cellular kinetics in HepG2 cells exposed for 24 h and 72 h; A) negative control (24 h), B) hot water extract (24 h), C) methanol extract (24 h), D) negative control (72 h), E) hot water extract (72 h), F) methanol extract (72 h). Significant difference relative to the respective time points of the negative control: ★  $p < 0.05$ , ★★  $p < 0.01$  and ★★★  $p < 0.001$ . ..... **110**
- Figure 30:** The effect of the IC<sub>50</sub> of *A. oppositifolia* on cellular viability in HepG2 cells exposed for 24 h and 72 h; A) negative control (24 h), B) hot water extract (24 h), C) methanol extract (24 h), D) negative control (72 h), E) hot water extract (72 h), F) methanol extract (72 h). Significant difference relative to the respective time points of the negative control: ★  $p < 0.05$ , ★★  $p < 0.01$  and ★★★  $p < 0.001$ . ..... **111**
- Figure 31:** The effect of the crude hot water extract of *B. disticha* in HepG2 cells; A) cell density, B)  $\Delta\Psi_m$ , C) ROS concentration, D) GSH concentration, E) fatty acid concentration, F) lipid peroxidation, G) ATP levels and H) caspase-3/7 activity. ... **113**
- Figure 32:** The effect of the crude methanol extract of *B. disticha* in HepG2 cells; A) cell density, B)  $\Delta\Psi_m$ , C) ROS concentration, D) GSH concentration, E) fatty acid concentration, F) lipid peroxidation, G) ATP levels and H) caspase-3/7 activity. ... **115**
- Figure 33:** The effect of the IC<sub>50</sub> of *B. disticha* on cellular kinetics in HepG2 cells exposed for 24 h and 72 h; A) negative control (24 h), B) hot water extract (24 h), C) methanol extract (24 h), D) negative control (72 h), E) hot water extract (72 h), F) methanol extract (72 h). ..... **116**
- Figure 34:** The effect of the IC<sub>50</sub> of *B. disticha* on cellular viability in HepG2 cells exposed for 24 h and 72 h; A) negative control (24 h), B) hot water extract (24 h), C) methanol extract (24 h), D) negative control (72 h), E) hot water extract (72 h), F) methanol extract (72 h). Significant difference relative to the respective time points of the negative control: ★  $p < 0.05$ , ★★  $p < 0.01$  and ★★★  $p < 0.001$ . ..... **117**
- Figure 35:** The effect of the crude hot water extract of *M. oleifera* in HepG2 cells; A) cell density, B)  $\Delta\Psi_m$ , C) ROS concentration, D) GSH concentration, E) fatty acid concentration, F) lipid peroxidation, G) ATP levels and H) caspase-3/7 activity. ... **119**
- Figure 36:** The effect of the crude methanol extract of *M. oleifera* in HepG2 cells; A) cell density, B)  $\Delta\Psi_m$ , C) ROS concentration, D) GSH concentration, E) fatty acid concentration, F) lipid peroxidation, G) ATP levels and H) caspase-3/7 activity. ... **120**
- Figure 37:** The effect of the 100  $\mu\text{g/mL}$  *M. oleifera* on cellular kinetics in HepG2 cells exposed for 24 h and 72 h; A) negative control (24 h), B) hot water extract (24 h), C) methanol extract (24 h), D) negative control (72 h), E) hot water extract (72 h), F) methanol extract (72 h). ..... **121**
- Figure 38:** The effect of the 100  $\mu\text{g/mL}$  *M. oleifera* on cellular viability in HepG2 cells exposed for 24 h and 72 h; A) negative control (24 h), B) hot water extract (24 h), C) methanol extract (24 h), D) negative control (72 h), E) hot water extract (72 h), F) methanol extract (72 h). Significant difference relative to the respective time points of the negative control: ★  $p < 0.05$ , ★★  $p < 0.01$  and ★★★  $p < 0.001$ . ..... **122**
- Figure 39:** The effect of the crude hot water extract of *S. aculeastrum* in HepG2 cells; A) cell density, B)  $\Delta\Psi_m$ , C) ROS concentration, D) GSH concentration, E) fatty acid concentration, F) lipid peroxidation, G) ATP levels and H) caspase-3/7 activity. ... **124**

- Figure 40:** The effect of the crude methanol extract of *S. aculeastrum* in HepG2 cells; A) cell density, B)  $\Delta\Psi_m$ , C) ROS concentration, D) GSH concentration, E) fatty acid concentration, F) lipid peroxidation, G) ATP levels and H) caspase-3/7 activity. ... **125**
- Figure 41:** The effect of the IC<sub>50</sub> of *S. aculeastrum* on cellular kinetics in HepG2 cells exposed for 24 h and 72 h; A) negative control (24 h), B) hot water extract (24 h), C) methanol extract (24 h), D) negative control (72 h), E) hot water extract (72 h), F) methanol extract (72 h). Significant difference relative to the respective time points of the negative control: ★★  $p < 0.01$  and ★★★  $p < 0.001$ . ..... **126**
- Figure 42:** The effect of the IC<sub>50</sub> of *S. aculeastrum* on cellular viability in HepG2 cells exposed for 24 h and 72 h; A) negative control (24 h), B) hot water extract (24 h), C) methanol extract (24 h), D) negative control (72 h), E) hot water extract (72 h), F) methanol extract (72 h). Significant difference relative to the respective time points of the negative control: ★★  $p < 0.01$  and ★★★  $p < 0.001$ . ..... **127**
- Figure 43:** The effect of the crude hot water extract of *T. elegans* in HepG2 cells; A) cell density, B)  $\Delta\Psi_m$ , C) ROS concentration, D) GSH concentration, E) fatty acid concentration, F) lipid peroxidation, G) ATP levels and H) caspase-3/7 activity. ... **129**
- Figure 44:** The effect of the crude methanol extract of *T. elegans* in HepG2 cells; A) cell density, B)  $\Delta\Psi_m$ , C) ROS concentration, D) GSH concentration, E) fatty acid concentration, F) lipid peroxidation, G) ATP levels and H) caspase-3/7 activity. ... **131**
- Figure 45:** The effect of 100  $\mu\text{g/mL}$  and the IC<sub>50</sub> of the hot water and methanol extract of *T. elegans*, respectively, on cellular kinetics in HepG2 cells exposed for 24 h and 72 h; A) negative control (24 h), B) hot water extract (24 h), C) methanol extract (24 h), D) negative control (72 h), E) hot water extract (72 h), F) methanol extract (72 h). Significant difference relative to the respective time points of the negative control: ★  $p < 0.05$  and ★★★  $p < 0.001$ . ..... **132**
- Figure 46:** The effect of 100  $\mu\text{g/mL}$  and the IC<sub>50</sub> of the hot water and methanol extract of *T. elegans*, respectively, on cellular viability in HepG2 cells exposed for 24 h and 72 h; A) negative control (24 h), B) hot water extract (24 h), C) methanol extract (24 h), D) negative control (72 h), E) hot water extract (72 h), F) methanol extract (72 h). Significant difference relative to the respective time points of the negative control: ★  $p < 0.05$  and ★★★  $p < 0.001$ . ..... **133**
- Figure 47:** The effect of the crude hot water extract of *T. sericea* in HepG2 cells; A) cell density, B)  $\Delta\Psi_m$ , C) ROS concentration, D) GSH concentration, E) fatty acid concentration, F) lipid peroxidation, G) ATP levels and H) caspase-3/7 activity. ... **135**
- Figure 48:** The effect of the crude methanol extract of *T. sericea* in HepG2 cells; A) cell density, B)  $\Delta\Psi_m$ , C) ROS concentration, D) GSH concentration, E) fatty acid concentration, F) lipid peroxidation, G) ATP levels and H) caspase-3/7 activity. ... **136**
- Figure 49:** The effect of the 100  $\mu\text{g/mL}$  *T. sericea* on cellular kinetics in HepG2 cells exposed for 24 h and 72 h; A) negative control (24 h), B) hot water extract (24 h), C) methanol extract (24 h), D) negative control (72 h), E) hot water extract (72 h), F) methanol extract (72 h) . Significant difference relative to the respective time points of the negative control: ★  $p < 0.05$ . ..... **137**

**Figure 50:** The effect of the 100 µg/mL *T. sericea* on cellular viability in HepG2 cells exposed for 24 h and 72 h; A) negative control (24 h), B) hot water extract (24 h), C) methanol extract (24 h), D) negative control (72 h), E) hot water extract (72 h), F) methanol extract (72 h). Significant difference relative to the respective time points of the negative control: ★★★  $p < 0.001$ . ..... 138

**Figure 51:** The effect of the crude methanol extract of *Z. mucronata* in HepG2 cells; A) cell density, B)  $\Delta\Psi_m$ , C) ROS concentration, D) GSH concentration, E) fatty acid concentration, F) lipid peroxidation, G) ATP levels and H) caspase-3/7 activity. ... 140

**Figure 52:** The effect of the crude methanol extract of *Z. mucronata* in HepG2 cells; A) cell density, B)  $\Delta\Psi_m$ , C) ROS concentration, D) GSH concentration, E) fatty acid concentration, F) lipid peroxidation, G) ATP levels and H) caspase-3/7 activity. ... 141

**Figure 53:** The effect of 100 µg/mL and the IC<sub>50</sub> of the hot water and methanol extract of *Z. mucronata*, respectively, on cellular kinetics in HepG2 cells exposed for 24 h and 72 h; A) negative control (24 h), B) hot water extract (24 h), C) methanol extract (24 h), D) negative control (72 h), E) hot water extract (72 h), F) methanol extract (72 h) . Significant difference relative to the respective time points of the negative control: ★  $p < 0.05$ , ★★  $p < 0.01$  and ★★★  $p < 0.001$ . ..... 142

**Figure 54:** The effect of 100 µg/mL and the IC<sub>50</sub> of the hot water and methanol extract of *Z. mucronata*, respectively, on cellular viability in HepG2 cells exposed for 24 h and 72 h; A) negative control (24 h), B) hot water extract (24 h), C) methanol extract (24 h), D) negative control (72 h), E) hot water extract (72 h), F) methanol extract (72 h). Significant difference relative to the respective time points of the negative control: ★  $p < 0.05$ , ★★  $p < 0.01$  and ★★★  $p < 0.001$ . ..... 143

**Figure 55:** Graphical representation of P-glycoprotein and other membrane transporters in the blood-brain barrier allowing for efflux of chemicals to protect the brain (as reproduced by Miller<sup>446</sup> with permission). ..... 176

**Figure 56:** Structurally-conserved regions of CYP450 enzymes in a structural overview (reproduced from Sirim *et al.*<sup>458</sup> with permission). The reference structure of CYP450 BM-3 is from *Bacillus megaterium*. The blue regions indicate structurally conserved regions, while the grey-green indicate variable regions. .... 180

**Figure 57:** Graphical representation of the structure of the Caco-2 bidirectional permeability assay supports that are implemented. .... 188

**Figure 58:** Effect of verapamil on Rh-123 accumulation in A) HepG2 and B) Caco-2 cells. Significance was determined against the negative control. .... 192

**Figure 59:** Effect of crude extracts of A) *B. africana*, B) *R. caffra*, C) *S. latifolius* and D) *S. aculeastrum* on Rh-123 accumulation in Caco-2 cells. Significance was determined against the negative control. .... 193

**Figure 60:** Effect of crude extracts of A) *M. sericea*, B) *P. capense* and C) *S. aculeastrum* on Rh-123 accumulation in HepG2 cells. Significance was determined against the negative control. .... 194

**Figure 61:** Chromatogram of nevirapine (10 µM) ..... 195

**Figure 62:** Calibration curve of nevirapine ..... 196

**Figure 63:** Nevirapine efflux ratio in verapamil-pretreated cells ..... 197

**Figure 64:** Nevirapine efflux ratio in crude extract-pretreated cells; VC: vehicle control; BaH: *B. africana* hot water extract, MsM: *M. sericea* methanol extract, RcM: *R. caffra* methanol extract, SIH: *S. latifolius* hot water extract, and SoM: *S. aculeastrum* methanol extract..... **197**

**Figure 65:** Controls for the CYP450 inhibitory activity assay indicating A) CYP2B6, B) CYP2D6 and C) CYP3A4 activity..... **198**

## List of Tables

<b>Table 1:</b> Plants investigated in this study, including ethnomedicinal use and botanical information. ....	<b>13</b>
<b>Table 2:</b> TLC parameters used for identification of crude extracts, as obtained from Bolliger <i>et al.</i> <sup>83</sup> .....	<b>16</b>
<b>Table 3:</b> Extraction yields of crude hot water and methanol extracts of plants investigated. ....	<b>19</b>
<b>Table 4:</b> Phytochemical classes detected in crude extracts using TLC screening...	<b>21</b>
<b>Table 5:</b> Quantitative analyses (n = 9) of flavonoids, phenolic acids and saponins in crude extracts.....	<b>22</b>
<b>Table 6:</b> ABTS <sup>•+</sup> scavenging activity of crude extracts and standards. ....	<b>25</b>
<b>Table 7:</b> Comparison of four cytotoxicity assays using eight crude extracts. ....	<b>41</b>
<b>Table 8:</b> Cytotoxicity of crude extracts in the HepG2 and Caco-2 cell lines (n = 9).	<b>44</b>
<b>Table 9:</b> IC <sub>50</sub> 's of plants selected for study (excluding those discussed in Chapter 4) as obtained from literature.....	<b>50</b>
<b>Table 10:</b> Summary of the cytotoxic properties of Amaryllidaceae-type isoquinoline alkaloids that have been identified in the studied plants .....	<b>58</b>
<b>Table 11:</b> Plants that carry a risk of exerting cytotoxic activity in the systemic circulation on liver cells, including amount of extract and plant material required (assuming full dissolution and absorption). ....	<b>70</b>
<b>Table 12:</b> Plants that carry a risk of exerting cytotoxic activity in the intestinal compartment, including amount of extract and plant material required (assuming full dissolution and absorption). ....	<b>70</b>
<b>Table 13:</b> Case reports where HILI was noted or suspected. ....	<b>73</b>
<b>Table 14:</b> The effect of the IC <sub>50</sub> of <i>A. oppositifolia</i> on cellular kinetics in HepG2 cells exposed for 24 h and 72 h summarized as the shift in phase from the respective negative control.....	<b>110</b>
<b>Table 15:</b> The effect of the IC <sub>50</sub> of <i>A. oppositifolia</i> on cellular viability in HepG2 cells exposed for 24 h and 72 h summarized as the shift in phase from the respective negative control.....	<b>112</b>
<b>Table 16:</b> The effect of the IC <sub>50</sub> of <i>B. disticha</i> on cellular kinetics in HepG2 cells exposed for 24 h and 72 h summarized as the shift in phase from the respective negative control.....	<b>116</b>
<b>Table 17:</b> The effect of the IC <sub>50</sub> of <i>B. disticha</i> on cellular viability in HepG2 cells exposed for 24 h and 72 h summarized as the shift in phase from the respective negative control.....	<b>117</b>
<b>Table 18:</b> The effect of the 100 µg/mL <i>M. oleifera</i> on cellular kinetics in HepG2 cells exposed for 24 h and 72 h summarized as the shift in phase from the respective negative control.....	<b>121</b>

**Table 19:** The effect of the 100 µg/mL *M. oleifera* on cellular viability in HepG2 cells exposed for 24 h and 72 h summarized as the shift in phase from the respective negative control..... **122**

**Table 20:** The effect of the IC<sub>50</sub> of *S. aculeastrum* on cellular kinetics in HepG2 cells exposed for 24 h and 72 h summarized as the shift in phase from the respective negative control..... **126**

**Table 21:** The effect of the IC<sub>50</sub> of *S. aculeastrum* on cellular viability in HepG2 cells exposed for 24 h and 72 h summarized as the shift in phase from the respective negative control..... **127**

**Table 22:** The effect of 100 µg/mL and the IC<sub>50</sub> of the hot water and methanol extract of *T. elegans*, respectively, on cellular kinetics in HepG2 cells exposed for 24 h and 72 h summarized as the shift in phase from the respective negative control. .... **132**

**Table 23:** The effect of 100 µg/mL and the IC<sub>50</sub> of the hot water and methanol extract of *T. elegans*, respectively, on cellular viability in HepG2 cells exposed for 24 h and 72 h summarized as the shift in phase from the respective negative control. .... **133**

**Table 24:** The effect of the 100 µg/mL *T. sericea* on cellular kinetics in HepG2 cells exposed for 24 h and 72 h summarized as the shift in phase from the respective negative control..... **137**

**Table 25:** The effect of the 100 µg/mL *T. sericea* on cellular viability in HepG2 cells exposed for 24 h and 72 h summarized as the shift in phase from the respective negative control..... **138**

**Table 26:** The effect of 100 µg/mL and the IC<sub>50</sub> of the hot water and methanol extract of *Z. mucronata*, respectively, on cellular kinetics in HepG2 cells exposed for 24 h and 72 h summarized as the shift in phase from the respective negative control. .... **142**

**Table 27:** The effect of 100 µg/mL and the IC<sub>50</sub> of the hot water and methanol extract of *Z. mucronata*, respectively, on cellular viability in HepG2 cells exposed for 24 h and 72 h summarized as the shift in phase from the respective negative control. .... **144**

**Table 28:** Summary of the hepatotoxicity of the selected crude extracts..... **145**

**Table 29:** Summary of the effects of indole/bisindole alkaloids that have been isolated from *T. elegans* on cellular cultures. .... **162**

**Table 30:** Summary of the effects of phytochemicals that have been isolated from *T. sericea* on cellular cultures..... **169**

**Table 31:** Distribution of transporters and enzymes in the gastrointestinal tract (reproduced from Pang, 2003<sup>440</sup> with permission)..... **176**

**Table 32:** Relative expression of CYP1, CYP2 and CYP3 subfamilies in different tissues (reproduced from Pavek & Dvorak<sup>452</sup> with permission). .... **181**

**Table 33:** A brief summary of substrates and polymorphisms for CYP2B6 and CYP2D6. .... **182**

**Table 34:** A brief summary of substrates and polymorphisms for CYP3A4. .... **184**

**Table 35:** Chromatographic conditions of nevirapine quantitation ..... **190**

**Table 36:** Mass spectrometry conditions of nevirapine quantitation..... **190**

**Table 37:** Substrates and positive controls used to assess CYP450 enzyme inhibitory activity ..... **191**

**Table 38:** CYP450 inhibitory activity of crude extracts expressed as the IC<sub>50</sub> values, and percentage inhibition of the methanol extracts against CYP3A4. .... **200**

**Table 39:** Plants that carry a risk of inhibiting intestinal or hepatic CYP2B6, including amount of extract and plant material required (assuming full dissolution and absorption). .... **206**

**Table 40:** Plants that carry a risk of inhibiting intestinal or hepatic CYP2D6, including amount of extract and plant material required (assuming full dissolution and absorption) ..... **206**

**Table 41:** Plants that carry a risk of inhibiting intestinal or hepatic CYP3A4, including amount of extract and plant material required (assuming full dissolution and absorption). .... **208**

## List of abbreviations

### Symbols and numerical values

°C	Degrees centigrade
%	Percentage
% w/v	Percentage weight to volume
% v/v	Percentage volume to volume
$\alpha$	Alpha
$\beta$	Beta
$\Delta$	Delta
$\Delta\Psi_m$	Electron chemical gradient / mitochondrial membrane potential
$\lambda_{em}$	Emission wavelength
$\lambda_{ex}$	Excitation wavelength
$\mu\text{g/mL}$	Microgram per milliliter
$\mu\text{m}$	Micrometer
$\mu\text{M}$	Micromolar
$\mu\text{L}$	Microliter
2n	Diploid
4n	Tetraploid

### A

Å	Angström
AAPH	2,2'-azobis(2-amidinopropane dihydrochloride)
ABC	ATP-binding cassette
ABTS <sup>•+</sup>	2,2'-azinobis-(3-ethyl benzothiazoline 6-sulfonic acid) radical
Ac-DEVD-AMC	Acetyl Asp-Glu-Val-Asp-7-amido-4-methylcoumarin

ACS	Acyl-CoA synthetases
ADME	Absorption, distribution, metabolism and excretion
ADP	Adenosine diphosphate
AhR	Aryl hydrocarbon receptor
AIDS	Acquired immune deficiency syndrome
AIF	Apoptosis-inducing factor
Akt	Protein kinase B
AMC	7-amido-4-coumarin
AMMC	3-[2-(N,N-diethyl-N-methylamino)ethyl]-7-methoxy-4-methylcoumarin
AMPK	Adenosine monophosphate-activated kinase
ANOVA	Analysis of variance
ANT	Adenine nucleotide translocator
Apaf-1	Apoptotic protease activating factor 1
ARE	Antioxidant response element
ASK1	Apoptosis signal-regulating kinase 1
ATCC	American Type Tissue Culture
ATP	Adenosine triphosphate
ATM	Ataxia telangiectasia mutated

## B

BCRP	Breast cancer resistance protein
BFC	7-Benzyl-trifluoromethylcoumarin
BRAC	Brea1-associated surveillance complex

## C

c	Concentration
---	---------------

C	Carbon
CAR	Constitutive androstane receptor
CCK-8	Cell Counting Kit-8
Cdk	Cyclin-dependent protein kinases
Chk	Checkpoint kinase
CKI	Cyclin kinase inhibitors
cm <sup>2</sup>	Centimeter squared
CO <sub>2</sub>	Carbon dioxide
CoA	Coenzyme A
CPT	Carnitine palmitoyltransferase
CYP450	Cytochrome P450 microsomal enzymes

## D

DCF	Dichlorofluorescein
DE	Diosgenin equivalents
DILI	Drug-induced liver injury
DISC	Death-inducing signalling complex
DILIN	Drug Induced Liver Injury Network
DMSO	Dimethyl sulfoxide
DNA	Deoxyribonucleic acid

## E

ED <sub>50</sub>	Half-maximal effective dose
EDTA	Ethylenediaminetetraacetic acid
EFC	7-Ethoxy-4-trifluoromethylcoumarin
EMEM	Eagle's Minimum Essential Medium
ERK	Extracellular signal regulated kinases



## F

FAD	Flavin adenine dinucleotide
FasL	Fas ligand
FasR	Fas receptor
FCS	Foetal calf serum
FITC	Fluorescein isothiocyanate

## G

g	Gram
<i>g</i>	Relative centrifugal forces
G1-phase	Post-mitotic gap phase
G2-phase	Pre-mitotic gap phase
GAE	Gallic acid equivalents
GSH	Reduced glutathione
GSSG	Oxidised glutathione disulphide

## H

HBSS	Hank's Balanced Saline Solution
H <sub>2</sub> -DCF	2',7'-dichlorodihydrofluorescein
H <sub>2</sub> -DCFDA	2',7'-dichlorodihydrofluorescein diacetate
h	Hour
HAART	Highly-active antiretroviral therapy
HILI	Herb-induced liver injury
HIV	Human immunodeficiency virus
4-HNE	4-Hydroxynonenal
LC-MS/MS	Liquid chromatography tandem mass spectrometry

## I

IC<sub>50</sub> Half-maximal inhibitory concentration

## J

JC-1 5,5',6,6'-tetrachloro-1,1',3,3'-  
tetraethylbenzimidazolylcarbocyanine iodide

JNK c-Jun *N*-terminal kinases

## K

kDa Kilodalton

## L

L Liter

LCFA Long-chain fatty acids

LogD Log partition coefficient at a specified pH

LogP Log partition coefficient water-octanol ratio

LT Lawrence Tshikudo

## M

m/z Mass-to-charge ratio

M-phase Mitosis-phase

M Molar

MAPK Mitogen-activated protein kinase

MDA Malondialdehyde

mg/g Milligram per gram

mM Millimolar

MDR-1 Multi-drug resistance-1

mg/mL	Milligram per millilitre
min	Minute
mL	Milliliter
MPTP	Mitochondrial permeability transition pore
MRP	Multidrug resistance-associated protein
MTT	3-(4,5-dimethylthiazol-2-yl)-2,5-diphenyltetrazolium bromide
mV	Millivolts

## N

n	Sample size
N	Haploid
NAD <sup>+</sup>	Oxidised nicotinamide adenine dinucleotide
NADH	Reduced nicotinamide adenine dinucleotide
NADP <sup>+</sup>	Oxidised nicotinamide dinucleotide phosphate
NADPH	Reduced nicotinamide dinucleotide phosphate
NBD	Nucleotide-binding domain
NCI	National Cancer Institute
NF-κB	Nuclear factor-kappa B
NH	Norbert Hahn
nm	Nanometer
nM	Nanomolar
NNRTI	Non-nucleoside reverse transcriptase inhibitor
Nrf2	Nuclear factor erythroid 2-related factor 2
NRTI	Nucleoside reverse transcriptase inhibitor

## O

OCT	Organic cation transporter
-----	----------------------------

## P

P <sub>app</sub>	Apparent permeability coefficient
PBR	Peripheral benzodiazepine receptor
PBS	Phosphate-buffered saline
PCNA	Proliferating cell nuclear antigen
PI3K	Phosphoinositide 3-kinase
P-gp	P-glycoprotein
pKa	Acid dissociation constant
PPAR- $\alpha$	Peroxisome proliferator-activated receptor-alpha
PS	Phosphatidylserine
PXR	Pregnane X receptor

## R

RE	Rutin equivalents
Rh-123	Rhodamine-123
RNA	Ribonucleic acid
ROS	Reactive oxygen species

## S

S-phase	DNA synthesis phase
SANBI	South African National Botanical Institute
SEM	Standard error of the mean
SOD	Superoxide dismutase
SRB	Sulforhodamine B

## T

TBARS	Thiobarbituric acid reactive substances
TCA	Trichloroacetic acid
TD <sub>50</sub>	Half-maximal toxic dose
TE	Trolox equivalents
TEER	Trans-epithelial electrical resistance
TMD	Transmembrane domains
TLC	Thin-layer chromatography

## U

U	Units
UPR	Unfolded protein response

## V

VDAC	Voltage-dependent anion channel
------	---------------------------------

## Chapter 1

# Introduction to herbal remedy usage, and its relevance in hepatotoxicity and drug-herb interactions

### 1.1. Literature review

#### 1.1.1. Phytopharmacology and phytotoxicity

As the philosopher Paracelsus stated: “Solely the dose determines that a thing is not a poison”,<sup>1</sup> all compounds may elicit toxicity depending on whether a high enough dosage is administered. Herbal remedies, although widely used for ailments, are often excluded from this rule by the general public due to a misconception that their ‘natural origins’ translate to greater safety than their allopathic, synthetic counterparts.<sup>2,3</sup>

Herbal remedies have a significant historical and cultural importance, and thus each country has introduced their own pharmacopoeia of indigenous medicinal plants.<sup>4</sup> Herbal remedy usage increases annually, resulting in greater availability from pharmacies, health shops, informal markets or online sources.<sup>4</sup> The clinical significance, efficacy and safety of these ethnomedicinal preparations is a controversial strife. An estimated 15% of the world’s plant resources have been investigated for potential therapeutic use, mostly on an *in vitro* basis.<sup>5</sup> In South Africa it is thought that more than 12% of the 24,000 plant species recognized are used medicinally for disease alleviation by more than 200,000 traditional healers.<sup>6,7</sup> It has been estimated that traditional healers outnumber allopathic doctors by 10 to 1,<sup>8</sup> further stressing the importance of medicinal plants in the country. Several reasons exist for their popularity, such as financial constraints and lack of medical resources,<sup>5</sup> as well as the belief that allopathic medications possess more severe adverse effects.<sup>9</sup> The latter has exposed a falsity in acceptance that herbal remedies do not pose serious toxicological threats. Furthermore, herbal remediation is oftentimes justified by a belief that a whole herbal extract produces synergistic effects compared to isolated components, and that the mixture presents a buffering against toxicity.<sup>10</sup> The latter statement may hold truth in certain cases, but it may just as well compound toxicity.

Unfortunately research into this is lacking, and as such it is haphazard statement to take as fact.

Due to a lack of pharmacological understanding, individuals often over-administer herbal remedies with subsequent greater risk of adverse effects, or do not disclose use when receiving further allopathic therapies.<sup>11</sup> As such, the use of polypharmacy is increasing, especially between herbal remedies and allopathic medications.<sup>12,13</sup>

Over- and co-administration of herbal remedies may lead to a plethora of adverse effects due to, amongst others, their potential to i) elicit inherent damage to cellular structures, or ii) interact with other compounds introduced in the body either pharmacokinetically or -dynamically. This may result in direct or indirect organotoxicity. Literature is scarce in Africa concerning the detrimental effects of herbal remedies on organ systems, including the liver. Furthermore, very little research has been done to elucidate the potential for interactions between herbal remedies and allopathic medications, such as antiretrovirals.<sup>14</sup> This is an area of importance due to the concomitant use of these drugs and herbal remedies during the treatment of diseases such as acquired immunity deficiency syndrome (AIDS).

### **1.1.2. Highly-active retroviral therapy**

Africa, consisting of developing countries, is afflicted with a range of potentially fatal communicable diseases, such as malaria and AIDS.<sup>14</sup> Human immunodeficiency virus (HIV) infection progressively debilitates the immune system, with subsequent progression to AIDS. It is implicated in more than 20 million deaths occur globally due to uncontrolled infections that cannot be combatted due to immune-suppression.<sup>15</sup>

HIV pharmacotherapy is generally administered as highly-active antiretroviral therapy (HAART), which follows a strict regimen of several antivirals, and requires adequate control to ensure that an effective reduction of viral load occurs. Therefore it is imperative that drug concentrations remain consistent for effective treatment, as alterations in the pharmacokinetic or pharmacodynamic profiles may result in severe consequences. Typical combinations in HAART comprise of protease inhibitors (e.g. saquinavir) and nucleoside reverse transcriptase inhibitors (NRTIs; e.g. azidothymidine), or NRTIs and non-nucleoside reverse transcriptase inhibitors

(NNRTIs; e.g. nevirapine). Inclusion of drugs with separate mechanisms of action ensures a multi-targeted attack occurs against viral replication, and thus allows for a greater viral clearance.<sup>16</sup>

Nevirapine, an NNRTI readily-available in fixed-dose combinations, is commonly used in Africa for HIV/AIDS pharmacotherapy and is effective in reducing mother-to-child transmission of viral particles.<sup>17,18</sup> Nevirapine, and most drugs present in HAART, induces marked hepatotoxicity in patients, such as acute hepatitis with subsequent risk of mortality.<sup>19,20</sup> During absorption, nevirapine undergoes first-pass metabolism and extensive biotransformation in the liver. It is known to be susceptible to interactions with drugs that alter P-glycoprotein (P-gp) and hepatic enzyme activity, and can result in fluctuations of drug plasma concentrations.<sup>13,19</sup>

As HIV/AIDS is incurable, polypharmacy with complementary and alternative often occurs due to desperation for disease alleviation. As Africa maintains a rich cultural belief in traditional therapies, the use of herbal remedies is even more likely during the HIV/AIDS wasting phase. It is necessary to ascertain the potential of further aggravating drug-induced hepatotoxicity, either through direct herbal toxicity or indirectly through fluctuations in drug plasma concentrations. However, pre-clinical assessment in hepatotoxicity related to herbal remedies in Africa is lacking, and thus it is imperative to further research this.

### **1.1.3. Herb-induced liver injury**

The liver, as primary site of metabolism, is susceptible to hepatocellular damage induced by xenobiotics, such as herbal remedies. Metabolic conversion may further potentiate damage through generation of toxic metabolites from parent compounds.<sup>12</sup> Hepatotoxicity is a large hurdle during drug discovery and development, as numerous pharmaceutical leads have undergone attrition due to clinically significant alterations in liver activity.<sup>21</sup> In the Westernized world, allopathic medications are proposed as the most likely candidates for xenobiotic-induced liver injury (regarded as drug-induced liver injury [DILI]), whereas herbal remedies are thought to be the primary malefactors (herb-induced liver injury [HILI]) in developing countries, including those in Africa.<sup>22,23</sup> HILI is common worldwide, though is often not suspected for hepatotoxicity due to an

assumption of safety<sup>23,24</sup> and denial of usage by patients.<sup>22</sup> Diagnosis of HILI is further problematic due to a variety of confounding factors, such as complex phytochemical matrices, dependence on geographic variation, misidentification of plants, microbial contamination or adulteration with potential toxins.<sup>25,26</sup> In America<sup>27</sup> and Asia<sup>22</sup> it is estimated that HILI is responsible for approximately 9% and 55% of hepatotoxicity cases, respectively, albeit these figures may be grossly underestimated.

Although hepatotoxicity is a multi-faceted disorder, several key processes have been noted to be important in toxicity: generation of reactive oxygen species (ROS), depletion of endogenous antioxidants (such as reduced glutathione [GSH]), loss of mitochondrial integrity (such as alterations in mitochondrial membrane potential [ $\Delta\Psi_m$ ]) or induction of cell death pathways (either apoptotic or necrotic death)<sup>21</sup> by phytochemicals or their active metabolites. Reduction in hepatocellular viability ultimately results in clinically significant hepatotoxicity with aggravation of morbidities and possibly leading to mortality.<sup>21</sup> These present in a variety of ways: hepatitis, cholestasis, drug-induced autoimmunity, lesions, fibrosis, hepatosteatorosis, veno-occlusive disease or hepatic failure.<sup>21,28</sup> Hepatotoxicity is generally either induced through direct or idiosyncratic mechanisms.<sup>29</sup>

Literature presents various *in vitro* or *in vivo* research, as well as case reports of HILI: *Polygonum multiflorum* (fo-ti),<sup>24</sup> *Piper methysticum* (kava),<sup>26</sup> *Chelidonium majus* (greater celandine),<sup>29</sup> *Dioscorea bulbifera* (air-potato),<sup>23</sup> *Symphytum officinale* (comfrey), *Atractylis gummifera* (kollies) and *Sassafras albidum* (sassafras).<sup>12</sup> Literature is sparse concerning African remedies though, and is often limited to case reports. In South Africa, reports of hepatotoxicity have been implicated with administration of *Senecio latifolius* (noxious ragwort)<sup>30</sup> or *Callilepis laureola* (Impila).<sup>28</sup> High concentrations of the pyrrolizidine alkaloids, senecionine and retrorsine, in *S. latifolius* result in veno-occlusive liver disease,<sup>31,32</sup> while atractyloside in *C. laureola* results in liver necrosis.<sup>28,31</sup> Regardless of known hepatotoxic effects, both these plants are still used to date for ethnomedicinal practices. Furthermore, these poisonings are oftentimes only observed after irreversible hepatocellular damage has occurred.<sup>31,32</sup> This further reiterates the importance of investigating the potential of HILI pre-clinically.

#### 1.1.4. Herb-drug interactions

Polypharmacy, although having justified benefits in various treatment regimens, also carry the risk of severe interactions. These can occur at various stages, either influencing the pharmacokinetic or pharmacodynamic profiles.<sup>33</sup> Bioactive constituents may interact with each other and shift the concentration into a subtherapeutic or toxic range (Figure 1) and thus decrease efficacy with subsequent treatment failure, or increase risk of adverse effects.<sup>33</sup> Pharmacokinetic herb-drug interactions can occur at any stage during the absorption, distribution, metabolism and excretion (ADME) phases (Figure 2).<sup>33</sup> Systemically, pharmacokinetics may be affected by a myriad of factors, such as changes in environmental pH, motility of the gastrointestinal tract, transporter activity, metabolic conversion or plasma protein concentrations.<sup>34–36</sup> Several recommendations have been made for pre-clinical drug-drug or herb-drug interaction assessment, which includes alterations to i) drug absorption<sup>13</sup>, ii) drug distribution<sup>37</sup> and iii) metabolism.<sup>38</sup> For absorption and distribution, transporter functionality (such as P-gp)<sup>36</sup> and intestinal efflux<sup>13</sup> are generally measured. Distribution of drugs may be affected by alterations in plasma protein binding,<sup>37</sup> while hepatic enzyme adjustments could affect metabolic clearance and bioactivation.<sup>38</sup>

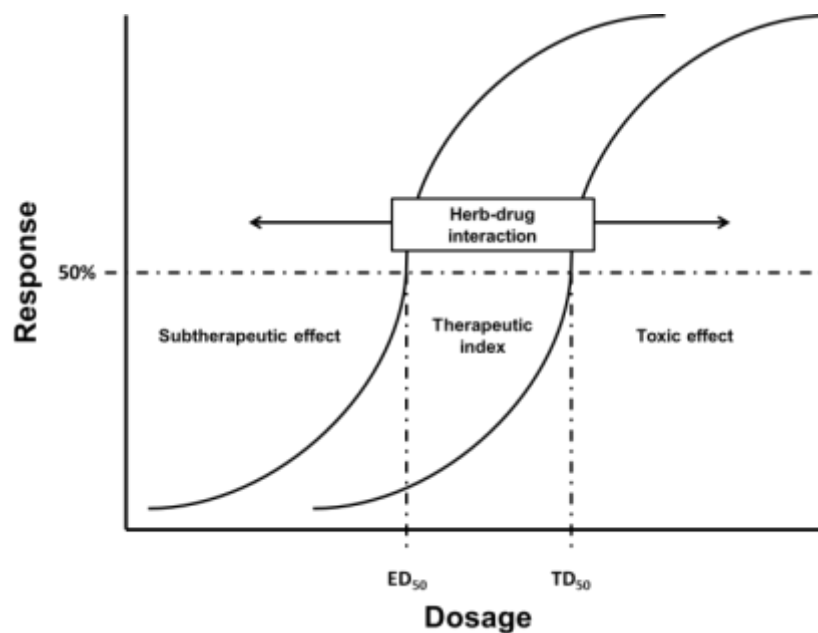


**Figure 1:** The effect that herb-drug interactions may elicit on drug efficacy and toxicity;  $ED_{50}$  = dose that results in an effect in 50% of individuals;  $TD_{50}$  = dose that results in toxicity in 50% of individuals.

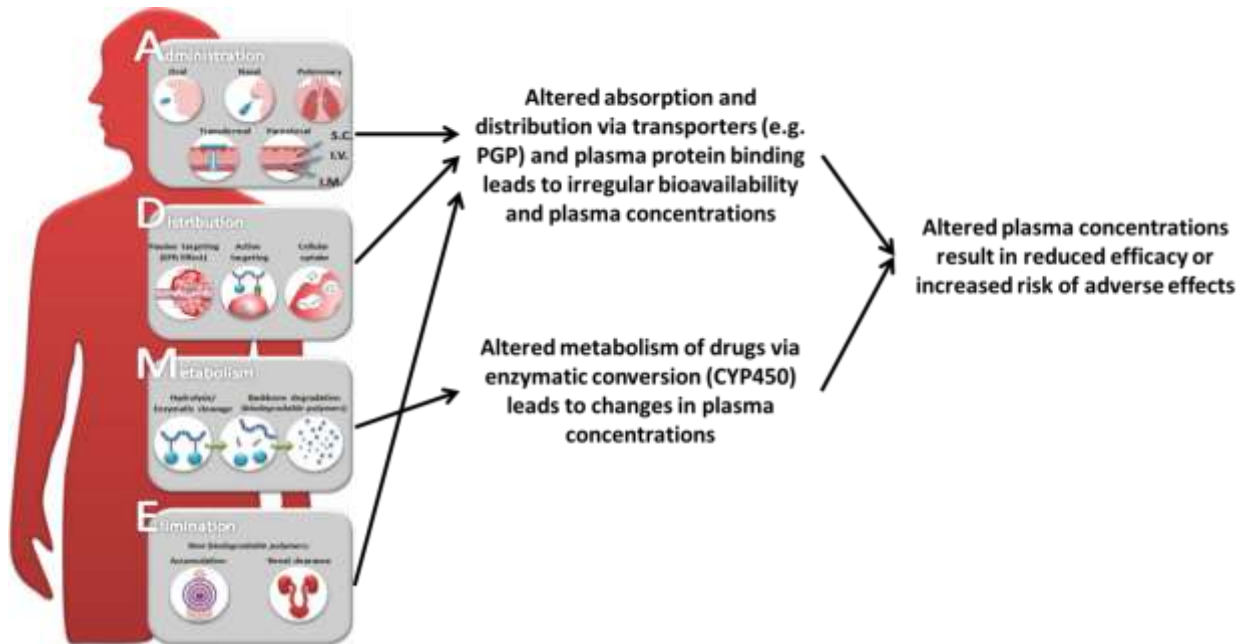


**Figure 2:** Phases of the pharmacokinetic profile where herbs are capable of inducing drug interactions (modified from Markovsky *et al.*<sup>39</sup>).

Significant clinical interactions have been widely published for various drug classes: angiotension-converting enzyme inhibitors and potassium-sparing diuretics (hyperkalaemia), verapamil and macrolide antibiotics (hypotension), digoxin and clarithromycin (digoxin toxicity), or warfarin and various drugs (increased bleeding tendencies).<sup>40</sup> Interactions are more likely to be significant when dealing with drugs displaying narrow therapeutic indices.<sup>37</sup> Although the abovementioned cases are between allopathic medications, the list of drug-herb interactions is ever-increasing: *Citrus paradisi* (grapefruit) and halofantrine (increased QT prolongation),<sup>41</sup> *Harpagophytum procumbens* (devil's claw) and anticoagulants (bleeding tendencies)<sup>42</sup> and *Hypericum perforatum* (St. John's wort) and verapamil (hypotensive treatment failure).<sup>43</sup> These studies generally focus on the more popularised herbal remedies, thus few have detailed those more commonly used in rural settings, like certain parts of Africa.<sup>14</sup>

## 1.2. Aim of the study

The aim of this study was to assess whether or not a panel of herbal remedies have the potential to display phytotoxicity through *in vitro* investigation of their i) hepatotoxic response in a model of hepatotoxicity, and ii) ability to interact with mechanisms of pharmacokinetic interactions.

## 1.3. Objectives

The main objectives of the study were to:

- 1.3.1. Determine the *in vitro* hepatotoxic potential of selected crude extracts by addressing several key hepatotoxic parameters.
- 1.3.2. Determine the *in vitro* potential of selected crude extracts to induce drug-herb interactions through measurement P-gp activity, nevirapine efflux and CYP450 activity.

## Chapter 2

### Extraction and crude phytochemical screening of herbal remedies

#### 2.1. Literature review

##### 2.1.1. Extraction of herbal remedies

Herbal remedies are used in high frequency by the populace in developing countries, especially in the rural setting. Use in developed countries is increasing as well. Traditional healers, even within the same location, compile their own pharmacopeias of medicinal plants with specific uses attributed to each part.<sup>44</sup> This ultimately makes it difficult to accurately establish a database of medicinal uses and dosages, as most differ in their methods of preparation and administration.

Typically aqueous or alcoholic liquids are used by traditional healers due to the lack of accessibility to lipophilic solvents.<sup>5</sup> Validation of ethnomedicinal claims would require that extraction procedures mimic that of traditional healers as closely as possible, such as the preparation of decoctions, infusions or teas. Although these methods are more typical in a traditional setting, industries have access to higher quality instrumentation and reagents and thus often use different methods of pharmaceutical extraction, such as alcoholic extraction.<sup>45</sup> Apart from infusion or decoction preparations, other extractions are used including vapour inhalation, enemas, douches, eye drops or poultices.<sup>44</sup>

When assessing herbal remedies for bioactivity, numerous factors need to be taken into account to ensure accurate interpretation. Although traditional healers have ascribed certain ethnomedicinal uses to different herbal remedies and their respective parts, bioactivity might not be apparent during *in vitro* assays for several different reasons: i) incorrect collection, storage or preparation methods, ii) combinations may be required, iii) their use may be for downstream symptoms of the disease, iv) bioactivation of phytochemicals may be required, or v) geographical and seasonal variation of the plant leading to fluctuations in phytochemical levels.<sup>46</sup> Understandably, this would also reflect in the phytotoxicity profile of the herbal remedies.

The National Cancer Institute (NCI) states that plant screening protocols for crude extracts define an upper limit for activity at 30 µg/mL, and although this is often taken with regards to cytotoxicity and anticancer activity,<sup>47</sup> this can be extrapolated to other areas as well. It is important to note that this is merely an empirical level to measure a cut-off of activity. Thus with respect to all assays performed, the potential to inflict bioactivity was set at ~30 µg/mL for all assays.

### **2.1.2. Phytochemical matrices and allelochemicals**

Plants synthesize a diverse range of secondary metabolites ( $\geq 100\,000$ ), which are generally stored at high concentrations (1 – 3% dry weight) in different cellular systems. These vary from nitrogen-containing or deficient molecules, creating a complex array of phytochemicals that can exist in different species and genera of plants. Furthermore, within the same species the phytochemical matrix may appear in different ratios depending on geographical variation.<sup>48,49</sup> As plants do not possess the typical panel of anti-predatory defence mechanisms that animals do, these secondary metabolites enable them to survive against harsh environmental stressors and predation from insects, herbivores and others.<sup>48,49</sup>

Allelochemicals are defined as chemicals, such as secondary metabolites, that are able to exert bioactivity in other organisms than the synthesising host. Subsequently these may elicit a positive or negative allelochemical effect by alleviating disease states or inducing toxicity, respectively.<sup>48</sup> It has long been known that some animals frequently employ plants to help protect them or treat illnesses, but can easily result in toxicity as well.<sup>48</sup> Extracts containing secondary metabolites can be used in various areas of biotechnology such as flavourants, medicines and perfumes (Figure 3).<sup>48</sup>

### **2.1.3. Phytochemical classes**

As stated earlier there are thousands of secondary metabolites. These are generally grouped based on their biosynthetic origin: terpenoids, alkaloids and phenylpropanoids (and associated phenolics).<sup>50,51</sup>



**Figure 3:** Uses of extracts (adapated from Wink<sup>48</sup>).

### 2.1.3.1. Alkaloids

Although too simplistic a definition to encompass the vastness of its groups, alkaloids are nitrogen-containing components that generally present with pharmacological activity, and are biosynthesised from amino acid sources.<sup>50,51</sup> Alkaloids perform an ecochemical function in plants, and as such prevent predation.<sup>51</sup> This can be seen in the potent physiological alterations that they induce in organisms.<sup>50</sup>

Alkaloids, such as the benzyloquinoline- (morphine) and tropane-types (atropine), are routinely used in medicine, though it is well-known that they all elicit severe toxicity if misused. Notable poisons throughout the ages have been identified as alkaloidal in nature.<sup>51</sup> Pyrrolizidine alkaloids, often found in Asteraceae family are highly toxic to mammals, especially when biotransformed by the CYP450 enzyme system<sup>50</sup> to pyrrolic esters.<sup>51</sup> Several are well-known hepatotoxins.<sup>51</sup> Steroidal glycoalkaloids, such as those present in the Solanaceae family, have been linked to several adverse effects and poisonings, such as haemolysis and cytolysis, cardiomyopathy and neuropathy.<sup>51</sup> Steroidal glycoalkaloids may cause necrotic cell death with inflammatory responses.<sup>51</sup>  $\alpha$ -Solanine, for example, is thought to be involved in the teratogenicity induced after ingestion of sprouting potatoes.<sup>50</sup>

### 2.1.3.2. Phenolic acids and flavonoids

Phenolic compounds are aromatic metabolites that contain, or previously contained, acidic hydrophilic groups attached to the aromatic arene.<sup>50</sup> Synthesis occurs through the shikimic acid or malonate/acetate pathway.<sup>50</sup> These compounds are often conjugated to sugars and other chemical moieties.<sup>51</sup> The group is typically divided into flavonoid and non-flavonoid entities.<sup>51</sup> Flavonoids are diverse polyphenolic compounds that include anthocyanins, proanthocyanidins/condensed tannins and isoflavonoids. Phenolic compounds typically act as feeding deterrents, defensive agents, structural support and signalling molecules.<sup>50</sup>

Polyphenolic compounds are well-known antioxidant compounds.<sup>52</sup> These are molecules that assist in the reduction of oxidative sources or free radicals that may deteriorate physiological systems.<sup>52,53</sup> It is important to note that free radicals, in homeostatic levels, function as important signalling molecules and do not always induce detriments, unless at high levels.<sup>54</sup> Antioxidants have important functions to ensure that free radicals do not overburden the system, and as such induce a state known as oxidative stress. During this state, endogenous antioxidants may not be able to attenuate the production of pro-oxidants, and thus attack on biological systems, such as proteins, lipids and nucleic acids may occur.<sup>52,53</sup> Thus the need for exogenous antioxidant supplementation may be required.<sup>53</sup> Under specific conditions, polyphenols may shift to pro-oxidant activities and induce production of free radicals.<sup>52</sup>

Coumarins are phenolic compounds<sup>50,55</sup> that are widespread in the plant kingdom.<sup>55</sup> It is thought to act as defensive molecules against predation and microbial contamination.<sup>50</sup> Many coumarins and/or their metabolites may result in toxicities such as bleeding (dicoumarol) or dermatitis (psoralen),<sup>50,55</sup> which are considered undesirable.<sup>51</sup>

### 2.1.3.3. Terpenoids

Terpenoids, also known as terpenes or isoprenoids, form due to repetitive assimilation of branched C<sub>5</sub>-units (referred to as isoprene units), of which the primary precursors are isopentenyl diphosphate and dimethylallyl pyrophosphate.<sup>50</sup> Terpenoid moieties are commonly found in other secondary metabolite classes.<sup>50,51</sup> Terpenoids are

classified according to the number of isoprene units: monoterpenes (C<sub>10</sub>), sesquiterpenes (C<sub>15</sub>), diterpenes (C<sub>20</sub>), triterpenes (C<sub>30</sub>), tetraterpenes (C<sub>40</sub>) and polyterpenes (C<sub>>40</sub>).<sup>50,51</sup>

Monoterpenes are well-known volatile constituents of essential oils, and are often used in perfumes and flavourants.<sup>50</sup> Sesquiterpenes are also found in essential oils, and often act as phytoalexins.<sup>50</sup> Diterpenes act as plant hormones, resins and phytoalexins, though are well-known pharmacologically-active compounds as well, such as taxol (anticancer) and forskolin (anti-glaucoma).<sup>50</sup> Ubiquinone is a polyterpene that acts as an electron carrier and is important in energy production.<sup>50,51</sup>

Saponins are oxygenated triterpenoid glycosidic structures that have detergent-like properties<sup>50</sup> and cause foaming in aqueous solutions.<sup>51</sup> These compounds present with toxicity towards various organisms, including vertebrates,<sup>50</sup> and may result in disruption of membranes with subsequent cytolysis.<sup>51</sup> This is due to its surface-active properties related to its polar (sugar) and non-polar (steroid or triterpenoid) moieties that allow for binding to phospholipids, membrane proteins and cholesterol.<sup>56</sup>

#### **2.1.4. Panel of herbal remedies chosen for this study**

The selection of plants for this study was done based on their popularity and ethnomedicinal uses (Table 1, Figure 4). Furthermore, most of their uses fall within the scope of symptoms that could present during the wasting phase of HIV/AIDS, including wounds, microbial infections and other factors that would reduce feelings of well-being.

#### **2.1.5. Aim of extraction and phytochemical screening**

The aim of the extract and phytochemical screening was to prepare crude extracts of seventeen herbal remedies, as well as to determine some phytochemical parameters.

The objectives were to:

- Identify phytochemical classes in crude extracts.
- Determine flavonoid, phenolic and saponin content of crude extracts.
- Determine of antioxidant activity of crude extracts.

**Table 1:** Plants investigated in this study, including ethnomedicinal use and botanical information.

Family	Plant	Vernacular	Part	Voucher number	Ethnomedicinal use
Amaryllidaceae	<i>Boophane disticha</i> (L.f.) Herb.	Poison bulb (E) Ibhade (Z)	Bulbs	SANBI gift	Wounds, rheumatism and pain <sup>5</sup>
	<i>Crinum bulbispermum</i> (Burm.f.) Milne-Redhead & Schweickherdt	Orange river lily (E) Umnduze (Z)	Roots	SANBI gift	Aching joints, wounds, kidney and bladder infections <sup>5</sup>
	<i>Scadoxus puniceus</i> (L.) I.Friis & I.Nordal	Snake lily (E) Umgola (Z)	Bulbs	SANBI gift	Coughs, gastrointestinal problems <sup>57</sup>
Anacardiaceae	<i>Rhus lancea</i> L.	Karee (E) Hlokoshiyne (Z)	Leaves	SANBI gift	Papules, pustules, coughs <sup>44</sup>
Apocynaceae	<i>Acokanthera oppositifolia</i> (Lam.) Codd	Bushman's poison (E) inHlungunyembe (Z)	Root-bark	LT0019	Pain, snake bites, anthrax and parasitic infections <sup>58</sup>
	<i>Rauvolfia caffra</i> Sond.	Quinine tree (E) umKhadluvungu (Z)	Bark	LT007	Epilepsy, eye sickness <sup>44</sup>
	<i>Tabernaemontana elegans</i> Stapf	Toad tree (E) umKhadlu (Z)	Roots	NH1920	Tuberculosis, wounds, venereal diseases <sup>44</sup>
Asteraceae	<i>Callilepis laureola</i> DC.	Ox-eye daisy (E) Impila (Z)	Tubers	Mai Mai market	Emetic, vermifuge, cough remedy <sup>31</sup>
	<i>Senecio latifolius</i> DC.	Noxious ragwort (E) Iyeza lasekhaya (X)	Stems	OVC	Wounds, burns, abortifacient <sup>32</sup>
Combretaceae	<i>Terminalia sericea</i> (Roxb.) Wight & Arn.	Silver cluster-leaf (E) amaNgwe-amhlope (Z)	Roots and leaves	NH1878	Diarrhoea, gonorrhoea <sup>44</sup>
Fabaceae	<i>Burkea africana</i> Hook	Wild syringa (E)	Bark	LT0015	Heavy menstruation, abdominal pain, inflammation <sup>59</sup>
	<i>Mundulea sericea</i> (Willd.) A. Chev.	Cork bush (E) umSindandlovu (Z)	Roots	LT0025	Pregnancy tonic <sup>60</sup>
Lamiaceae	<i>Leonotis leonurus</i> (L.) R.Br.	Wild dagga (E) Imvovo (X)	Leaves	SANBI gift	Tuberculosis, bronchitis, flu <sup>61</sup>
Moringaceae	<i>Moringa oleifera</i> Lam.	Horseradish tree (E)	Leaves	University of Pretoria	Diabetes, inflammation, microbial infections, wound healing <sup>62</sup>
Piperaceae	<i>Piper capense</i> L.f	Wild pepper (E)	Root-bark	LT0016	Anthelmintic <sup>63</sup>
Rhamnaceae	<i>Ziziphus mucronata</i> Willd.	Buffalo thorn (E) umPhafa (X)	Roots	NH1809	Pain, coughs, dysentery, lumbago <sup>64</sup>
Solanaceae	<i>Solanum aculeastrum</i> Dunal	Soda nightshade (E) Itunga (X)	Fruits	LT0017	Breast cancer, jigger wounds and gonorrhoea <sup>65</sup>

SANBI – South African National Botanical Institute, OVC – Onderstepoort Veterinary Campus, Pretoria; E – English, X – Xhosa, Z - Zulu

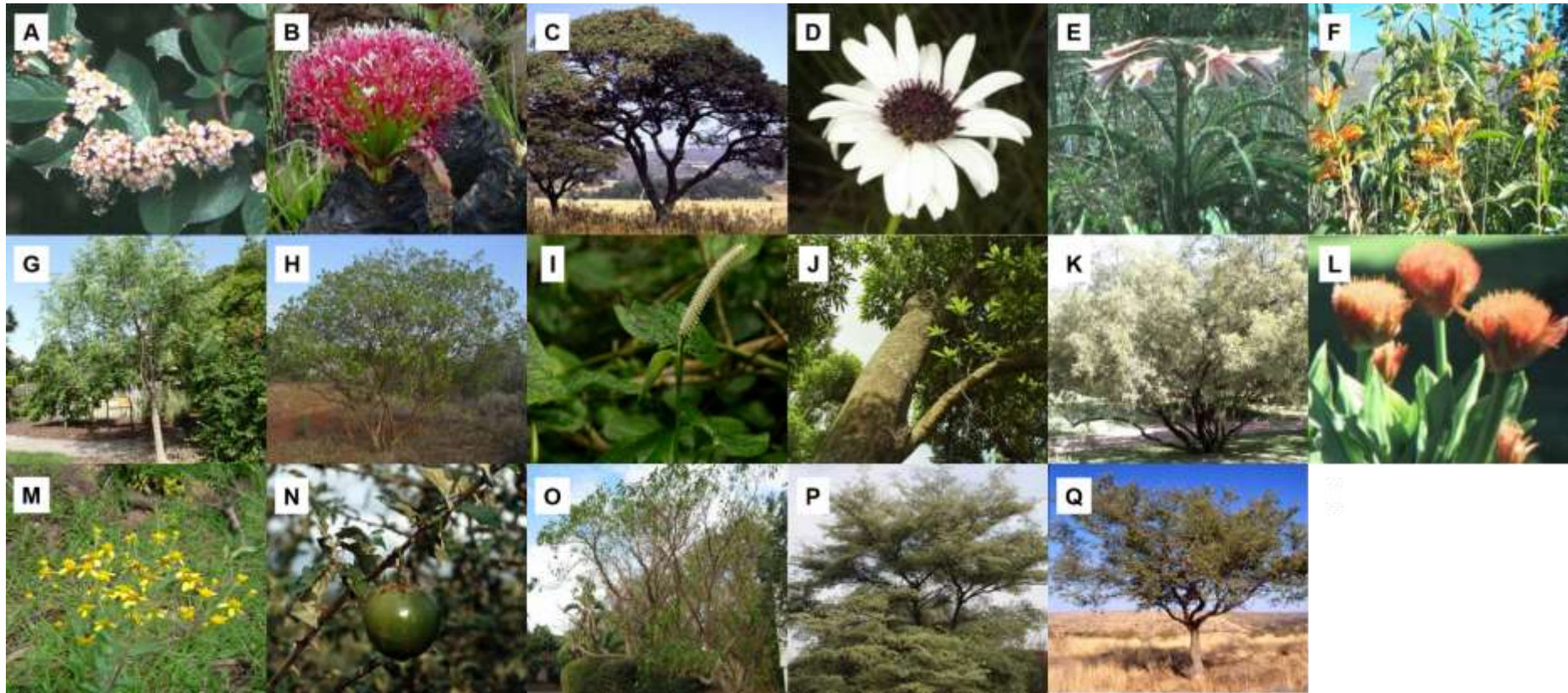


**Figure 4:** Plants investigated during the study. A) *A. oppositifolia*,<sup>66</sup> B) *B. disticha*,<sup>67</sup> C) *B. africana*,<sup>68</sup> D) *C. laureola*,<sup>69</sup> E) *C. bulbispermum*,<sup>70</sup> F) *L. leonurus*,<sup>71</sup> G) *M. oleifera*,<sup>72</sup> H) *M. sericea*,<sup>73</sup> I) *P. capense*,<sup>74</sup> J) *R. caffra*,<sup>75</sup> K) *R. lancea*,<sup>76</sup> L) *S. puniceus*,<sup>77</sup> M) *S. latifolius*,<sup>78</sup> N) *S. aculeastrum*,<sup>79</sup> O) *T. elegans*,<sup>80</sup> P) *T. sericea*<sup>81</sup> and Q) *Z. mucronata*<sup>82</sup>

## **2.2. Materials and Methods**

Ethical approval to carry out this study was obtained from the University of Pretoria Research Ethics Committee (276/2013, Appendix II). A detailed list of all reagents used in the study, as well as the preparation thereof, is provided (Appendix III).

### **2.2.1. Preparation of crude extracts**

#### **2.2.1.1. Collection and preparation of plant material**

Plant material (parts provided in Table 1) was either collected in the wild by Mr Lawrence Tshikudo (LT) or Dr Norbert Hahn (NH), provided by the South African National Botanical Institute (SANBI) or provided by Prof ES du Toit from the Department of Plant Production and Soil Science (University of Pretoria). Plant material was cleaned, air-dried at ambient temperature, finely ground (YellowLine Grinder, Merck) and stored in air-tight, amber bottles. Voucher specimens are stored at the Department of Toxicology (Onderstepoort Veterinary Institute, Pretoria, South Africa) and Soutpansbergensis Herbarium (Makado) for those noted with LT and NH, respectively.

#### **2.2.1.2. Crude extraction of plant material**

##### **2.2.1.2.1. Hot water extraction**

Hot water extracts were prepared by soaking 10 g plant material in 100 mL boiling distilled water. Extracts were stirred for 15 min to simulate the brewing of tea, and allowed to cool to room temperature.

##### **2.2.1.2.2. Methanol extraction**

Methanol extracts were prepared by sonicating (Branson 52, Branson Cleaning Equipment Co.) 10 g plant material in 100 mL absolute methanol for 30 min, after which it was agitated for 2 h and incubated for 16 h at 4°C. Methanol was decanted and replenished, the process repeated thrice from agitation and the supernatants pooled.

### 2.2.1.2.3. Extract concentration

All extracts were centrifuged (1000g, 5 min) and filtered (0.22 µm). Extracts were concentrated through lyophilization (Freezone® Freeze Dry System, Labconco) or rotary-evaporation (Büchi Rotovapor R-200, Büchi) for hot water and methanol extracts, respectively. Methanol extracts were further reconstituted in distilled water completely and lyophilized to yield a dry mass for storage. Extraction yields were determined gravimetrically. Aliquots of 25 mg/mL (dry extract weight/volume) were prepared in dimethyl sulfoxide (DMSO) or phosphate-buffered saline (PBS) for methanol and hot water extracts, respectively. The latter were filter-sterilised (0.22 µm) and aliquots stored at -80°C.

## 2.2.2. Phytochemical screening

### 2.2.2.1. Thin layer chromatography

Crude phytochemical classes were identified using thin-layer chromatography (TLC) with various mobile phases and spray reagents (Table 2). TLC silica gel F254 aluminium-backed plates were loaded with 10 µg crude extract (diluted with methanol) or respective positive controls, allowed to develop in saturated TLC chambers and visualised under short-wave (254 nm) and long-wave (366 nm) ultraviolet light before and after spraying with respective spray reagents.

**Table 2:** TLC parameters used for identification of crude extracts, as obtained from Bolliger *et al.*<sup>83</sup>

Phytochemical class	Mobile phase	Spray reagent	Positive control
<b>Alkaloids</b>	Chloroform:Methanol:Formic acid (25:70:5)	Dragendorff's reagent	Galanthamine
<b>Anthrones</b>	Distilled water:Methanol (1:20)	5% methanolic potassium hydroxide	-
<b>Athraquinones</b>			-
<b>Coumarins</b>			Dicoumarol
<b>Flavonoids</b>	Chloroform:Acetone:Formic acid (60:60:10)	1% Aluminium trichloride	Rutin
<b>Glycosides</b>	Chloroform:Methanol:Formic acid (188:12:1)	20% antimony trichloride	Digoxigenin
<b>Phenolic acids</b>	Chloroform:Acetone:Formic acid (60:60:10)	Folin-Ciocalteu reagent	Gallic acid
<b>Saponins</b>	Chloroform:Methanol:Distilled water (80:12:8)	1% vanillin (in sulphuric acid:ethanol 4:1)	Diosgenin
<b>Tannins</b>	Chloroform:Acetone:Formic acid (60:60:10)	1% methanolic vanillin	Catechin
<b>Terpenoids</b>	Chloroform:Methanol:Formic acid (188:12:1)	1% vanillin (in sulphuric acid:ethanol 4:1)	Oleonolic acid

#### 2.2.2.2. Total flavonoid content

The aluminium trichloride assay was used to determine the total flavonoid content of the crude extracts as described by Dewanto *et al.*<sup>84</sup> Rutin hydrochloride was used to prepare a standard curve of 0 to 100 µg/mL in reaction. Into a 96-well plate was pipetted: 20 µL rutin (0, 0.1, 0.2, 0.3, 0.4, 0.5, 0.6, 0.7, 0.8, 0.9 and 1 mg/mL) or crude extracts (1 mg/mL), followed by 60 µL sodium nitrate solution (1.25% w/v), 60 µL aluminum trichloride solution (0.4% w/v) and 60 µL sodium hydroxide solution (1 M). Absorbance was measured at 765 nm (ELx800 Universal Microplate Reader, Bio-Tek Instruments, Inc.) and results expressed as rutin equivalents (RE mg/g extract) as determined by the following equation:

$$RE = \frac{c \times v}{m}$$

where, c = concentration obtained from standard curve (in mg/mL); v = volume of extract in assay (in mL); and m = mass of extract in assay (in g).

#### 2.2.2.3. Total phenolic content

The Folin-Ciocalteu assay was used to determine the total phenolic content of the crude extracts as described by Slinkard and Singleton.<sup>85</sup> Gallic acid was used to prepare a standard curve of 0 to 100 µg/mL in reaction. Into a 96-well plate was pipetted: 20 µL gallic acid (0, 0.1, 0.2, 0.3, 0.4, 0.5, 0.6, 0.7, 0.8, 0.9 and 1 mg/mL) or crude extracts (1 mg/mL), 90 µL Folin-Ciocalteu reagent (10% v/v) and after 8 min incubation 90 µL sodium carbonate solution (7% w/v). Plates were incubated for 1 h in the dark and the absorbance measured at 765 nm (ELx800 Universal Microplate Reader, Bio-Tek Instruments, Inc.). Results are expressed as gallic acid equivalents (GAE mg/g extract) as determined by the equation in Section 2.1.2.2.

#### 2.2.2.4. Total saponin content

The vanillin-sulphuric assay was used to determine the total saponin content of the crude extracts as described by Makkar *et al.*<sup>56</sup> Diosgenin was used to prepare a standard curve of 0 to 100 µg/mL in reaction. Into a 96-well plate was pipetted: 20 µL diosgenin (0, 0.1, 0.2, 0.3, 0.4, 0.5, 0.6, 0.7, 0.8, 0.9 and 1 mg/mL) or crude extracts (1 mg/mL), followed by 20 µL ethanolic vanillin (250 mg/mL) and 160 µL aqueous sulphuric acid (75%). Plates were incubated for 10 min at 50°C, after which it was cooled to room temperature in the dark. Absorbance was measured at 570 nm and

results expressed as diosgenin equivalents (DE mg/g extract) as determined by the equation in Section 2.1.2.2.

#### **2.2.2.5. 2,2'-azinobis-(3-ethyl benzothiazoline 6-sulfonic acid) radical scavenging assay**

The ABTS<sup>•+</sup> scavenging assay was used to determine the antioxidant activity of the crude extracts.<sup>86</sup> ABTS<sup>•+</sup> (7.46 mM) was prepared in distilled water and oxidized using 2.5 mM potassium peroxodisulfate at 4°C for 16 h. The oxidized solution was diluted with distilled water to an absorbance of  $0.70 \pm 0.02$  at 734 nm (Lambda UV/VIS Spectrophotometer, Perkin Elmer). Trolox was used to prepare a standard curve of 0 to 10 µg/mL in reaction. Into a 96-well plate was pipetted: 20 µL Trolox (dilutions of 0.1 mg/mL), crude extracts (half-log dilutions of 1 mg/mL) or various known antioxidants (half-log dilutions of 1 mg/mL) followed by 180 µL ABTS<sup>•+</sup>. Absorbance was measured at 405 nm after 15 min incubation in the dark. Results are expressed as the half-maximal inhibitory concentration (IC<sub>50</sub>) and Trolox equivalents (TE) as determined by the following equation:

$$TE = \frac{\text{slope}(T)}{\text{slope}(S)}$$

where, slope(T) = slope of Trolox standard curve; slope(S) = slope of sample curve.

#### **2.2.3. Statistics**

All experiments were performed using at least three technical and biological replicates. Results were compiled using Microsoft Excel 2010 (Microsoft) and analysed statistically using GraphPad Prism 5.0 (GraphPad Software). All results are expressed as the mean  $\pm$  the standard error of the mean (SEM). The IC<sub>50</sub> was determined through non-linear regression (normalized variable slope). TE was calculated through linear regression and expressed as the ratio of the sample slope to the Trolox slope. Phenolic, flavonoid and saponin content was interpolated from a standard curve.

## 2.3. Results

### 2.3.1. Extraction yields

The majority of extracts displayed a higher extraction yield with methanol as solvent (Table 3), except for the extracts of *B. disticha*, *C. bulbispermum*, *L. leonurus*, *R. lancea* and *T. elegans*. High extraction yields were noted for the methanol extract of *B. africana*, *M. sericea* and *S. aculeastrum*, as well as both extracts of *C. laureola* and *M. oleifera*.

**Table 3:** Extraction yields of crude hot water and methanol extracts of plants investigated.

Plant	Hot water extracts (%)	Methanol extracts (%)
<i>A. oppositifolia</i>	6.1	8.1
<i>B. disticha</i>	15.5	9.5
<i>B. africana</i>	15.9	32.4
<i>C. laureola</i>	23.0	26.6
<i>C. bulbispermum</i>	6.7	6.4
<i>L. leonurus</i>	13.0	12.0
<i>M. oleifera</i>	22.6	26.1
<i>M. sericea</i>	4.8	24.5
<i>P. capense</i>	4.8	8.7
<i>R. caffra</i>	5.9	6.7
<i>R. lancea</i>	7.5	5.6
<i>S. puniceus</i>	1.5	5.5
<i>S. latifolius</i>	9.0	21.8
<i>S. aculeastrum</i>	13.8	19.5
<i>T. elegans</i>	10.9	7.4
<i>T. sericea</i>	7.6	13.3
<i>Z. mucronata</i>	4.8	6.8

### 2.3.2. Phytochemical screening

Qualitative TLC-based visualisation was employed to identify phytochemical classes in crude extracts. Alkaloids, anthrones, flavonoids, glycosides, phenolic acids and saponins were present in most of the extracts, while anthroquinones, coumarins, tannins and terpenoids were absent from the majority of extracts (Table 4).

Quantitative analyses were performed to determine the relative abundance of flavonoids, phenolic acids and saponins in crude extracts (Table 5, Figures 5 - 7). It should be noted that these contents are expressed relative to that of a standard, and thus is a representative value and not a true quantitation. It is therefore possible for

extracts to contain greater phytochemical content where cumulative potency exceeds that of the standard. High variability was apparent for the total saponin content assay. In the majority of cases the methanol extract possessed a greater flavonoid, phenolic acid and saponin content than the hot water extract, but exceptions did exist for the i) flavonoid content of *L. leonurus*, ii) phenolic content of *A. oppositifolia* and *L. leonurus*, and iii) saponin content of *B. disticha*, *C. laureola*, *P. capense* and *R. lancea*. Although all extracts displayed a measurable phenolic content at 100 µg/mL, both extracts of *B. disticha*, *C. laureola*, *C. bulpispermum*, *P. capense*, *S. puniceus* and *T. elegans*, as well as the hot water extract of *M. sericea* and *R. lancea* did not possess a high enough flavonoid content to be determined. This was also true for the saponin content of both extracts of *S. puniceus*, as well as the hot water extract of *M. oleifera* and *T. sericea*. Overall, *B. africana*, *T. sericea* and *Z. mucronata* possessed the highest quantities of the three phytochemicals tested. The greatest flavonoid content was found in *B. africana*, followed by *Z. mucronata* and *T. sericea*. Phenolic content was highest in *T. sericea*, followed by *B. africana* and *Z. mucronata*. *Z. mucronata* possessed the highest saponin content, followed by *B. africana* and *T. sericea*. Interestingly enough, the hot water extract of *T. sericea* did not possess any determinable saponin content.

### 2.3.3. Antioxidant activity

The antioxidant activity of the crude extracts was determined as a measure of their ABTS<sup>•+</sup> scavenging abilities. Both the IC<sub>50</sub> and TE of the crude extracts were determined, as well as a panel of known antioxidant standards for comparison (Table 6, Figure 8). All comparisons were made with regards to the slope of Trolox, which was taken as the comparative standard – thus TE<1 is weaker than Trolox, while a value >1 displays higher antioxidant activity. In all cases, except for *A. oppositifolia*, *B. disticha* and *L. leonurus*, the methanol extract displayed higher antioxidant activity than the hot water extract.

**Table 4:** Phytochemical classes detected in crude extracts using TLC screening.

Plant	Extract	Alkaloids	Anthrones	Anthro-quinones	Coumarins	Flavonoids	Glycosides	Phenolic acids	Saponins	Tannins	Terpenoids
<i>A. oppositifolia</i>	Hot water	X	X			X	X	X	X		
	Methanol	X	X			X	X	X	X		
<i>B. disticha</i>	Hot water		X					X	X		
	Methanol	X	X		X		X	X			X
<i>B. africana</i>	Hot water	X	X			X	X	X	X	X	
	Methanol	X	X			X	X	X	X	X	
<i>C. laureola</i>	Hot water	X					X	X	X		
	Methanol	X					X	X	X		
<i>C. bulbispermum</i>	Hot water							X	X		
	Methanol	X	X		X		X	X	X		X
<i>L. leonurus</i>	Hot water					X		X	X	X	
	Methanol	X	X	X		X	X	X	X	X	X
<i>M. oleifera</i>	Hot water	X	X			X		X			
	Methanol	X		X		X	X	X	X		X
<i>M. sericea</i>	Hot water						X	X	X		
	Methanol	X			X	X	X	X	X		
<i>P. capense</i>	Hot water						X	X	X		
	Methanol	X					X	X			
<i>R. caffra</i>	Hot water	X	X		X	X	X	X	X		X
	Methanol	X	X		X	X	X	X	X		X
<i>R. lancea</i>	Hot water	X					X	X	X	X	
	Methanol	X		X		X	X	X	X	X	
<i>S. puniceus</i>	Hot water		X					X		X	
	Methanol	X	X				X	X			
<i>S. latifolius</i>	Hot water	X	X			X	X	X	X		
	Methanol	X				X	X	X	X		
<i>S. aculeastrum</i>	Hot water	X	X			X	X	X	X		X
	Methanol	X	X			X	X	X	X		X
<i>T. elegans</i>	Hot water	X			X		X	X	X		
	Methanol	X			X		X	X	X	X	X
<i>T. sericea</i>	Hot water	X				X	X	X		X	
	Methanol					X	X	X	X	X	
<i>Z. mucronata</i>	Hot water	X				X	X	X	X	X	
	Methanol	X			X	X	X	X	X	X	

**Table 5:** Quantitative analyses (n = 9) of flavonoids, phenolic acids and saponins in crude extracts.

Plant	Extract	Flavonoids (RE mg/g extract)	Phenolic acids (GAE mg/g extract)	Saponins (DE mg/g extract)
<i>A. oppositifolia</i>	Hot water	130.32 ± 7.84	46.27 ± 1.63	21.09 ± 31.76
	Methanol	167.34 ± 8.66	40.48 ± 0.99	167.81 ± 14.2
<i>B. disticha</i>	Hot water	Negligible	14.99 ± 0.19	41.58 ± 136.87
	Methanol	Negligible	15.56 ± 1.18	0.61 ± 67.04
<i>B. africana</i>	Hot water	805.11 ± 12.14	481.30 ± 13.20	2704.42 ± 378.63
	Methanol	1350.01 ± 15.76	624.33 ± 8.30	4877.51 ± 616.21
<i>C. laureola</i>	Hot water	Negligible	13.55 ± 0.42	69.82 ± 67.94
	Methanol	Negligible	12.61 ± 0.27	37.70 ± 32.03
<i>C. bulbispermum</i>	Hot water	Negligible	16.59 ± 0.77	11.13 ± 139.29
	Methanol	Negligible	16.36 ± 0.73	33.27 ± 94.86
<i>L. leonurus</i>	Hot water	70.13 ± 4.11	33.98 ± 1.34	107.46 ± 32.17
	Methanol	50.75 ± 3.38	30.16 ± 0.50	291.83 ± 60.01
<i>M. oleifera</i>	Hot water	12.35 ± 3.37	25.43 ± 0.42	Negligible
	Methanol	36.57 ± 7.29	27.00 ± 1.44	98.61 ± 26.81
<i>M. sericea</i>	Hot water	Negligible	18.34 ± 0.71	282.97 ± 131.09
	Methanol	11.31 ± 3.71	29.41 ± 1.48	756.90 ± 63.13
<i>P. capense</i>	Hot water	Negligible	8.37 ± 0.29	22.76 ± 82.60
	Methanol	Negligible	12.02 ± 0.45	0.06 ± 124.61
<i>R. caffra</i>	Hot water	61.27 ± 5.64	39.25 ± 0.45	499.45 ± 131.28
	Methanol	94.34 ± 5.84	49.10 ± 1.13	769.08 ± 107.31
<i>R. lancea</i>	Hot water	Negligible	24.48 ± 1.38	114.66 ± 45.83
	Methanol	5.78 ± 3.34	34.54 ± 0.44	104.14 ± 65.66
<i>S. puniceus</i>	Hot water	Negligible	11.34 ± 0.76	Negligible
	Methanol	Negligible	22.03 ± 1.34	Negligible
<i>S. latifolius</i>	Hot water	4.74 ± 2.31	19.33 ± 0.29	2.27 ± 33.34
	Methanol	29.65 ± 8.38	23.80 ± 1.13	163.38 ± 18.56
<i>S. aculeastrum</i>	Hot water	5.08 ± 3.38	25.64 ± 0.59	58.19 ± 59.60
	Methanol	233.42 ± 8.29	48.58 ± 1.44	277.99 ± 119.24
<i>T. elegans</i>	Hot water	Negligible	17.11 ± 3.15	91.41 ± 131.29
	Methanol	Negligible	23.42 ± 3.55	177.22 ± 150.92
<i>T. sericea</i>	Hot water	363.55 ± 5.09	837.94 ± 25.66	Negligible
	Methanol	799.47 ± 56.7	2840.44 ± 39.99	1467.69 ± 257.32
<i>Z. mucronata</i>	Hot water	306.92 ± 11.13	239.78 ± 12.32	2296.10 ± 246.28
	Methanol	994.53 ± 37.24	438.09 ± 16.38	4934.60 ± 404.65

Negligible levels refer to values that fall outside of the calibration curve, and could thus not be quantified.

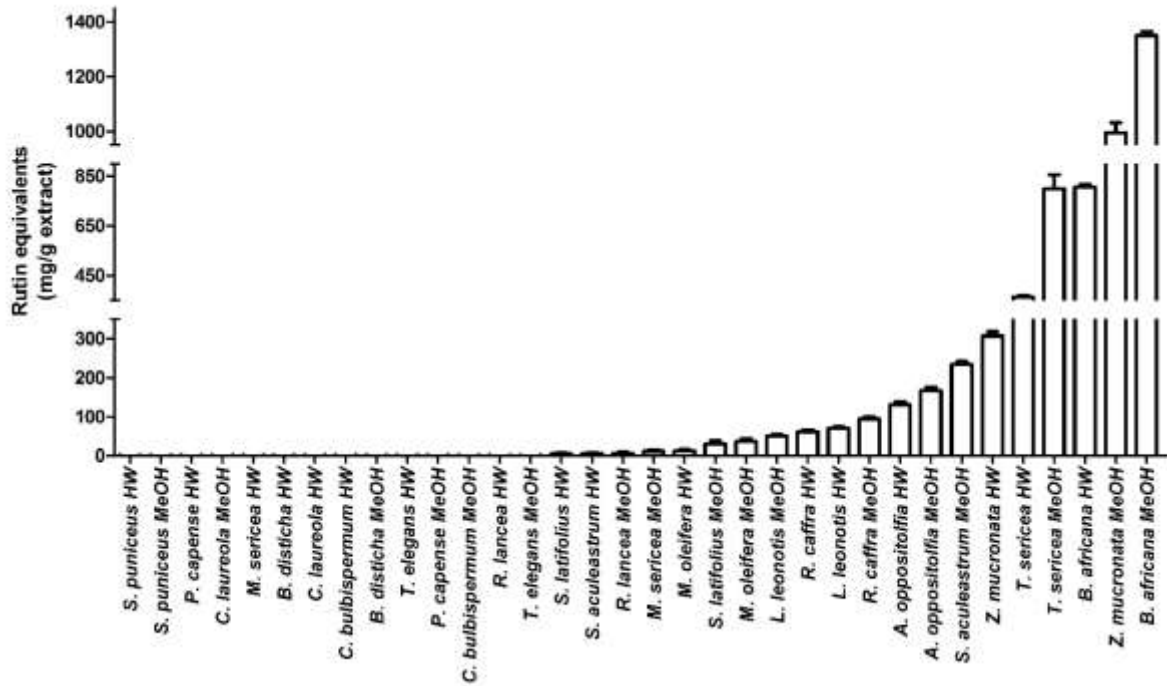


**Figure 5:** Total flavonoid content of crude extracts, arranged by increasing relative abundance. HW – hot water extract; MeOH – methanol extract.

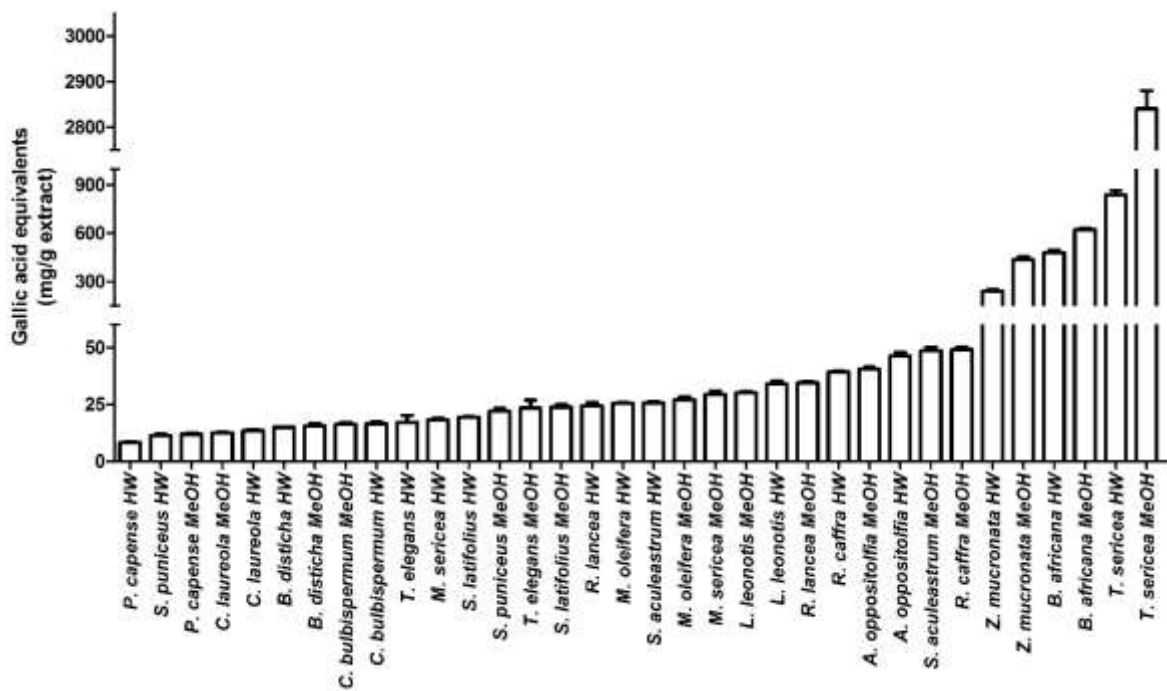


**Figure 6:** Total phenolic content of crude extracts, arranged by increasing relative abundance. HW – hot water extract; MeOH – methanol extract.

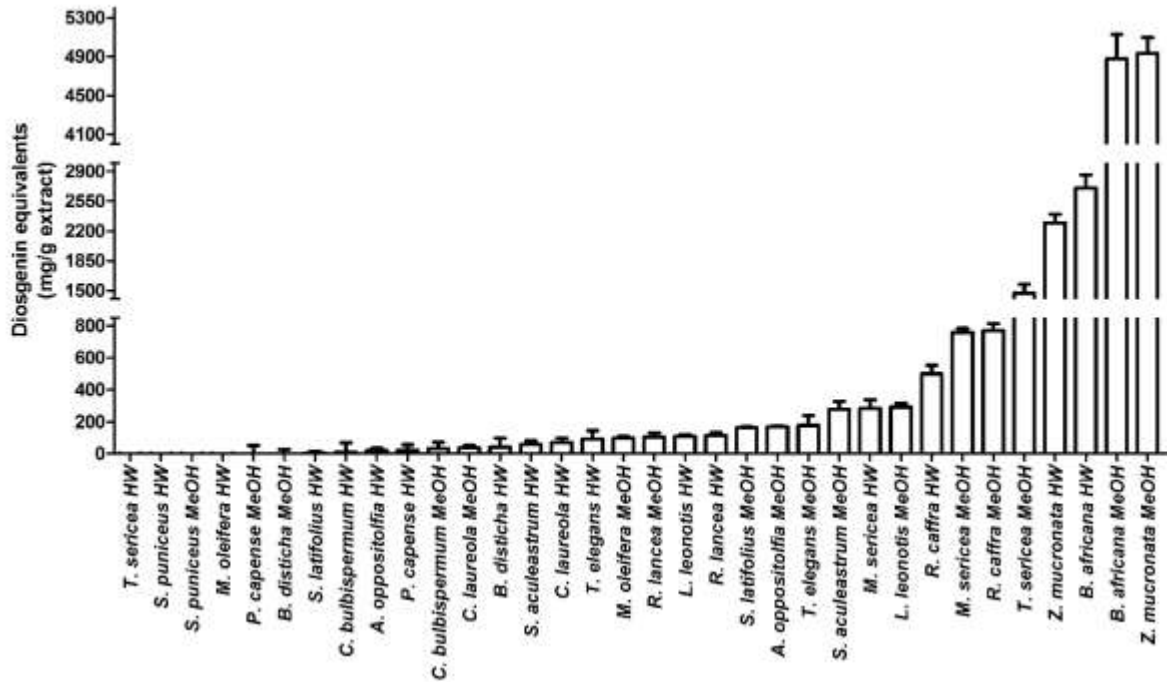


**Figure 7:** Total saponin content of crude extracts, arranged by increasing relative abundance. HW – hot water extract; MeOH – methanol extract.

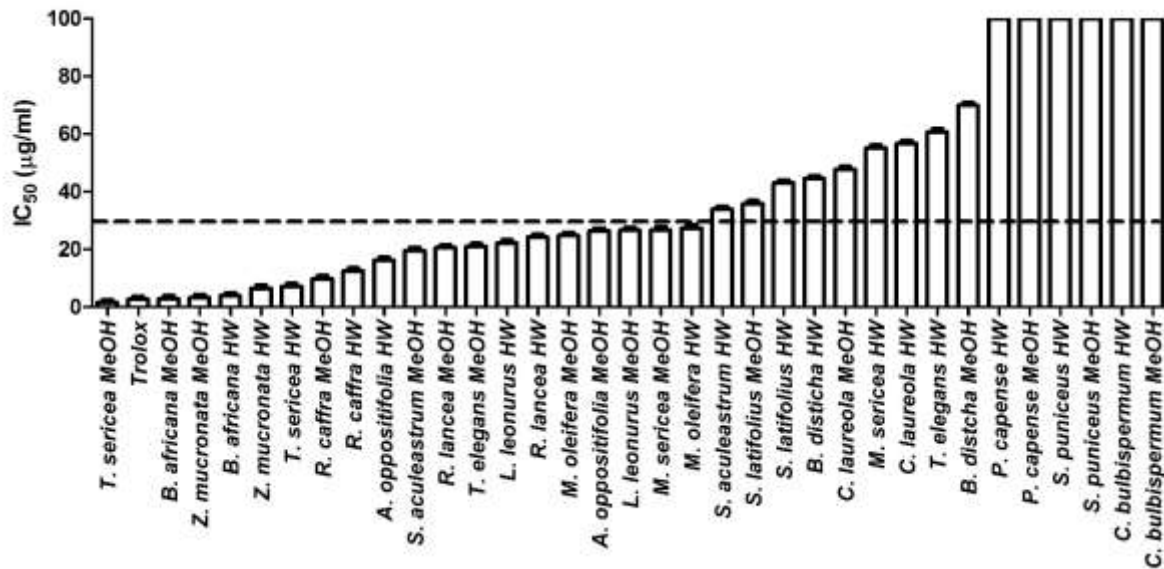


**Figure 8:** Antioxidant activity, expressed as the IC<sub>50</sub>, of the crude extracts arranged from strongest to weakest activity (black dashed line represents the active threshold). Antioxidant activity at 100 µg/mL represents a value >100 µg/mL. HW – hot water extract; MeOH – methanol extract.

**Table 6:** ABTS<sup>•+</sup> scavenging activity of crude extracts and standards.

Plant	Extract	IC <sub>50</sub> ± SEM (µg/mL)	TE ± SEM (ratio)
<i>A. oppositifolia</i>	Hot water	16.17 ± 1.03	0.15 ± 0.00
	Methanol	26.39 ± 1.02	0.11 ± 0.00
<i>B. disticha</i>	Hot water	44.54 ± 1.02	0.05 ± 0.00
	Methanol	69.85 ± 1.03	0.04 ± 0.00
<i>B. africana</i>	Hot water	3.86 ± 1.05	0.56 ± 0.01
	Methanol	2.90 ± 1.06	0.58 ± 0.03
<i>C. laureola</i>	Hot water	56.71 ± 1.03	0.05 ± 0.00
	Methanol	47.71 ± 1.03	0.05 ± 0.00
<i>C. bulbispermum</i>	Hot water	>100	0.02 ± 0.00
	Methanol	>100	0.02 ± 0.00
<i>L. leonurus</i>	Hot water	22.24 ± 1.02	0.12 ± 0.00
	Methanol	26.64 ± 1.02	0.11 ± 0.00
<i>M. oleifera</i>	Hot water	27.38 ± 1.05	0.11 ± 0.01
	Methanol	24.82 ± 1.03	0.12 ± 0.00
<i>M. sericea</i>	Hot water	55.14 ± 1.03	0.05 ± 0.00
	Methanol	26.72 ± 1.14	0.12 ± 0.01
<i>P. capense</i>	Hot water	>100	0.02 ± 0.00
	Methanol	>100	0.03 ± 0.00
<i>R. caffra</i>	Hot water	12.52 ± 1.03	0.24 ± 0.01
	Methanol	9.82 ± 1.05	0.29 ± 0.01
<i>R. lancea</i>	Hot water	24.24 ± 1.03	0.12 ± 0.00
	Methanol	20.50 ± 1.03	0.13 ± 0.00
<i>S. puniceus</i>	Hot water	>100	0.02 ± 0.00
	Methanol	>100	0.02 ± 0.00
<i>S. latifolius</i>	Hot water	42.98 ± 1.03	0.06 ± 0.00
	Methanol	35.83 ± 1.03	0.06 ± 0.00
<i>S. aculeastrum</i>	Hot water	33.89 ± 1.04	0.09 ± 0.00
	Methanol	19.58 ± 1.03	0.13 ± 0.00
<i>T. elegans</i>	Hot water	60.68 ± 1.08	0.06 ± 0.01
	Methanol	21.02 ± 1.03	0.13 ± 0.00
<i>T. sericea</i>	Hot water	7.12 ± 1.04	0.43 ± 0.01
	Methanol	1.50 ± 1.04	1.54 ± 0.05
<i>Z. mucronata</i>	Hot water	6.46 ± 1.04	0.44 ± 0.01
	Methanol	3.20 ± 1.06	0.56 ± 0.02
Antioxidant standards	Ascorbic acid	2.80 ± 1.03	1.19 ± 0.04
	Caffeic acid	2.04 ± 1.03	1.30 ± 0.04
	Catechin	1.02 ± 1.02	3.18 ± 0.08
	p-Coumaric acid	1.83 ± 1.04	2.36 ± 0.11
	Curcumin	4.49 ± 1.05	0.84 ± 0.03
	Ferulic acid	1.11 ± 1.04	3.00 ± 0.08
	Gallic acid	0.61 ± 1.03	4.08 ± 0.10
	Quercetin	0.92 ± 1.03	3.79 ± 0.14
	Rutin	8.67 ± 1.04	0.35 ± 0.02
	Sinapic acid	2.17 ± 1.04	1.08 ± 0.04
	Syringic acid	2.08 ± 1.03	2.31 ± 0.08
	Tannic acid	1.42 ± 1.04	2.35 ± 0.08
	Trolox	2.73 ± 1.01	1.00 ± 0.01

Only two antioxidant standards did not match or exceed the activity of Trolox, namely curcumin (TE 0.85) and rutin (TE 0.35). The only crude extract to display higher activity than Trolox was the methanol extract of *T. sericea* with a TE of 1.57. Nineteen extracts, which comprise of hot water and methanol extracts of eight plants (*A. oppositifolia*, *B.*

*africana*, *L. leonurus*, *M. oleifera*, *R. caffra*, *R. lancea*, *T. sericea* and *Z. mucronata*), as well as the methanol extracts of *M. sericea*, *S. aculeastrum* and *T. elegans* displayed high antioxidant activity, albeit not as potent as Trolox. The most potent antioxidant activity was displayed by the methanol extract of *T. sericea* (1.5 µg/mL), both extracts of *B. africana* (3 – 4 µg/mL), and *Z. mucronata* (3 – 6 µg/mL).

## 2.4. Discussion

Although crude screening does not identify specific phytochemicals, it does lead to a broad indication of the groups that are present within an extract. Phytochemical classes have specific characteristics ascribed to them, and thus it is possible to make inferences based on bioactivity observed. An antioxidant IC<sub>50</sub> of 30 µg/mL was selected as a noteworthy cut-off point for bioactivity,<sup>47</sup> while <100 mg/g, 100-500 mg/g and >500 mg/g was selected as cut-off points for low, moderate and high content, respectively. The latter three ranges were selected as a representative zone of activity based on experimentation. As observed from the total saponin content, large variation was found, which may indicate the relative non-selectivity of the vanillin-sulphuric acid method. Due to the diverse selection of plants, discussion is done based upon family groupings. Although direct phytochemical detection was not done, inferences are made based on phytochemical literature available, and correlating this to the phytochemical screening performed in the project.

### 2.4.1. Amaryllidaceae

Research in plants from the Amaryllidaceae-family are generally focussed on the range of isoquinoline alkaloids specific to the family (colloquially known as the Amaryllidaceae-type alkaloids).<sup>87</sup> These have been described as being neuro- and cardioactive, as well as highly toxic.<sup>88</sup> These alkaloids are largely classified into three groups: the lycorane-, galanthamine- and crinane-types.<sup>88</sup>

Both crude extracts of *B. disticha* (Figure 4B) were found to contain anthrones and phenolic acids, while only the hot water extract tested positive for saponins, and the

methanol extract for alkaloids, coumarins, glycosides and terpenoids (Table 4). Flavonoid content was considered negligible, while low levels of phenolic acids were detected, as well as low of saponins in the hot water extract, and negligible concentrations in the methanol extract (Table 5). It has been estimated that the fresh bulb contains up to 0.31% alkaloids.<sup>87</sup> Twelve alkaloids have been isolated from the bulbs, including buphenadrine (the major constituent and toxin),<sup>87,88</sup> undulatin, buphanisine, buphanamine, nerbowdine, crinine, distichamine, crinamidine, acetylnerbowdine, lycorine and buphacetine,<sup>87</sup> and recently 6 $\alpha$ -hydroxycrinamine.<sup>89</sup> Distichamine, acetylnerbowdine and buphacetine appear to be specific to *B. disticha*.<sup>88</sup> Antioxidant activity, which is correlated to phenolic and flavonoid content,<sup>59</sup> was not seen as highly active (Table 6), and is supported by the low content screening and literature (ABTS<sup>•+</sup> IC<sub>50</sub>>125  $\mu$ g/mL).<sup>90</sup> Other organic compounds that have been isolated include furfuraldehyde, acetovannilone, chelidonic acid, laevulose, pentatriacontane, phytosterols, ipuranol and fatty acids.<sup>91</sup>

*C. bulbispermum* (Figure 4E) crude extracts were found to contain phenolic acids (albeit low levels) and saponins (more concentrated in the methanol extract), however in the methanol extract alkaloids, anthrones, coumarins, glycosides and terpenoids were identified (Tables 4 and 5). Flavonoid content was considered negligible for both extracts (Table 5). *C. bulbispermum* contains Amaryllidaceae-type alkaloids: crinine,<sup>92</sup> powelline, lycorine,<sup>57,92</sup> crinamine, bulbispermine, acetylcaranine, ambelline, crinasiadine, crinasiatine, galanthamine, heppeastrine,<sup>57</sup> norbelladine,<sup>92</sup> 11,12-dehydrolycorine, trishaeridine, vittatine, crinane acetate, 11-12-didehydroanhydrolycorine, buphanidine, undulatine, macronine, crinimadine, bowdensine.<sup>93</sup> No antioxidant activity was detected (Table 6), although literature does describe low-to-moderate activity (ABTS<sup>•+</sup> IC<sub>50</sub> = 68.5  $\mu$ g/mL).<sup>94</sup>

*S. puniceus* (Figure 4L) crude extracts tested positive for anthrones and phenolic acids (low levels), while only the hot water extract contained tannins, and the methanol extract alkaloids and glycosides. Negligible flavonoid and saponin content was found (Tables 4 and 5). Haemanthamine, haemanthidine,<sup>57,95</sup> and 6-hydroxycrinamine<sup>95</sup> have been detected in extracts. The lack of antioxidant activity (Table 6) is supported by literature, although being from a different solvent extract system.<sup>94</sup>

#### 2.4.2. Anacardiaceae

*R. lancea* (Figure 4K) crude extracts tested positive for alkaloids, glycosides, phenolic acids, saponins (low-to-moderate levels, slightly higher in the hot water extract) and tannins, while anthroquinones and flavonoids were only present in the methanol extract (Tables 4 and 5). Flavonoid content, although low, may contain kaempferol, quercetin and myricetin, as well as 7,4'-di-O-methylmyricetin and its galactoside, which have been isolated from ethanolic leaf extracts.<sup>96</sup> Essential oils consisting of  $\alpha$ -pinene, benzene,  $\delta$ -3-carene, isopropyl and trans-caryophyllene have been identified in leaves.<sup>97</sup> The presence of phenolic acids, flavonoids, gallotannins and condensed tannins is supported by literature.<sup>98</sup> Antioxidant activity was observed ( $IC_{50}$ 's < 25  $\mu$ g/mL), which was slightly higher in the methanol extract (Table 6). This is supported by the higher phenolic content identified in the methanol extract, compared to the hot water extract.

#### 2.4.3. Apocynaceae

Plants belonging to the Apocynaceae family are known to be toxic, which is oftentimes ascribed to the presence of potent cardiac glycosides.<sup>99</sup> Both crude extracts of *A. oppositifolia* (Figure 4A) tested positive for alkaloids, anthrones, flavonoids, glycosides, phenolic acids and saponins (Table 4). Flavonoid content was moderate, with a greater content in the methanol extract. The hot water extract contained more phenolic acids than the methanol extract. The methanol extract possessed moderate levels of saponins, ~8-fold the amount of the hot water extract. Overall, flavonoid content was greater than phenolic content (Table 5), a trend that was described in a previous study.<sup>100</sup> *Acokanthera* species are reported to contain the cardenolide cardiac glycosides,<sup>57,101</sup> ouabain and acovenoside A.<sup>57,102</sup> Antioxidant activity was considered high relative to the majority of extracts, especially in the hot water extract, which may be due to the higher phenolic content (Table 6). Antioxidant activity has been ascribed to the extracts of *A. oppositifolia*,<sup>103</sup> but not to the extent seen in the present study. Geographical variation may potentially be responsible for this.

Alkaloids, anthrones, coumarins, flavonoids, glycosides, phenolic acids, saponins and terpenoids were found to be present in the crude extracts of *R. caffra* (Figure 4J),

however were devoid of anthroquinones and tannins (Table 4). Low levels of flavonoids and phenolic acids were present, with moderate levels of saponins (Table 5). The presence of alkaloids, terpenoids, saponins and cardiac glycosides in the stem-bark is supported by literature.<sup>104</sup> Twenty-eight alkaloids have been identified: corynane, strictamine, sarpagan, akuammicine, pleiocarpamine, indolenine, dihydroindole, peraksine, heteroyohimbine, hydroxyheteroyohimbine, oxindole, 2-acyl-indole, suaveoline and yohimbine types. Ajmaline, norajmaline, ajmalicine, ajmalicine, geissoschizol, pleiocarpamine and heteroyohimbine are considered the main alkaloids.<sup>105</sup> Notable antioxidant activity was present in the crude extracts of *R. caffra* (Table 6), which is supported by literature pertaining to the stem-bark and leaves.<sup>104</sup>

While both crude extracts of *T. elegans* (Figure 4O) contained alkaloids, coumarins, glycosides, phenolic acids and saponins, only the methanol extract tested positive for tannins and terpenoids (Table 4). The presence of alkaloids, amines, essential oils, phenolic acids, saponins and sterols/steroids has been reported.<sup>61,106</sup> Flavonoid content was negligible, with low levels of phenolic acids. Low and moderate levels of (an approximate ~2-fold increase from hot water to methanol) was present in the hot water and methanol extracts, respectively (Table 5). Alkaloids of *T. elegans* have been extensively researched<sup>107</sup> leading to the identification of 3-oxo-isovoacangine, 3-*R/S*-hydroxyisovoacangine, coronaridine, isositsirikine, geissoschizol, tabernaemontanine, vobasine,<sup>107,108</sup> vobasinol, apparicine, 16-hydroxy-16,22-dihydroapparicine, tubotaiwine, 3-*R/S*-hydroxyconodurine, monogagaine,<sup>107</sup> dregamine,<sup>106,108</sup> elaganine A,  $\beta$ -carbolines (tabernines A–C),<sup>108</sup> alosmontamine A,<sup>109</sup> voacangine,<sup>106</sup> 16-epidregamine and tabernaelegantinine B.<sup>110</sup> The hot water extract displayed low levels of antioxidant activity, while the methanol extract presented with noteworthy activity (Table 6). The hot water extract's lack of activity has been described in literature.<sup>61</sup>

#### 2.4.4. Asteraceae

Both crude extracts of *C. laureola* (Figure 4D) tested positive for alkaloids, glycosides, phenolic acids and saponins (Table 4). The main diterpenoid glycosides that have been identified are atractyloside and carboxyatractyloside (which thermally decomposes to the former). These are considered as the primary phytotoxins.<sup>31,111</sup>

Previously phenolic acids, phytosterols, flavonoids, reducing sugars and gums have been detected.<sup>112</sup> In the present study flavonoid content was negligible, while low levels of phenolic acids and saponins were identified. In both cases the hot water extract contained a greater content than the methanol extract (Table 5). Moderate antioxidant activity was present, which was greater in the methanol extract (Table 6). Antioxidant activity has been attributed to *C. laureola* extracts, but only at high concentrations.<sup>113</sup>

Alkaloids, flavonoids, glycosides, phenolic acids and saponins were present in both crude extracts of *S. latifolius* (Figure 4M), although anthrones were only present in the methanol extract (Table 4). A number of alkaloids have been isolated from *S. latifolius* which includes sceleratine, sceleratine-N-oxide, merenskine, merenskine-N-oxide, retronecine, scleraneic bislactone, retrorsine, isatidine, isatinecine, chlorodeoxyscleratine,<sup>114</sup> senecifolidine and senecifoline.<sup>115</sup> Flavonoid and saponin content was low in the hot water extract, albeit ~2- and 72-fold higher in the methanol extract, respectively. Phenolic acid content was relatively low for both extracts (Table 5), as was antioxidant activity (Table 6).

#### 2.4.5. Combretaceae

Flavonoids, glycosides, phenolic acids and tannins were found to be present in both crude extracts of *T. sericea* (Figure 4P), while alkaloids and saponins were only detected in the hot water and methanol extract, respectively (Table 4). Phenolic and flavonoid compounds, such as ellagic acid derivatives, ellagitannins, gallic acid, catechins, stilbenes<sup>116</sup> and resveratrol,<sup>117</sup> as well as hydroxystilbene glycosides (3'5'-dihydroxy-4-[2-hydroxy-ethoxy] resveratrol-3-O- $\beta$ -rutinoside<sup>117</sup> and reseedveratrol-3-O- $\beta$ -D-rutinoside<sup>118</sup> have been isolated previously. Furthermore, lignans (anolignan B<sup>119</sup> and termilignan B<sup>120</sup>) and sterols ( $\beta$ -sitosterol<sup>117</sup>,  $\beta$ -sitosterol-3-acetate, stigma-4-ene-3-one<sup>121</sup> and stigmasterol<sup>117</sup>) have been reported. Although not identified using TLC, *T. sericea* is known to contain the triterpenoids sericic acid, sericoside,<sup>122</sup> terminoic acid,<sup>123</sup> arjunic acid,<sup>120</sup> arjugenin,<sup>117</sup> and lupeol.<sup>121</sup> While negligible saponin content was observed in the hot water extract, all other phytochemical quantities were high, increasing greatly from the hot water to methanol extract (Table 5). Potent antioxidant activity was observed for both extracts, with the methanol extract exceeding the

activity of the positive control (Trolox). The antioxidant activity observed in the present study (Table 6) is supported by previous studies,<sup>94,124–126</sup> and correlates with tannin content.<sup>126</sup> This was observed in a cellular system where the neutrophil respiratory burst was reduced by methanol extracts of *T. sericea*.<sup>127</sup>

#### 2.4.6. Fabaceae

Both crude extracts of *B. africana* (Figure 4C) tested positive for alkaloids, anthrones, flavonoids, glycosides, phenolic acids, saponins and tannins (Table 4). The presence of alkaloids, flavonoids, glycosides, phenolic acids, saponins<sup>59,128</sup> and tannins is known.<sup>128</sup> Very high levels of flavonoids, phenolic acids and saponins were observed, which in all cases were greater in the methanol extract (Table 5). With regards to phenolic acids and flavonoids, these may consist of proanthocyanidins such as fisetinidol-(4 $\alpha$ -8)-catechin 3-gallate and bis-fisetinidol-(4 $\alpha$ -6,4 $\alpha$ -8)-catechin 3-gallate, as well as catechin and epicatechin.<sup>129</sup> Potent antioxidant activity was observed for both crude extracts (Table 6), which corresponds to literature.<sup>59,128–130</sup> This activity has also been displayed in a cellular model exposed to 2,2'-azobis(2-amidinopropane dihydrochloride) (AAPH)-mediated oxidation.<sup>59</sup>

Glycosides, phenolic acids and saponins were identified in both extracts of *M. sericea* (Figure 4H). Only the methanol extract contained alkaloids, coumarins and flavonoids. Low flavonoid and phenolic content was detected, while mild-to-moderate levels of saponins were identified (Table 5). Phytochemical content was greater in the methanol extract than hot water extract. Flavonoids (mundulone, munetone and sericetin),<sup>131</sup> rotenoids (deguelin, tephrosin, [-]-13 $\alpha$ -hydroxytephrosin and [-]-13 $\alpha$ -hydroxydeguelin), chalcones (munsericin, 4-hydroxyonchocarpin)<sup>132</sup> as well as phytosterols, have been isolated from the bark.<sup>131</sup> Low antioxidant potential was observed for the hot water extract, which was higher in the methanol extract (Table 6).

#### 2.4.7. Lamiaceae

The crude extracts of *L. leonurus* (Figure 4F) contained flavonoids, phenolic acids, saponins and tannins, while only the methanol extract was found to possess alkaloids,

anthrones, anthroquinones, glycosides and terpenoids (Table 4). Flavonoid, phenolic and saponin content was moderate, low-to-moderate and high, respectively (Table 5). Flavonoids isolated from *L. leonurus* include apigenin 6-C- $\alpha$ -arabinoside-8-C- $\beta$ -glucoside, apigenin 8-C- $\beta$ -glucoside, apigenin 7-O- $\beta$ -glucoside, luteolin 7-O- $\beta$ -glucoside, luteolin 7-O- $\beta$ -glucoside-3'-methyl ether, apigenin 7-O-(6'-O-*p*-coumaroyl)- $\beta$ -glucoside, 6-methoxyluteolin-4'-methyl ether, luteolin 3'-methyl ether, luteolin and apigenin.<sup>133</sup> Aqueous extracts have been shown to contain alkaloids, saponins, tannins,<sup>134,135</sup> phenolic acids, flavonoids,<sup>135,136</sup> and glycosides.<sup>135</sup> As with the methanol extract, other organic extracts of the leaves have been reported to contain flavonoids, phenolic acids and terpenoids.<sup>137</sup> The labdane diterpenoids<sup>138</sup> leonurun, premarrubiin, marrubiin,<sup>139</sup> leonurenones A-C, luteolin 7-O- $\beta$ -glucoside and luteolin<sup>140</sup> have been isolated. Moderate antioxidant activity was observed in the present study, which appears to be greater than that found in other studies (Table 6). Low antioxidant activity has been described for both aqueous<sup>136,141,142</sup> and methanol extracts.<sup>142</sup> This may be attributed to difference in geographical location and extraction procedure.

#### 2.4.8. Moringaceae

*M. oleifera* (Figure 4G) crude extracts were found to contain alkaloids, flavonoids, phenolic acids and saponins. Additionally anthrones were detected in the hot water extract, and anthroquinones, glycosides and terpenoids in the methanol extract (Table 4). Low concentrations of flavonoids, phenolic acids and saponins were detected, however saponin levels were moderately increased in the methanol extract (Table 5). The presence of alkaloids, glycosides, terpenoids, saponins, flavonoids and phenolic acids in the leaves, as well as carbohydrates, tannins and fat stores have been confirmed.<sup>143–148</sup> Phenolic and flavonoid compounds previously detected include catechin, caffeic acid, epicatechin, rutin, ferulic acid, ellagic acid, chlorogenic acid, gallic acid, quercetin, myricetin, kaempferol and vanillin.<sup>149–151</sup> The alkaloid, trigonelline<sup>152</sup> and various glycosides (niazirin, niaziridin,<sup>153</sup> niazarin (4-( $\alpha$ -L-rhamnopyranosyloxy)phenylacetone)nitrile, pyrrolemarumine 4''-O- $\alpha$ -L-rhamnopyranoside, marumoside A, marumoside B, methyl 4-( $\alpha$ -L-rhamnopyranosyloxy)-benzylcarbamate, benzyl  $\beta$ -D-glucopyranoside, benzyl  $\beta$ -D-xylopyranosyl-(1 $\rightarrow$ 6)- $\beta$ -D-glucopyranoside, kaempferol 3-O- $\beta$ -D-glucopyranoside and

quercetin 3-O- $\beta$ -D-glucopyranoside<sup>154</sup>) have been described, as well as protease inhibitors.<sup>155,156</sup> Moderate antioxidant activity was observed (Table 6), which is supported by literature both in cell-free<sup>150,157,158</sup> and cellular systems.<sup>159,160</sup>

#### 2.4.9. Piperaceae

Both extracts of *P. capense* (Figure 4I) tested positive for glycosides and phenolic acids. The hot water and methanol extract contained saponins and alkaloids, respectively (Table 4). Phenolic and saponin content were low (Table 5). The presence of phenolic acids.<sup>94</sup> Roots have been found to contain lignans and neolignans,<sup>161,162</sup> sesquiterpenes (capentin),<sup>63</sup> amides (piperine and 4,5-dihydropiperine),<sup>163,164</sup> essential oils,<sup>165</sup> and quinones (plumbagin) have been reported.<sup>166</sup> No antioxidant activity was observed in the present study (Table 6), although organic extracts of *P. capense* have been described to contain low-to-moderate activity.<sup>94,166</sup> This could be explained by the relatively low phenolic content found in the prepared extracts.

#### 2.4.10. Rhamnaceae

Whereas only the crude methanol extract of *Z. mucronata* (Figure 4Q) contained coumarins, both extracts possessed alkaloids, flavonoids, glycosides, phenolic acids, saponins and tannins (Table 4). Flavonoid and phenolic content was moderate-to-high, while saponin content was very high, exceeding that of the standard (diosgenin) used (Table 5). In all cases the methanol extract contained higher levels of phytochemicals than the hot water extract. The presence of flavonoids, glycosides, phenolic acids, saponins and tannins is supported by literature.<sup>94,167–169</sup> Flavonoid and phenolic acid concentrations were found to be lower than in other studies,<sup>94,167,168</sup> whereas high saponin content has been described in literature.<sup>169</sup> *Z. mucronata* is known to contain cyclopeptide alkaloids (numerous mucronines and abyssenines),<sup>64,170</sup> phenolic acids,<sup>171</sup> quonones, flavonoids, anthocyanins and terpenoids.<sup>172</sup> High antioxidant activity was observed (Table 6), which is supported by other studies.<sup>94,167–169</sup>

#### 2.4.11. Solanaceae

Both crude extracts of *S. aculeastrum* (Figure 4N) contained alkaloids, anthrones, flavonoids, glycosides, phenolic acids, saponins and terpenoids (Table 4). Flavonoid content in the hot water extract was relatively low, while moderate in the methanol extract. Phenolic acid content was low in both extracts, while saponin content was moderate in the methanol extract (Table 5). The fruits have been reported to be rich in steroidal glucosaponins and glucoalkaloids,<sup>173</sup> which includes the steroidal alkaloids ( $\beta$ -solamarine, solamargine,<sup>174</sup> solanine, solasonine,<sup>175</sup> solasodine,<sup>175,176</sup> and tomatodine.<sup>176</sup> Antioxidant activity was noteworthy in the methanol extract (Table 6), which is supported by literature.<sup>177</sup>

#### 2.5. Conclusion

The objectives of the chapter were met. An all-encompassing conclusion is provided in Chapter 6. The presence of phytochemical classes will aid in the discussion of the results of the subsequent biological assays. It was observed that the solvent extraction system allowed for differential extraction of phytochemical classes, although there were some similarities. Relative quantitative analyses provided an indication of the phytochemical content of phenolic acids, flavonoids and saponins. It should be noted, however, that the saponin content displayed high levels of variability, most likely due to method non-specificity.

## Chapter 3

### **Preliminary phytotoxicological assessment of herbal remedies in the HepG2 hepatocarcinoma and Caco-2 colon carcinoma cell lines**

#### **3.1. Literature review**

##### **3.1.1. Cytotoxic processes**

Although widely used, the safety of most herbal remedies is generally not researched. Patients are frequently admitted with suspected poisoning due to herbal remedy usage. These remedies are often not well-described by traditional healers, or specific administration details are omitted, which makes diagnosis problematic.<sup>44</sup> With regards to their medicinal usage, plants (or their respective parts) should be used that have minimal toxic effects attributed to them.<sup>5</sup> Herbal poisoning was listed as one of the 20 most common causes for infant mortality in South Africa between 1997 and 2007 during a 2012 Medical Research Council report.<sup>178</sup> Mortality rates due to herbal and traditional medicine use appear to be higher in children.<sup>179</sup>

Herbal remedies carry direct (intrinsic) and indirect (extrinsic) risks of toxicity with their usage. Direct risks include inherent phytochemical toxicity, incorrect preparation or misidentification of plant material. Indirect risks refer to, amongst others, the potential of herbal remedies to interact with other medicinal preparations, with subsequent adverse effects due to altered pharmacokinetic and pharmacodynamic profiles.<sup>180</sup> Phytotoxicity mainly manifests as damage to the kidneys, liver and heart.<sup>180</sup>

Plant species have, through evolution, adopted numerous defensive mechanisms against predatory attacks, including the *de novo* synthesis of chemical entities. Plants that accumulate toxic phytochemicals have been used as toxins for arrows or darts, or even the surreptitious murdering of individuals.<sup>99</sup> However, as much as their toxicity is often highlighted through their cultural uses or even their naming, they remain highly regarded as medicinal preparations.<sup>99</sup>

Allelochemicals can act as toxins through interactions with various molecular targets, which amongst others include the cellular membrane, proteinaceous structures (such

as receptors, transporters and structural units) and nucleic acids.<sup>181</sup> These compounds often mimic that of endogenous substances (such as neurotransmitters), allowing them the ability to alter physiological pathways necessary for survival of the organism. In high enough quantities, these can ultimately perturb physiological homeostasis with resulting adverse effects.<sup>181</sup>

The cellular membrane is mostly affected by lipophilic or amphiphilic molecules (such as saponins and terpenoids), resulting in potential interactions with membrane channels, transporters, receptors or the inner lipophilic core. This allows for potential alteration of membrane functionality, including destabilization and degradation.<sup>181</sup> Subsequent destruction of the cell can occur due to loss of structural integrity.<sup>51</sup> These types of interactions are often not selective, and can therefore result in non-specific toxicity across different taxa and species.<sup>181</sup>

As proteinaceous structures require a highly specific conformation to maintain bioactivity, any changes to this can greatly diminish their functionality. Secondary metabolites, such as reactive polyphenolic molecules and certain terpenoids, are capable of binding to the functional groups of proteins. Effects may include attenuated enzyme activity, structural changes or degradation of proteins.<sup>51,56,181</sup>

Nucleic acid alkylations or chelations result in alteration of genetic material, resulting in altered expression of endogenous substances and potential downstream toxicity.<sup>51</sup> As such these can result in mutations which can be highly detrimental if not corrected.<sup>181</sup>

### **3.1.2. Aim of phytotoxicological assessment**

The aim of the phytotoxicological assessment was to determine the cytotoxic potential of the panel of crude extracts using the HepG2 and Caco-2 cell lines in order to determine which extracts would be assessed during further mechanistic studies. The objective was to:

- Determine the cytotoxic potential of the crude extracts in the HepG2 and Caco-2 cell lines with the selected cytotoxicity assay.

## 3.2. Materials and Methods

A detailed list of all reagents used in the study, as well as the preparation thereof, is provided (Appendix III).

### 3.2.1. Cell culture, seeding and exposure of cells to crude extracts

*In vitro* cytotoxic assessment has a wide panel of potential confounding factors, and it is thus imperative to determine the most applicable model to be used. The two cell lines chosen for this study have well-described uses as cytotoxicity and interaction models. The Caco-2 cell line is a commercially available colorectal adenocarcinoma cell line (American Type Tissue Collection [ATCC] #HTB-37) originally isolated from a 72-year old male.<sup>182</sup> The cell line is widely researched and used for *in vitro* studies on intestinal absorption. Monolayers are able to differentiate to structurally- and functionally-similar cells that simulate small intestinal epithelium, making them appropriate for intestinal absorption studies.<sup>183,184</sup> On the other hand, the commonly used HepG2 hepatocellular carcinoma cell line (ATCC #HB-8065) was originally isolated from a 15-year old male.<sup>185</sup> HepG2's are a well-characterised model for hepatotoxicity, although they do succumb to certain disadvantages, such as being metabolically incompetent and cancerous. This does present the potential of not taking into account enzymatic bioactivation during induction of hepatotoxicity.<sup>186</sup>

The HepG2 and Caco-2 cell lines were maintained in Eagle's Minimum Essential Medium (EMEM). Medium was supplemented with 10% foetal calf serum (FCS) and grown in 75 cm<sup>2</sup> flasks at 37°C and 5% CO<sub>2</sub> in a humidified incubator. Once flasks reached a confluence of 75%, cells were detached using Trypsin/Versene solution for 5 min. Detached cells were harvested through centrifugation (200g, 5 min), counted using the trypan blue exclusion assay (0.1%) and a haemocytometer, and diluted to 2 x 10<sup>5</sup> cells/mL (HepG2) or 1 x 10<sup>5</sup> cells/mL (Caco-2) in 10% FCS-supplemented medium. Cells (100 µL) were seeded into sterile, clear 96-well plates at 2 x 10<sup>4</sup> cells/well (HepG2) or 1 x 10<sup>4</sup> cells/well (Caco-2), and incubated for 24 h at 37°C and 5% CO<sub>2</sub> in a humidified incubator to allow for attachment. Blanks containing 200 µL FCS (5%)-supplemented medium alone was used to account for background noise

and sterility. After attachment, cells were exposed to 100  $\mu\text{L}$  medium (negative control), DMSO (0.8%; vehicle control), crude extracts (2, 6.4, 20, 64 and 200  $\mu\text{g}/\text{mL}$ ) or tamoxifen (2, 6.4, 20, 64 and 200  $\mu\text{M}$ ; positive control) prepared in FCS-negative medium for 72 h at 37°C and 5%  $\text{CO}_2$  in a humidified incubator.

### **3.2.2. Effect of crude extracts on cellular status**

Although various assays exist for the determination of cellular viability and cytotoxicity, a few have gained popularity. These generally entail the generation of a coloured or fluorescent product either through metabolic conversion<sup>187</sup> or staining of cellular components.<sup>188</sup> These can then be compared to untreated cultures to give relative estimations of cellular viability or survival. Ultimately an assay should be cost-effective, reproducible, inert, indicate an accurate representation of viable cells, not interfere with test samples, offer high-throughput use and not add to potential cytotoxic activity.

#### **3.2.2.1. Sulforhodamine B staining assay**

Cell enumeration assays, such as sulforhodamine B (SRB),<sup>188</sup> aim to quantify the cellular elements through staining in a stoichiometric fashion. SRB is a pink aminoxanthene dye with two sulfonic groups. It associates with basic amino acid functional groups of trichloroacetic acid-fixed proteins under acidic conditions, while dissociating under basic conditions. Such an assay is considered inert, as compounds very rarely result in interactions with staining substrate.<sup>188</sup> Care must be taken though to ensure compounds themselves do not result in staining of cellular elements.

Cell density was determined by staining fixed protein elements with SRB in the HepG2 and Caco-2 cell lines as described by Vichai and Kirtikara<sup>188</sup> with minor modifications. Cells were fixed with 50  $\mu\text{L}$  trichloroacetic acid (TCA; 50%) for 16 h at 4°C, washed thrice with slow-running tap water and stained using 100  $\mu\text{L}$  SRB solution (0.057% in 1% acetic acid) for 30 min. Stained cells were washed thrice with 100  $\mu\text{L}$  acetic acid (1%), air-dried and the stain solubilized using 200  $\mu\text{L}$  Tris-buffer (10 mM, pH 10.5). Absorbance was measured at 510 nm with a reference of 630 nm (Synergy 2, Bio-Tek

Instruments, Inc.) and adjusted by subtracting the blank. Percentage cell density relative to the negative control was expressed using the following equation:

$$\text{Cell density (\% relative to negative control)} = \frac{A_s}{A_c} \times 100$$

where,  $A_s$  = the blank-adjusted absorbance of the sample, and  $A_c$  = the blank-adjusted average absorbance of the negative control.

### 3.2.2.2. Neutral red staining assay

Neutral red is a red weakly cationic dye that accumulates in lysosomes through electrostatic hydrophobic binding.<sup>189</sup> Cell number as a function of lysosome integrity was determined by the staining of lysosomes with neutral red in the HepG2 cell line as described by Repetto *et al.*<sup>189</sup> with minor modifications. After incubation with the extracts, as described in Section 3.2.1., medium was aspirated and replaced with 100 µg/mL neutral red-supplemented EMEM. Plates were incubated for 4 h, after which they were washed thrice with PBS (200g for 5 min). Dye was extracted from stained cells through the use 200 µL neutral red eluent (distilled water:ethanol:acetic acid [50:49:1]). Absorbance was measured at 540 nm with a reference of 630 nm and lysosome integrity determined as described in Section 3.2.2.1.

### 3.2.2.3. MTT conversion assay

Conversion assays utilize cellular metabolism to enzymatically convert a substrate (preferably colourless) to a differently coloured product.<sup>190</sup> Due to the need for unperturbed enzymes, only viable cells are able to convert the dye.<sup>190</sup> The 3-(4,5-dimethylthiazol-2-yl)-2,5-diphenyltetrazolium bromide (MTT) assay allows for the conversion of yellow tetrazolium salt to purple formazan crystals.<sup>190</sup> MTT is popular as a cell enumeration assay to support cytotoxicity testing.<sup>187</sup> Although being useful for indicating the metabolic activity of cells, they do suffer from a number of limitations. Cells which have reached confluence may undergo contact inhibition with attenuated metabolic function, thus conversion may be decreased.<sup>187</sup> Furthermore, these dyes are often susceptible to interactions, either through direct conversion by the sample

(such as seen with reducing compounds) or through alterations in metabolic efficiency, resulting in inaccurate determination of cellular viability.<sup>187</sup> An increased conversion may then give a false indication that cells are still functional and living, or might even be misconstrued as a proliferation.

Metabolic activity was determined by the conversion of yellow MTT to insoluble purple formazan crystals in the HepG2 cell line as described by Mosmann<sup>190</sup> with minor modifications. After incubation with the extracts, as described in Section 3.2.1., an aliquot of 20  $\mu$ l MTT (5 mg/mL) was added to all wells and allowed to incubate for 3 h. Plates were washed thrice with PBS (200g for 5 min) and the pelleted formazan crystals dissolved with 200  $\mu$ L DMSO. Absorbance was measured at 570 nm with a reference of 630 nm and metabolic activity determined as described in Section 3.2.2.1.

#### 3.2.2.4. Resazurin conversion assay

The resazurin conversion assay is similar to the MTT assay, as blue/purple resazurin is converted to pink resorufin.<sup>187</sup> Metabolic activity was determined in the HepG2 cell line as described by Riss *et al.*<sup>187</sup> with minor modifications. After incubation with the extracts, as described in Section 3.2.1., medium was aspirated and replaced with 100  $\mu$ L resazurin (10  $\mu$ M in PBS). Plates were incubated for 2 h after which the fluorescence was measured at  $\lambda_{ex}$  = 544 nm and  $\lambda_{em}$  = 590 nm. Percentage metabolic activity relative to the negative control was expressed using the following equation:

$$\text{Metabolic activity (\% relative to negative control)} = \frac{FIs}{FIc} \times 100$$

where, FIs = the blank-adjusted fluorescence of the sample, and FIc = the blank-adjusted average fluorescence of the negative control.

#### 3.2.3. Statistics

All experiments were performed using at least three technical and three biological replicates. Results were compiled using Microsoft Excel 2010 and analysed statistically using GraphPad Prism 5.0. All results are expressed as the mean  $\pm$  SEM. The IC<sub>50</sub> was determined using non-linear regression (normalized variable slope).

### 3.3. Results

#### 3.3.1. Comparison of cytotoxicity assays

A panel of four plants (eight extracts) were initially screened for their effects on HepG2 cellular viability to determine which cytotoxicity assay would be most applicable to the study. The comparison (in terms of the IC<sub>50</sub>) is presented in Table 7. The resazurin assay under-estimated cytotoxicity (as no IC<sub>50</sub> could be determined  $\leq 100$   $\mu\text{g/mL}$ ), whereas the neutral red staining and MTT conversion assays offered the highest sensitivity for both extracts of two plants (*B. disticha* [17.17 – 33.16  $\mu\text{g/mL}$ ] and *S. aculeastrum* [11.28 – 34.16  $\mu\text{g/mL}$ ]) in comparison to SRB (*B. disticha* [45.45 – 69.32  $\mu\text{g/mL}$ ] and *S. aculeastrum* [21.87 – 63.41  $\mu\text{g/mL}$ ]). For all other extracts cytotoxicity data compared well amongst the MTT, neutral red and SRB assays. The SRB and resazurin assays proved to offer the least technical and biological variability.

The largest difference between resazurin and the other assays was found for the methanol extract of *T. elegans*, where no IC<sub>50</sub> could be determined for the former (Table 7 and Figure 9). Furthermore, a slight increase in metabolic activity was noted for the methanol extract of *T. elegans* in the resazurin assay at lower concentrations ( $\leq 32$   $\mu\text{g/mL}$ ) (Figure 9).

**Table 7:** Comparison of four cytotoxicity assays using eight crude extracts.

Plant	Extract	IC <sub>50</sub> ( $\mu\text{g/mL}$ ) $\pm$ SEM			
		Resazurin	SRB	Neutral red	MTT
<i>A. oppositifolia</i>	Hot water	>100	13.86 $\pm$ 1.05	9.59 $\pm$ 1.07	11.52 $\pm$ 1.12
	Methanol	>100	26.63 $\pm$ 1.05	30.19 $\pm$ 1.00	22.20 $\pm$ 1.10
<i>B. disticha</i>	Hot water	>100	69.32 $\pm$ 1.08	32.77 $\pm$ 1.15	33.16 $\pm$ 1.17
	Methanol	>100	45.45 $\pm$ 1.07	18.07 $\pm$ 1.12	17.17 $\pm$ 1.21
<i>S. aculeastrum</i>	Hot water	>100	63.41 $\pm$ 1.02	22.02 $\pm$ 1.11	34.16 $\pm$ 1.10
	Methanol	>100	21.87 $\pm$ 1.10	11.28 $\pm$ 1.05	15.93 $\pm$ 1.06
<i>T. elegans</i>	Hot water	>100	>100	>100	>100
	Methanol	>100	3.57 $\pm$ 1.09	2.86 $\pm$ 1.00	4.76 $\pm$ 1.13

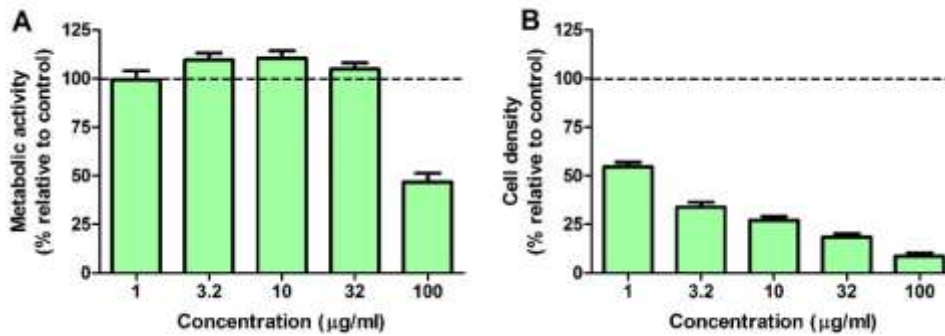


**Figure 9:** Comparison of the effect of the methanol extract of *T. elegans* on metabolic activity and cell density using the A) resazurin and B) SRB assays, respectively.

From the results obtained for the resazurin assay, it was decided to incubate the crude extracts with resazurin in the absence of cells to determine whether a spontaneous conversion was taking place. It was found that fluorescence was only slightly increased by the extract at 100 µg/mL, and largely by the positive control (1 mg/mL ascorbate) (Figure 10).

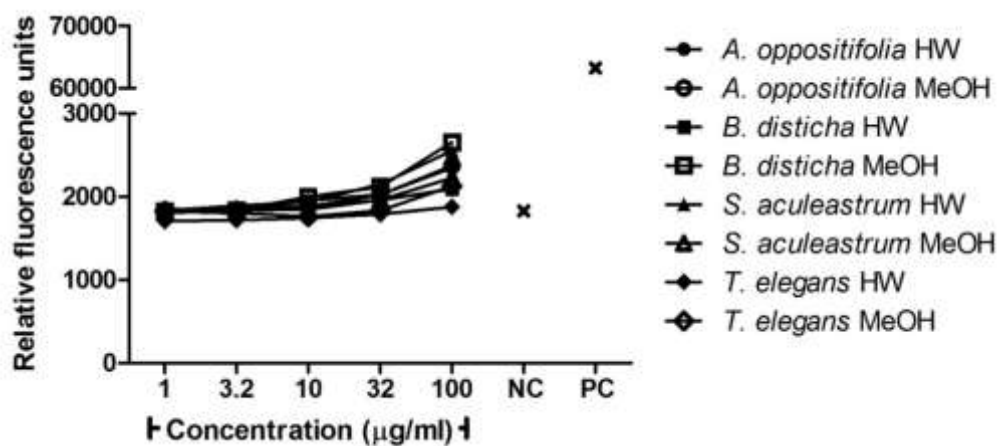


**Figure 10:** The effects of crude extracts on resazurin conversion in absence of cells; HW – hot water, MeOH – methanol; NC – negative control; PC – positive control (1 mg/mL ascorbate)

As resazurin was unable to detect cytotoxicity in the panel of crude extracts, and the MTT and neutral red assays proved to be more expensive, laborious, variable and presented with similar results for most of the extracts, it was decided that the SRB assay would be used to determine cytotoxic effects for the remainder of the study.

### 3.3.2. Determination of cytotoxic effects of crude extracts

The positive control, tamoxifen, induced a dose-dependent decrease in cell density (Figure 11), with an IC<sub>50</sub> of 6.18 µg/mL (16.63 µM) and 10.67 µg/mL (28.71 µM) in the HepG2 and Caco-2 cell lines, respectively (Table 8). Furthermore, the observed cytotoxicity had a narrow cytotoxicity index with a sharp decrease in cell density between 10 and 32 µg/mL (Figure 11).

Thirteen and twelve of the thirty-four extracts resulted in the inhibition of cell density by more than 50% at the highest concentration tested in the HepG2 and Caco-2 cell lines, respectively (Table 8). These crude extracts induced a dose-dependent decrease in cell density in both HepG2 (Figure 12) and Caco-2 cells (Figure 13). The crude extracts of *M. sericea* (Figure 12E and Figure 13D) and *S. aculeastrum* (Figure 12G and Figure 13G) presented with a narrow toxicity index similar to that of tamoxifen.

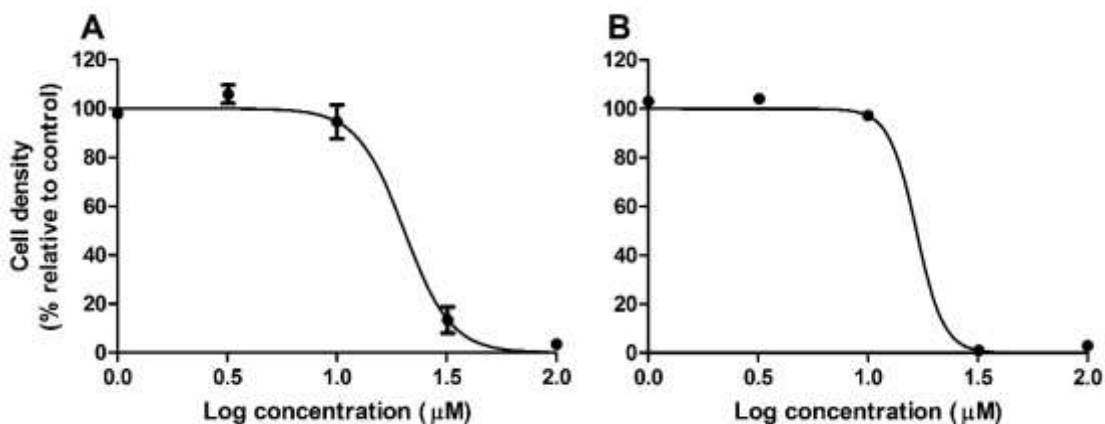


**Figure 11:** The effect of tamoxifen on A) Caco-2 and B) HepG2 cells



**Table 8:** Cytotoxicity of crude extracts in the HepG2 and Caco-2 cell lines (n = 9).

Plant	Extract	IC <sub>50</sub> ± SEM (µg/mL)	
		HepG2	Caco-2
<i>A. oppositifolia</i>	Hot water	13.86 ± 1.05	2.32 ± 1.05
	Methanol	26.63 ± 1.05	3.14 ± 1.06
<i>B. disticha</i>	Hot water	69.32 ± 1.08	18.72 ± 1.05
	Methanol	45.45 ± 1.07	13.36 ± 1.05
<i>B. africana</i>	Hot water	>100	>100
	Methanol	68.81 ± 1.07	>100
<i>C. laureola</i>	Hot water	>100	>100
	Methanol	>100	>100
<i>C. bulbispermum</i>	Hot water	>100	64.25 ± 1.03
	Methanol	67.24 ± 1.06	31.20 ± 1.05
<i>L. leonurus</i>	Hot water	>100	>100
	Methanol	>100	>100
<i>M. oleifera</i>	Hot water	>100	>100
	Methanol	>100	>100
<i>M. sericea</i>	Hot water	19.82 ± 1.08	>100
	Methanol	6.78 ± 1.05	15.43 ± 1.03
<i>P. capense</i>	Hot water	>100	>100
	Methanol	>100	72.94 ± 1.09
<i>R. caffra</i>	Hot water	>100	>100
	Methanol	>100	>100
<i>R. lancea</i>	Hot water	>100	>100
	Methanol	>100	>100
<i>S. puniceus</i>	Hot water	>100	>100
	Methanol	30.40 ± 1.06	30.75 ± 1.03
<i>S. latifolius</i>	Hot water	>100	>100
	Methanol	>100	>100
<i>S. aculeastrum</i>	Hot water	63.41 ± 1.02	40.24 ± 1.05
	Methanol	21.87 ± 1.1	22.23 ± 1.43
<i>T. elegans</i>	Hot water	>100	>100
	Methanol	3.57 ± 1.09	3.41 ± 1.06
<i>T. sericea</i>	Hot water	>100	>100
	Methanol	>100	>100
<i>Z. mucronata</i>	Hot water	>100	>100
	Methanol	82.08 ± 1.04	>100
Tamoxifen (µM)		16.63 ± 1.07	28.71 ± 1.10

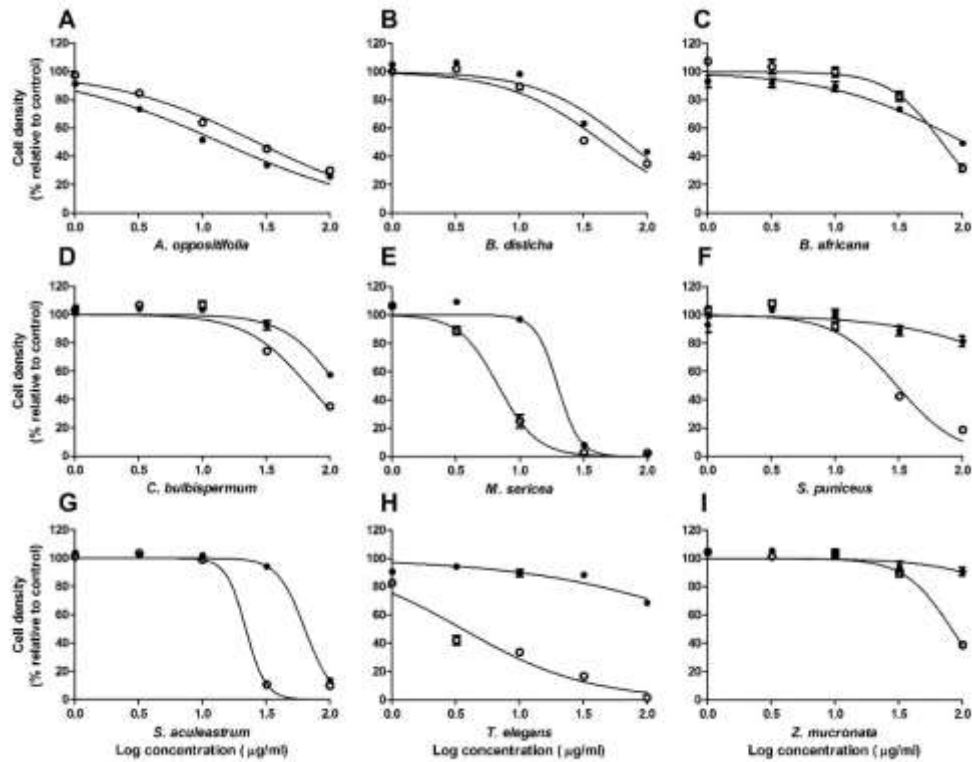


**Figure 12:** The effect of crude extracts of A) *A. oppositifolia*, B) *B. disticha*, C) *B. africana*, D) *C. bulbispermum*, E) *M. sericea*, F) *S. puniceus*, G) *S. aculeastrum*, H) *T. elegans* and I) *Z. mucronata* on the cell density of HepG2 cells. ● hot water extracts, ○ methanol extracts.

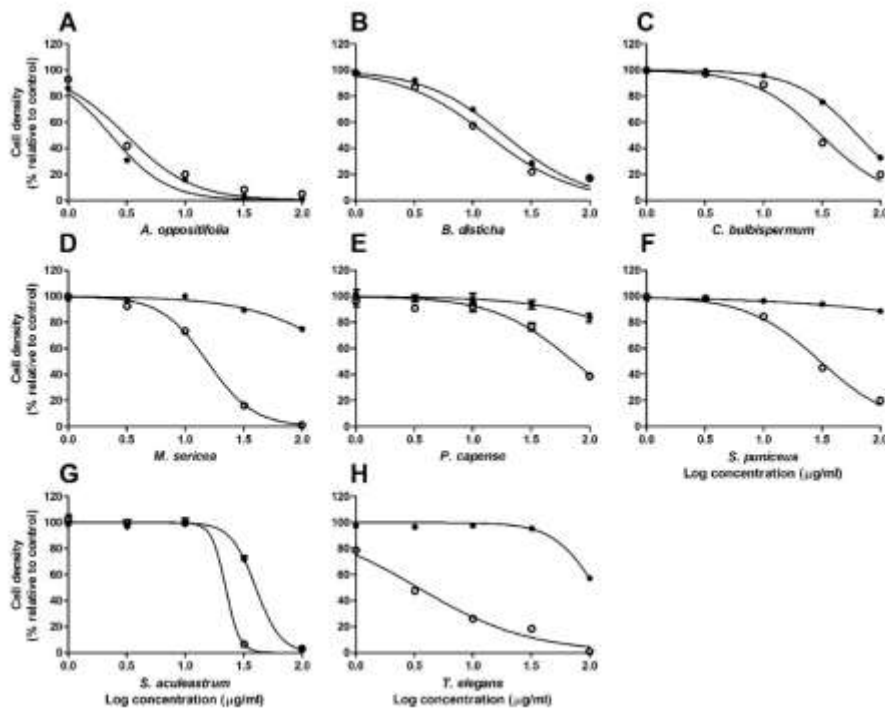


**Figure 13:** The effect of crude extracts of A) *A. oppositifolia*, B) *B. disticha*, C) *C. bulbispermum*, D) *M. sericea*, E) *P. capense*, F) *S. puniceus*, G) *S. aculeastrum* and H) *T. elegans* on the cell density of Caco-2 cells. ● hot water extracts, ○ methanol extracts.

With the exception of the crude extracts of *A. oppositifolia*, the methanol extracts were more cytotoxic than the hot water extracts. Cytotoxicity was generally higher in the Caco-2 cell line (nine extracts) than HepG2 cell line (four extracts). In the HepG2 cell line both extracts of *M. sericea*, and the methanol extracts of *B. africana* and *Z. mucronata* were more cytotoxic than for the Caco-2 cell line. Both extracts of *A. oppositifolia*, *B. disticha*, *C. bulbispermum* and *P. capense*, as well as the hot water extract of *S. aculeastrum*, were more cytotoxic to the Caco-2 cell line than the HepG2 cell line.

The potential for cytotoxicity is defined as high when an  $IC_{50} \leq 30 \mu\text{g/mL}$  is obtained.<sup>47</sup> In the HepG2 cell line high cytotoxicity was present for both extracts of *A. oppositifolia* (14 – 27  $\mu\text{g/mL}$ ) and *M. sericea* (7 – 20  $\mu\text{g/mL}$ ), as well as the methanol extracts of *S. puniceus* (30.4  $\mu\text{g/mL}$ ), *S. aculeastrum* (21.9  $\mu\text{g/mL}$ ) and *T. elegans* (3.57  $\mu\text{g/mL}$ ) (Table 8, Figure 14). In the Caco-2 cell line this was noted for both extracts of *A. oppositifolia* (2 – 3  $\mu\text{g/mL}$ ) and *B. disticha* (13 – 19  $\mu\text{g/mL}$ ), as well as the methanol extracts of *C. bulbispermum* (31.2  $\mu\text{g/mL}$ ), *M. sericea* (15.4  $\mu\text{g/mL}$ ), *S. puniceus* (30.8  $\mu\text{g/mL}$ ), *S. aculeastrum* (22.2  $\mu\text{g/mL}$ ) and *T. elegans* (3.4  $\mu\text{g/mL}$ ) (Table 8, Figure 14).

Four extracts increased cell density slightly in the Caco-2 cell line: both extracts of *B. africana* (Figure 15A, ~10%), and the methanol extracts of *R. caffra* (Figure 15B, 21.00%) and *S. latifolius* (Figure 15C, 28.88%). However, this increase was only dose-dependent for the extract of *S. latifolius* (Figure 15C).

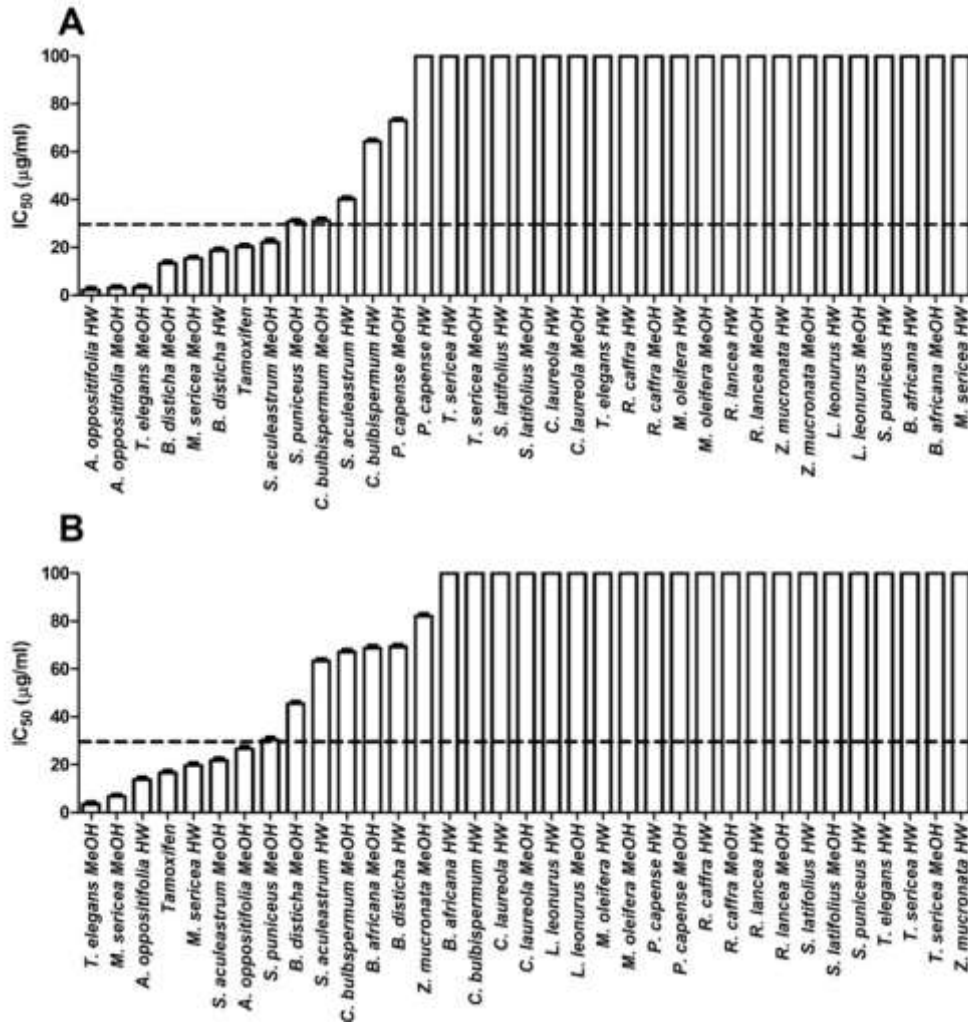


**Figure 14:** Cytotoxicity, expressed as the IC<sub>50</sub>, of the crude extracts arranged by reduction of cell density (black dashed line represents the active threshold) in the A) Caco-2 and B) HepG2 cell lines. Cytotoxicity at 100 µg/mL represents a value >100 µg/mL. HW – hot water extract; MeOH – methanol extract.

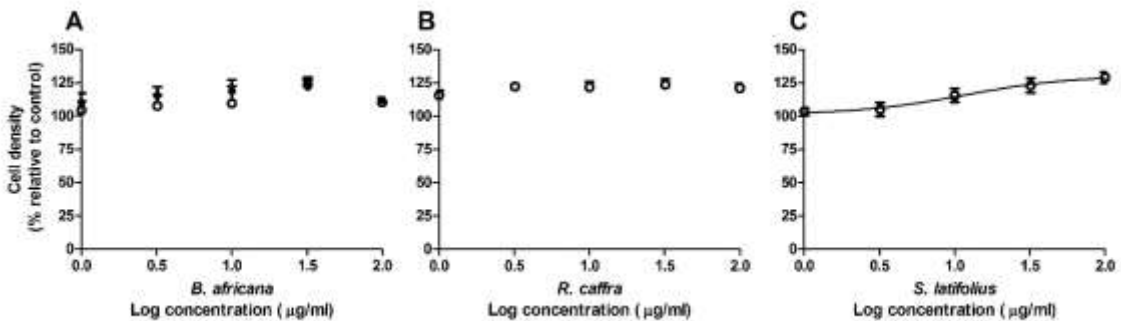


**Figure 15:** The effect of crude extracts of A) *B. africana*, B) *R. caffra* and C) *S. latifolius* on Caco-2 cells. ● hot water extracts, ○ methanol extracts. *S. latifolius* was the only crude extract that displayed an accurate dose-response fit using stimulatory non-linear regression.

### 3.4. Discussion

#### 3.4.1. The selection of cytotoxicity assay

A hormetic effect was evident in the resazurin assay when cells were exposed to the methanol extract of *T. elegans*, where metabolic activity increased at lower concentrations. This could indicate an adaptive, metabolic change within the cells to counteract the phytotoxicity of the crude extracts. To assess whether the extracts were directly converting resazurin to resorufin, cell-free assays were performed for further elucidation. Although a slight dose-dependent increase in fluorescent activity was found, this was not considered significant enough to explain the interference noted. As cells were necessary for this interaction to occur, it can be inferred that an upregulation of metabolic enzyme activity is needed for the conversion of resazurin. No correlation between the interaction and solvent type was present.

The interaction observed appeared to be specific towards the metabolic conversion of resazurin, as MTT was unaffected. As many mitochondrial and cytosolic enzymes are involved in the metabolic conversion,<sup>191</sup> it is possible that any of them may have been influenced without allowing for an overlap with MTT conversion. In support of the specific effect that may take place, glycolysis inhibitors have been shown to influence MTT conversion without altering resazurin.<sup>192</sup> Thus some substrate-specificity may be involved in the conversion, even though similar enzyme systems are involved. Spontaneous conversion of resorufin to non-fluorescent dihydroresorufin does occur, but only after a prolonged incubation period,<sup>191</sup> and thus this was not considered a likely possibility taking into consideration the time-course of the experiment. Although few compounds have been reported to alter resazurin conversion, many have been implicated in interference with MTT, such as dicoumarol,<sup>193</sup> epigallocatechin gallate,<sup>194</sup> various antioxidants, phytoestrogens and different plant extracts.<sup>195</sup> To the best of the authors knowledge, no literature was present describing phytochemical interference with resazurin, though it has been reported for some redox cycling compounds (that increase ROS production)<sup>196</sup> and nanoparticles<sup>197</sup>. As only the HepG2 cell line was studied, it is possible that a different scenario may be apparent in other cell lines.

The SRB and resazurin assays proved to be less variable than the MTT and neutral red assays. Cytotoxicity was underestimated for the resazurin assay, while the MTT

and neutral red offered higher sensitivity for four of the extracts. This could be due to potential selective toxicity against mitochondria or lysosomes, respectively, and brings to light the importance of multiple assessment criteria. As SRB proved to be reproducible and offered high sensitivity, which is also supported by literature,<sup>188</sup> it was chosen for the remainder of cytotoxicity testing.

### 3.4.2. Effects of crude extracts on the HepG2 and Caco-2 cell lines

Preliminary cytotoxicity screening using the HepG2 and Caco-2 cell lines was performed to determine which plants would be selected to undergo further hepatotoxic evaluation, and to account for possible confounding factors in future drug-herb interaction assays. Three groups of plants were subsequently selected: i) those presenting with a mixture of high hepatotoxic potential (*A. oppositifolia*, *S. aculeastrum* and *T. elegans*), ii) moderate cytotoxicity (*B. disticha*) and iii) those presenting with low cytotoxic potential and beneficial health effects as supported by literature (*M. oleifera*, *T. sericea* and *Z. mucronata*). These three groups were selected to provide toxicological information on the spectrum of toxicity. These results will be discussed separately in Chapter 4.

Phytotoxicology with regards to hepatic and intestinal cytotoxicity is poorly described in literature, and as such the results obtained aim to increase the toxicological knowledge of the plants investigated. It is important to note that the cell lines used in this study are of cancerous origin, and thus may present with an altered response towards cytotoxins, though they do provide a model for further assessment. In general cytotoxicity was more prominent in the Caco-2 cell line, indicating a potential selective cytotoxicity for intestinal cells, rather than for those of hepatic origin. As an area of main absorption for oral administered drugs, this may incur gastrointestinal irregularities and toxicity. A discussion on the cytotoxicity will be approached from the perspective of the different plant families. Cytotoxicity data that could be obtained for the plants discussed in this chapter have been summarised in Table 9.

**Table 9:** IC<sub>50</sub>'s of plants selected for study (excluding those discussed in Chapter 4) as obtained from literature.

Family	Plant	Part	Extract	Cell line used	Cytotoxicity assay	Time point	IC <sub>50</sub> (µg/mL)	References
Amaryllidaceae	<i>C. bulbispermum</i>	Bulbs	Ethyl acetate	SH-SY5Y neuroblastoma	SRB	72 h	>100	198
			Methanol				46.18	
		Flowering bulbs	Ether fraction of alkaline extract	N/A	Brine shrimp	24 h	73	92
		Non-flowering bulbs	Butanol fraction of acidic extract				63.10	
		Roots	Ethyl acetate	SH-SY5Y neuroblastoma	MTT / NR	72 h	10.71 - 12.53	200
	<i>S. puniceus</i>	Bulbs	Ethyl acetate	SH-SY5Y neuroblastoma	SRB	72 h	37.40	198
			Hot water	MCF-7 breast carcinoma	SRB	72 h	>100	Appendix IV
				MDA-MB-231 breast carcinoma			>100	
				SK-Br-3 breast carcinoma			>100	
			Methanol	MCF-7 breast carcinoma	SRB	72 h	13.27	
				MDA-MB-231 breast carcinoma			23.95	
				SK-Br-3 breast carcinoma			56.78	
	Methanol	SH-SY5Y neuroblastoma	SRB	72 h	20.75	198		

Family	Plant	Part	Extract	Cell line used	Cytotoxicity assay	Time point	IC <sub>50</sub> (µg/mL)	References	
Anacardiaceae	<i>R. lancea</i>	Bark	Hexane	N/A	Brine shrimp	24 h	>5000	201	
			Methanol				>5000		
			Water				3900		
		Fruits	Dichloromethane	MCF-7 breast carcinoma	SRB	48 h	16.66*	202	
				TK10 renal carcinoma			15*		
				UACC62 melanoma			13.33*		
		Leaves	Hexane	N/A	Brine shrimp	24 h	>5000	201	
							Methanol		1000
							Water		600
		Stems	Dichloromethane	MCF-7 breast carcinoma	SRB	48 h	19.12*	202	
				TK10 renal carcinoma			14.71*		
				UACC62 melanoma			13.56*		
Apocynaceae	<i>R. caffra</i>	Roots	Dichloromethane	L6 murine skeletal myocyte	RZN	68 h	46.60	203	
Asteraceae	<i>C. laureola</i>	Roots	Aqueous	HepG2 hepatocarcinoma	MTT	24 h	3500#	111	
Fabaceae	<i>B. africana</i>	Bark	Aqueous	3T3-L1 pre-adipocytes	NR	72 h	84.50	59	
				C2C12 myeloblasts			42.50		
				Normal human dermal fibroblasts			>100		
				U937 monoblastic cells			>100		

Family	Plant	Part	Extract	Cell line used	Cytotoxicity assay	Time point	IC <sub>50</sub> (µg/mL)	References	
Fabaceae	<i>B. africana</i>	Bark	Methanol	3T3-L1 pre-adipocytes	NR	72 h	28.50	59	
				C2C12 myeloblasts			16		
				Normal human dermal fibroblasts			>100		
				U937 monoblastic cells			>100		
		Stem	Ethanol	N/A		Brine shrimp	24 h	87.24	204
	<i>M. sericea</i>	Roots	Hot water		MCF-7 breast carcinoma	SRB	72 h	64.34	Appendix IV
					MDA-MB-231 breast carcinoma			>100	
					SK-Br-3 breast carcinoma			36.44	
			Methanol	MCF-7 breast carcinoma	2.39				
				MDA-MB-231 breast carcinoma	9.25				
SK-Br-3 breast carcinoma				19.28					
Lamiaceae	<i>L. leonurus</i>	Flowers	Aqueous	Brine shrimp	Brine shrimp	24 h	>1000	142	
				K562 myelogenous leukaemia	MTT	20 h	>1000		
			Hydro-methanol	H460 lung carcinoma	SRB	48 h	>10	133	
				HCT116 colon carcinoma			>10		
				HeLa cervical carcinoma			>10		

Family	Plant	Part	Extract	Cell line used	Cytotoxicity assay	Time point	IC <sub>50</sub> (µg/mL)	References
Lamiaceae	<i>L. leonurus</i>	Flowers	Hydro-methanol	HepG2 hepatocarcinoma	SRB	48 h	>10	133
				MCF-7 breast carcinoma			>10	
				U251 brain tumour			>10	
		Methanol	Brine shrimp	Brine shrimp	24 h	>1000	142	
			K562 myelogenous leukaemia	MTT	20 h	>1000		
		Aqueous	Brine shrimp	Brine shrimp	24 h	>1000		
			K562 myelogenous leukaemia	MTT	20 h	>1000		
		Leaves	Dichloromethane-methanol	L6 murine skeletal myocyte	RZN	68 h	14.10	203
			Methanol	Brine shrimp	Brine shrimp	24 h	>1000	142
		K562 myelogenous leukaemia		MTT	20 h	>1000		
		Roots	Tannin-free aqueous	A-549 lung epithelial	MTT	25 h	>500	205
				HL-60 acute promyelocytic leukaemia			>500	
HT-29 colon adenocarcinoma	>500							
K562 chronic myelogenous leukaemia	>500							

Family	Plant	Part	Extract	Cell line used	Cytotoxicity assay	Time point	IC <sub>50</sub> (µg/mL)	References
Lamiaceae	<i>L. leonurus</i>	Roots	Tannin-free aqueous	MCF-7 breast carcinoma	MTT	25 h	>500	205
			Tannin-free methanol	A-549 lung epithelial	MTT	25 h	269.02	
				HL-60 acute promyelocytic leukaemia			262.09	
				HT-29 colon adenocarcinoma			327.46	
				K562 chronic myelogenous leukaemia			62.47	
				MCF-7 breast carcinoma			145.90	
Piperaceae	<i>P. capense</i>	Aerial	Chloroform	THP-1 monocytes	PI	72 h	>50	206
			Methanol				>50	
		Fruits	Essential oils	A375 malignant melanoma	MTT	72 h	76	207
				HCT116 colon carcinoma			22.70	
				MDA-MB-231 breast carcinoma			26.30	
		Root-bark	Acetone	C2C12 myeloblasts	MTT	72 h	43.89	166
				PHA-stimulated human lymphocytes			28.13	
				Resting human lymphocytes			16.82	

Family	Plant	Part	Extract	Cell line used	Cytotoxicity assay	Time point	IC <sub>50</sub> (µg/mL)	References
Piperaceae	<i>P. capense</i>	Root-bark	Chloroform partition of methanol extract	KB oral epidermoid carcinoma	SRB	72 h	>20	46
			Hexane	C2C12 myeloblasts	MTT	72 h	3.01	166
				PHA-stimulated human lymphocytes			0.62	
				Resting human lymphocytes			1.64	
			Methanol	C2C12 myeloblasts			11.94	
				PHA-stimulated human lymphocytes			28.42	
				Resting human lymphocytes			6.23	
			Water	C2C12 myeloblasts			144.44	
				PHA-stimulated human lymphocytes			52.30	
		Resting human lymphocytes		49.74				
		Seeds	Methanol	AML12 hepatocytes	RZN	48 h	>40	208
				CCRF-CEM leukaemia	MTS	48 h	7.03	209
				CCRF-CEM leukaemia	RZN	48 h	6.95	208
CCRF-CEM/ADR5000 resistant leukaemia	MTS			48 h	6.56	208		

Family	Plant	Part	Extract	Cell line used	Cytotoxicity assay	Time point	IC <sub>50</sub> (µg/mL)	References
Piperaceae	<i>P. capense</i>	Seeds	Methanol	HCT116 p53-/- resistant colon carcinoma	RZN	48 h	4.62	208
				HCT116 p53+/+ colon carcinoma			4.64	
				HepG2 hepatocarcinoma			16.07	
				HL-60 acute promyelocytic leukaemia			8.16	
				HL-60/AR resistant leukaemia			11.22	
				Human umbilical vein epithelial cells	MTS	48 h	>80	208
				MDA-MB-231 breast carcinoma	RZN	48 h	4.17	208
				MDA-MB-231-BCRP resistant breast carcinoma			19.45	
				Mia PaCa2 prostate carcinoma	MTS	48 h	8.92	208
				U87MG glioblastoma	RZN	48 h	13.48	208
U87MGΔEGFR resistant glioblastoma	7.44							

N/A – not applicable; SRB – sulphorhodamine B protein staining assay; MTT - 3-(4,5-dimethylthiazol-2-yl)-2,5-diphenyltetrazolium bromide conversion assay; NR – neutral red lysosome staining assay; RZN – resazurin conversion assay; PI – propidium iodide; MTS - 3-(4,5-dimethylthiazol-2-yl)-5-(3-carboxymethoxyphenyl)-2-(4-sulfophenyl)-2H-tetrazolium conversion assay. \* – total growth inhibition values; # – concentration deemed as dried plant material per mL diluent

### 3.4.2.1. Amaryllidaceae

The hot water extract of *C. bulbispermum* displayed little cytotoxicity in the HepG2 cell line (42.67% at 100 µg/mL), while its methanol counterpart was more active (IC<sub>50</sub> = 67.24 µg/mL). The Caco-2 cell line (hot water IC<sub>50</sub> = 64.25 µg/mL; methanol = 31.20 µg/mL) was more susceptible to cytotoxic effects. It is apparent that moderate cytotoxicity is induced by organic extracts of *C. bulbispermum*.<sup>198</sup> The methanol extract of the bulbs induced moderate cytotoxicity in the SH-SY5Y neuroblastoma cell line (Table 9).<sup>198</sup> The ethyl acetate extract of the bulbs displayed no cytotoxic potential,<sup>198</sup> while the ethyl acetate extract of the roots displayed prominent cytotoxicity (Table 9).<sup>199</sup> Ether and butanol fractions of pH-adjusted extracts of the flowering and non-flowering bulbs, respectively, induced moderate toxicity in the brine shrimp assay (Table 9).<sup>92</sup> While the hot water extract of *S. puniceus* was not highly cytotoxic in the HepG2 and Caco-2 cell lines (18.76% and 11.34% cell death at 100 µg/mL, respectively), the methanol extract induced similar cytotoxicity in both cell lines (IC<sub>50</sub> = ~30 µg/mL). This may imply a non-specific mechanism of cytotoxicity. The low cytotoxic potential of the hot water extract (Appendix IV), and greater cytotoxicity of the organic extracts has been described in literature<sup>198</sup> (Appendix IV).

*C. bulbispermum* and *S. puniceus* belong to the Amaryllidaceae family, and the isoquinoline-alkaloids (**Error! Not a valid bookmark self-reference.**) are believed to be responsible for toxicity due to their poisonous nature.<sup>57</sup> The phytochemicals most likely responsible for the reduction in cell density observed after exposure to *C. bulbispermum* may be bulbispermine,<sup>210</sup> 6-hydroxycrinamine,<sup>89</sup> lycorine<sup>211–215</sup> and vittatine.<sup>216</sup> Buphanidrine<sup>217</sup> and caranine<sup>212</sup> appear to be less active. Lycorine may serve as the main contributor to the effects seen. Mechanistically lycorine incurs greater antiproliferative activity than cytotoxicity, as do many other Amaryllidaceae alkaloids.<sup>212</sup> Lycorine may induce a G0/G1-<sup>213</sup> or G2/M-arrest,<sup>214</sup> with subsequent apoptosis through either the intrinsic or extrinsic pathway.<sup>211</sup> As alkaloids were only identified in the methanol extract, it may shed some light on lack of cytotoxicity present in the hot water extract, as lycorine and associated alkaloid content might have been too low to induce significant cytotoxic effects. The membrane-rupturing capabilities of saponins are well-known.<sup>218,219</sup> Saponins appear to generally have low bioavailability due to poor intestinal absorption,<sup>219</sup> and thus may exert a much more potent effect in

the intestine. Supporting this is the higher potency seen for *C. bulbispermum* and *B. disitcha*

**Table 10:** Summary of the cytotoxic properties of Amaryllidaceae-type isoquinoline alkaloids that have been identified in the studied plants

Alkaloids	Present in	Cell line used	Cytotoxicity assay	Time point	IC <sub>50</sub> (µM)	Additional effects	References
Ambelline	<i>C. bulbispermum</i>	A549 lung carcinoma	MTT	72 h	>10	Inactivity due to β-ethano bridge	212
		OE21 oesophageal squamous carcinoma			86		
		Hs 683 glioma			>10		
		U373 asatocytoma			>10		
		SKMEL melanoma			>10		
		B16F10 murine melanoma			>10		
Bulbispermine	<i>C. bulbispermum</i>	HL-60 acute promyelocytic leukaemia			17.80	Activity related to C-3β-methoxy group and hydrogenation of double bond between -1 and C2	210
Buphanamine	<i>B. disticha</i>	A549 lung carcinoma			>10	Inactivity due to β-ethano bridge	212
		OE21 oesophageal squamous carcinoma			>10		
		Hs 683 glioma			>10		
		U373 asatocytoma	>10				
		SKMEL melanoma	>10				
		B16F10 murine melanoma	>10				
Buphanidrine	<i>C. bulbispermum</i>	CEM leukaemia	>50	-	217		
		K562 myelogenous leukaemia	Calcein-AM			>50	

Alkaloids	Present in	Cell line used	Cytotoxicity assay	Time point	IC <sub>50</sub> (μM)	Additional effects	References
Buphanidrine	<i>C. bulbispermum</i>	MCF-7 breast carcinoma	Calcein-AM		>50	-	217
		HeLa cervical carcinoma			>50		
		G-361 melanoma			>50		
		BJ fibroblast			>50		
Buphanisine	<i>B. disticha</i>	A549 lung carcinoma	MTT	72 h	>10	Inactivity due to β-ethano bridge	212
		OE21 oesophageal squamous carcinoma			97		
		Hs 683 glioma			>10		
		U373 asatrocytoma			>10		
		SKMEL melanoma			>10		
		B16F10 murine melanoma			>10		
Caranine	<i>C. bulbispermum</i>	A549 lung carcinoma	MTT	72 h	>10	Inactivity due to lack of C-2 hydroxy group	212
		OE21 oesophageal squamous carcinoma			>10		
		Hs 683 glioma			>10		
		U373 asatrocytoma			>10		
		SKMEL melanoma			>10		
		B16F10 murine melanoma			>10		
Distichamine	<i>B. disticha</i>	CEM leukaemia	Calcein-AM		4.50	Dose-dependent G2/M-block and apoptotic activity	217

Alkaloids	Present in	Cell line used	Cytotoxicity assay	Time point	IC <sub>50</sub> (µM)	Additional effects	References
Distichamine	<i>B. disticha</i>	K562 myelogenous leukaemia	Calcein-AM	72 h	4.10	-	217
		MCF-7 breast carcinoma			2.30		
		HeLa cervical carcinoma			2.20		
		G-361 melanoma			14.70		
		BJ fibroblast			10.50		
Galanthamine	<i>C. bulbispermum</i>	CEM leukaemia			>50		
		K562 myelogenous leukaemia			>50		
		MCF-7 breast carcinoma			>50		
		HeLa cervical carcinoma			>50		
		G-361 melanoma			>50		
		BJ fibroblast			>50		
Haemanthamine	<i>S. puniceus</i>	A549 lung carcinoma	MTT	72 h	4.50	Cytostatic effect observed with videomicroscopy, no cytotoxicity. Activity due to α-ethano bridge	212
		OE21 oesophageal squamous carcinoma			6.80		
		Hs 683 glioma			7.00		
		U373 asatrocytoma			7.70		
		SKMEL melanoma			8.50		
		B16F10 murine melanoma			6.80		
		CEM leukaemia			2.10		
		K562 myelogenous leukaemia	Calcein-AM	3.40	-	217	

Alkaloids	Present in	Cell line used	Cytotoxicity assay	Time point	IC <sub>50</sub> (μM)	Additional effects	References
Haemanthamine	<i>S. puniceus</i>	MCF-7 breast carcinoma	Calcein-AM	72 h	8.10	-	217
		HeLa cervical carcinoma			7.00		
		G-361 melanoma			3.70		
		BJ fibroblast			2.70		
		Caco-2 colon carcinoma	MTT		0.99		215
		HT-29 gastrointestinal carcinoma			0.59		
		FHs 74 Int			19.50		
		HL-60 acute promyelocytic leukaemia			2.00		
HSC-2 oral squamous cell carcinoma		33.20					
HL-60 acute promyelocytic leukaemia		2.00			210		
HSC-2 oral squamous cell carcinoma		13.30					
A549 lung carcinoma		4.00					
OE21 oesophageal squamous carcinoma		3.70					
Haemanthidine			Hs 683 glioma				4.30
	U373 asatrocytoma		3.80				
	SKMEL melanoma		4.20				

Alkaloids	Present in	Cell line used	Cytotoxicity assay	Time point	IC <sub>50</sub> (µM)	Additional effects	References
Haemanthidine	<i>S. puniceus</i>	B16F10 murine melanoma	MTT	72 h	3.10	Cytostatic effect observed with videomicroscopy, no cytotoxicity. Activity due to α-ethano bridge	212
		Caco-2 colon carcinoma			3.30		-
		HT-29 gastrointestinal carcinoma			1.70		
		FHs 74 Int			11.60		
6-Hydroxycrinamine	<i>B. disticha</i> <i>C. bulbispermum</i> <i>S. puniceus</i>	SH-SY5Y neuroblastoma	MTT and NR		54.50 – 61.70		89
Lycorine	<i>B. disticha</i> <i>C. bulbispermum</i>	A549 lung carcinoma	MTT		4.20	Cytostatic effect observed with videomicroscopy, no cytotoxicity. Unmodified C-ring and C/D-ring junction important for activity	212
		OE21 oesophageal squamous carcinoma			4.50		
		Hs 683 glioma			6.90		
		U373 asatrocytoma			7.60		
		SKMEL melanoma			8.40		
		B16F10 murine melanoma		6.30			
		CEM leukaemia	Calcein-AM	1.60	-	217	
		K562 myelogenous leukaemia		3.60			
		MCF-7 breast carcinoma		13.00			
		HeLa cervical carcinoma		10.60			
G-361 melanoma	5.00						
BJ fibroblast	1.90						

Alkaloids	Present in	Cell line used	Cytotoxicity assay	Time point	IC <sub>50</sub> (µM)	Additional effects	References
Lycorine	<i>B. disticha</i> <i>C. bulbispermum</i>	Hey1B ovarian carcinoma	Alamar Blue	46 h	1.20	Dose-dependent G2/M-block	214
		Caco-2 colon carcinoma	MTT	72 h	0.99	-	215
		HT-29 gastrointestinal carcinoma			1.20		
		FHs 74 Int			22.70		
		K562 myelogenous leukaemia	CCK-8	48 h	N/S	G0/G1-block as a result of histone deacetylase inhibition, and upregulation of p53 and p21	213
		KM3 multiple myeloma	MTT		1.25	G0/G1-block, and apoptotic activity from intrinsic and extrinsic pathway	211
Vittatine	<i>C. bulbispermum</i>	HT-29 colon adenocarcinoma	SRB	N/S	21.91	-	216
		H460 non-small cell lung carcinoma			15.88	-	
		RXF393 renal cell carcinoma			29.57	-	

CCK-8 – Cell Counting Kit-8; MTT - 3-(4,5-dimethylthiazol-2-yl)-2,5-diphenyltetrazolium bromide conversion assay; N/S – not stated; NR – neutral red staining assay; RZN – resazurin conversion assay; SRB – sulforhodamine B staining

Haemanthamine,<sup>210,212,215,217</sup> haemanthidine<sup>210,212,215</sup> and to a lesser extent, 6-hydroxycrinamine,<sup>89</sup> have been described to elicit cytotoxicity. These three phytochemicals have previously been identified in *S. puniceus* and reported in literature. Haemanthamine and haemanthidine are active in the low micromolar range, and furthermore appear to offer more of a cytostatic than a cytotoxic effect<sup>212</sup>. As with *C. bulbispermum*, no alkaloids were present in the hot water extract, which was devoid of a cytotoxic effect. Thus it can be summarised that alkaloidal presence is required for cytotoxicity.

#### **3.4.2.2. Anacardiaceae**

Both extracts of *R. lancea* presented with negligible cytotoxicity, only inducing between 6.34% and 11.17% at 100 µg/mL in both cell lines. The low cytotoxic potential of the bark and leaves has been described in literature (Table 9),<sup>220</sup> while cytotoxicity appears to be confined to the stems and fruits (Table 9).<sup>202</sup>

#### **3.4.2.3. Apocynaceae**

Neither extracts of *R. caffra* displayed prominent cytotoxicity in the HepG2 and Caco-2 cell lines, inducing between 6.06% to 14.42% reduction of cell density at 100 µg/mL. Furthermore, the methanol extract increased cellular density by up to 21.00% in the Caco-2 cell line. Apart from a study indicating moderate cytotoxic effects in the L6 murine skeletal myocyte cell line by a dichloromethane extract of the root, no other reports could be found (Table 9).<sup>203</sup>

#### **3.4.2.4. Asteraceae**

The extracts of *C. laureola* did not induce any alteration in cell density in the HepG2 cell line, while in the Caco-2 cell line approximately 13% reduction of cell density occurred. Although no significant changes in cell density were noted in the present study, research highlights the cytotoxic effects of *C. laureola* (although the concentration tested was not stated).<sup>221</sup> A decoction at 10 mg/mL (based on root

powder per mL of diluent) induced approximately 80% cellular death in HepG2 cells after 24 h, though concurrent treatment with n-acetylcysteine reduced this significantly to 40%. Also, GSH concentrations were adversely affected in a time-dependent manner, which could be the mechanism behind its hepatotoxic response.<sup>221</sup> Furthermore, in HuH-7 hepatoma cells it was shown that a decoction induced slight apoptosis and G2/M cell cycle arrest, as well as destruction of cytoplasmic tubulin, and nuclear condensation.<sup>111</sup> Although not inducing cytotoxicity in human peripheral blood mononuclear cells, *C. laureola* at 10 mg/mL (dried plant material per mL diluent) induced slight genotoxicity as a hot water extract (1.4-fold), but significantly more for the methanol extract (2.8-fold).<sup>113</sup>

*C. laureola* is known as a highly toxic plant,<sup>101</sup> so much so that a suggestion for its ban by the KwaZulu-Natal Provincial Department of Health was made in 1995.<sup>222</sup> It contains diterpenoid toxins, though its major toxic phytochemical is thought to be the kaurene glycoside atractyloside and carboxyatractyloside.<sup>57,111</sup> It is possible that the lack of metabolic competence in the HepG2 cell line may have decrease conversion to carboxyatractyloside, and thus may have contributed to the lack of effects observed. *C. laureola* has been implicated in sporadic reports of hepatotoxicity, though the role of atractyloside in this has been subject to controversy.<sup>28</sup> Mitochondrial toxicity, with subsequent activation of apoptotic or necrotic pathways may be incurred by high enough concentrations of atractyloside in some hepatic cell lines,<sup>111</sup> which may also be inactive in other cells.<sup>221</sup> It appears that atractyloside acts as a potent nephrotoxin,<sup>31</sup> thus the true hepatotoxin may still be unidentified.

While the hot water extract of *S. latifolius* displayed slight reduction of cell density at 100 µg/mL (6.59% and 14.30% in the HepG2 and Caco-2 cell line, respectively), the methanol extract induced no alteration in the HepG2 cell line and a 28.88% increase in the Caco-2 cell line. The latter increase was dose-dependent. Hot water decoctions (10 mg/mL) have been shown to reduce HepG2 cell viability (approximately 40% after 6 h exposure) due to a depletion of GSH and induction of apoptosis.<sup>32</sup> The cytotoxicity was shown to be attenuated through the use of n-acetylcysteine and caspase inhibitor IDN-1965, further highlighting the involvement of GSH and caspases in the induction of *S. latifolius*-induced apoptosis.<sup>32</sup> Furthermore, a hot water retrorsine-containing extract was found to induce cellular death through apoptosis, with cytoskeletal and nuclear damage.<sup>223</sup> The high concentrations used in the published studies could

explain the lack of cytotoxicity seen in the current project. The slight increase in Caco-2 cell density induced by the methanol extract may be an indication of a proliferative ability, though this would need to be ascertained using validated proliferation studies. Whether or not this can be considered a carcinogenic activity is debatable. Retrorsine and *S. latifolius* supplementation (albeit a hot water extract) was found to alter nuclear morphology in HuH-7 hepatoma, which may be downstream carcinogenicity.<sup>223</sup> If this would result in increased proliferation, it may elude to the mechanism behind the increase in cell density.

Pyrrrolizidine alkaloids are commonly found in many plant families, including the Asteraceae, of which a large quantity are classified as hepatotoxins. Otonecine- and retronecine-type pyrrrolizidine alkaloids are considerably more cytotoxic when metabolised by the liver to pyrroles, which may then bind to cellular proteins.<sup>224</sup> The macrocyclic pyrrrolizidine alkaloids, retrorsine and istaidine, display strong liver carcinogenicity and mutagenicity,<sup>225</sup> and elicit cytotoxicity in HepG2 cells (although at high concentrations)<sup>32,224</sup> and rat hepatocytes.<sup>226</sup> As the cytotoxicity of many of these pyrrrolizidine alkaloids, such as retrorsine,<sup>227</sup> are dependent on metabolic activation which may be reduced in the metabolically incompetent HepG2 cell line, it is proposed that the lack of effect seen in the present study may either be low concentrations of the alkaloids, or a lack of pyrrole formation.

#### **3.4.2.5. Fabaceae**

While the hot water extract of *B. africana* presented with cytotoxicity (50.63% at 100 µg/mL) in the HepG2 cell line, the methanol extract was significantly more cytotoxic (IC<sub>50</sub> = 68.81 µg/mL). No cytotoxicity was apparent in the Caco-2 cell line (approximately 110% cell density for both extracts), which indicates selective cytotoxicity towards liver cells. The higher cytotoxic potential of the methanol extract is supported by literature in which 3T3-L1 pre-adipocytes and C2C12 myoblast cells were affected to a greater extent than in the current study (Table 9).<sup>59</sup> Alcoholic extracts of stems also appear to offer a certain degree of cytotoxicity (Table 9).<sup>204</sup> However, the absence of cytotoxicity seen in the Caco-2 cell line is supported by the results obtained in U937 monocytic and normal human dermal fibroblast cells (Table 9).<sup>59</sup> It is thus apparent that alcoholic extractions are more cytotoxic, though the

phytochemical matrix is selective in cytotoxicity, and does not appear to offer broad detrimental effects.

Cytotoxicity was more prominent in the HepG2 cell line for extracts of *M. sericea*. While the hot water extract failed to induced cytotoxicity in the Caco-2 cell line (25.11%), its effect was greater in the HepG2 cell line ( $IC_{50} = 19.82 \mu\text{g/mL}$ ). Cytotoxicity was more prominent in the HepG2 than the Caco-2 cell line, with  $IC_{50}$ 's of  $6.78 \mu\text{g/mL}$  and  $15.43 \mu\text{g/mL}$ , respectively. The methanol extract has previously been found to display greater cytotoxicity than the hot water extract, though the latter does appear to offer moderate cytotoxicity in different cell lines (Appendix IV).

*M. sericea* is a well-known fish poison, which may also induce toxicity in humans. Rotenoids are inhibitors of the mitochondrial respiratory chain, and thus reduce cellular respiration and energy production.<sup>228</sup> Rotenoids (deguelin), flavonoids (munetone), and chalcones (munsericin) have been shown to reduce ornithine decarboxylase-mediated cellular proliferation when stimulated with various cancerous agents.<sup>132,229,230</sup> Ornithine decarboxylase is a rate-limiting enzyme required for the synthesis of polyamines, essential components for cellular proliferation.<sup>230</sup> Thus inhibition of this enzyme will ultimately induce an antiproliferative effect and reduction of cancerous growth.<sup>132</sup> Furthermore, deguelin attenuates the glycogen synthase-3  $\beta/\beta$ -catenin,<sup>231</sup> epidermal growth factor<sup>232</sup> and nuclear factor-kappa B (NF- $\kappa$ B) pathway,<sup>230</sup> which reduces proliferation, and promotes apoptotic pathways. Of concern is the fact that the hot water extract of *M. sericea* induced a prominent hepatotoxic effect, which although it supports its use as a fish poison, highlights the possibly of poisoning during use.

#### **3.4.2.6. Lamiaceae**

The extracts of *L. leonurus* were not cytotoxic to either cell line. The hot water extract (12.51%) induced a greater effect in the HepG2 cell line than the methanol extract (3.67%) at  $100 \mu\text{g/mL}$ . Reduction of cell density was slightly higher in the Caco-2 cell line, with the methanol extract (30.09%) inducing more cytotoxicity than the hot water extract (17.73%). The low cytotoxic potential of the leaves,<sup>142</sup> flowers<sup>133,142</sup> and roots<sup>205</sup> are supported by literature (Table 9). It is important to note though that the

flowers were not tested at concentrations greater than 10 µg/mL.<sup>133</sup> Only two reports could be found of high to moderate cytotoxicity of leaves<sup>203</sup> and roots<sup>205</sup> (Table 9). The cytotoxicity presented for the former was seen in a slightly less polar extract,<sup>203</sup> thus it is conceivable that non-polar moieties from *L. leonurus* are more detrimental to cellular health and may thus explain why this was not seen in the present study. However, a *in vivo* Wistar rat study described potential toxicity with regards to haematological, liver and kidney parameters at moderately high concentrations,<sup>233</sup> thus caution is suggested when used.

#### 3.4.2.7. Piperaceae

Both extracts of *P. capense* displayed negligible cytotoxicity in the HepG2 cell line (between 5.70% and 26.54% at 100 µg/mL), as well as the hot water extract in the Caco-2 cell line (16.15% at 100 µg/mL). The methanol extract however displayed moderate cytotoxicity with an IC<sub>50</sub> of 72.94 µg/mL in the Caco-2 cell line. The low cytotoxic potential of the aerial parts has been described in literature,<sup>206</sup> though moderate to high cytotoxicity has been ascribed to the essential oil of the fruits,<sup>207</sup> organic extracts of the root-bark<sup>166</sup> and methanol extracts of seeds<sup>209</sup> (Table 9). Although water extracts of the root-bark did induce cytotoxicity, it was to a lower extent than the organic counterparts (Table 9),<sup>166</sup> which is similar to what was found in the current study. Conflicting evidence is present with regards to the tumour selectivity of the root-bark and seed extracts compared to primary cell lines (Table 9),<sup>46,209</sup> thus it is uncertain whether or not the extract displays a non-selective cytotoxic effect. Mechanistically methanol extracts of the seeds induced cytotoxicity through G0/G1 cell cycle arrest, mitochondrial toxicity and apoptosis,<sup>209</sup> though no evidence is present to suggest that the methanol extract of the root-bark inflicted this.

Slight cytotoxicity has been noted for components of the aerial parts in the THP-1 monocytic carcinoma cell line: kaousine (IC<sub>50</sub> = 34 µg/mL) and apigenine dimethylether (IC<sub>50</sub> = 17 µg/mL), while less from Z-antiepilepsirine (IC<sub>50</sub> >50 µg/mL).<sup>234</sup> Furthermore, the cytotoxicity displayed by the essential oils of fruits did not seem to be attributed to β-pinene nor (*E*)-caryophyllene.<sup>207</sup> Piperine has been shown to promote cytotoxicity in various cell lines,<sup>235,236</sup> which may be due to pro-apoptotic activity.<sup>235</sup> In colon carcinoma cell lines, piperine was found to induce pro-apoptotic activity, G0/G1-arrest

and free radical generation,<sup>237</sup> which may explain why the only cytotoxicity seen was in the methanol extract in the Caco-2 cell line. Plumbagin displayed high cytotoxic activity in C2C12 fibroblast cells, as well as resting and stimulated lymphocytes, with a reduction of metabolic activity at concentrations  $\geq 3.2$   $\mu\text{g/mL}$  of between  $\sim 45\%$  and  $\sim 80\%$ .<sup>166</sup> Its cytotoxicity has been confirmed in other studies as well.<sup>238,239</sup> It is possible that cytotoxicity would have been more pronounced if this had been extracted in higher quantities, but as the extracts tested negative for quinones, it is possible that too little was present to elicit an effect.

### 3.4.3. Risk of cytotoxic effects in the intestinal and systemic compartments

If one assumes oral administration of the extracts studied, then a risk of intestinal and hepatic enzyme inhibition is possible. Taking into account the low volume of the intestinal tract, which at fasting is approximately 105 mL,<sup>240</sup> it would be much easier to obtain a high concentration of the crude extracts compared to a larger compartment such as the systemic circulation (5 L). Systemically, if one would assume full absorption and distribution into 5 L of blood, then much higher administrations would be required to reach these concentrations, and thus physiologically-relevant concentrations would be less likely to occur. To identify such a risk, an  $\text{IC}_{50} \leq 30$   $\mu\text{g/mL}$  and  $\leq 100$   $\mu\text{g/mL}$  was chosen as a risk factor for systemic circulation and intestinal circulation, respectively. To determine the amount of extract needed, calculations were done taking into considerations the  $\text{IC}_{50}$ 's obtained, the compartmental volumes and extraction yields. It is important to mention that such extrapolations are however speculative and based on the assumption of full absorption and dissolution of the extracts within the defined compartments. This is not a likely scenario as the absorptive profiles of each phytochemical would be different, however, it does present with a worst-case situation that may occur.

A total of seven (Table 11) and twelve (Table 12) extracts are identified as having a risk of hepatotoxicity and intestinal cytotoxicity, respectively. The highest risk of hepatotoxicity appears to be the methanol extract of *T. elegans*, where an oral dose of as little as 17.85 mg is required to reach the  $\text{IC}_{50}$ . Both extracts of *A. oppositifolia*, as well as the methanol extract of *T. elegans*, requires less than 0.36 mg to obtain the  $\text{IC}_{50}$ .

**Table 11:** Plants that carry a risk of exerting cytotoxic activity in the systemic circulation on liver cells, including amount of extract and plant material required (assuming full dissolution and absorption).

		Extract needed to reach IC <sub>50</sub> (mg)	Plant material needed to reach mass (mg)
<i>A. oppositifolia</i>	Hot water	69.30	1141.68
	Methanol	133.15	1641.80
<i>M. sericea</i>	Hot water	99.10	2077.57
	Methanol	33.90	138.59
<i>S. puniceus</i>	Methanol	152.00	2783.88
<i>S. aculeastrum</i>	Methanol	109.35	559.91
<i>T. elegans</i>	Methanol	17.85	242.53

**Table 12:** Plants that carry a risk of exerting cytotoxic activity in the intestinal compartment, including amount of extract and plant material required (assuming full dissolution and absorption).

		Extract needed to reach IC <sub>50</sub> (mg)	Plant material needed to reach mass (mg)
<i>A. oppositifolia</i>	Hot water	0.24	4.01
	Methanol	0.33	4.07
<i>B. disticha</i>	Hot water	1.97	12.66
	Methanol	1.40	14.78
<i>C. bulbispermum</i>	Hot water	6.75	101.45
	Methanol	3.28	50.95
<i>M. sericea</i>	Methanol	1.62	6.62
<i>P. capense</i>	Methanol	7.66	88.13
<i>S. puniceus</i>	Methanol	3.23	59.13
<i>S. aculeastrum</i>	Hot water	4.23	30.62
	Methanol	2.33	11.95
<i>T. elegans</i>	Methanol	0.36	4.86

### 3.5. Conclusion

The objectives of the chapter were met. An all-encompassing conclusion is provided in Chapter 6. The SRB staining assay was chosen as the representative cytotoxicity assay due to its higher accuracy, reproducibility and lack of interference. The resazurin assay proved to be ineffective in accurate determination of cytotoxicity, which was published as a peer-reviewed article. There is a high risk of inducing cytotoxicity in intestinal cell lines, while there is less in hepatic cells. The methanol extract of *T. elegans* displayed the greatest potency, however, cytotoxicity appeared to be non-selective between the Caco-2 and HepG2 cell lines. Of the crude extracts assayed, seven plants were selected to undergo mechanistic evaluation for underlying causes of cytotoxicity in HepG2 cells.

## Chapter 4

### ***In vitro* assessment of hepatotoxic potential of herbal remedies**

#### **4.1. Literature review**

##### **4.1.1. Hepatotoxicity induced by xenobiotics**

The liver is a key determinant in the maintenance of physiological responses and homeostasis in the body, which includes lipid,<sup>241</sup> carbohydrate, fat and protein metabolism,<sup>242</sup> xenobiotic detoxification<sup>243</sup> and biliary secretion.<sup>242</sup> Since xenobiotics and their metabolites pass through the liver via the hepatic artery, portal vein or lymphatic system, the liver is highly exposed to such compounds.<sup>244</sup> Xenobiotic metabolism aims to produce less reactive metabolites that are easier to eliminate from the body, and it thus functions as an aid to protect the body from foreign molecules.<sup>243,244</sup>

Although drug metabolism pathways are discussed in more detail in Chapter 5, a brief overview is provided for background. Metabolism occurs as phase I and II reactions, and although not necessary for all xenobiotics, they often work together to increase the hydrophilicity of compounds to aid in their elimination. Phase I reactions primarily expose vulnerable sites of compounds so that phase II reactions can occur unhindered. Phase I reactions are mostly mediated by the CYP450 enzyme system, but others do assist in oxidative mechanisms. Phase II reactions conjugate phase I metabolites, or those amenable to conjugation, through sulfation, glucuronidation and glutathione systems to form large, hydrophilic compounds.<sup>245</sup> Unfortunately, due to its role as primary metaboliser, the liver is susceptible to hepatotoxic effects from high xenobiotic exposure.<sup>243</sup> Both phase I and phase II metabolites have been implicated in hepatic adverse effects due to their involvement in the production of reactive metabolites.<sup>246</sup> These reactions may deplete GSH, leading to subsequent susceptibility to oxidative stress.<sup>246</sup> Most drugs that are metabolised by more than 50% by the liver have been suggested to present with a risk of hepatic side effects.<sup>246</sup>

DILI accounts for significant drug attrition.<sup>247</sup> Apart from the financial loss that pharmaceutical companies incur, the detrimental effects on patients can result in

reduced quality of life, as well as increased morbidity and mortality.<sup>247,248</sup> Problematically, DILI is oftentimes discovered late in drug development or during post-marketing. DILI may be a rare occurrence for certain drugs, and thus may only appear in susceptible individuals, making it difficult to diagnose or identify.<sup>249,250</sup> Although HILI is less well-described, its frequency is ever-increasing, with detrimental effects similar to DILI.<sup>10</sup> It is important to note that although HILI specifically refers to herb-induced toxicity, it is still referred to under the broader term DILI.

Drug-induced hepatotoxicity has been implicated as one of the major causes of acute liver failure.<sup>248</sup> Combination therapy may increase the risk of patients developing DILI or HILI.<sup>248</sup> Herbal remedies/dietary supplements were suspected in 9.3% of potential DILI cases in an American study in 2003, of which green tea was reported in 21.4% of those cases.<sup>251</sup> Due to a lack of international standards which address diagnosis, it is difficult to attribute an accurate value on DILI incidences.<sup>248,249,252</sup> The Drug Induced Liver Injury Network (DILIN) is a cooperative agreement between National Institutes of Health, academic clinical centres and data coordinating centres to establish an accurate record of DILI, as well as diagnostic and management systems.<sup>251</sup>

Hepatotoxicity is categorised as intrinsic (predictable), or idiosyncratic (unpredictable).<sup>253</sup> While the former presents itself in a large proportion of the population in a dose-dependent manner, the latter which occurs only in susceptible individuals, does not follow dose-dependent toxicity and has variable latency periods.<sup>248,253</sup> Clinically, DILI symptoms are often initially non-specific, and include nausea, fatigue, fever and abdominal pain. As severity increases several other features may present, such as jaundice, pruritis, ascites, encephalopathy and possibly immune reactions.<sup>252</sup> Discontinuation of the assaulting therapy (albeit it drug or herb) may result in varying results. In most cases liver function improves after cessation of use, but certain types of hepatotoxicity may persist or worsen for some time.<sup>248</sup>

DILI and HILI are difficult to diagnose since liver disease is most often indistinguishable from drug/herb-induced hepatotoxicity. Furthermore, no clear biomarker exists to identify whether or not a xenobiotic can be implicated in liver dysfunction.<sup>249,253</sup> Assessment of DILI or HILI requires careful scrutiny of the treatment regimen, appearance of adverse effects and co-morbidities. Factors, such as alcohol usage or viral hepatitis, must be taken into account to accurately determine whether

or not DILI or HILI has occurred. At best DILI or HILI can be defined as present, absent or possible based upon an exclusion-based diagnosis.<sup>248,249</sup> Various criteria have been implemented to determine this, but most have been scrutinized for lack of accuracy or reliability, such as the Roussel Uclaf Causality Assessment Method.<sup>248</sup>

Numerous cases of HILI have been published or documented, however the accuracy of these reports are debatable<sup>10,254,255</sup> since HILI can present in a predictable or unpredictable fashion.<sup>10</sup> Hepatotoxicity has been linked to various herbal preparations, either single or polyherbal preparations, where toxicity most often presents as jaundice, elevated liver markers, localised pain, pruritis and acute hepatitis (Table 13). In several case reports it has been indicated that patients did not disclose or denied use of herbal preparations.<sup>256–260</sup>

**Table 13:** Case reports where HILI was noted or suspected.

Herbal preparation	Clinical presentation	Recovery upon cessation?	Probable hepatotoxic constituent	Reference
Aloe tablets ( <i>Aloe vera</i> )	Acute hepatitis with inflammation Jaundice and pruritis Elevated liver markers	Yes	None identified	258
Andawali ( <i>Tinospora crispa</i> )	Jaundice Elevated liver markers	Yes	Furanoditerpenoids from <i>Tinospora crispa</i>	261
Bakuchi ( <i>Psoralea corylifolia</i> )	Jaundice Pruritis Elevated liver markers	Yes	Psoralens from <i>Psoralea corylifolia</i>	262
Black cohosh ( <i>Cimicifuga racemosa</i> )	Cholestasis with necrosis Jaundice Elevated liver markers	Yes	None identified	260
Black cohosh ( <i>Cimicifuga racemosa</i> )	Acute hepatitis with inflammation and necrosis Jaundice and ascites Elevated liver markers	Successful liver transplant	None identified	263
Buchu-Rooibos tea ( <i>Agathosma</i> sp. and <i>Aspalathus linearis</i> )	Jaundice and pruritis Elevated liver markers	Yes	None identified	264



Herbal preparation	Clinical presentation	Recovery upon cessation?	Probable hepatotoxic constituent	Reference
Chinese knotweed ( <i>Polygonum multiflorum</i> )	25 individual cases Mixed or acute hepatitis Most often jaundice Elevated liver markers	Majority recovered, one successful liver transplant and one death	Anthroquinones from Chinese knotweed ( <i>Polygonum multiflorum</i> )	265
Impila ( <i>Callilepis laureola</i> )	Centrilobular zonal engorgement and necrosis	No	None identified	266
Impila ( <i>Callilepis laureola</i> )	50 individual cases Acute hepatitis Jaundice Confusion Elevated liver markers	Majority not	Atractyloside from <i>Callilepis laureola</i>	267
Impila ( <i>Callilepis laureola</i> )	Acute hepatitis with necrosis Jaundice Elevated liver markers	No	Atractyloside from <i>Callilepis laureola</i>	256
Impila ( <i>Callilepis laureola</i> )	Jaundice Elevated liver markers	Yes	Atractyloside from <i>Callilepis laureola</i>	256
Jin Bu Huan ( <i>Lycopodium serratum</i> )	Chronic hepatitis with inflammation Moderate fibrosis and steatosis Elevated liver markers	Yes	None identified	268
Muti	Venoocclusive liver disease Jaundice Elevated liver markers	High mortality rate, though some recovered	Pyrrolizidine alkaloids from <i>Senecio</i> sp.	257
Noni juice ( <i>Morinda citrifolia</i> )	Acute hepatitis, cholestasis and inflammation Zonal necrosis Jaundice Elevated liver markers	Yes	None identified	269
Polyherbals Bu-gu-zhi and Qu Bai Ba Bu Qi Pian	Jaundice Elevated liver markers	Yes	Psoralens from <i>Psoralea coryfolia</i>	270
Polyherbal Cascara sagrada	Intrahepatic cholestasis Portal hypertension and inflammation Jaundice and ascites Elevated liver markers	Yes	Anthracene glycosides from Cascara buckthorn ( <i>Rhamnus purshiana</i> )	271

In South Africa, hepatotoxicity induced by *C. laureola* is commonplace. It is suspected that a large majority of centrilobular zonal liver necrosis in African patients is due ingestion of *C. laureola*,<sup>266</sup> especially in children.<sup>267</sup> The hepatotoxicity induced by *C. laureola* is thought to be as a result of atractyloside ingestion, an inhibitor of oxidative phosphorylation. However, research seems to be controversial with regards to its involvement and thus the main hepatotoxin may still be undiscovered.<sup>221</sup> A second primary contributor to HILI in South Africa is *Senecio* spp. poisoning. This genus contains pyrrolizidine alkaloids, which can result in the development of veno-occlusive liver disease after chronic ingestion. Mortality rates have been shown to be as high as 40% in suspected poisonings, with children being most at risk.<sup>257</sup>

#### **4.1.2. Mechanisms underlying hepatotoxicity**

##### **4.1.2.1. Mitochondrial functioning and toxicity**

Mitochondria are energy-producing organelles<sup>272</sup> that produce the largest quantity of ATP, especially in times of fasting.<sup>247</sup> Morphologically, mitochondria contain an outer and inner lipid bilayer separated by an intermembrane space. The inner mitochondrial membrane encloses the hydrophilic matrix which contains mitochondrial DNA and enzymes.<sup>247,272</sup> The inner membrane is folded upon itself to create cristae, which increases the surface area. As the inner membrane is not freely permeable, transfer of compounds into the matrix is highly protein-mediated and –regulated.<sup>247,273</sup> The membrane is embedded with protein systems, such as those of the electron transport chain complexes (including ubiquinone), ATP synthase and the adenine nucleotide translocator (ANT).<sup>272,273</sup> The matrix side of the inner mitochondrial membrane is negatively charged and slightly alkaline. As a result of this mitochondria can accumulate positively charged lipophilic compounds and certain acidic compounds, which explains the selective mitochondrial toxicity some compounds elicit.<sup>272</sup>

Cells require energy to maintain their survival and functionality.<sup>274</sup> In mitochondria, energy is produced from the conversion of dietary carbohydrates and fats to reducing equivalents.<sup>275</sup> Synthesis of energy in the form of ATP occurs through oxidative degradation of compounds, which includes pyruvate, fatty acids and amino acids. Pyruvate (from glycolysis) and fatty acids (from lipolysis) are ultimately converted to

acetyl-coenzyme A (CoA) under aerobic conditions in the mitochondria by pyruvate dehydrogenase and  $\beta$ -oxidation, respectively.<sup>247,274,275</sup>

The process of  $\beta$ -oxidation is a complex enzymatic cascade which progressively oxidizes free fatty acids to acetyl-CoA (Figure 16). This occurs in most tissues, with the exception of the CNS and erythrocytes.<sup>247</sup> Although short- and medium-chain fatty acids can cross the mitochondrial membrane passively, long-chain fatty acids require active transport. Carnitine-palmitoyltransferase 1 catalyses the transport of long-chain fatty acids across the membrane with the aid of CoA and L-carnitine.<sup>247</sup> The latter occurs during fasting conditions in ketogenic organs, such as the liver. The products serve as substrates for oxidative energy production in extra-hepatic tissues (such as the kidneys, muscles and brain).<sup>247,274</sup> Alternatively, fatty acid oxidation of long-chain and very long-chain fatty acids can occur via extra-mitochondrial enzyme systems, though this may result in mitochondrial dysfunction and increased free radical production.<sup>247</sup> Acetyl-CoA enters the Krebs-cycle to form several intermediaries, including reduced nicotinamide adenine dinucleotide (NADH), which donates electrons to the respiratory chain to produce ATP during oxidative phosphorylation.<sup>275</sup>

Due to electrogenic proton pumping, mitochondria generate an electrochemical gradient, also referred to as the  $\Delta\Psi_m$ .<sup>247,272</sup> Mitochondria produce ATP from the  $\Delta\Psi_m$  by transporting protons through the F0 portion of ATP synthase (complex V) back into the matrix, which releases energy. The F1 portion uses released energy for the phosphorylation of adenosine diphosphate (ADP) to ATP.<sup>247</sup> Matrix-generated ATP is transported across the membrane through the ANT, in exchange for ADP, for use by cellular systems.<sup>273</sup> This potential is necessary for the electrophoretic or protonophoric transport of several different substrates.<sup>247</sup> The  $\Delta\Psi_m$  is produced from an electrical membrane potential (generally between -180 and -200 mV) and a pH gradient ( $\Delta 0.4 - 0.6$  U) across the inner mitochondrial membrane. Respiration is linked to  $\Delta\Psi_m$ , thus a high  $\Delta\Psi_m$  results in decreased respiration, and vice versa. Low  $\Delta\Psi_m$  can translate to an increase in metabolic respiration and oxygen consumption.<sup>272</sup>

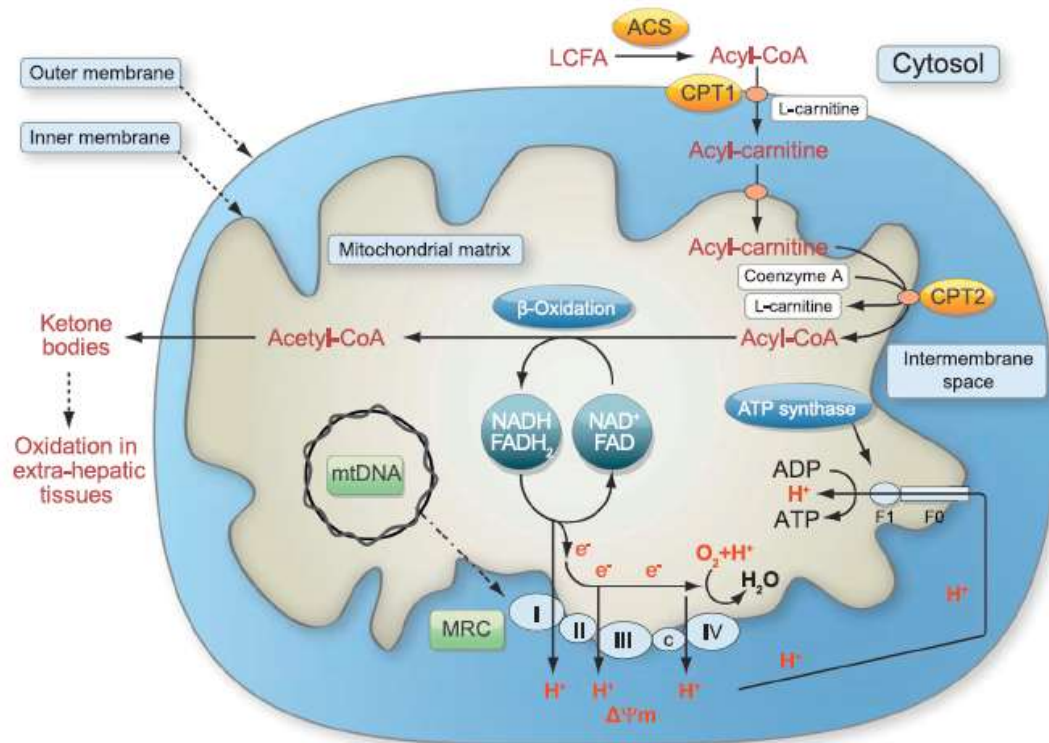


**Figure 16:** Schematic representation of the mitochondrial fatty acid  $\beta$ -oxidation and oxidative phosphorylation pathways in liver mitochondria (reproduced from Begrich *et al.* with permission).<sup>247</sup>; ACS – acyl-CoA synthetases; acyl-CoA – acyl-conenzyme A; CPT – carnitine palmitoyltransferase; LCFA – long-chain fatty acids; MRC – mitochondrial respiratory chain; mtDNA – mitochondrial DNA

Mitochondrial toxicity can arise from multiple points, including i) uncoupling of the respiratory chain by lipophilic or slightly acidic compounds, ii) disruption of electron shuffling from mitochondrial respiration to oxygen, iii) altered redox cycling, iv) opening of the mitochondrial permeability transition pore (MPTP) with resultant calcium influx or oxidative stress, v) impaired fatty acid oxidation or vi) inhibited mitochondrial DNA synthesis.<sup>276</sup> Mitochondrial dysfunction can result in downstream toxicities, including oxidative stress, energy shortages, steatosis, cell cycling disturbances, alterations in differentiation and cellular death.<sup>247,272</sup> The intermembrane space contains proapoptotic factors, which upon release may activate cell death pathways.<sup>273</sup>

Damage to the mitochondrial membranes may result in structural and functional loss, with increased membrane permeability. Except for mitochondrial membrane rupturing, another factor that decreases membrane stability involves the opening of the MPTP. The MPTP complex is an association of several proteins located on the outer and inner membrane of the mitochondrion that assemble upon stimulation and allows for

increased permeability.<sup>247,273</sup> It is primarily formed from the two most abundant proteins in the outer and inner membrane, namely the voltage-dependent anion channel (VDAC) and ANT, respectively. The pore is formed between the outer and inner membrane proteins, which also involves the association of the peripheral benzodiazepine receptor (PBR) on the outer membrane, creatine kinase in the intermembrane space, hexokinase II linked to VDAC on the cytosolic portion of the outer membrane, cyclophilin D in the matrix, as well as Bax and Bcl-2.<sup>247,273</sup> As interactions occur between these proteins, modulation of either may affect the activity of the other, and thus influence MPTP formation.<sup>273</sup> Depolarization of the mitochondrial membrane (evident by a reduced  $\Delta\Psi_m$ ) is thought to be indicative of MPTP opening.<sup>277</sup> Mediators of mitochondrial membrane permeabilisation have differential effects on the outer and inner mitochondrial membrane. This may be followed by matrix swelling and rupture, but it is not necessarily a definite response.<sup>273</sup>

Mitochondrial toxicity has been implicated as a centralised component in the induction of DILI.<sup>250</sup> This can be induced through different mechanisms, such as alterations to mitochondrial DNA, altered mitochondrial proteins, disruption of mitochondrial membranes or induction of oxidative stress.<sup>250</sup> Various drugs, directly or indirectly, inhibit mitochondrial respiration or  $\beta$ -oxidation, reducing formation of ATP or producing oxidative stress.<sup>250</sup> Respiration may be blocked through inhibition of the respiratory chain protein complexes, or critical enzymes involved in it, such as ATPase.<sup>250</sup> Moderate inhibition may result in cellular dysfunction, but at a larger scale hepatocyte necrosis may occur, with induction of cholestatic or fibrotic outcomes.<sup>250</sup>

#### **4.1.2.2. Oxidative stress and antioxidant systems**

ROS are amongst the most abundant and important free radical species produced in the physiological system. ROS are produced through various mechanisms, including disruptions of the mitochondrial respiratory chain, metabolic activity of the CYP450 enzyme system (particularly in the liver during detoxification of xenobiotics) and its reductases, and by intracellular oxidases.<sup>241,278</sup> Mitochondria are responsible for a large percentage of ROS formation due to leakage of electrons from complex I and II from the mitochondrial respiratory chain, which react with oxygen through one-electron reduction to become superoxide anions radicals.<sup>247,250,275</sup> Homeostasis of ROS is

important for proper cellular functioning, thus diminished or excessive production may influence proliferation or viability.<sup>279</sup> Macromolecules may be affected in such a way as to inactivate or alter protein function, peroxidise lipid membranes thus altering membrane stability or resulting in DNA damage or strand breaks.<sup>275</sup>

ROS at low concentrations act as second messengers or signalling molecules by altering the cellular redox state and its redox-sensitive proteins, which may activate or inhibit pathways.<sup>280</sup> As hydrogen peroxide has a relatively long half-life, exhibits membrane permeability and can reach high cellular concentrations, it is generally considered one of the main reactive signalling molecules of ROS.<sup>280</sup> ROS has been implicated in the modulation of mitogen-activated protein kinase (MAPK) pathways, which in turn activates cell proliferation, differentiation, survival and apoptosis.<sup>280</sup> The concentration of ROS is pertinent to the type of cellular effect that will be elicited upon activation.<sup>280</sup>

Although biological systems are equipped with endogenous antioxidants to combat free radical production, oxidative stress will occur once a physiological excess of ROS is present and insufficient levels of endogenous scavengers or antioxidants are available to combat this.<sup>275,278</sup> ROS are capable of damaging macromolecules, for example through protein and lipid peroxidation, and nucleic acid degradation. Damage can vary from slight alterations to severe structural and functional loss.<sup>276,278</sup> Lipid peroxidation occurs once lipids and membrane components undergo oxidation to form reactive intermediates. In ROS-induced liver injury, lipid peroxidation has been implicated as one of the most likely mechanisms of cell death, though it may be a consequence of liver injury as well. Ultimately it is thought that high levels of lipid peroxidation is required for significant clinical toxicity, and may require specific conditions (such as decreased antioxidant protection) to elicit severe damage.<sup>278</sup> Oxidative stress depletes endogenous antioxidants, thus cells are unable to withstand hydrogen peroxide formation. Accumulation of hydrogen peroxide is linked to increased mitochondrial dysfunction and MPTP opening, activation of MAPK pathways and ultimately cell death.<sup>247</sup>

Several antioxidant systems are available to combat oxidative stress. GSH is an abundant biomolecule containing a free thiol group in its cysteinyl residue, which allows it to act as a free radical scavenger.<sup>281</sup> GSH is synthesised in an energy-

dependent fashion, with ATP being used to power the process.<sup>282</sup> Although the cytosol contains approximately 80 – 85% of the cellular GSH pool, the mitochondrial GSH concentration is similar to that of the cytosol (9 – 12 mM).<sup>281,282</sup> This is due to the lower mitochondrial volume compared to the cytosol. In hepatocytes, the cytosolic GSH concentration is approximately 10 mM. Mitochondrial GSH enters the cytosol through transport mechanisms, where it is mainly kept in the matrix by the inner mitochondrial membrane. The fluidity of this membrane alters the ability of GSH to exit the mitochondria, thus an increased microviscosity allows for greater mitochondrial GSH depletion (such as seen in alcoholic liver diseases).<sup>281,282</sup> The ratio of GSH to oxidized glutathione disulphide (GSSG) helps maintain redox homeostasis in cells, and also assists in the proper functioning of signalling cascades, enzymatic processes and survival pathways. As GSH is approximately 100 to 10 000-fold greater than other reducing couples, such as oxidized nicotinamide dinucleotide phosphate (NADP<sup>+</sup>)/reduced nicotinamide dinucleotide phosphate (NADPH) and thioredoxin, it is the major determinant of intracellular redox potential.<sup>281,282</sup> GSH quenches ROS by acting as a hydrogen donor to glutathione peroxidase, and thereby maintains an environment free of excessive oxidation. Proteins with an exposed cysteine become susceptible to redox reactions once the sulfhydryl group becomes deprotonated to a thiolate form. GSH coupling allows proteins to be protected against such redox reactions, and assists in regulation of their functionality. GSH may also conjugate to xenobiotics through glutathione-S-transferase to assist in the efflux of compounds out of the intracellular compartment.<sup>281</sup> Oxidative stress may induce genetic transcription at the antioxidant response element (ARE), which increases GSH and glutathione-S-transferase levels. This implies that higher levels of free radicals can be cleared, and oxidative stress attenuated.<sup>250</sup>

Cellular GSH concentrations regulate several signalling pathways. Some, such as the c-Jun *N*-terminal kinases (JNK) pathway, involve a very tightly controlled redox status.<sup>281,283</sup> Generation of reactive metabolites from xenobiotics is a common occurrence in the liver, and is primarily removed through detoxification or conjugation to GSH. The depletion of GSH has long been known to be a marker of hepatotoxic events.<sup>276</sup> Formation of reactive, toxic metabolites is known to be one of the primary malefactors of DILI. These toxic metabolites may be conjugated by GSH for removal from the hepatic system, or may result in degradation of hepatic macromolecules

leading to inflammatory responses.<sup>250,282</sup> GSH depletion leaves cells vulnerable to increasing concentrations of ROS and oxidative by-products, and interferes with metabolism, survival and proliferation pathways.<sup>281</sup> During mitochondrial permeabilisation, uncoupling of the respiratory chain and release of cytochrome c may occur, which results in a higher burden of superoxide formation, reduced concentrations of redox equivalents and subsequent ROS-mediated damage as oxidative stress.<sup>273</sup>

#### **4.1.2.3. Fatty acid accumulation and steatosis**

Lipids are hydrophobic or amphipathic molecules essential for the maintenance of cellular integrity, production of energy and are used for cellular signalling pathways. Bioactive lipids act as signalling molecules in cell proliferation, growth, differentiation survival and death pathways, and offers membrane integrity, thus alterations may affect membrane permeability.<sup>284</sup> Fatty acids and lipoproteins deliver lipids to hepatocytes through passive diffusion mechanisms. Free fatty acids are converted to triglycerides, used in the synthesis of phospholipids, inflammatory mediators, and transporters, or act as an energy source. Excess fatty acids are usually stored as triglycerides until required as an energy source.<sup>244,284</sup> Inhibition of enzymes or substrates involved in  $\beta$ -oxidation may result in accumulation of fatty acids to toxic levels, and thus aid in the development of different pathologies, including hepatotoxicity.<sup>284</sup> A number of drugs have been shown to induce steatotic hepatotoxicity through these mechanisms.<sup>250</sup>

Steatosis is an accumulation of fatty acids and triglycerides in the liver, due to, amongst others, an inhibition of  $\beta$ -oxidation.<sup>244,276</sup> It may lead to steatohepatitis, inflammatory and fibrotic lesions resulting from fatty acid accumulation and necrotic events in the liver.<sup>250</sup> Impaired  $\beta$ -oxidation of mitochondrial fatty acids results in accumulation of fatty acyl-CoA and non-esterified fatty acids. These products are esterified into triglycerides, which are stored within the liver giving rise to steatosis.<sup>250</sup> Depending on the intensity or frequency of  $\beta$ -oxidation impairment, micro-, macro- or mixed-vesicular steatosis may occur.<sup>250</sup> Xenobiotics cause steatosis through inhibition of acyl-CoA synthases, depletion of cytosolic or intramitochondrial CoA, deficiencies in reducing factors such as oxidised nicotinamide adenine dinucleotide (NAD<sup>+</sup>) or

flavin adenine dinucleotide (FAD), as well as carnitine palmitoyl transferase (CPT) I or acyl-CoA dehydrogenases.<sup>250,274</sup> Steatosis may also arise when fat transporting systems aimed at removing fat from the hepatic tissues become dysfunctional.<sup>250</sup> Increased hepatic fatty acid synthesis, release of free fatty acids from adipose tissue or uptake into the hepatic tissue also increases fatty acid accumulation.<sup>250</sup> If coupled to free radical exposure lipid peroxidation may occur, with toxic aldehyde formation as a result (such as 4-hydroxynonenal [4-HNE] and malondialdehyde [MDA]). This may in turn exacerbate mitochondrial dysfunction and increase the likelihood of xenobiotic-induced hepatocellular cytotoxicity.<sup>276</sup>

#### **4.1.2.4. The cell cycle and cellular kinetics**

Eukaryotic cells follow a distinct, highly-regulated progression of cell growth and division, which is known as the cell cycle.<sup>285</sup> The cell cycle is largely categorized into the interphase and mitotic phase. During interphase cells grow and replicate their DNA in preparation for the mitotic phase. The mitotic phase allows for chromosomal separation into daughter cells, and subsequent cytokinesis, relating to the division of cells and cytoplasm into two daughter cells.<sup>285,286</sup> The mitotic phase is shorter, only lasting about 1 h of the typical 24 h for human cells to progress through the cell cycle.<sup>285</sup> Rapidly proliferating cells generally have a cell cycle of 24 h, which is divided into 11 h, 8 h, 4 h and 1 h for the post-mitotic gap (G1)-, DNA synthesis (S)-, pre-mitotic gap (G2)- and mitosis (M)-phase, respectively.<sup>285</sup> The time required to complete cycling is dependent on the cell type, as well as its environment.<sup>285</sup> The cell cycle is divided into four discrete phases, each comprising of its own specific characteristics and functions: G1, S, G2 and M (Figure 17).<sup>285,287</sup> Although growth is continuously occurring, synthesis of DNA only occurs within one phase of the interphase, after which the duplicated genetic material is equally distributed between daughter cells.<sup>285</sup> During the G1-phase cells grow and are metabolically active, but do not replicate DNA. During the S-phase, DNA replicates after which it enters the G2-phase, where growth continues and mitotic-dependent proteins are synthesised. During the M-phase, cells divide and then generally undergo cytokinesis required for division into daughter cells.<sup>285</sup>

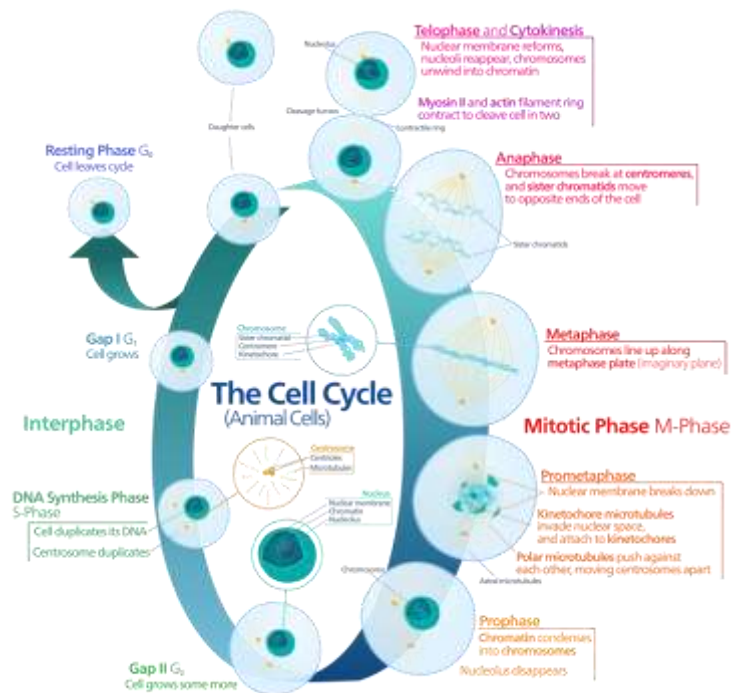


**Figure 17:** The cell cycle (reproduced from Wikipedia with permission).<sup>288</sup>

The amount of DNA differs throughout the cell cycle, and as such they can be classified accordingly. Cells in the G<sub>1</sub>-phase are diploid due to the presence of two chromosomal copies (2N). As DNA replication occurs, cells become tetraploid (4N). Thus cells in the S-phase contain a DNA content of 2N to 4N, while those in the G<sub>2</sub>- and M-phase contain 4N. As cytokinesis occurs cells become diploid once again.<sup>285</sup> The cell cycle is highly regulated to ensure that cellular proliferation continues unperturbed and damaged cellular material does not duplicate.<sup>285</sup> Cell cycle progression is affected by different extracellular and intracellular factors.<sup>285</sup> As cells undergo growth in the G<sub>1</sub>-phase, they reach a restriction point that controls movement from G<sub>1</sub>- to S-phase. The restriction point assesses the availability of proliferation-dependent growth factors. If not present, cells may undergo transition to a quiescent G<sub>0</sub>-phase, where cells do not actively proliferate, though still remain metabolically active. As soon as growth factors are supplied, cells may continue to move to the S-phase.<sup>285,289</sup> Cells, such as those of the liver, may enter the G<sub>0</sub>-phase and only re-enter the G<sub>1</sub>-phase once liver-injury has occurred or if repair is required.<sup>285,286</sup>

Cell cycle checkpoints ensure that coordination of the different phases take place and that sequential transition occurs,<sup>285</sup> and that genomic stability and the

nucleocytoplasmic ratio stay within physiological range.<sup>290</sup> Cell cycle checkpoints consist of an error-detecting sensor, a sensor-generated signal and a signal-induced response element aiming to remedy the error.<sup>286</sup> An incomplete cell cycle phase inhibits progression to subsequent stages.<sup>290</sup> The checkpoints are categorised as follows: DNA damage checkpoint (arresting cells in any phase until repair occurs); DNA replication checkpoint (ensures cells do not divide until full chromosomal duplication occurs); and the spindle assembly checkpoint (ensures all chromosomes are attached to kinetochores on the spindle before mitosis occurs).<sup>286</sup>

DNA damage may arrest cells at the G1/S-checkpoint,<sup>290</sup> where repair can be done before chromosomes are replicated with incorrect genetic material. This checkpoint is primarily controlled by the p53 protein, which is rapidly induced by damaged DNA.<sup>285</sup> The G2/M-checkpoint in the G2-phase prevents transition to the M-phase until all chromosomes have been duplicated fully and do not contain damaged DNA.<sup>290</sup> Thus cells undergo cell cycle arrest and are allowed to finalise or repair the S-phase DNA replication before M-phase transition takes place.<sup>285</sup> At the end of the M-phase, a metaphase/anaphase-checkpoint exists<sup>290</sup> that ensures chromosomes are aligned correctly on the mitotic spindle. Without this checkpoint chromosomes may be aberrantly distributed between daughter cells, and thus arrest may occur until arrangement has been properly completed.<sup>285</sup> Minichromosome maintenance proteins ensure that cells in the G2-phase do not enter the S-phase and thereby cause chromosomal replication more than is needed. Binding of these proteins in the G1-phase allows cells to undergo chromosomal replication in the S-phase.<sup>285</sup>

Modulators of checkpoints may act as accelerators, inducing cell cycle progression (e.g. growth factors, nutrients and appropriate size), or decelerators, inhibiting phase transition (e.g. genomic instability).<sup>290</sup> Cell cycle progression is mainly controlled by cyclin-dependent protein kinases (Cdks) and their individual regulatory subunits (cyclins).<sup>286,291</sup> Cyclin-Cdk-complexes enzymatically catalyse the covalent binding of ATP-derived phosphate groups to protein groups. This phosphorylation alters protein functioning.<sup>286</sup> Each cyclin-Cdk complex is responsible for a different effect, though slight overlap occurs and thus flexible control is granted.<sup>291</sup> Three general classes have been suggested: G1 cyclin-Cdk complex (G1/S-phase transition), S cyclin-Cdk complex (initiation and completion of DNA duplication), and M cyclin-Cdk complex (initiates mitosis and blocks re-entry into the G1-phase). Modulation of these

complexes occurs via three primary routes, namely cyclin availability, stoichiometric inhibition and inhibitory phosphorylation.<sup>289,290</sup> The cyclin-Cdk complex is the primary modulator of its own regulatory processes, and thus feedback systems are created in this manner.<sup>290</sup> Stoichiometric inhibition occurs through inactivation by cyclin kinase inhibitors (CKIs) which form inactive trimer complexes with cyclin-Cdks. Human cells possess various CKIs, such as those originating from the p15/p16/p17<sup>INK4a</sup>, p21<sup>Cip1</sup> or p27<sup>Kip1</sup> families.<sup>290</sup>

The redox status of cells is a key determinant in cell cycle progression. Critical aspects are controlled through regulated ROS bursts, which aim to shift the redox state in accordance to cellular kinetics.<sup>282</sup> Depending on the state, this can either result in progression or arrest of the cell cycle.<sup>282</sup> Intracellular ROS, in small quantities, act as proliferation signals by activating mitogenic pathways and Cdks, as well as inactivating retinoblastoma protein through phosphorylation to suppress its antiproliferative properties.<sup>282</sup> As such GSH concentrations are lower during the initial G1-phase to accompany the rise in ROS, and as progression occurs adaptive GSH synthesis takes place to counteract oxidation.<sup>282</sup> Distribution of intracellular GSH throughout the cell is imperative in cell cycle control.<sup>282</sup> A low level oxidative state in the cytosol is necessary for transition throughout the G1-phase, while a more reductive environment is required to progress through the G2/M-phases.<sup>282</sup> Excessive oxidation may, however, damage DNA, and activate DNA repair pathways such as the DNA damage response (DDR) system.<sup>282,292</sup>

Lipid biosynthesis is critical for cell proliferation, and lipids may act as mitogenic modulators. Similarly, various anticancer agents may produce cellular death or stasis through interference with lipid metabolism.<sup>284</sup> Short-chain fatty acids may cause growth arrest in certain cell types due to histone hyperacetylation.<sup>284</sup> Steatotic liver cells present with cell cycle arrest.<sup>293</sup>

#### **4.1.2.5. Cell death**

Cell death is a tightly regulated system that can deviate into several characteristic types or mechanisms, such as apoptosis, necrosis, aponecrosis and autophagy.<sup>275,294</sup> Although being functionally and morphologically different, all processes involve

several overlapping mediators and it is thus possible for compounds to shift their preference to either mechanism depending on the condition.<sup>294</sup> Cell death occurs in several steps, involving the initiation, commitment and ultimate execution of cellular decay.<sup>295</sup> Hepatic cell death may frequently appear as a mixture of apoptotic and necrotic events.<sup>296</sup>

Selective mitochondrial membrane permeability is a common occurrence in activation of cellular death.<sup>273</sup> During permeabilisation of the mitochondrial membrane, several specific steps occur. Cells initially accumulate mediators required for permeabilisation, with subsequent reduced integrity of the membrane and release of catabolic intermediaries necessary for cell degradation.<sup>273</sup> Depending on the pathway invoked, permeabilisation of the membrane can either be sudden and large resulting in necrotic death, or step-wise and more subtle inducing apoptotic events (Figure 18).<sup>273</sup> The mode of cell death thus depends on the level of mitochondrial toxicity and number of mitochondria with open MPTP.<sup>247</sup>

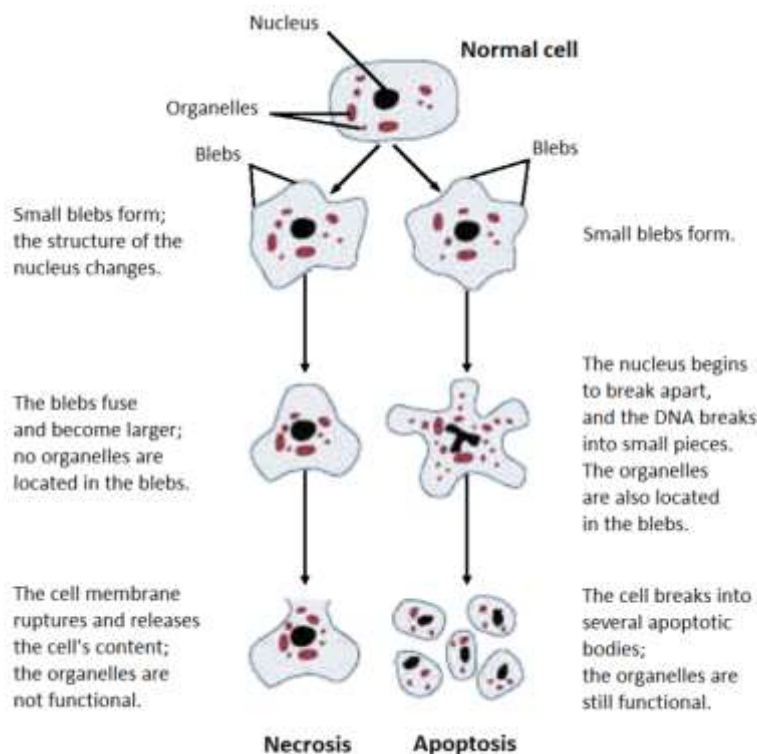


**Figure 18:** Differentiation between necrotic and apoptotic cell death (reproduced from Wikipedia<sup>297</sup> with permission).

#### 4.1.2.5.1. Apoptosis

Apoptosis, or programmed cell death, is a controlled cellular death that under physiological conditions systematically removes damaged or decayed cells without severe repercussions,<sup>294,298</sup> such as the inflammatory response.<sup>295</sup> As mitogenesis occurs at a constant rate, damaged cells will be replaced by newer cells.<sup>294,298</sup> Excessive or deficient apoptotic events have been linked to a large variety of pathologies, and therefore the importance of a well-regulated apoptotic system is further brought to light.<sup>294</sup> Uncontrolled or excessive apoptosis due to xenobiotics can result in severe hepatic damage, including hepatitis and liver failure.<sup>298</sup> Morphologically, apoptosis is characterised by nuclear condensation and fragmentation, compaction of cytoplasm and cellular organelles, subtle alterations to plasma membranes (membrane blebbing and phosphatidyl serine flipping), shrinkage of cellular volume (due to formation of apoptotic bodies) and ultimately phagocytosis of the apoptotic cells.<sup>295</sup> Intranucleosomal cleavage may occur at a late apoptotic stage to degrade DNA,<sup>295</sup> together with formation of apoptotic bodies which house intact cytoplasmic organelles or nuclear fragments.<sup>275</sup> During this event few morphological changes are observed in the mitochondria, and ATP levels remain relatively stable or high.<sup>294</sup> All these changes occur with minimal alteration to the barrier integrity of the cellular membrane, thus the cellular components remain housed within the cytosol enclosed with an intact membrane.<sup>294</sup> These morphological changes are primarily modulated through intracellular cysteine proteases, namely caspases.<sup>299</sup>

All caspases possess an active cysteine site and cleave substrates at aspartate residues, though each caspase present with their own specificity.<sup>299</sup> Caspases are synthesised as inactive proenzymes, which are then activated by initiator caspases through cleavage of aspartate residues.<sup>295</sup> Although apoptosis is mediated through numerous modulators, caspases are the primary executioners of programmed cell death. Caspases result in a sequential activation of themselves and other downstream mediators. Specific cleavage of cellular structures accounts for characteristic apoptotic morphological events such as cell shrinkage, membrane blebbing or loss of cellular shape. Caspase-3, -6 and -7 are executioner caspases and are the most active of the caspase cascade.<sup>299</sup> Caspases act either as upstream (extrinsic pathway) or downstream (intrinsic) effectors of membrane permeabilisation.<sup>273</sup> Ultimately DNase activation occurs through caspase-3 activity, resulting in intranucleosomal

cleavage.<sup>299</sup> Apoptotic cells undergo a translocation of phosphatidylserine residues from the inner membrane leaflet to the outer surface of the plasma membrane (referred to as the PS-flip). Phosphatidyl serine, and other surface molecules, are recognised by neighbouring phagocytosing cells, such as immune cells, where they are removed through phagocytosis to diminish the immune response.<sup>275,300</sup> Hepatocytes undergoing apoptosis are mainly digested by Kupffer cells.<sup>296</sup> Although caspases are of great importance in apoptotic cell death, it seems apparent that programmed cell death may take place independent of caspase-activation. Morphological features of programmed cell death in the absence of caspase activation often resembles necrotic cell death more than the classical hallmarks of apoptosis.<sup>299</sup>

A variety of endogenous proteins act as amplifiers or inhibitors of apoptotic cell death, aiding in the regulation of spontaneous or mediated apoptosis.<sup>273</sup> Non-protein pro-apoptotic signals include excessive cytosolic calcium influxes (such as those seen with mitochondrial rupturing), lipid mediators (such as saturated fatty acids or ceramide), non-mitochondrial or mitochondrial ROS and lipid peroxidation byproducts (4-HNE) which may result in mitochondrial membrane permeabilisation and subsequent apoptosis.<sup>273,277,283</sup>

Apoptosis is generally divided into two largely independent pathways: the extrinsic death-receptor or the intrinsic mitochondrial apoptotic pathways (Figure 19). While the extrinsic pathway relies on complex formation of ligands and surface death-receptors, the intrinsic pathway is mediated through mitochondria-derived pro-apoptotic molecules released due to exposure to intrinsic cellular damage intermediaries.<sup>299</sup> Although the extrinsic pathway does converge with the intrinsic pathway at the level of caspase-3 activation, it is possible that involvement of the mitochondria during the extrinsic pathway may take place.<sup>300</sup>

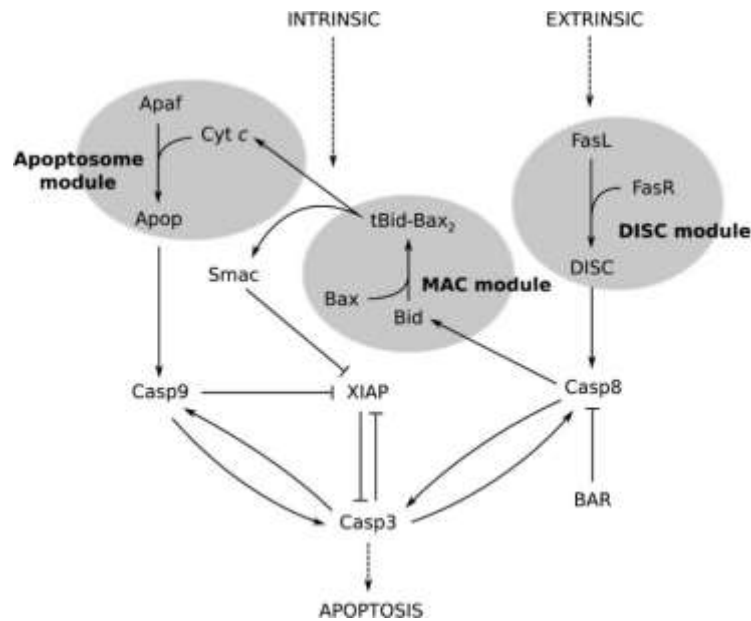


**Figure 19:** The intrinsic and extrinsic apoptotic pathways (reproduced from Wikipedia<sup>301</sup> with permission); Apaf - apoptotic protease activating factor 1; DISC – death inducing signal complex; FasL –Fas ligand; FasR – Fas receptor.

#### 4.1.2.5.2. Necrosis

Unlike apoptosis, necrosis is a more destructive form of cellular death, resulting in large scale effects and detriments.<sup>294</sup> During necrotic cell death the cytoplasm and mitochondrial matrix swells, with subsequent rupturing of the cellular membrane and leakage of intracellular contents. Organelle dysfunction and degradation occurs as well. Release of the intracellular contents into the extracellular space is accompanied by inflammatory responses.<sup>294</sup> Necrosis may occur through a death-receptor or mitochondrial pathway, though requires different signalling cascades than those present in apoptosis.<sup>284</sup>

Whether or not the cell undergoes apoptotic or necrotic cell death is dependent on a complex system of competing factors. Cells may undergo apoptosis when MPTP opening is gradual, and allows for activation of caspases. If MPTP opening is too quick, severe and widespread, mitochondrial lysis may occur due to rapid depolarisation and uncoupling of the respiratory chain.<sup>275,294</sup> Opening of the MPTP results in the passive re-entry of protons into the mitochondrial matrix, and thus ATP formation is hindered, which may produce necrotic cell death.<sup>250</sup> As the mitochondria contain high calcium concentrations, rupturing creates a large cytosolic calcium influx.<sup>277</sup> This bypasses

activation of caspases and depletes ATP stores. The latter is due to failure of the plasma membrane calcium ATPase, required for the efflux of calcium out of the cell.<sup>247,294</sup> Necrotic events may follow under these conditions, with activation of the inflammatory system.<sup>275,294</sup> Necroptosis may occur when cells are programmed for cellular death through apoptotic means, but some interference shifts the process into a necrotic state, for example a sudden depletion of ATP or inhibition of pro-apoptotic executioners.<sup>296</sup> This pathway is caspase-independent, though requires receptor interaction with protein kinases.<sup>284</sup> Inhibition in any critical apoptotic step will allow necrotic cell death to take preference.<sup>281</sup>

#### 4.1.3. Plants selected for mechanistic evaluation of hepatotoxic potential

*A. oppositifolia* is a small tree with thick leaves, white flowers and red berries (Figure 4A). It is commonly known as the Bushman's poison due to aqueous decoctions of the bark and root being used as an arrow poison. These have also been implemented as an analgesic, in the treatment of snake bites, and against anthrax.<sup>58</sup>

*B. disticha* is a highly poisonous psychoactive bulb that is either classified as *Boophone*, *Boophane*, *Buphane* and *Buphone* (Figure 4B). The bulb is often used for wounds, headaches, abdominal pains and various eye conditions, while the psychoactive properties are used for divination properties.<sup>302</sup> It is a recognized hallucinogen, and has been used as a means of suicide and arrow poisoning.<sup>87</sup> One study details mortal wounding of a person, as well as grievous injury of several others, after an individual experienced severe hallucinations brought about by the bulb extract.<sup>303</sup> However, no hepatotoxic data has been established.

*M. oleifera*, otherwise known as the horseradish or miracle tree,<sup>143,151,304,305</sup> is a medium-sized tree<sup>306</sup> that has been used by the Greeks, Romans and Egyptians since ancient times (Figure 4G).<sup>307</sup> *M. oleifera* is used to treat various diseases and disorders, including inflammatory, hepatorenal and cardiovascular pathologies,<sup>308</sup> but is also considered versatile and nutritious.<sup>309,310</sup> Extracts of *M. oleifera* have not indicated potential risk for hepatotoxicity, and thus due to its proposed safety and great commercial value, it was considered a non-hepatotoxic control. However one can never assume safety without assessment of mechanistic parameters.

*S. aculeastrum*, or the goat bitter apple, is a thorny, perennial plant with white flowers and lemon-shaped berries found in the Limpopo, Mpumalanga, KwaZulu-Natal, Western and Eastern Cape provinces (Figure 4N).<sup>311</sup> Berries become yellow-green when ripened, and are used as a treatment for jigger wounds and gonorrhoea.<sup>312</sup> Extracts of berries are rich in steroidal glucosaponins and steroidal glucoalkaloids.<sup>173,174</sup> *Solanum* spp. are described as poisonous due to the presence of steroidal glucoalkaloids, and was thus included based on the cytotoxicity observed in the phytotoxicity testing phase of the project.

*T. elegans*, or the toad tree, is a small tree that is distributed throughout tropical and subtropical regions, including Africa (Figure 4O).<sup>109</sup> Ethnomedicinal uses include the treatment of pulmonary disorders, cancers, heart disease and as an aphrodisiac.<sup>106</sup> Bioactivity has mostly been ascribed to the presence of potent indole alkaloids.<sup>109</sup> Due to the potent cytotoxic effects observed in the phytotoxicity testing phase of the project, *T. elegans* was included as a high risk of hepatotoxicity.

*T. sericea*, or the silver cluster leaf,<sup>313</sup> is a tree widespread in Africa (Figure 4P). It ethnomedicinal uses include the treatment of tuberculosis, diabetes, diarrhoea and gonorrhoea.<sup>314</sup> Due to relatively low cytotoxicity that were observed in the phytotoxicity testing phase of the project, *T. sericea* was included as a low cytotoxic risk.

*Z. mucronata*, also known as the buffalo thorn tree, is used ethnomedicinally for the treatment of pain, skin infections, dysentery and coughs (Figure 4Q).<sup>64</sup> *Z. mucronata* displayed a moderate-to-low risk of inducing cytotoxic effects in the phytotoxicity testing phase of the project, thus was included for further assessment.

#### 4.1.4. Aim of hepatotoxicity assessment

The aim of the hepatotoxicity assessment was to determine to the effect of the selected herbal remedies on various hepatocellular parameters that could elucidate the mechanism of phytotoxicity. The objectives was to:

- Determine the effect of selected herbal remedies on hepatocellular parameters relevant to hepatotoxicity.

## 4.2. Materials and Methods

A detailed list of all reagents used in the study, as well as the preparation thereof, is provided (Appendix III). Preparation of crude extracts has been described in Chapter 2.

### 4.2.1. Determination of hepatotoxicity using a single-plate method

A rapid, repeatable, sensitive and affordable multi-endpoint, single microplate method has been developed in our department which allows for the determination of *in vitro* hepatotoxicity in hepatocytes from an immortalized cell line.<sup>21</sup> Further optimization of the established model has allowed for the assessment of pre-clinical toxicity with regards to: intracellular ROS concentration, depletion of GSH, impairment of mitochondrial stability (through determination of changes in  $\Delta\Psi_m$ ), induction of apoptosis (through measurement of caspase-3/7 activity), reduction of cellular viability and potential steatotic changes (through determination of fatty acid accumulation). These parameters are recognized indicators of pre-lethality<sup>276</sup> and therefore serve as a basis for pre-clinical assessment of hepatotoxicity. Based on the predicted results, it is pertinent to also assess the involvement of lipid peroxidation and fluctuations of ATP levels, which may give further indication of the effects on cellular viability and cellular kinetics.

#### 4.2.1.1. Seeding of cells and exposure to crude extracts

HepG2 cells (100  $\mu$ L) were seeded into sterile, white 96-well plates at  $2 \times 10^4$  cells/well (Figure 20). Plates were incubated for 24 h at 37°C and 5% CO<sub>2</sub> in a humidified incubator to allow for attachment. Blanks (200  $\mu$ L) consisting of 5% FCS-supplemented EMEM alone were included to assess background noise and sterility. Cells were exposed to 100  $\mu$ L DMSO (0.8%, negative vehicle control), crude extracts (2, 6.4, 20, 64 and 200  $\mu$ g/mL) or the respective positive control prepared in FCS-negative EMEM for 72 h. Hepatotoxic parameters were determined after the designated exposure time as described hereafter.

	CD	ROS	GSH	MMP	FA	CAS-3/7
Crude extracts	○	○	○	○	○	○
	○	○	○	○	○	○
	○	○	○	○	○	○
	○	○	○	○	○	○
	○	○	○	○	○	○
Blank	○	○	○	○	○	○
Negative control	○	○	○	○	○	○
Positive control	○	○	○	○	○	○

**Figure 20:** Plate template used for the determination of hepatotoxicity (CD – cell density, ROS – ROS concentration, GSH – GSH concentration, MMP –  $\Delta\Psi_m$ , FA –fatty acid concentration, CAS-3/7 – caspase-3/7)

#### 4.2.1.2. Cell density

The SRB assay has been described in Chapter 3. Initially the resazurin conversion assay was idealised for its fluorescent activity and high sensitivity, but unfortunately the high level of interaction between the crude extracts and the dye made this assay incompatible.<sup>315</sup> Cell density was determined by protein staining using SRB as described in Chapter 3. Staurosporine (10  $\mu\text{M}$  in reaction) was used as positive control. Aliquots of solubilized dye (100  $\mu\text{L}$ ) were transferred to a clear 96-well plate and the absorbance measured spectrophotometrically.

#### 4.2.1.3. Reactive oxygen species concentration

Oxidative stress can be measured fluorometrically by using 2',7'-dichlorodihydrofluorescein diacetate (H<sub>2</sub>-DCFDA). The dye enters the cell passively where it is hydrolysed by intracellular esterases to remove the diacetate. The resultant 2',7'-dichlorodihydrofluorescein (H<sub>2</sub>-DCF) is captured intracellularly and oxidized by free radicals to the highly fluorescent dichlorofluorescein (DCF).<sup>276</sup>

Intracellular ROS concentration was determined using the enzymatic conversion and activation of H<sub>2</sub>-DCF-DA to the highly-fluorescent DCF.<sup>316</sup> Potassium peroxodisulfate

(150  $\mu$ M in reaction) was used as positive control. Medium was replaced with 100  $\mu$ L H<sub>2</sub>-DCF-DA (10  $\mu$ M in PBS) for 2 h and the fluorescent intensity measured at  $\lambda_{\text{ex}} = 485$  nm and  $\lambda_{\text{em}} = 520$  nm (gain 750) (FLUOstar Optima, BMG Labtech). The SRB assay was performed post-measurement to account for sample-induced cell death. Fluorescent intensity was adjusted by subtracting the blanks, standardised according to the cell density and the fold-change of the intracellular ROS concentration relative to the negative control expressed using the following equation:

$$\text{Intracellular ROS concentration (fold – change)} = \frac{\text{FIs}}{\text{Fic}}$$

where, FIs = the standardised, blank-adjusted fluorescent intensity of the sample, and Fic = the standardised, blank-adjusted average fluorescent intensity of the negative control.

#### **4.2.1.4. Reduced glutathione concentration**

Monochlorobimane is a non-fluorescent molecule that diffuses readily into cells and undergoes enzymatic conjugation to GSH through glutathione-S-transferase. Once conjugated the monochlorobimane adduct fluoresces intensely, and thus alterations in intensity would either indicate GSH depletion (lower intensity) or *de novo* synthesis/supplementation (higher intensity).<sup>317</sup>

Intracellular GSH concentration was determined using the conjugation of monochlorobimane to GSH to form a fluorescent adduct.<sup>59</sup> n-Ethylmaleimide (10  $\mu$ M in reaction) was used as positive control. Medium was replaced with 100  $\mu$ L monochlorobimane (16  $\mu$ M in PBS) for 2 h and the fluorescent intensity measured at  $\lambda_{\text{ex}} = 355$  nm and  $\lambda_{\text{em}} = 460$  nm (gain 1250). The fold-change of the intracellular GSH concentration was determined as described in Section 4.2.1.3.

#### **4.2.1.5. Mitochondrial membrane potential**

The mitochondrial-selective, lipophilic dye, 5,5',6,6'-tetrachloro-1,1',3,3'-tetraethylbenzimidazolylcarbocyanine iodide (JC-1), exists in two forms, either as its monomer or aggregates of itself which exhibits intense green or red fluorescence, respectively.<sup>316</sup> In healthy cells JC-1 preferentially accumulates in mitochondria ( $\Delta\Psi_{\text{m}} -180 - 200$  mV) and undergoes aggregation to J-aggregates. In compromised or

apoptotic cells JC-1 remains in its monomer form in the cytosol due to an increase in  $\Delta\Psi_m$  ( $\approx 0$  mV). The mitochondrial selectivity of JC-1 is only dependent on the  $\Delta\Psi_m$ , and thus other factors such as size, shape and density are not taken into account. By determining the red-to-green fluorescence ratio the effect of compounds on the mitochondrial stability can be determined, where a decrease reflects mitochondrial depolarization (an increase in aggregate formation due to decreased  $\Delta\Psi_m$ ), while an increase indicates hyperpolarization (a decrease in aggregate formation due to increased  $\Delta\Psi_m$ ).<sup>316</sup>

MMP was determined by expressing the ratio of red fluorescent J-aggregates (healthy cells) to green fluorescent JC-1 monomers (unhealthy cells).<sup>316</sup> Rotenone (100 nM in reaction) was used as positive control. Medium was replaced with 100  $\mu$ L JC-1 (10  $\mu$ M in PBS) for 2 h and the fluorescent intensity measured at  $\lambda_{ex} = 492$  nm and  $\lambda_{em} = 590$  nm (gain 1000) and  $\lambda_{ex} = 485$  nm and  $\lambda_{em} = 520$  nm (gain 1000), respectively. Fluorescent intensity was adjusted by subtracting the blanks and the ratio of JC-1 monomers to J-aggregates determined. The fold-change of  $\Delta\Psi_m$  relative to the negative control was expressed using the following equation:

$$\Delta\Psi_m (\text{fold - change}) = \frac{R_s}{R_c}$$

where,  $R_s$  = the ratio of blank-adjusted fluorescent intensity of the sample, and  $R_c$  = the ratio of blank-adjusted average fluorescent intensity of the negative control.

#### 4.2.1.6. Fatty acid concentration

Nile red is a lipophilic dye that generally does not fluoresce when in a polar solvent, though when dissolved in lipid-rich media it emits intense red fluorescence. The dye accumulates within lipid droplets, and thus cells containing high quantities of intracellular fatty acids will fluoresce strongly.<sup>318</sup> In HepG2 cells this will occur during fatty acid accumulation, and thus may be an indication of steatosis.

Intracellular fatty acid concentration was determined using cellular accumulation of Nile red as a measure of steatosis.<sup>319</sup> Oleic acid (200  $\mu$ M in reaction) was used as positive control. Medium was replaced with 100  $\mu$ L Nile red (1  $\mu$ M) for 2 h and the fluorescent intensity measured at  $\lambda_{ex} = 544$  nm and  $\lambda_{em} = 590$  nm (gain 1000). The fold-change of the intracellular acid concentration was determined as described in Section 4.2.1.3.

#### 4.2.1.7. Apoptosis

Acetyl Asp-Glu-Val-Asp-7-amido-4-methylcoumarin (Ac-DEVD-AMC) is a synthetic tetrapeptide substrate that is cleaved by activated caspases-3/7 to free the bound fluorogenic 7-amido-4-coumarin (AMC).<sup>316</sup> Intracellular caspase-3/7 is released from cells through the use of membrane lytic solutions where it can be exposed to the selective substrate. As caspase-3/7 is only activated through pro-apoptotic pathways, fluorescence indicates an induction of programmed cell death.<sup>316</sup>

Apoptosis was determined using the enzymatic cleavage of Ac-DEVD-AMC by activated caspase-3/7 to release the fluorescent AMC molecule.<sup>316</sup> Staurosporine (10  $\mu$ M in reaction) served as positive control. Medium was replaced with 25  $\mu$ l cold lysis buffer and incubated for 15 min on ice. After lysis, 100  $\mu$ L caspase-3/7 substrate buffer containing Ac-DEVD-AMC was added. Plates were incubated for 4 h at 37°C, and a further 16 h at 4°C. The fluorescent intensity was measured at  $\lambda_{\text{ex}} = 355$  nm and  $\lambda_{\text{em}} = 460$  nm (gain 750). Fluorescent intensity was adjusted by subtracting the blanks, standardised according to the relative cell density and the fold change of the caspase-3/7 activity relative to the negative control expressed using the following equation:

$$\text{Caspase - 3/7 activity (fold - change)} = \frac{\text{FIs}}{\text{FIc}}$$

where, FIs = the standardised, blank-adjusted fluorescent intensity of the sample, and FIc = the standardised, blank-adjusted average fluorescent intensity of the negative control.

#### 4.2.2. Determination of lipid peroxidation

The TBARS assay functions as a measure of lipid hydroperoxide formation, which occurs during oxidation and thus suggests oxidative stress. These products include MDA, which binds to thiobarbituric acid to form a fluorescent adduct. Increased fluorescence would then suggest of oxidative stress.<sup>320</sup>

Lipid peroxidation was determined using the TBARS assay.<sup>320</sup> HepG2 cells were seeded into sterile, clear 96-well plates and exposed as described in Section 4.2.1.1. AAPH (500  $\mu$ M in reaction) was used as positive control. Medium (200  $\mu$ L) was aspirated into 5 mL tubes, after which cells were chemically detached using 100  $\mu$ L

Trypsin/Versene and added to the respective supernatant. To each tube was added: 100  $\mu\text{L}$  TCA (16.5%) and 100  $\mu\text{L}$  thiobarbituric acid (2.5% in 0.1 M sodium hydroxide and 50  $\mu\text{M}$  ethylenediaminetetraacetic acid [EDTA]). Tubes were vortex-mixed and placed in a warm waterbath (95°C) for 20 min, after which 250  $\mu\text{L}$  butanol was added. Tubes were vortex-mixed once more, and left to separate into an aqueous and organic layer. Aliquots (100  $\mu\text{L}$ ) of the organic layer were transferred to a white 96-well plate and the fluorescent intensity measured at  $\lambda_{\text{ex}} = 544 \text{ nm}$  and  $\lambda_{\text{em}} = 590 \text{ nm}$  (gain 750). The fold-change of the intracellular lipid peroxidation levels were determined as described in Section 4.2.1.3.

#### 4.2.3. Determination of ATP levels

Chemiluminescent signalling relies on the production of light from a bioluminescent source. Luciferase catalyses the interaction between the substrate luciferin and ATP, which yields significant flash of light production. This can then be measured using a luminometer, and thus gives a proportional indication of ATP content within a cell.<sup>321</sup>

ATP levels were determined using the ApoSENSOR™ ATP cell viability chemiluminescence kit.<sup>321</sup> HepG2 cells were seeded and exposed as described in Section 4.2.1.1 in sterile, white 96-well plates. Saponin (1% in reaction) was used as positive control. Medium was replaced with 100  $\mu\text{L}$  nucleotide releasing buffer and incubated for 5 min on a shaker. After lysis, 10  $\mu\text{L}$  ATP monitoring enzyme was added, and plates measured immediately using a chemiluminescence protocol. End-point luminescent intensity was adjusted by subtracting the blanks, standardised according to the relative cell density and the fold change of the ATP level relative to the negative control expressed using the following equation:

$$\text{ATP level (fold – change)} = \frac{\text{LIs}}{\text{LIc}}$$

where, LIs = the standardised, blank-adjusted luminescent intensity of the sample, and LIc = the standardised, blank-adjusted average luminescent intensity of the negative control.

## 4.2.4. Determination of cellular kinetics and mode of cell death

### 4.2.4.1. Synchronisation of HepG2 cells for cellular kinetics

Assessment of the cell cycle requires that the majority of cells be synchronised into one cellular phase to limit variability that can occur from asynchronicity.<sup>322</sup> From this a more accurate picture can be drawn with regards to the type of effects that are elicited on cellular kinetics. Methods range from low to high cell manipulation which upon removal will theoretically allow for cells to continue cycling in a synchronised fashion for a defined period of time.<sup>322</sup> Although traditional synchronisation methods have been scrutinised as not producing truly synchronised populations,<sup>323</sup> their use in literature is widely employed. Serum deprivation is an often-used technique to induce a G1-phase arrest, as cells require several growth factors to proceed into the subsequent phases.<sup>322</sup> The withdrawal of serum, however, has been shown to reduce cellular viability,<sup>322</sup> and a higher level of baseline cytotoxicity can be observed upon experimentation. In-house experimentation has shown that a variety of cell lines, including the HepG2 cell line, undergo detachment and DNA fragmentation when deprived of serum for 24 to 48 h (data not shown), making this method unsuitable. The mitotic shake-off method is based on the principle that cells undergoing division display low adhesion to the culture surface, and thus can be dislodged upon agitation.<sup>324</sup> This however produces a low yield of synchronised cells, thus exceptionally large populations need to be used initially to obtain an adequate amount of synchronised cells.<sup>322</sup> The method ultimately utilised for experimentation in the current project was the double thymidine block method. Through sequential treatment with excessive thymidine concentrations, cells are arrested in the S-phase through a feedback inhibition of DNA replication by affecting ribonucleotide reductase.<sup>322,324</sup>

HepG2 cells were synchronised into the S-phase of the cell cycle using the double thymidine block as described by Chiang *et al.*<sup>325</sup> for determination of cellular kinetics. HepG2 cells were maintained in EMEM supplemented with 10% FCS and grown in 75 cm<sup>2</sup> flasks at 37°C and 5% CO<sub>2</sub> in a humidified incubator till 75% confluent. Cells were rinsed with PBS and incubated for 16 h in 3 mM thymidine-fortified EMEM supplemented with 10% FCS, after which flasks were rinsed and incubated for 10 h in EMEM supplemented with 10% FCS. After incubation, cells were rinsed once more and incubated for a further 16 h with 3 mM thymidine-fortified EMEM supplemented with 10% FCS. Cells were detached using Trypsin/Versene solution and counted using

the trypan blue exclusion assay as described in Chapter 3. An aliquot of the synchronised cells were fixed as described in Section 4.2.4.3. to follow.

#### **4.2.4.2. Seeding of cells and exposure to crude extracts**

Synchronised and non-synchronised HepG2 cells were used for determination of cellular kinetics and mode of cell death, respectively. HepG2 cells (600  $\mu$ L) were seeded into sterile, clear 24-well plates at  $1 \times 10^5$  cells/well. Plates were incubated for 24 h at 37°C and 5% CO<sub>2</sub> in a humidified incubator to allow for attachment. Cells were exposed to 600  $\mu$ L EMEM (negative control), crude extracts (2 x IC<sub>50</sub>, or 200  $\mu$ g/mL if no IC<sub>50</sub> was obtained) or the respective positive control prepared in FCS-negative EMEM for both 24 h and 72 h.

#### **4.2.4.3. Determination of cellular kinetics using cell cycle analysis**

The incorporation of fluorescent or radioactive DNA markers has been the staple of cell cycle analysis, and different methods are available. Propidium iodide, an analogue of ethidium bromide, is a double stranded DNA and ribonucleic acid (RNA) intercalating agent that displays increased fluorescence (20 – 30-fold) once bound to a nucleic acid.<sup>287</sup> As propidium iodide is unable to permeate intact cellular membranes, fixation and lysis is required for successful staining to occur.<sup>287</sup> To ensure only DNA is stained during sample preparation, RNA can be degraded through the addition of RNase A.<sup>287,326</sup> As cells in each phase contain different DNA content, fluorescent activity will differ throughout. As such a flow cytometric histogram is created (Figure 21), displaying the distribution of cells in each phase. Utilizing propidium iodide staining allows for four distinct phases to be presented, namely the sub-G1-, G1-, S- and G2/M-phase. The sub-G1-phase refers to DNA content  $<2N$ , thus represents hypodiploid cells with fragmented DNA, an indicator of potential apoptotic cell death.<sup>327</sup> As DNA content of the G2- and M-phases are similar, it is not possible to differentiate between the two using the proposed method. Statistical analysis of the cell cycle can be achieved by incorporating deconvolution software to the collected data if a large enough number of cells have been counted, which utilizes Gaussian distributions to model the different phases.<sup>287</sup> Important to note is that each phase (G1, S, G2/M)

contributes to the total amount displayed (100%). The sub-G1 phase itself is represented as a different set, and thus does not contribute to the total cell cycle phases. Furthermore, due to the abovementioned, although the cell cycle distribution may appear diminished at times, it is still represented relative to the whole cell cycle.

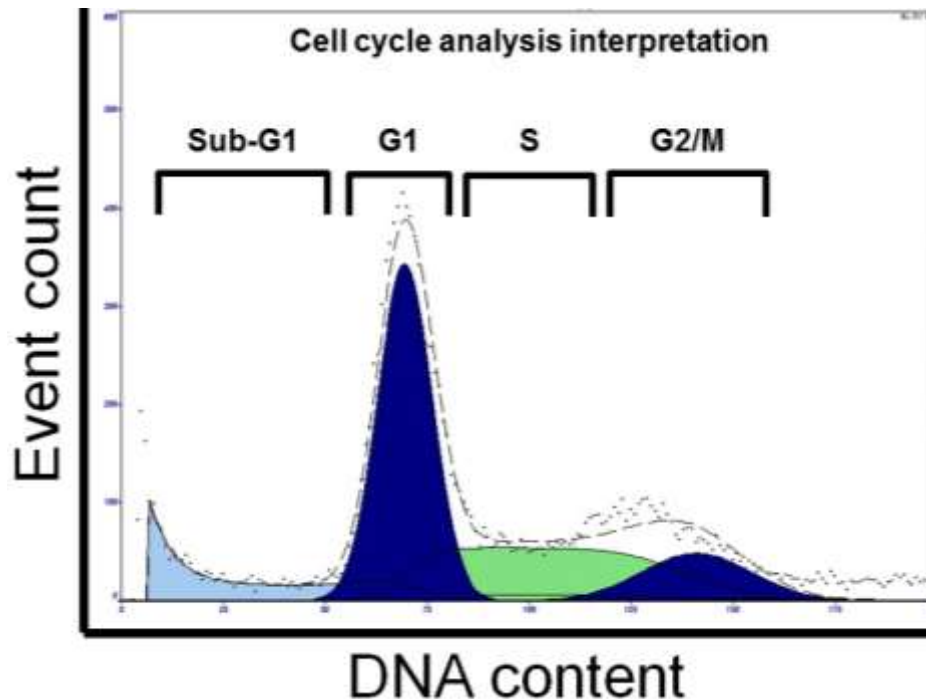


**Figure 21:** Interpretation of cell cycle kinetics using deconvolution software, where DNA content was determined through propidium iodide staining.

The effects of the crude extracts on cellular kinetics was determined using the propidium iodide staining method according to Darzynkiewicz and Juan.<sup>328</sup> Positive controls included the following: i) for induction of a G1-block, medium was replaced with FCS-free EMEM, and ii) for induction of a S- and G2/M-block, cells were exposed to 10  $\mu$ M methotrexate and 20  $\mu$ M curcumin in reaction, respectively for 14 h. Cells were trypsinised and washed once with PBS supplemented with 1% FCS. Cells were fixed by adding 3 mL cold ethanol (70%) in a drop-wise fashion while being vortex-mixed, after which cells were incubated at 4°C overnight. Cells were lysed and stained using a propidium iodide staining solution (containing 100  $\mu$ g/mL RNase, 40  $\mu$ g/mL propidium iodide and 0.1% Triton X-100) for 40 min at 37°C. Flow cytometric analysis (FC500 Series, Beckman-Coulter) was carried out to determine the distribution of DNA using FL-3. Deconvolution software (Multicycle V3.0, WinCycle) was employed to interpret the different phases of the cell cycle.

#### 4.2.4.4. Determination of mode of cell death through PS-flip and membrane integrity

As apoptotic and necrotic cells present with different characteristics, it is possible to separate them flow cytometrically into distinct quadrants through the use of differential staining methods. Such is the case with Annexin V-fluorescein isothiocyanate (FITC) and propidium iodide dual staining. Annexin V is a calcium-dependent phospholipid-binding protein with high affinity for phosphatidylserine residues. As a PS-flip occurs in apoptotic cells, cells may be stained positively through the use of a FITC-conjugated Annexin V molecule. Propidium iodide, a vital dye, cannot cross intact cellular membranes. Thus only cells with disrupted cellular membrane integrity can be stained positive.<sup>329</sup> By using both dyes, cells may be divided into different quadrants, namely Annexin V<sup>-</sup>/propidium iodide<sup>-</sup> (viable), Annexin V<sup>+</sup>/propidium iodide<sup>-</sup> (early apoptotic), Annexin V<sup>+</sup>/propidium iodide<sup>+</sup> (late apoptotic/aponecrotic) or Annexin V<sup>-</sup>/propidium iodide<sup>+</sup> (necrotic) (Figure 22). These quadrants can be defined using unstained or differentially-stained populations of cells. Density plots can then be utilised to express the amount of cells within each specific quadrant, and representative images used to indicate this.

The effect of crude extracts on the mode of cell death was assessed using the Annexin V-FITC/propidium iodide assay as described by Hingorani *et al.*<sup>329</sup> Positive controls included the following: i) for induction of apoptosis, cells were exposed to 50 nM rotenone in-reaction, and ii) for induction of necrosis, trypsinised cells were lysed with cold absolute ethanol and sonicated for 3 min. Cells were trypsinised and washed once with PBS supplemented with 1% FCS. Cells were stained for 15 min in the dark with 2.5  $\mu$ L Annexin V-FITC solution, after which 2.5  $\mu$ L propidium iodide (3 mM) was added. Quadrant flow cytometric analysis was carried out to determine the distribution of cells in either the FL-1-positive (Annexin V-FITC, early apoptosis), FL-3-positive (propidium iodide, necrosis) or FL-1 and FL-3 positive (late apoptosis, or aponecrosis) quadrants.

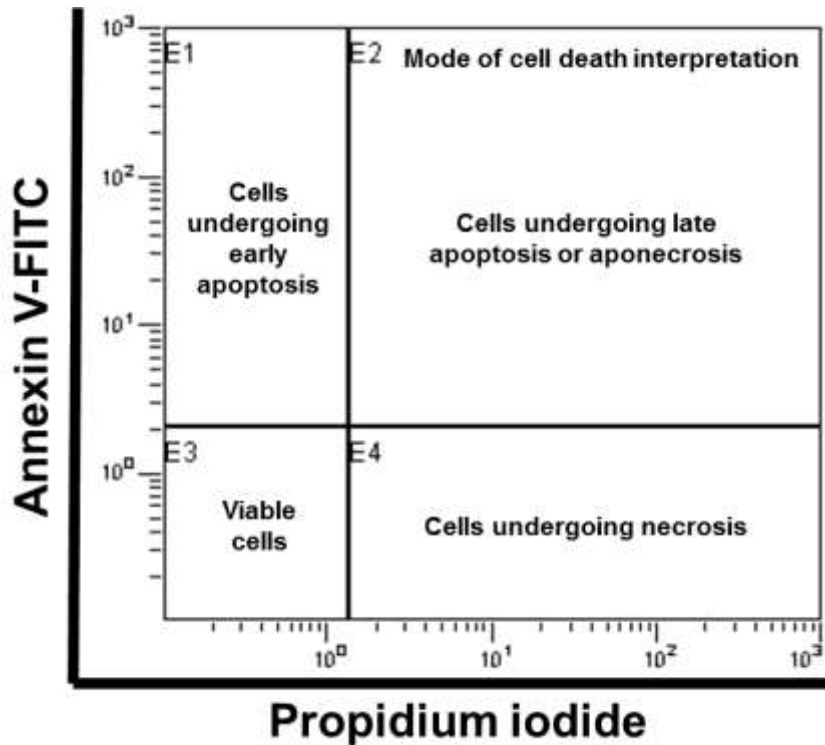


**Figure 22:** Interpretation of mode of cell death.

#### 4.2.5. Statistics

All experiments were performed using at least two technical and three biological replicates. Results were compiled using Microsoft Excel 2010 and analysed statistically with GraphPad Prism 5.0. All results were expressed as the mean  $\pm$  SEM. The  $IC_{50}$  was determined using non-linear regression (normalized, variable slope). For the hepatotoxicity model, significant differences were determined between the negative control and treated cells using Kruskal-Wallis and a post-hoc Dunns test. For the flow cytometric results, significant difference were determined between the negative and the treated cells using two-way analysis of variance (ANOVA) and a post-hoc Bonferroni test. Significance was defined as  $p < 0.05$ .

## 4.3. Results

### 4.3.1. Use of sulforhodamine B for normalization against protein content

As fluorescent data could be skewed due to an alteration in cellular viability, normalization of the data relative to protein content is often done to more accurately express results. The Bradford protein content assay is usually followed, but due to specific parameters of the hepatotoxicity model it was decided that a more robust technique would be better suited. As the SRB assay also stains for protein content, it was assessed whether a correlation was present between cell number and protein content. A high correlation ( $r^2 = 0.9688$ ) that was statistically significant ( $p < 0.001$ ) was found for protein content between the Bradford and SRB assays (Figure 23). Subsequent experiments were normalized to SRB-determined cellular density to express the fluorescent data obtained.

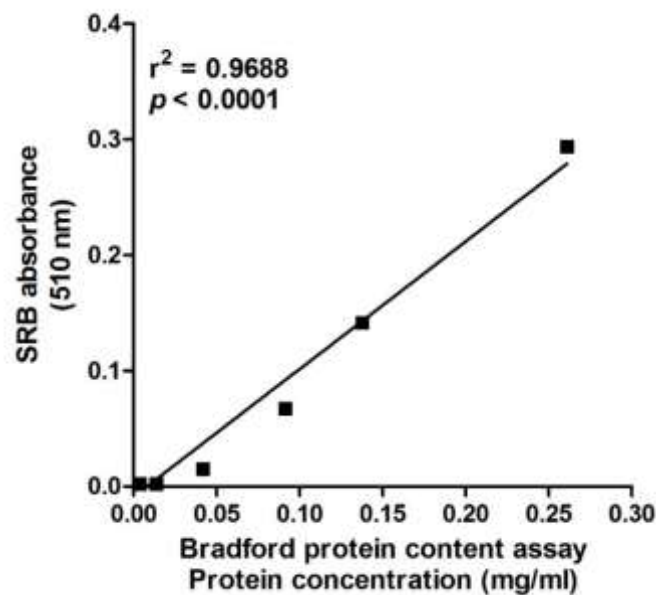


**Figure 23:** Correlation between the Bradford protein content and SRB assay.

### 4.3.2. Positive controls for the hepatotoxicity assays

Positive controls for all assays resulted in the expected alterations to the hepatocyte parameters, indicating that all assays displayed suitable sensitivity and responses to the measured parameters. With regards to the hepatotoxicity model: cell density

(Figure 24A),  $\Delta\Psi_m$  (Figure 24B), GSH concentrations (Figure 24D) and ATP levels (Figure 24G) were decreased by 94.2%, 0.34-, 0.85- and 0.99-fold after exposure to staurosporine, rotenone, n-ethylmaleimide and saponin, respectively. ROS concentration (Figure 24C), fatty acid concentration (Figure 24E), lipid peroxidation (Figure 24F) and caspase-3/7 activity (Figure 24H) was increased by 2-, 2.5-, 1.93- and 2.2-fold after exposure to potassium peroxodisulfate, oleic acid, AAPH and staurosporine, respectively.

Cells were successfully synchronised in the S-phase of the cell cycle using the double thymidine blocking method, resulting in 71.18% of cells retained in this phase upon experimentation (Figure 25C). Although not significant, an increase of 8.83% of cells in the G1-phase was induced after 24 h FCS-depletion (G1-block) (Figure 25D). Exposure to methotrexate and curcumin induced an increase of 16.69% and 14.25% of cells in the S- and G2/M-phase, respectively (Figure 25E and F). Negative controls displayed similar cellular kinetics at the 24 h and 72 h mark (Figure 25A and B).

Cells were successfully maintained in the culture conditions and displayed high cellular viability (approximately 92%) with minimal cell death, which primarily presented as necrosis (approximately 6%) (Figure 26A and B). Cells exposed to rotenone for 24 h displayed apoptotic (45.94%) and necrotic cell death (14.57%) (Figure 26C). Sonication in 70% cold ethanol for 5 min resulted in a large increase in necrotic cells (95.10%) (Figure 26D).

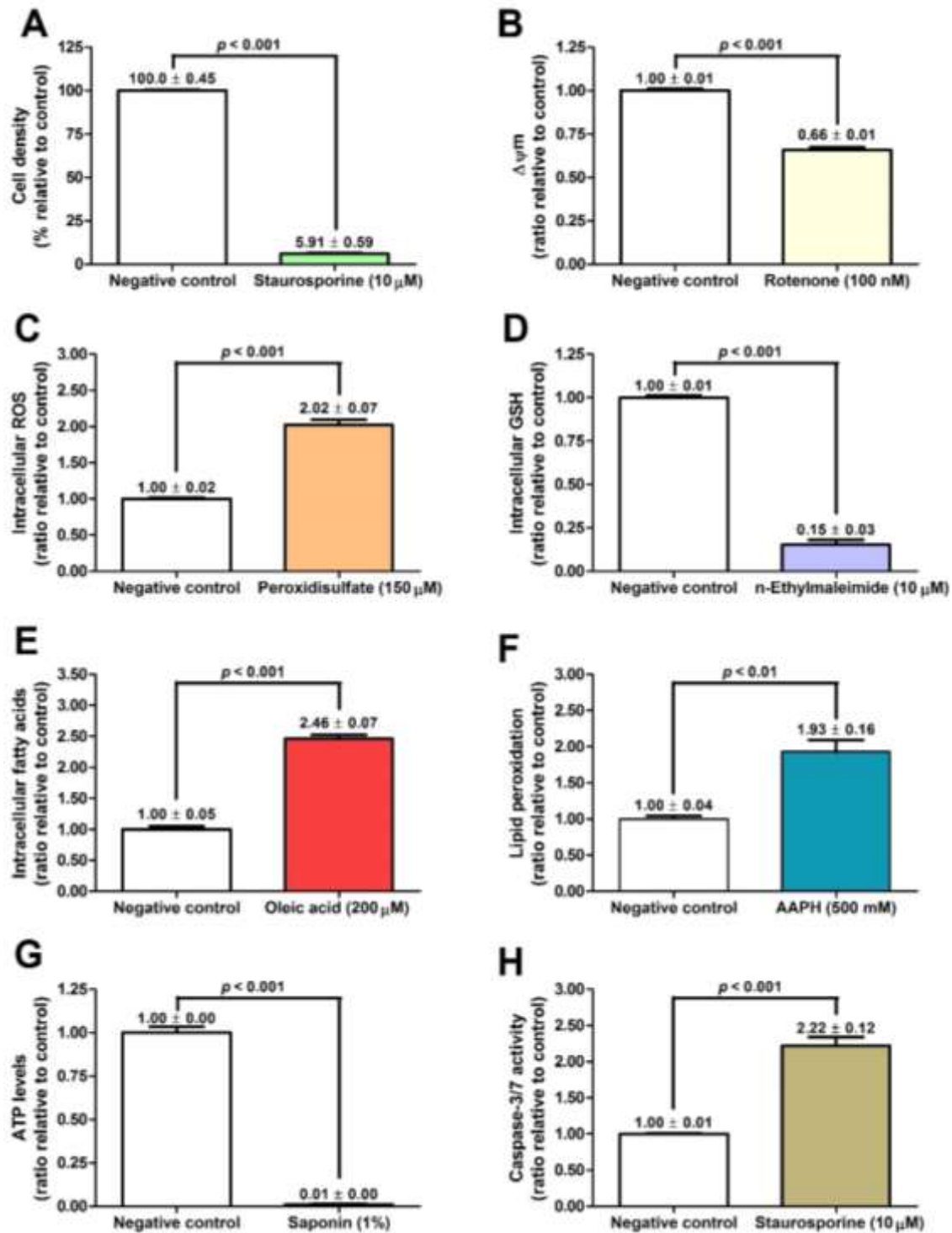


**Figure 24:** The effect of positive controls on A) cell density (staurosporine), B)  $\Delta\Psi_m$  (rotenone), C) ROS concentration (potassium peroxidisulfate), D) GSH concentration (n-ethylmaleimide), E) fatty acid concentration (oleic acid), F) lipid peroxidation (AAPH), G) ATP levels (saponin) and H) caspase-3/7 activity (staurosporine) in HepG2 cells; significance was determined against the negative control.

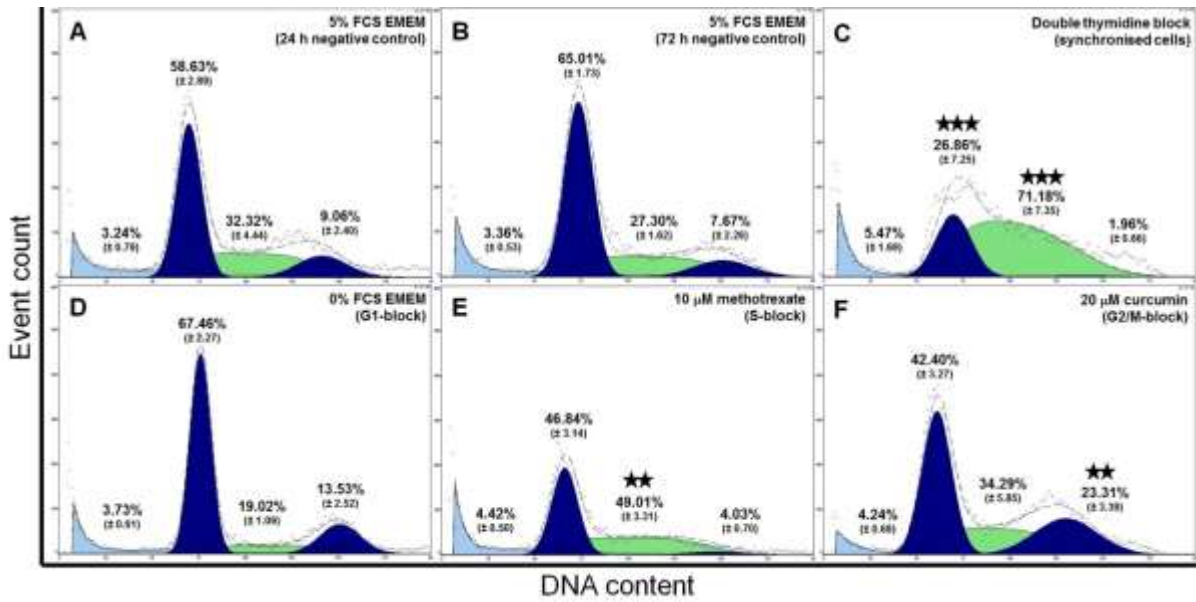


**Figure 25:** The effect of positive controls on the cell cycle kinetics of HepG2 cells exposed to A) negative control for 24 h, B) negative control for 72 h, C) double thymidine block (synchronised cells), D) FCS-depleted EMEM (G1-block) for 24 h, E) methotrexate (S-block) for 14 h, and F) curcumin (G2/M-block) for 14 h. Significance determined relative to the 24 h negative control: ★★  $p < 0.01$ , ★★★  $p < 0.001$ .

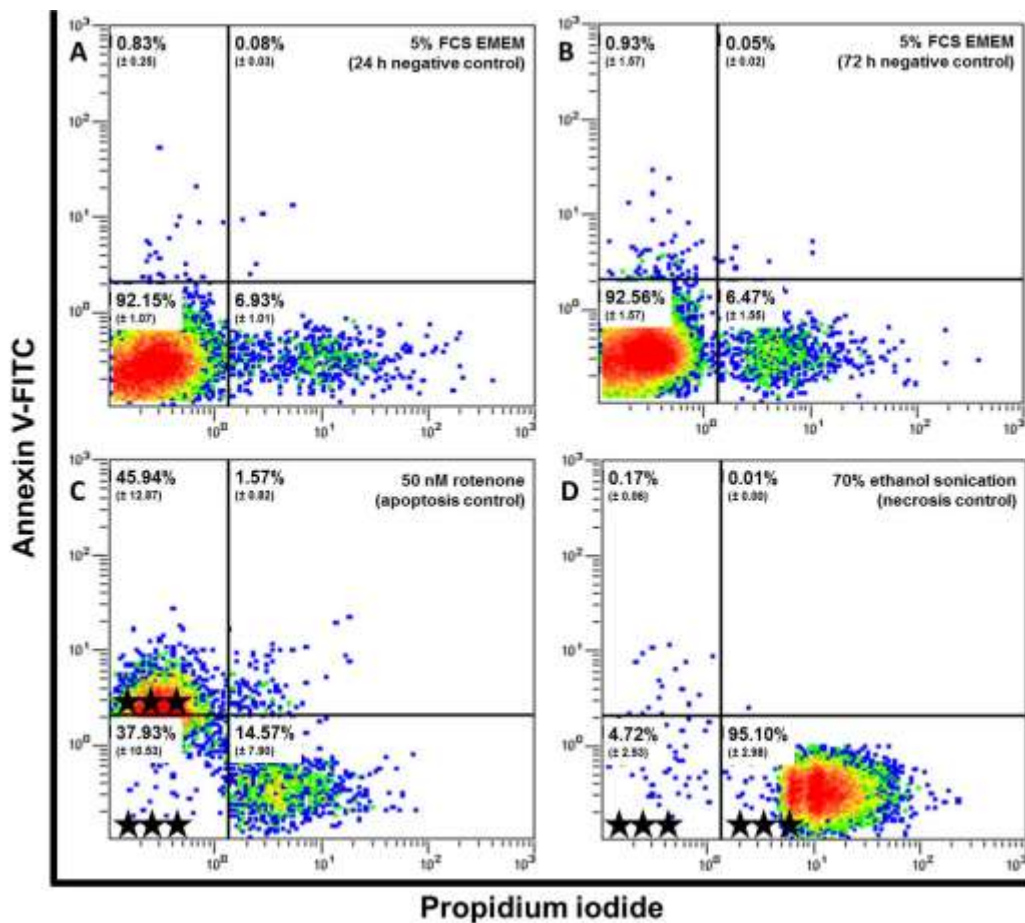


**Figure 26:** The effect of positive controls on the viability of HepG2 cells exposed to A) negative control for 24 h, B) negative control for 72 h, C) rotenone (apoptosis) for 24 h, and D) 70% ethanol sonication (necrosis) for 5 min. Significance determined relative to the 24 h negative control: ★★★  $p < 0.001$ .

### 4.3.3. Selected plant extracts

#### 4.3.3.1. *Acokanthera oppositifolia*

The hot water extract of *A. oppositifolia* decreased cell density significantly ( $p < 0.01$ ) at  $\geq 10$   $\mu\text{g/mL}$ , with an  $\text{IC}_{50}$  of 24.26  $\mu\text{g/mL}$  and maximum reduction of 65.95% at 100  $\mu\text{g/mL}$  (Figure 27A).  $\Delta\Psi\text{m}$  was reduced to below baseline at all concentrations, but was only significant ( $p < 0.01$ ) at  $\geq 10$   $\mu\text{g/mL}$  (up to 0.84-fold at 100  $\mu\text{g/mL}$ ) (Figure 27B). Intracellular ROS concentrations were slightly reduced below baseline, although this was not significant (Figure 27C). Intracellular GSH concentrations decreased to below baseline at all concentrations, but were only significant ( $p < 0.05$ ) at  $\geq 3.2$   $\mu\text{g/mL}$ , and reached a plateau at  $\geq 10$   $\mu\text{g/mL}$  (0.56-fold) (Figure 27D). Fatty acid concentrations increased significantly ( $p < 0.001$ ) at  $\geq 10$   $\mu\text{g/mL}$ , though no dose-dependent effect was observed (2.33- and 2.00-fold at 32  $\mu\text{g/mL}$  and 100  $\mu\text{g/mL}$ , respectively) (Figure 27E). Lipid peroxidation was not significantly altered, though a slight increase of 1.24-fold was apparent at 3.2  $\mu\text{g/mL}$  (Figure 27F). ATP levels were dose-dependently decreased at all concentrations ( $p < 0.05$ ), ranging between 0.42- and 0.08-fold (Figure 27G). Although not significant, caspase-3/7 activity was below baseline at  $\leq 3.2$   $\mu\text{g/mL}$  (approximately 0.35-fold reduction), while at  $\geq 10$   $\mu\text{g/mL}$  it was induced by up to 1.98-fold at 100  $\mu\text{g/mL}$  (Figure 27H).

The methanol extract decreased cell density significantly ( $p < 0.05$ ) at  $\geq 3.2$   $\mu\text{g/mL}$ , with an  $\text{IC}_{50}$  of 26.16  $\mu\text{g/mL}$  and maximum reduction of 72.14% at 100  $\mu\text{g/mL}$  (Figure 28A).  $\Delta\Psi\text{m}$  was reduced dose-dependently by up to 0.74-fold at 100  $\mu\text{g/mL}$ , with significant ( $p < 0.01$ ) reduction at  $\geq 10$   $\mu\text{g/mL}$  (Figure 28B). Similar to the hot water extract, ROS concentrations were below baseline at all concentrations, although a significant ( $p < 0.05$ ) reduction was observed at  $\geq 32$   $\mu\text{g/mL}$  (complete abolishment at 100  $\mu\text{g/mL}$ ) (Figure 28C). GSH concentrations were significantly ( $p < 0.01$ ) decreased at 3.2  $\mu\text{g/mL}$  to 32  $\mu\text{g/mL}$  (0.29-fold to 0.43-fold reduction), with a slight increase of 1.20-fold at 100  $\mu\text{g/mL}$  (Figure 28D). Dose-dependent fatty acid accumulation was observed, significant ( $p < 0.05$ ) at  $\geq 10$   $\mu\text{g/mL}$  (4.61-fold at 100  $\mu\text{g/mL}$ ) (Figure 28E). Little to no alteration in lipid peroxidation occurred (Figure 28F). ATP levels decreased significantly ( $p < 0.05$ ) at all concentrations between 0.53- and 0.19-fold (Figure 28G). Caspase-3/7 activity was similarly increased, with elevated activity at  $\geq 10$   $\mu\text{g/mL}$ , although it was only significant ( $p < 0.05$ ) at 100  $\mu\text{g/mL}$  (5.82-fold) (Figure 28H).

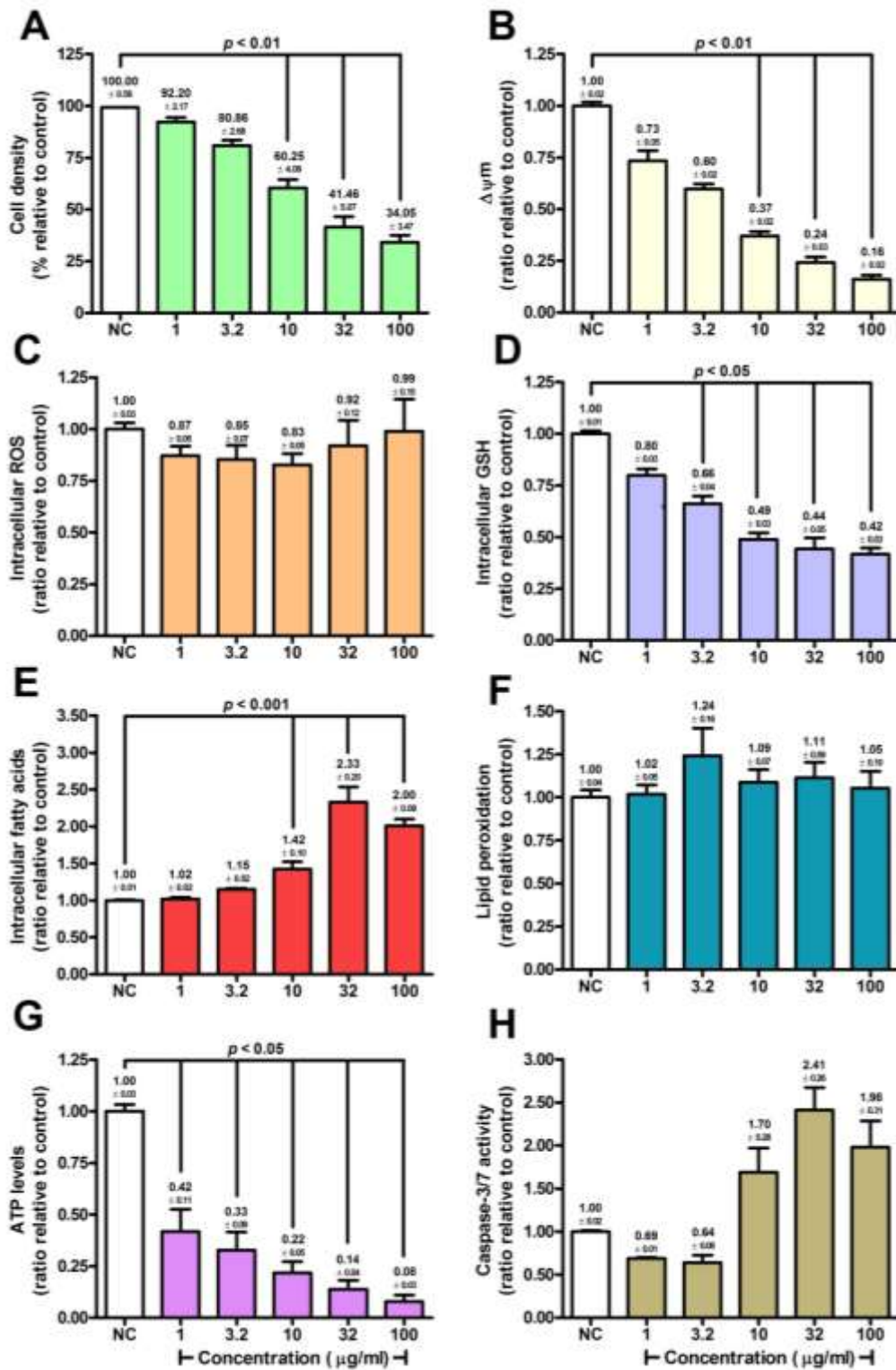


**Figure 27:** The effect of the crude hot water extract of *A. oppositifolia* in HepG2 cells; A) cell density, B)  $\Delta\psi_m$ , C) ROS concentration, D) GSH concentration, E) fatty acid concentration, F) lipid peroxidation, G) ATP levels and H) caspase-3/7 activity.

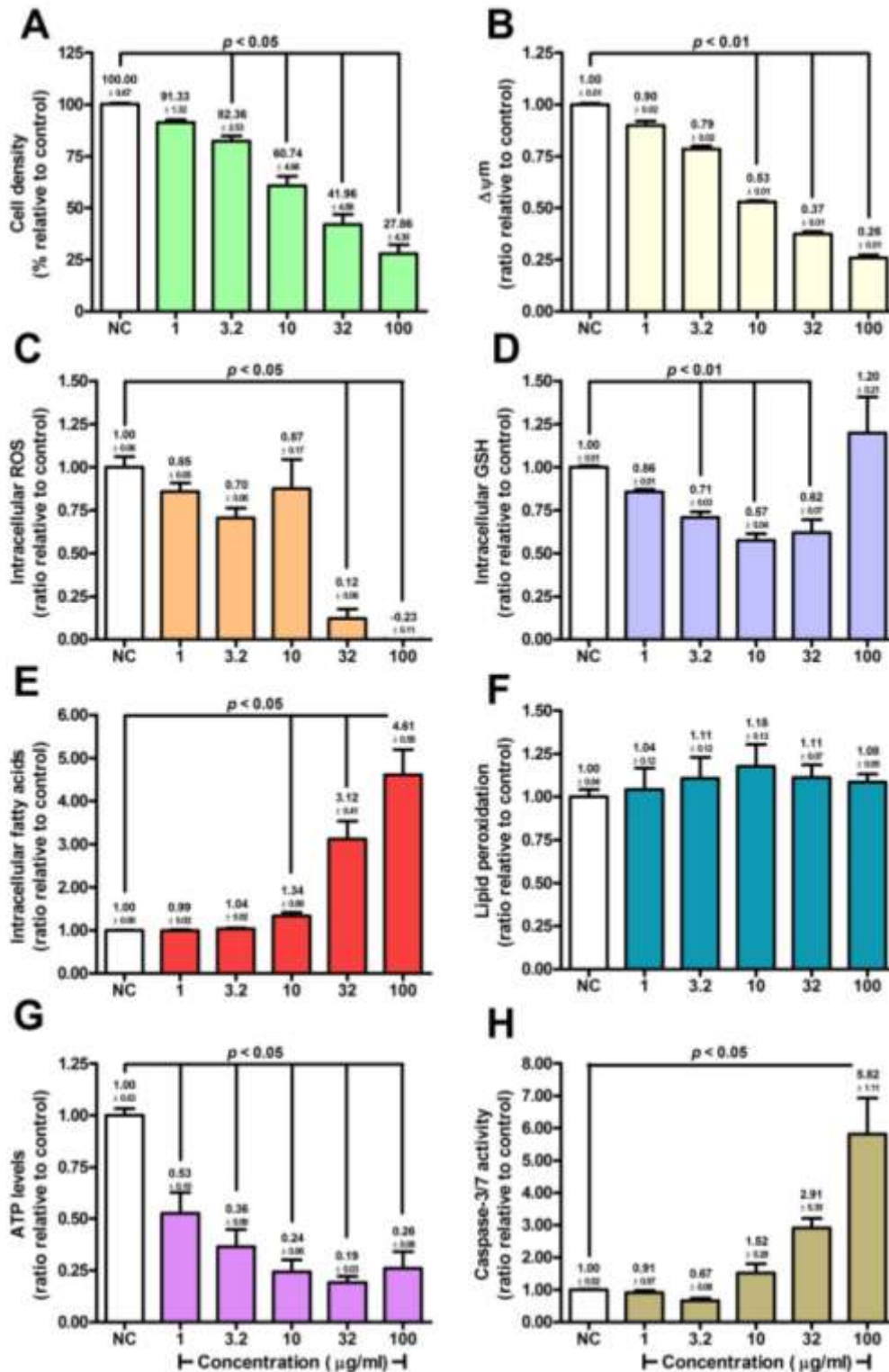


**Figure 28:** The effect of the crude methanol extract of *A. oppositifolia* in HepG2 cells; A) cell density, B)  $\Delta\Psi_m$ , C) ROS concentration, D) GSH concentration, E) fatty acid concentration, F) lipid peroxidation, G) ATP levels and H) caspase-3/7 activity.

After 24 h exposure to the hot water extract, a 3.03% increase, 15.10% reduction ( $p < 0.01$ ), 5.66% increase and 9.44% increase in the percentage of cells in the sub-G1-,

G1-, S- and G2/M-phase was observed, respectively (Figure 29B, Table 14). After 72 h exposure to the hot water extract, the percentage of sub-G1-phase cells increased by 17.53% ( $p < 0.05$ ), the G1-phase decreased by 27.70% ( $p < 0.001$ ), and the S- and G2/M-phase increased by 17.76% ( $p < 0.05$ ) and 10.54%, respectively (Figure 29E, Table 14). Exposure to the methanol extract for 24 h led to an increase of 4.21%, reduction of 4.90% and increases of 0.70% and 4.19% for the sub-G1-, G1-, S- and G2/M-phase, respectively (Figure 29C, Table 14). After 72 h exposure to the methanol extract, the G1-phase was reduced by 20.37% ( $p < 0.05$ ), while the sub-G1-, S- and G2/M-phase was increased by 14.69%, 1.50% and 18.87% ( $p < 0.05$ ), respectively (Figure 29F, Table 14).

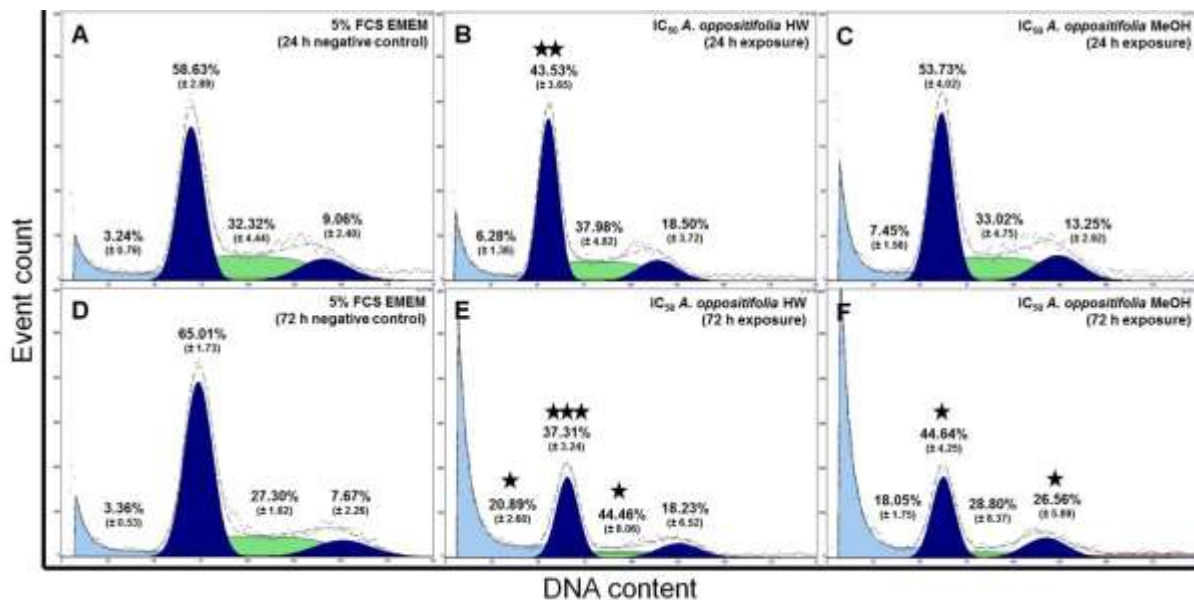


**Figure 29:** The effect of the IC<sub>50</sub> of *A. oppositifolia* on cellular kinetics in HepG2 cells exposed for 24 h and 72 h; A) negative control (24 h), B) hot water extract (24 h), C) methanol extract (24 h), D) negative control (72 h), E) hot water extract (72 h), F) methanol extract (72 h). Significant difference relative to the respective time points of the negative control: ★  $p < 0.05$ , ★★  $p < 0.01$  and ★★★  $p < 0.001$ .

**Table 14:** The effect of the IC<sub>50</sub> of *A. oppositifolia* on cellular kinetics in HepG2 cells exposed for 24 h and 72 h summarized as the shift in phase from the respective negative control.

Phase of cell cycle	Shift in cell cycle phase after exposure to <i>A. oppositifolia</i> (%)			
	Hot water extract		Methanol extract	
	24 h	72 h	24 h	72 h
Sub-G1	↑ 3.03	↑ 17.54*	↑ 4.21	↑ 14.69
G1	↓ 15.10**	↓ 27.70***	↓ 4.90	↓ 20.37*
S	↑ 5.66	↑ 17.16*	↑ 0.70	↑ 1.50
G2/M	↑ 9.44	↑ 10.54	↑ 4.19	↑ 18.87*

Significant difference relative to the respective time points of the negative control: ★  $p < 0.05$ , ★★  $p < 0.01$  and ★★★  $p < 0.001$ .

After 24 h exposure to the hot water extract, cellular viability decreased by 30.71% ( $p < 0.001$ ), while necrotic cells increased by 29.98% (Figure 30B, Table 15). At 72 h exposure to the hot water extract cellular viability was reduced by 20.83% ( $p < 0.01$ ), while early apoptotic, late apoptotic and necrotic cells increased by 2.3%, 1.38% and 17.13% ( $p < 0.05$ ), respectively (Figure 30E, Table 15). Twenty-four hour exposure to the methanol extract decreased cellular viability by 21.77% ( $p < 0.05$ ), with an increase of 3.08%, 1.19% and 17.51% of early apoptotic, late apoptotic and necrotic cells, respectively (Figure 30C, Table 15). At 72 h exposure the methanol extract decreased cellular viability by 20.53% ( $p < 0.01$ ), with a 4.22%, 3.09% and 13.21% increase in early apoptotic, late apoptotic and necrotic cells, respectively (Figure 30F, Table 15)

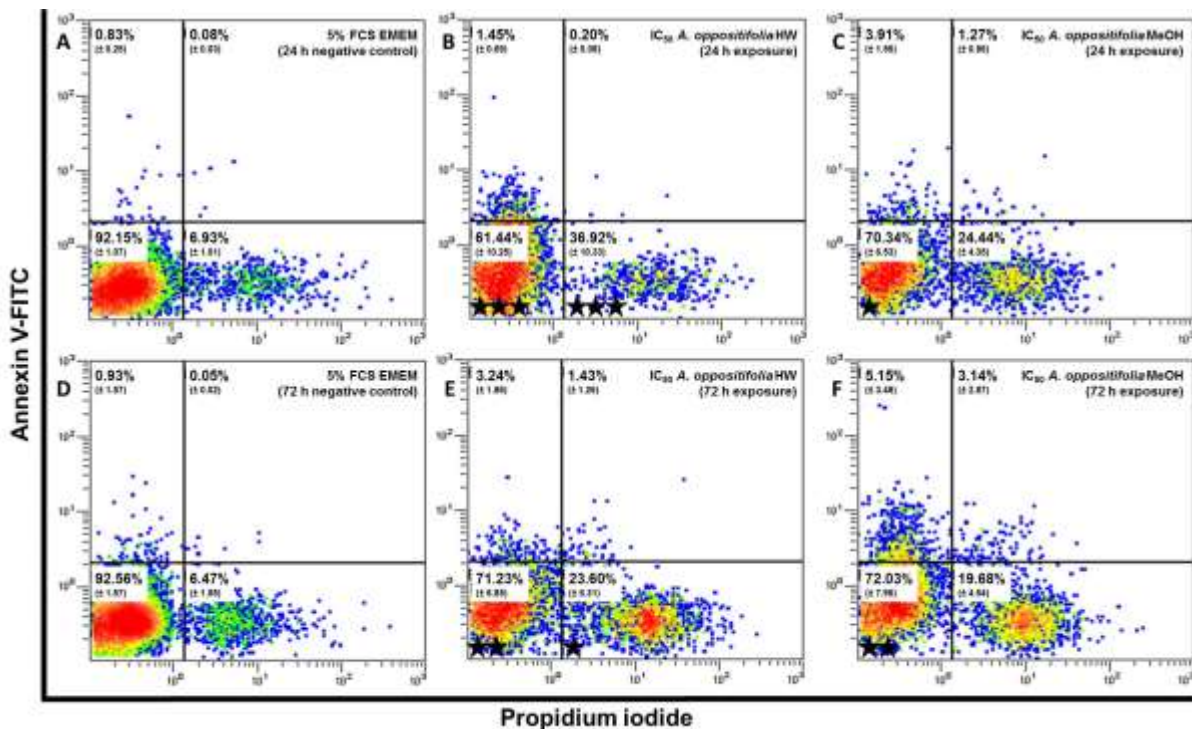


**Figure 30:** The effect of the IC<sub>50</sub> of *A. oppositifolia* on cellular viability in HepG2 cells exposed for 24 h and 72 h; A) negative control (24 h), B) hot water extract (24 h), C) methanol extract (24 h), D) negative control (72 h), E) hot water extract (72 h), F) methanol extract (72 h). Significant difference relative to the respective time points of the negative control: ★  $p < 0.05$ , ★★  $p < 0.01$  and ★★★  $p < 0.001$ .

**Table 15:** The effect of the IC<sub>50</sub> of *A. oppositifolia* on cellular viability in HepG2 cells exposed for 24 h and 72 h summarized as the shift in phase from the respective negative control.

State of viability	Shift in viability after exposure to <i>A. oppositifolia</i> (%)			
	Hot water extract		Methanol extract	
	24 h	72 h	24 h	72 h
<b>Viable</b>	↓ 30.71***	↓ 20.83**	↓ 21.77*	↓ 20.53**
<b>Early apoptosis</b>	↑ 0.61	↑ 2.3	↑ 3.08	↑ 4.22
<b>Late apoptosis</b>	↑ 0.12	↑ 1.38	↑ 1.19	↑ 3.09
<b>Necrosis</b>	↑ 29.98***	↑ 17.13*	↑ 17.51	↑ 13.21

Significant difference relative to the respective time points of the negative control: ★  $p < 0.05$ , ★★  $p < 0.01$  and ★★★  $p < 0.001$ .

From the results it is suggested that the hot water extract debilitates cells to a greater extent than the methanol extract, although cell density was decreased to a similar extent at the highest concentration tested. The hot water extract reduced GSH concentrations,  $\Delta\Psi_m$  and ATP levels more than the equivalent methanol extract. The methanol extract increased fatty acid content and caspase-3/7 activity. The hot water extract did not affect ROS content whereas the methanol extract abolished this at higher concentrations. Lipid peroxidation did not appear to be a factor in the cytotoxicity. Both the hot water and methanol extracts increased the sub-G1-phase after 72 h, while the former increased the percentage of cells in the S- and G2/M-phase of the cell cycle, and the latter only increased the G2/M-phase. While both extracts decreased cellular viability and increased the amount of necrotic cells as early as 24 h, the hot water extract was more potent at inducing this.

#### 4.3.3.2. *Boophane disticha*

The hot water extract of *B. disticha* displayed cytotoxicity at concentrations  $\geq 10$   $\mu\text{g/mL}$ , with an IC<sub>50</sub> of 51.39  $\mu\text{g/mL}$  and maximum cell density reduction of 61.88% at 100  $\mu\text{g/mL}$  (Figure 31A). Slight, but significant ( $p < 0.05$ ), reduction in  $\Delta\Psi_m$  was observed at  $\geq 32$   $\mu\text{g/mL}$ , with a maximum reduction of 0.35-fold (Figure 31B). Intracellular ROS concentrations were reduced below baseline at all concentration, with a minimum reduction of 0.23-fold at 1  $\mu\text{g/mL}$  to plateau at  $\geq 32$   $\mu\text{g/mL}$  by approximately 0.61-fold (Figure 31C). Intracellular GSH concentrations were reduced at  $\geq 3.2$   $\mu\text{g/mL}$  significantly ( $p < 0.05$ ) by up to 0.39-fold, while only a slight reduction of 0.28-fold was present at 100  $\mu\text{g/mL}$  (Figure 31D). A slight reduction of 0.10-fold in fatty acid content was noted at concentrations from 1  $\mu\text{g/mL}$  to 10  $\mu\text{g/mL}$ , while a dose-dependent increase was observed at  $\geq 10$   $\mu\text{g/mL}$  by up to 2.92-fold at 100  $\mu\text{g/mL}$  (Figure 31E).

Lipid peroxidation remained largely unaltered (Figure 31F). ATP levels were non-significantly increased at  $\geq 32 \mu\text{g/mL}$  by up to 2.72-fold (Figure 31G). Caspase-3/7 activity was below baseline for all concentrations, and was only significant ( $p < 0.01$ ) at 10  $\mu\text{g/mL}$  and 32  $\mu\text{g/mL}$  with a reduction of 0.44- and 0.63-fold, respectively, while at 100  $\mu\text{g/mL}$  only a slight reduction of 0.31-fold was observed (Figure 31H).

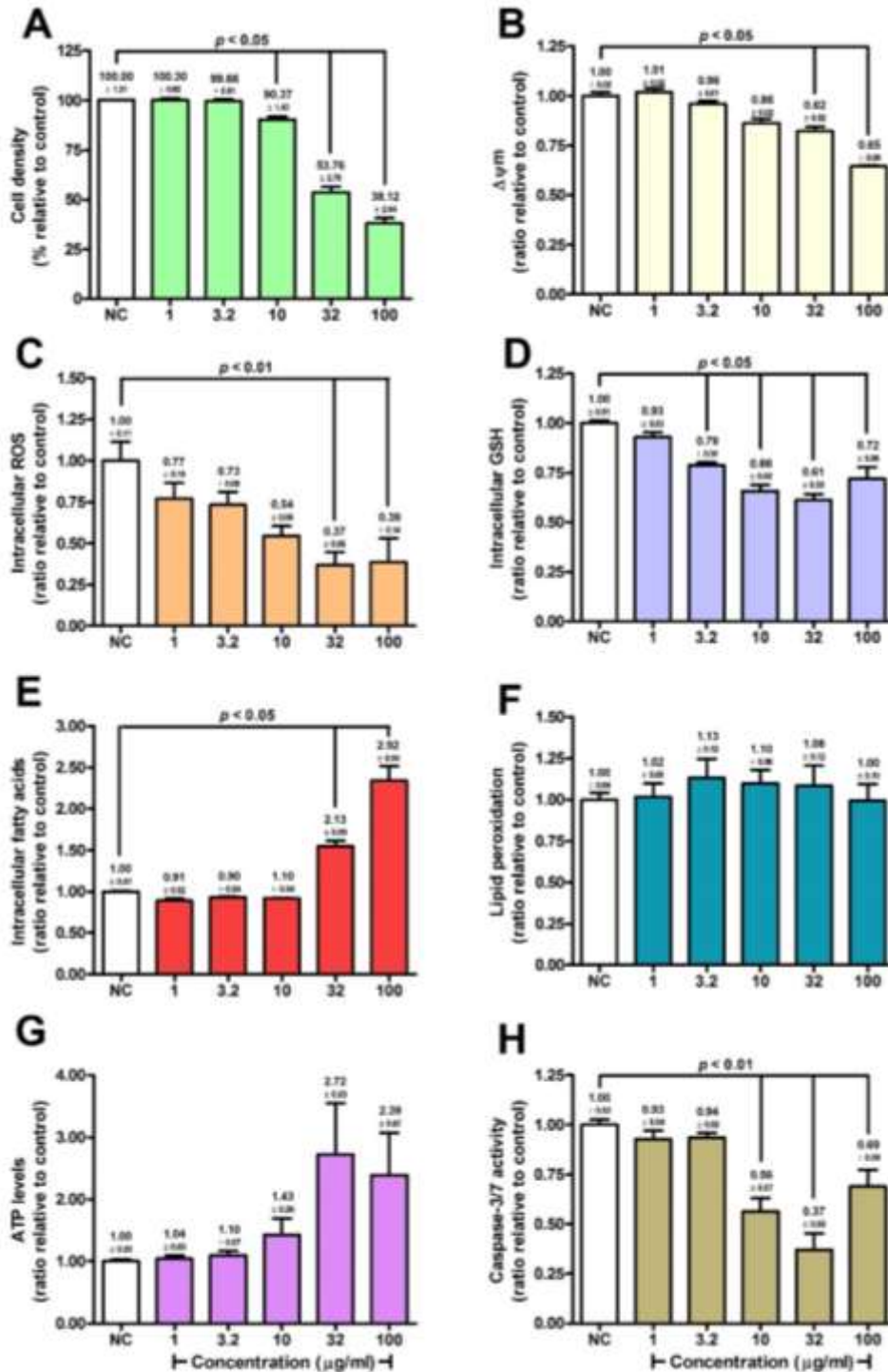


**Figure 31:** The effect of the crude hot water extract of *B. disticha* in HepG2 cells; A) cell density, B)  $\Delta\Psi\text{m}$ , C) ROS concentration, D) GSH concentration, E) fatty acid concentration, F) lipid peroxidation, G) ATP levels and H) caspase-3/7 activity.

The methanol extract displayed significant ( $p < 0.05$ ) cytotoxicity at concentrations  $\geq 10$   $\mu\text{g/mL}$ , with an  $\text{IC}_{50}$  of 35.11  $\mu\text{g/mL}$  and maximum cell density reduction of 66.43% at 100  $\mu\text{g/mL}$  (Figure 32A).  $\Delta\Psi\text{m}$  decreased gradually, with a maximum significant ( $p < 0.01$ ) reduction of 0.43-fold at 100  $\mu\text{g/mL}$  (Figure 32B). Intracellular ROS concentrations were decreased at all concentrations, with a minimum reduction of 0.09-fold at 1  $\mu\text{g/mL}$  to 0.56-fold at 100  $\mu\text{g/mL}$  (Figure 32C). Intracellular GSH concentrations decreased significantly ( $p < 0.001$ ) at 3.2  $\mu\text{g/mL}$  and 10  $\mu\text{g/mL}$  by 0.27- and 0.34-fold, while at  $\geq 32$   $\mu\text{g/mL}$  it started increasing to 1.37-fold at 100  $\mu\text{g/mL}$  (Figure 32D). Fatty acid concentration was reduced by approximately 0.10-fold at 1 and 3.2  $\mu\text{g/mL}$ , but increased significantly ( $p < 0.05$ ) by 2.12- and 2.86-fold at 32  $\mu\text{g/mL}$  and 100  $\mu\text{g/mL}$ , respectively (Figure 32E). Lipid peroxidation increased dose-dependently by up to 1.24-fold, though this was not significant.  $\Delta\Psi\text{m}$  decreased gradually, with a maximum significant ( $p < 0.01$ ) reduction of 0.43-fold at 100  $\mu\text{g/mL}$  (Figure 32F). ATP levels increased dose-dependently by up to 1.94-fold at 32  $\mu\text{g/mL}$ , but returned to baseline at 100  $\mu\text{g/mL}$ .  $\Delta\Psi\text{m}$  decreased gradually, with a maximum significant ( $p < 0.01$ ) reduction of 0.43-fold at 100  $\mu\text{g/mL}$  (Figure 32G). Caspase-3/7 activity was decreased significantly ( $p < 0.05$ ) by 0.36- and 0.52-fold at 10  $\mu\text{g/mL}$  and 32  $\mu\text{g/mL}$ , respectively, with only a slight reduction of 0.12-fold at 100  $\mu\text{g/mL}$  (Figure 32H).

Exposure to the hot water extract for 24 h resulted in an increase of 0.81%, 0.18% and 4.47% in the cells of the sub-G1-, S- and G2/M-phase, respectively and a 4.70% reduction of in the G1-phase (Figure 33B, Table 16). After 72 h exposure the hot water extract reduced the sub-G1 and S-phase by 1.40% and 7.71%, respectively, while the G1- and G2/M-phase were increased by 6.47% and 1.24%, respectively (Figure 33E, Table 16). The methanol extract resulted in a 0.08% and 4.18% increase in the sub-G1- and G2/M-phase, respectively, and decreased the G1- and S-phase by 4.05% and 0.12%, respectively (Figure 33C, Table 16). After 72 h the methanol extract decreased the sub-G1- and S-phase by 2.11% and 5.10%, respectively, and increased the G1- and G2/M-phase by 1.92% and 3.18%, respectively (Figure 33F, Table 16).

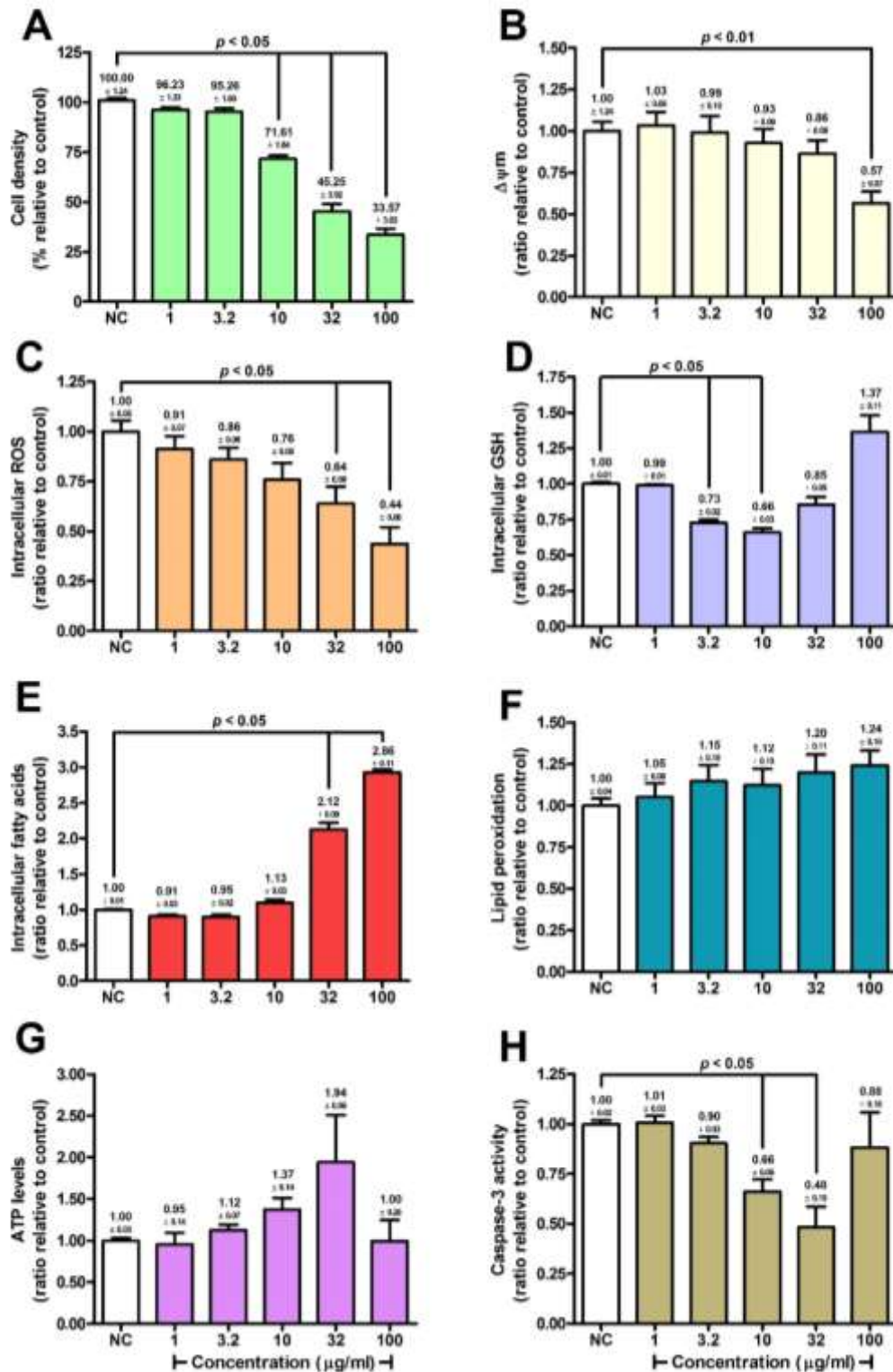


**Figure 32:** The effect of the crude methanol extract of *B. disticha* in HepG2 cells; A) cell density, B)  $\Delta\Psi_m$ , C) ROS concentration, D) GSH concentration, E) fatty acid concentration, F) lipid peroxidation, G) ATP levels and H) caspase-3/7 activity.

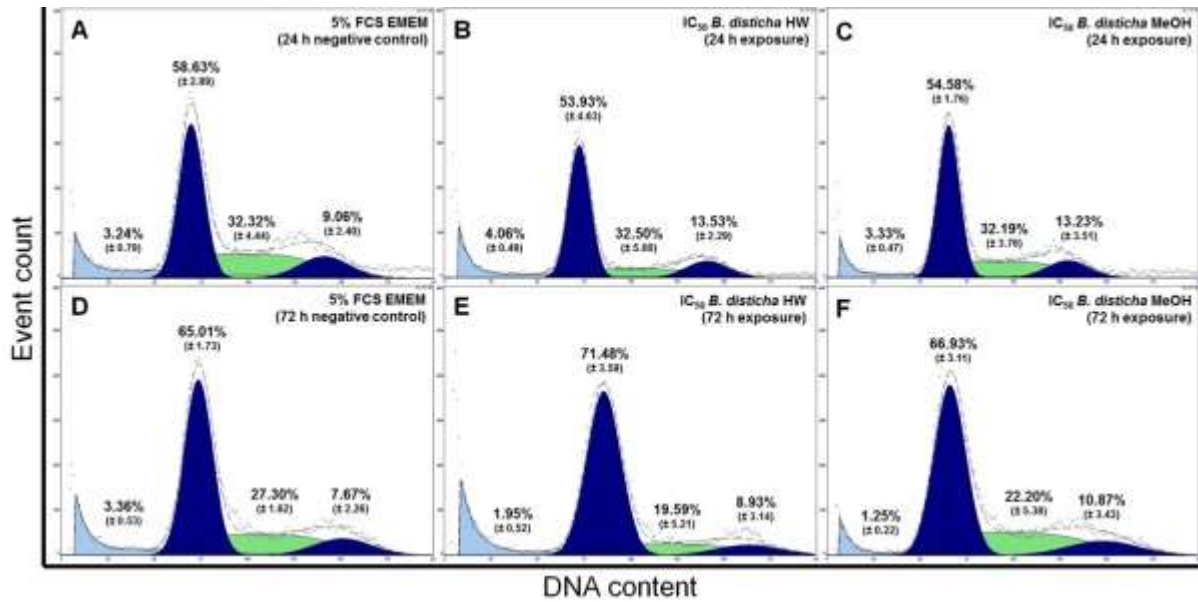


**Figure 33:** The effect of the IC<sub>50</sub> of *B. disticha* on cellular kinetics in HepG2 cells exposed for 24 h and 72 h; A) negative control (24 h), B) hot water extract (24 h), C) methanol extract (24 h), D) negative control (72 h), E) hot water extract (72 h), F) methanol extract (72 h).

**Table 16:** The effect of the IC<sub>50</sub> of *B. disticha* on cellular kinetics in HepG2 cells exposed for 24 h and 72 h summarized as the shift in phase from the respective negative control.

Phase of cell cycle	Shift in cell cycle phase after exposure to <i>B. disticha</i> (%)			
	Hot water extract		Methanol extract	
	24 h	72 h	24 h	72 h
<b>Sub-G1</b>	↑ 0.81	↓ 1.40	↑ 0.08	↓ 2.11
<b>G1</b>	↓ 4.70	↑ 6.47	↓ 4.05	↑ 1.92
<b>S</b>	↑ 0.18	↓ 7.71	↓ 0.12	↓ 5.10
<b>G2/M</b>	↑ 4.48	↑ 1.24	↑ 4.18	↑ 3.18

After 24 h exposure to the hot water extract there was a decrease of 6.18% ( $p < 0.05$ ) in viable cells and 3.07% in necrotic cells, while an increase of 8.43% and 0.82% occurred in early and late apoptotic cells, respectively (Figure 34, Table 17). At 72 h exposure to the hot water extract an increase of 3.17% occurred in early apoptotic cells, while a decrease of 3.77% was evident for necrotic cells (Figure 34, Table 17). The methanol extract reduced cell viability by 10.27% ( $p < 0.01$ ) and necrosis by 2.42% after 24 h exposure, while early and late apoptotic cells increased by 10.88% ( $p < 0.001$ ) and 1.81%, respectively (Figure 34, Table 17). After 72 h exposure the methanol extract reduced cell viability and necrosis by 2.10% and 3.43%, respectively, while early apoptotic cells increased by 5.07% (Figure 34, Table 17).

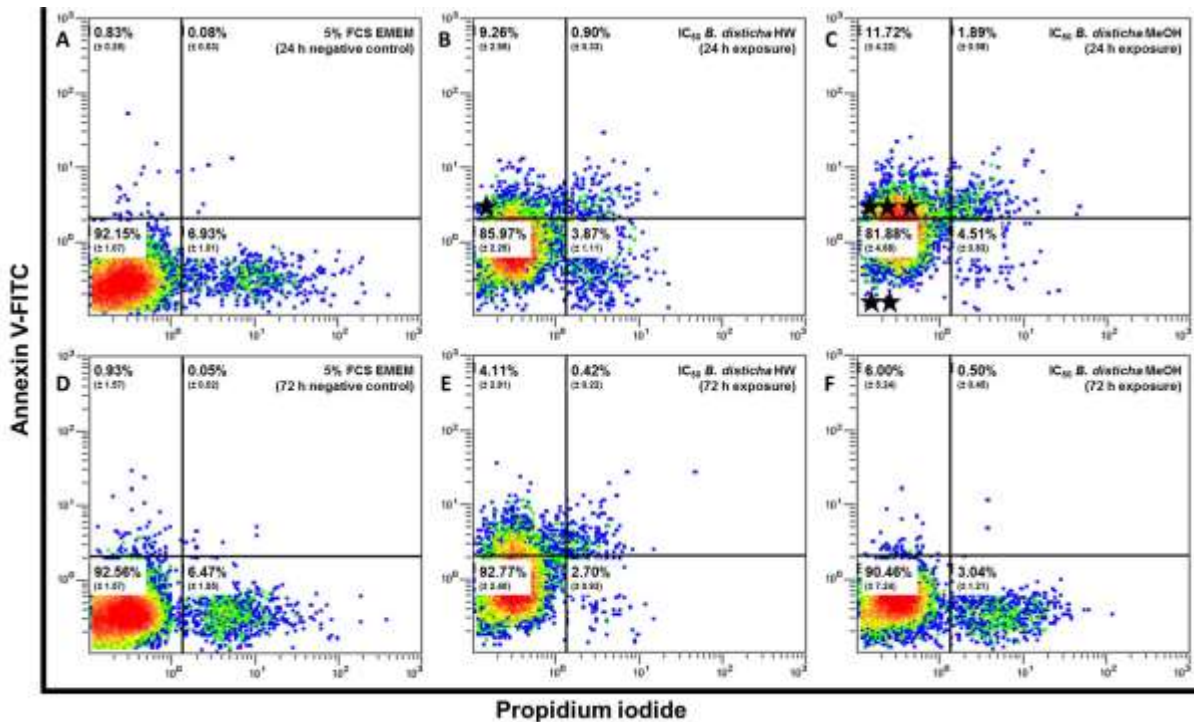


**Figure 34:** The effect of the IC<sub>50</sub> of *B. disticha* on cellular viability in HepG2 cells exposed for 24 h and 72 h; A) negative control (24 h), B) hot water extract (24 h), C) methanol extract (24 h), D) negative control (72 h), E) hot water extract (72 h), F) methanol extract (72 h). Significant difference relative to the respective time points of the negative control: ★  $p < 0.05$ , ★★  $p < 0.01$  and ★★★  $p < 0.001$ .

**Table 17:** The effect of the IC<sub>50</sub> of *B. disticha* on cellular viability in HepG2 cells exposed for 24 h and 72 h summarized as the shift in phase from the respective negative control.

State of viability	Shift in viability after exposure to <i>B. disticha</i> (%)			
	Hot water extract		Methanol extract	
	24 h	72 h	24 h	72 h
<b>Viable</b>	↓ 6.18★	↑ 0.21	↓ 10.27★★	↓ 2.10
<b>Early apoptosis</b>	↑ 8.43	↑ 3.17	↑ 10.88★★★	↑ 5.07
<b>Late apoptosis</b>	↑ 0.82	↑ 0.38	↑ 1.81	↑ 0.45
<b>Necrosis</b>	↓ 3.07	↓ 3.77	↓ 2.42	↓ 3.43

Significant difference relative to the respective time points of the negative control: ★  $p < 0.05$ , ★★  $p < 0.01$  and ★★★  $p < 0.001$ .

Although the methanol extract had a more deleterious effect on cellular density across the exposure range, the maximum reduction was similar in both extracts. Alterations to hepatotoxic parameters followed a similar trend after exposure to both solvent extracts. The methanol extract resulted in an increase in GSH concentrations at the highest concentration tested. Effects on ROS,  $\Delta\Psi_m$ , fatty acid concentrations and caspase-3/7 activity were similar in hot water and methanol extracts. ATP levels were increased after exposure to both extracts, though this effect was nullified at the highest concentration for the methanol extract. Cell number was slightly increased in the

G2/M-phase of the cellular phase for both extracts, with a further increase in the G1-phase following exposure to the hot water extract. Annexin V-FITC staining indicated that cellular viability remained high, with only a slight increase in early apoptotic cells.

#### 4.3.3.3. *Moringa oleifera*

No significant alterations to cell density (Figure 35A), GSH concentrations (Figure 35D) and lipid peroxidation (Figure 35F) occurred after exposure to the hot water extract of *M. oleifera*. While ROS concentrations were reduced by approximately 0.20-fold at <100 µg/mL, it increased significantly ( $p < 0.05$ ) by 1.99-fold at 100 µg/mL.  $\Delta\Psi_m$  was reduced dose-dependently, displaying significance ( $p < 0.05$ ) at 100 µg/mL (0.35-fold) (Figure 35B). At 100 µg/mL fatty acid concentrations (Figure 35E) and caspase-3/7 activity (Figure 35H) was significantly ( $p < 0.05$ ) reduced by 0.15-fold and 0.30-fold, respectively. ATP levels were reduced at concentrations  $\geq 32$  µg/mL by up to 0.56-fold (Figure 35G).

The methanol extract did not induce any significant alterations to cell density (Figure 36A), GSH concentrations (Figure 36D), ATP levels (Figure 36G) and caspase-3/7 activity (Figure 36H) after exposure to the methanol extract of *M. oleifera*. Cell density displayed an increasing trend at higher concentrations. ROS concentrations were reduced to below baseline for all concentrations (Figure 36C), with a significant ( $p < 0.05$ ) reduction at  $\geq 32$  µg/mL (up to 0.50-fold at 100 µg/mL).  $\Delta\Psi_m$  was reduced similarly to that of the hot water extract (Figure 36B), but not as much (0.28-fold). Fatty acid concentrations were reduced at concentrations  $\geq 3.2$  µg/mL (Figure 36E), but only attained significance at 100 µg/mL (0.43-fold). Lipid peroxidation displayed a trend to increase dose-dependently by up to 1.48-fold (Figure 36F), though this was not significant. Caspase-3/7 activity was not significantly altered, although a slight reduction was noted at 100 µg/mL (0.14-fold) (Figure 36H).

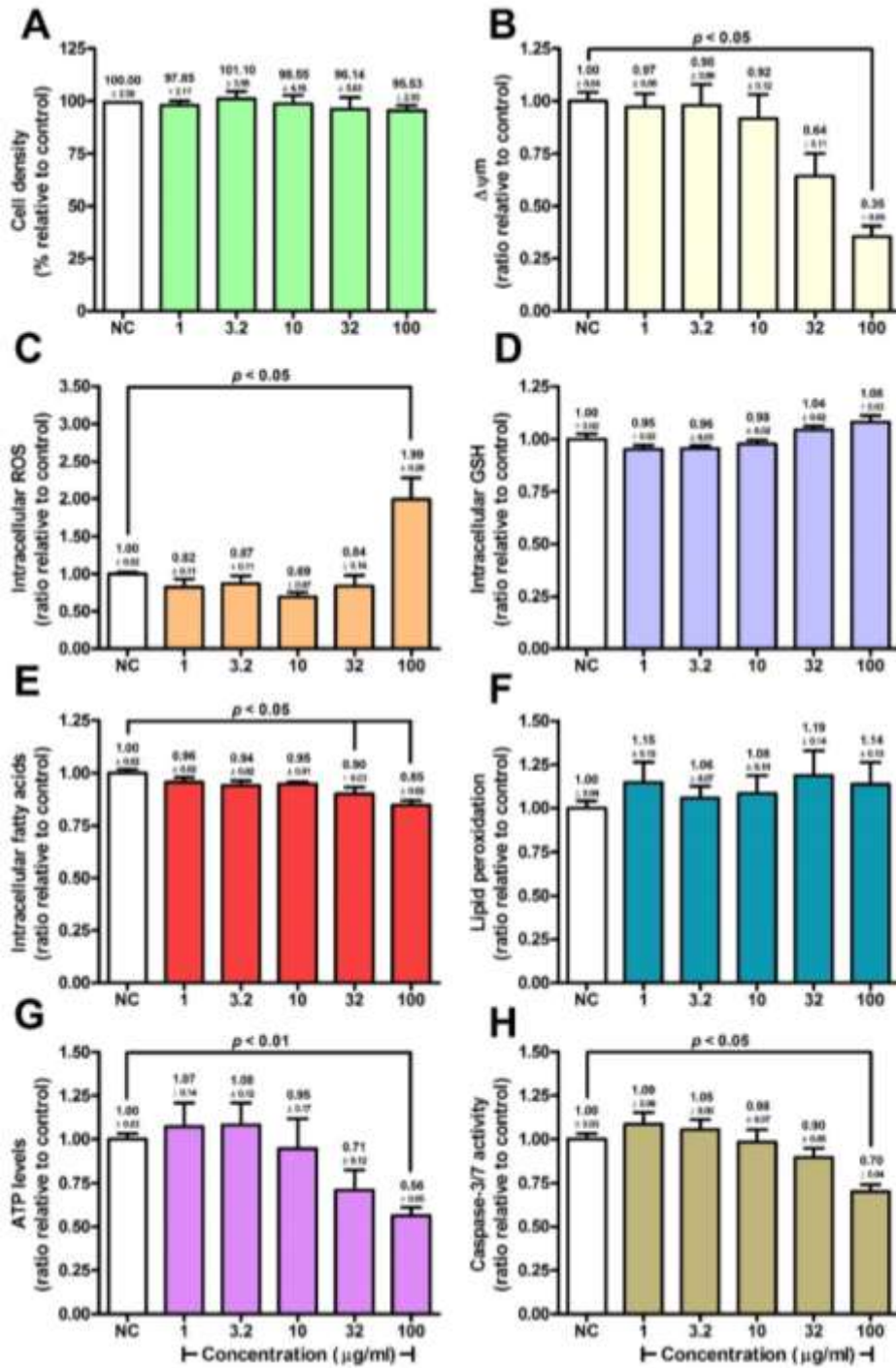


**Figure 35:** The effect of the crude hot water extract of *M. oleifera* in HepG2 cells; A) cell density, B)  $\Delta\Psi_m$ , C) ROS concentration, D) GSH concentration, E) fatty acid concentration, F) lipid peroxidation, G) ATP levels and H) caspase-3/7 activity.

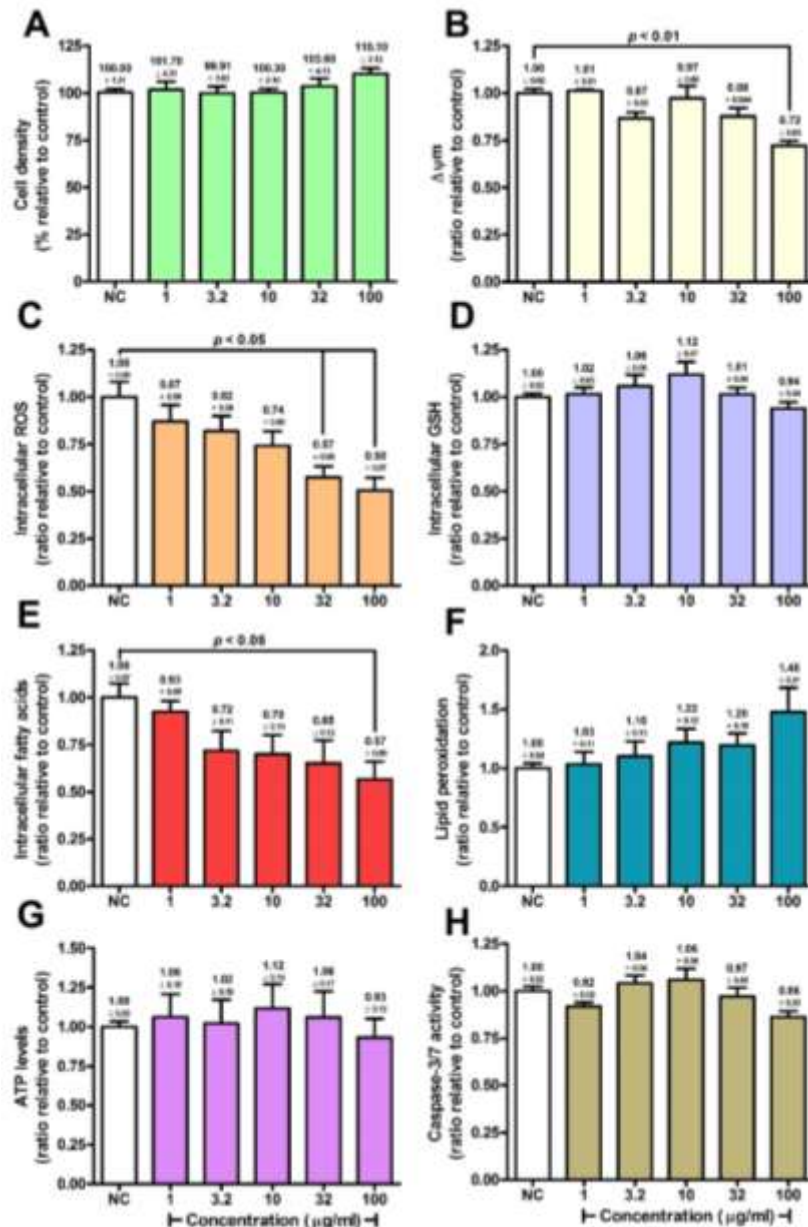


**Figure 36:** The effect of the crude methanol extract of *M. oleifera* in HepG2 cells; A) cell density, B)  $\Delta\Psi_m$ , C) ROS concentration, D) GSH concentration, E) fatty acid concentration, F) lipid peroxidation, G) ATP levels and H) caspase-3/7 activity.

Exposure to the hot water extract did not result in significant changes to the cell cycle after 24 h (Figure 37B, Table 18), but after 72 h an increase of 6.22% was observed in the G1-phase, with a reduction of 5.1% in the S-phase (Figure 37E, Table 18). Exposure to the methanol extract for 24 h increased the sub-G1-, G1- and G2/M-phase by 1.32%, 3.53% and 1.64%, respectively, with a reduction of 5.17% in the S-phase (Figure 37C, Table 18). After 72 h the methanol extract increased the G1- and G2/M-phase by 2.12% and 3.96%, respectively, and decreased the S-phase by 6.08% (Figure 37F, Table 18).

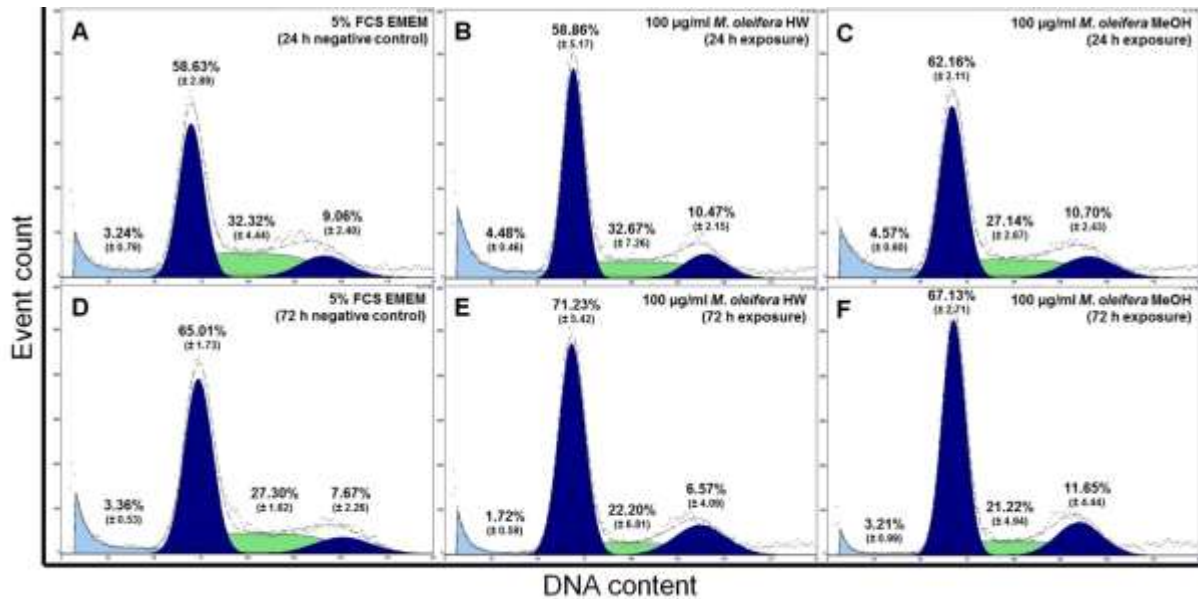


**Figure 37:** The effect of the 100 µg/mL *M. oleifera* on cellular kinetics in HepG2 cells exposed for 24 h and 72 h; A) negative control (24 h), B) hot water extract (24 h), C) methanol extract (24 h), D) negative control (72 h), E) hot water extract (72 h), F) methanol extract (72 h).

**Table 18:** The effect of the 100 µg/mL *M. oleifera* on cellular kinetics in HepG2 cells exposed for 24 h and 72 h summarized as the shift in phase from the respective negative control.

Phase of cell cycle	Shift in cell cycle phase after exposure to <i>M. oleifera</i> (%)			
	Hot water extract		Methanol extract	
	24 h	72 h	24 h	72 h
<b>Sub-G1</b>	↑ 1.65	↓ 1.64	↑ 1.32	↓ 0.14
<b>G1</b>	↓ 1.77	↑ 6.22	↑ 3.53	↑ 2.12
<b>S</b>	↑ 0.36	↓ 5.10	↓ 5.17	↓ 6.08
<b>G2/M</b>	↑ 1.41	↓ 1.12	↑ 1.64	↑ 3.96

Exposure to the hot water extract decreased cell viability by 8.96% ( $p < 0.05$ ) after 24 h, and increased early apoptotic and necrotic cells by 5.43% and 3.05%, respectively (Figure 38B, Table 19). After 72 h exposure the hot water extract reduced cell viability by 8.74%, while increasing early apoptotic and necrotic cells by 2.66% and 5.62%, respectively (Figure 38E, Table 19). The methanol extract induced 13.74% ( $p < 0.001$ ) reduction in cell viability after 24 h exposure, while increasing early apoptotic, late apoptotic and necrotic cells by 1.31%, 1.02% and 11.41% ( $p < 0.01$ ), respectively (Figure 38C, Table 19). After 72 h exposure cell viability was decreased by 11.08% ( $p < 0.05$ ), while early apoptotic and necrotic cells increased by 3.97% and 6.22%, respectively (Figure 38F, Table 19).

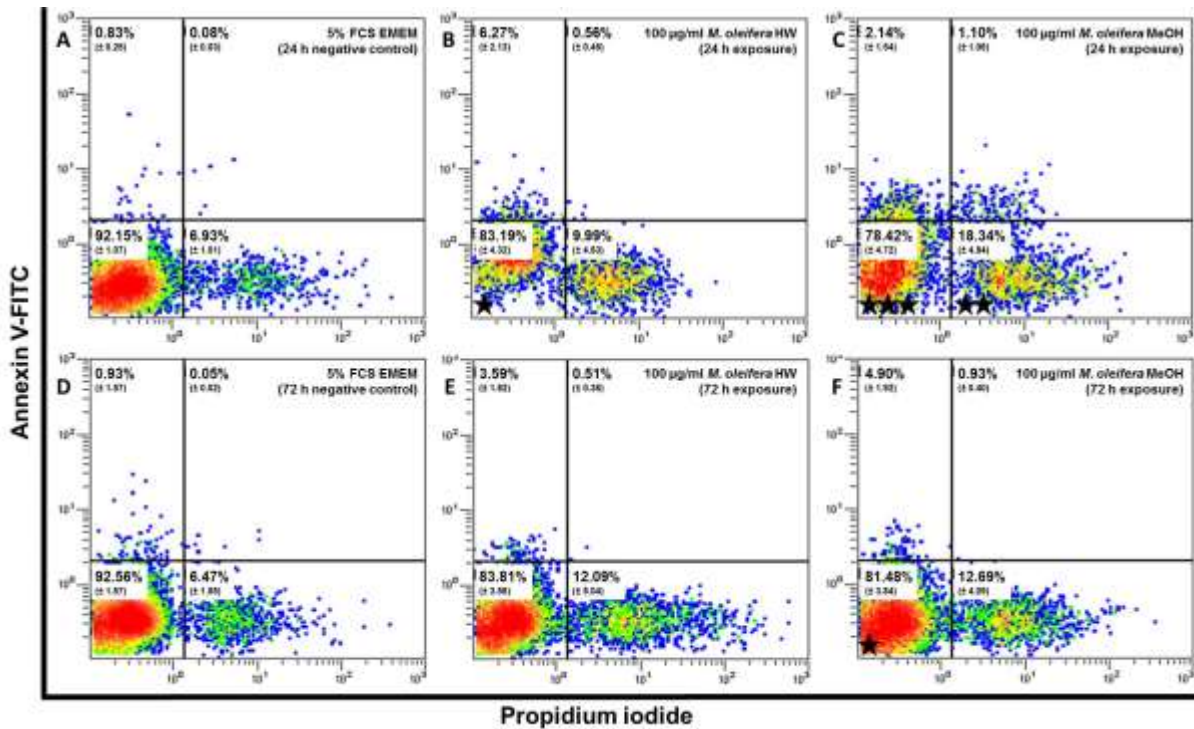


**Figure 38:** The effect of the 100 µg/mL *M. oleifera* on cellular viability in HepG2 cells exposed for 24 h and 72 h; A) negative control (24 h), B) hot water extract (24 h), C) methanol extract (24 h), D) negative control (72 h), E) hot water extract (72 h), F) methanol extract (72 h). Significant difference relative to the respective time points of the negative control: ★  $p < 0.05$ , ★★  $p < 0.01$  and ★★★  $p < 0.001$ .

**Table 19:** The effect of the 100 µg/mL *M. oleifera* on cellular viability in HepG2 cells exposed for 24 h and 72 h summarized as the shift in phase from the respective negative control.

State of viability	Shift in viability after exposure to <i>M. oleifera</i> (%)			
	Hot water extract		Methanol extract	
	24 h	72 h	24 h	72 h
Viable	↓ 8.96★	↓ 8.74	↓ 13.74★★★	↓ 11.08★
Early apoptosis	↑ 5.43	↑ 2.66	↑ 1.31	↑ 3.97
Late apoptosis	↑ 0.48	↑ 0.46	↑ 1.02	↑ 0.89
Necrosis	↑ 3.05	↑ 5.62	↑ 11.41★★	↑ 6.22

Significant difference relative to the respective time points of the negative control: ★  $p < 0.05$ , ★★  $p < 0.01$  and ★★★  $p < 0.001$ .

Although both extracts induced similar effects, the hot water extract did result in a higher reduction of  $\Delta\Psi_m$  and caspase-3/7 activity, and a large increase in ROS at the highest concentration tested. The methanol extract however greatly decreased fatty acid concentrations. While the hot water extract decreased ATP levels, the methanol extract did not affect it, but increased lipid peroxidation slightly. The hot water and methanol extract increased cells in the G1-phase slightly after 72 h. The methanol extract also increased G2/M-phase cell percentage. Both extracts decreased cell

viability slightly (more prominent with the methanol extract), while increasing necrotic cells to a large extent, and early apoptotic cells slightly.

#### 4.3.3.4. *Solanum aculeastrum*

The hot water extract of *S. aculeastrum* displayed moderate cytotoxicity, with an IC<sub>50</sub> of 67.83 µg/mL and maximum cell density reduction of 71.82% at 100 µg/mL (Figure 39A).  $\Delta\Psi_m$  was reduced dose-dependently, with maximal reduction of 0.88-fold at 100 µg/mL (Figure 39B). ROS concentrations were decreased, with maximal reduction of 0.36-fold at 100 µg/mL (Figure 39C). GSH concentrations remained unaffected except for a sharp increase of 1.92-fold at 100 µg/mL (Figure 39D). A significant accumulation of fatty acids of 1.41- and 4.25-fold was observed at 32 µg/mL and 100 µg/mL, respectively (Figure 39E). Lipid peroxidation tended to increase up to 32 µg/mL (1.25-fold), though reduced at 100 µg/mL (1.12-fold) (Figure 39F). ATP levels increased by 1.21-fold at 10 µg/mL, but were abolished at higher concentrations (Figure 39G). Caspase-3/7 activity was increased significantly ( $p < 0.01$ ) by 1.40- and 2.15-fold at 32 µg/mL and 100 µg/mL, respectively (Figure 39H).

The methanol extract reduced cell density sharply and significantly ( $p < 0.001$ ) from  $\geq 32$  µg/mL where it seemed to reach a plateau at approximately 85% reduction (Figure 40A) and an IC<sub>50</sub> of 17.91 µg/mL.  $\Delta\Psi_m$  was reduced dose-dependently with a maximal reduction of 0.82-fold at 100 µg/mL (Figure 40B). ROS concentrations were not significantly altered for concentrations  $\leq 32$  µg/mL except for complete abolishment at 100 µg/mL (Figure 40C). GSH concentrations decreased sharply ( $p < 0.05$ ) at 32 µg/mL by 0.49-fold, but increased by 1.25-fold at 100 µg/mL (Figure 40D). Fatty acid accumulation was observed at 32 µg/mL and 100 µg/mL by 4.83- and 6.31-fold, respectively (Figure 40E). Lipid peroxidation tended to increase slightly at higher concentrations (Figure 40F). ATP levels were completely abolished at  $\geq 32$  µg/mL (Figure 40G). Although caspase-3/7 activity increased non-significantly by 1.65-fold at 10 µg/mL, there was a significant ( $p < 0.05$ ) reduction of 0.81- and 0.93-fold at 32 µg/mL and 100 µg/mL, respectively (Figure 40F).

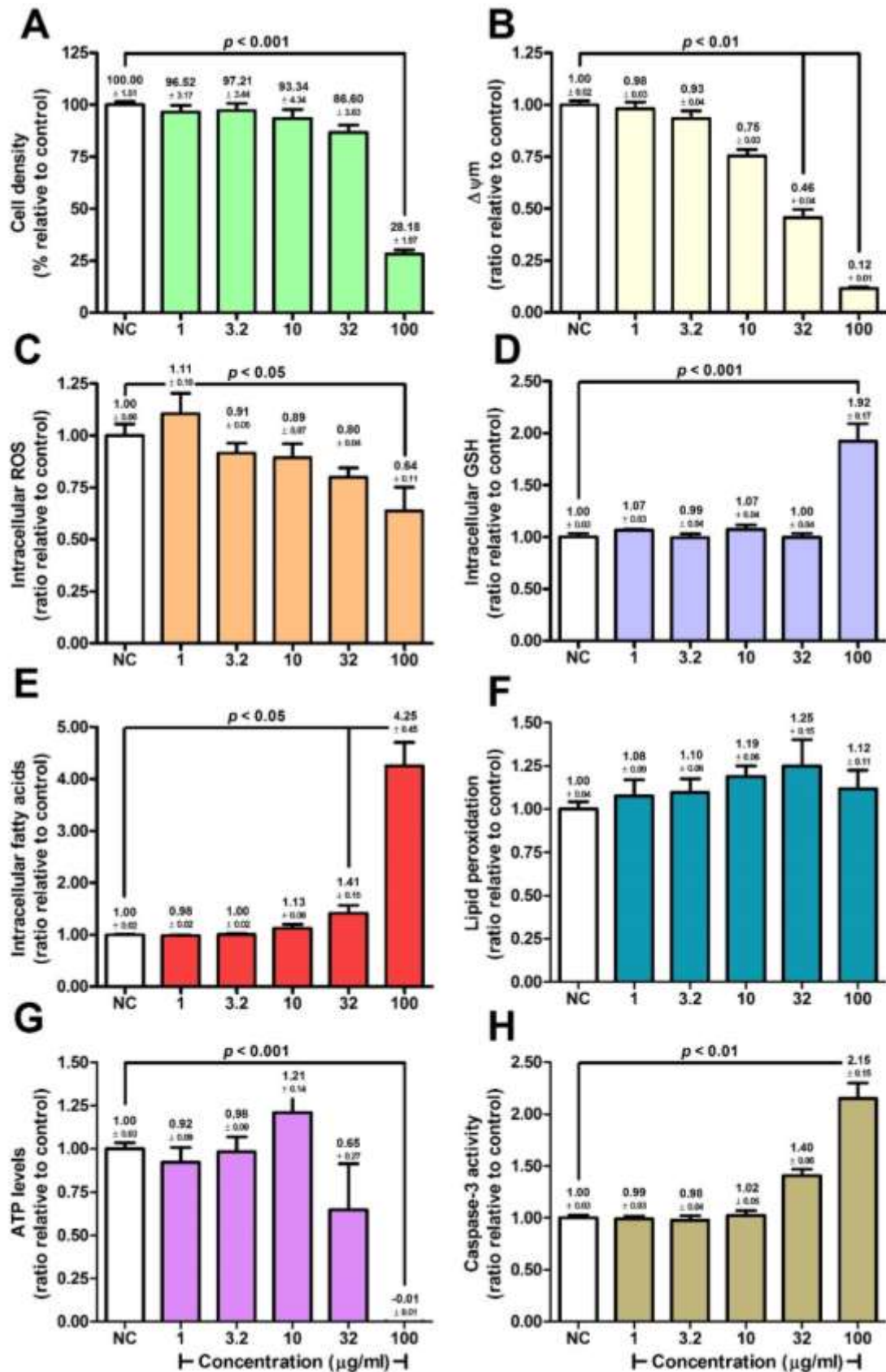


**Figure 39:** The effect of the crude hot water extract of *S. aculeastrum* in HepG2 cells; A) cell density, B)  $\Delta\Psi_m$ , C) ROS concentration, D) GSH concentration, E) fatty acid concentration, F) lipid peroxidation, G) ATP levels and H) caspase-3/7 activity.

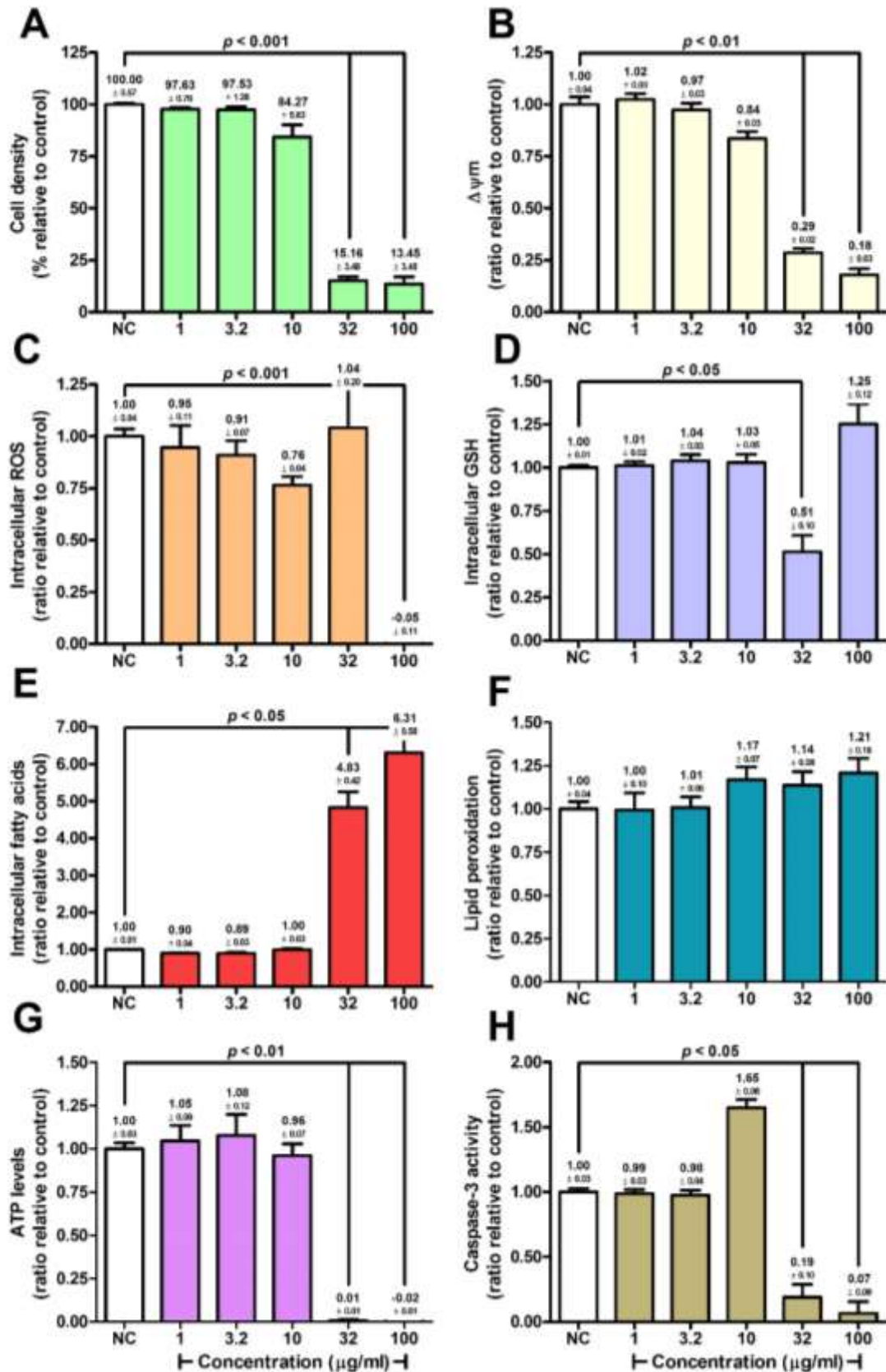


**Figure 40:** The effect of the crude methanol extract of *S. aculeastrum* in HepG2 cells; A) cell density, B)  $\Delta\Psi_m$ , C) ROS concentration, D) GSH concentration, E) fatty acid concentration, F) lipid peroxidation, G) ATP levels and H) caspase-3/7 activity.

After 24 h exposure to the hot water extract there was a decrease of 14.75% ( $p < 0.001$ ) in cells in the G1-phase, and increase of 18.75% ( $p < 0.001$ ) in the S-phase (Figure 41B, Table 20). After 72 h there was an increase of 50.31% ( $p < 0.001$ ) and 25.36% ( $p < 0.001$ ) in the sub-G1- and S-phase, respectively, while a reduction of 24.55% ( $p < 0.001$ ) occurred in the G1-phase (Figure 41E, Table 20). The methanol extract induced a reduction of 4.69% and 6.45% in the G1- and S-phase, respectively, and an increase of 1.2% and 11.14% ( $p < 0.01$ ) in the sub-G1- and G2/M-phase after 24 h (Figure 41C, Table 20). After 72 h a decrease of 9.14% occurred in the G1-phase, while the sub-G1-, S- and G2/M-phase increased by 14.8% ( $p < 0.001$ ), 6.25% and 2.89%, respectively (Figure 41F, Table 20).

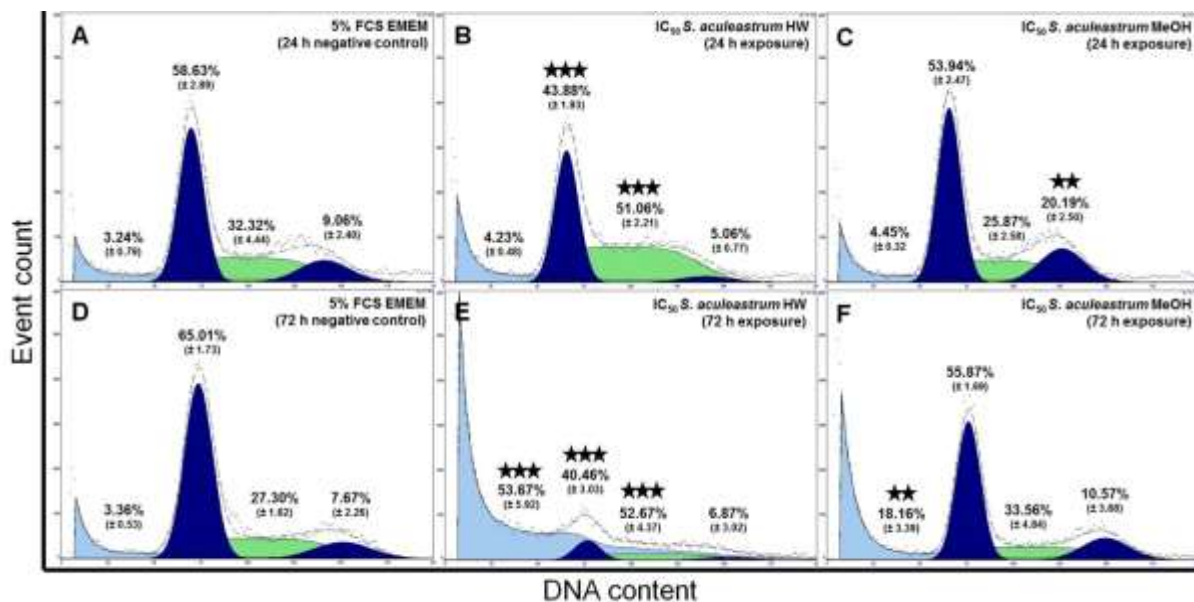


**Figure 41:** The effect of the IC<sub>50</sub> of *S. aculeastrum* on cellular kinetics in HepG2 cells exposed for 24 h and 72 h; A) negative control (24 h), B) hot water extract (24 h), C) methanol extract (24 h), D) negative control (72 h), E) hot water extract (72 h), F) methanol extract (72 h). Significant difference relative to the respective time points of the negative control: \*\*  $p < 0.01$  and \*\*\*  $p < 0.001$ .

**Table 20:** The effect of the IC<sub>50</sub> of *S. aculeastrum* on cellular kinetics in HepG2 cells exposed for 24 h and 72 h summarized as the shift in phase from the respective negative control.

Phase of cell cycle	Shift in cell cycle phase after exposure to <i>S. aculeastrum</i> (%)			
	Hot water extract		Methanol extract	
	24 h	72 h	24 h	72 h
Sub-G1	↑ 0.99	↑ 50.31***	↑ 1.20	↑ 14.80**
G1	↓ 14.75***	↓ 24.55***	↓ 4.69	↓ 9.14
S	↑ 18.75***	↑ 25.36***	↓ 6.45	↑ 6.25
G2/M	↓ 4.00	↓ 0.81	↑ 11.14**	↑ 2.89

Significant difference relative to the respective time points of the negative control: \*\*  $p < 0.01$  and \*\*\*  $p < 0.001$ .

The hot water extract decreased cell viability by 74.05% ( $p < 0.001$ ) after 24 h, and increased late apoptotic and necrotic cells by 1.03% and 74.28% ( $p < 0.001$ ), respectively (Figure 42B, Table 21). After 72 h exposure the extract induced a reduction of 77.43% ( $p < 0.001$ ) in cell viability, while increasing early apoptotic, late apoptotic and necrotic cells by 2.03%, 1.14% and 74.26% ( $p < 0.001$ ), respectively (Figure 42E, Table 21). The methanol induced a 19.10% ( $p < 0.001$ ) reduction in cell viability, and a 2.60%, 2.89% and 13.62% ( $p < 0.001$ ) increase in early apoptotic, late apoptotic and necrotic cells, respectively (Figure 42C, Table 21). After 72 h cell viability was decreased by 21.19% ( $p < 0.01$ ), while increasing early apoptotic, late apoptotic and necrotic cells by 1.11%, 0.82% and 19.25% ( $p < 0.01$ ), respectively (Figure 42F, Table 21).

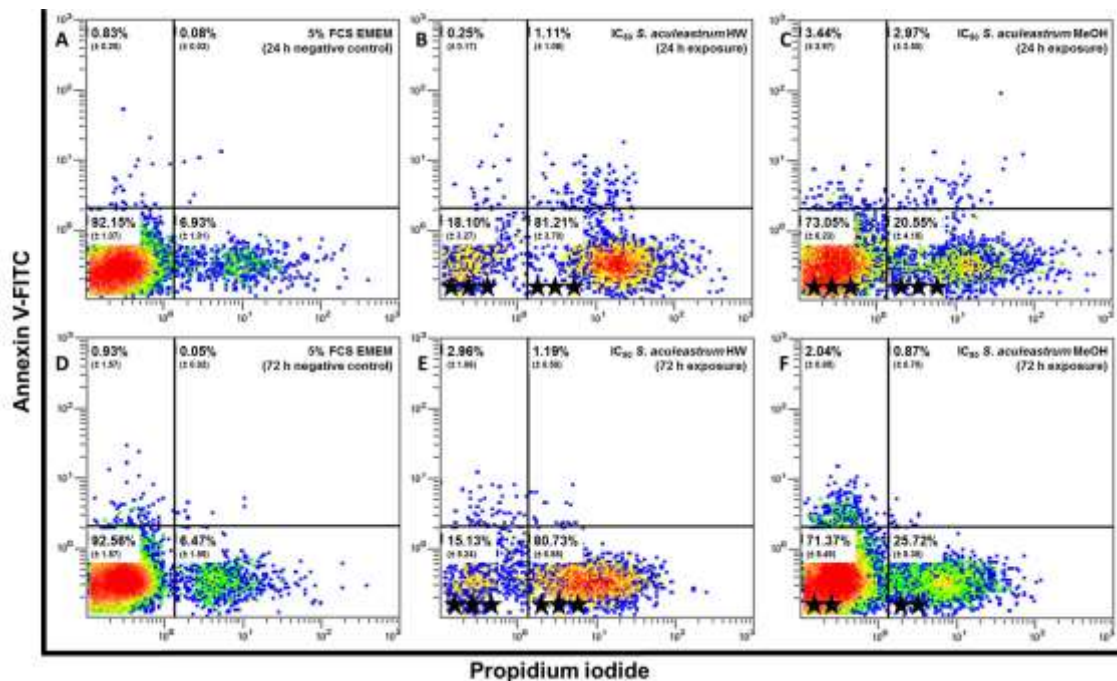


**Figure 42:** The effect of the IC<sub>50</sub> of *S. aculeastrum* on cellular viability in HepG2 cells exposed for 24 h and 72 h; A) negative control (24 h), B) hot water extract (24 h), C) methanol extract (24 h), D) negative control (72 h), E) hot water extract (72 h), F) methanol extract (72 h). Significant difference relative to the respective time points of the negative control: ★★  $p < 0.01$  and ★★★  $p < 0.001$ .

**Table 21:** The effect of the IC<sub>50</sub> of *S. aculeastrum* on cellular viability in HepG2 cells exposed for 24 h and 72 h summarized as the shift in phase from the respective negative control.

State of viability	Shift in viability after exposure to <i>S. aculeastrum</i> (%)			
	Hot water extract		Methanol extract	
	24 h	72 h	24 h	72 h
<b>Viable</b>	↓ 74.05***	↓ 77.43***	↓ 19.1***	↓ 21.19**
<b>Early apoptosis</b>	↓ 0.58	↑ 2.03	↑ 2.6	↑ 1.11
<b>Late apoptosis</b>	↑ 1.03	↑ 1.14	↑ 2.89	↑ 0.82
<b>Necrosis</b>	↑ 74.28***	↑ 74.26***	↑ 13.62***	↑ 19.25**

Significant difference relative to the respective time points of the negative control: ★  $p < 0.05$ , ★★  $p < 0.01$  and ★★★  $p < 0.001$ .

The methanol extract displayed greater hepatotoxicity than the hot water extract with regards to cytotoxicity, GSH concentrations,  $\Delta\Psi_m$  and fatty acid accumulation. While the hot water extract appeared to increase caspase-3/7 activity, the methanol extract reduced this at higher concentrations. The hot water extract increased the percentage of S-phase cells as early as 24 h, while the methanol extract increased the amount of cells in the G2/M-phase at 24 h, and then at 72 h in the S-phase. Both extracts decreased cell viability and increased necrotic cells as early as 24 h, after it plateaued. Although the methanol extract appeared to have a greater effect during screening, further assays indicated a larger hepatotoxic effect from the hot water extract.

#### 4.3.3.5. *Tabernaemontana elegans*

The hot water extract of *T. elegans* displayed a significant ( $p < 0.01$ ) reduction in cell density by 43.99% at 100  $\mu\text{g/mL}$  (Figure 43A).  $\Delta\Psi_m$  was gradually decreased, but was only significant ( $p < 0.05$ ) at 100  $\mu\text{g/mL}$  with a 0.35-fold reduction (Figure 43B). All concentrations decreased ROS concentration below baseline, with approximately 0.30-fold reduction between 3.2 and 32  $\mu\text{g/mL}$ , and a smaller reduction of 0.06-fold at 100  $\mu\text{g/mL}$  (Figure 43C). GSH concentrations were unaffected up to 32  $\mu\text{g/mL}$  and sharply increased by 1.45-fold at 100  $\mu\text{g/mL}$  ( $p < 0.05$ ) (Figure 43D). Although not significant, fatty acid concentration was reduced by 0.10-fold at 1  $\mu\text{g/mL}$  and gradually increased by 1.13-fold at 100  $\mu\text{g/mL}$  (Figure 43E). Lipid peroxidation was increased at 1  $\mu\text{g/mL}$ , but gradually decreased to baseline as the concentration increased (Figure 43F). ATP concentrations were slightly increased at lower concentrations, but were reduced by 0.2-fold at 100  $\mu\text{g/mL}$  (Figure 43G). A gradual activation of caspase-3/7 was observed at low concentrations, with an increase of 1.36- and 1.86-fold at 32  $\mu\text{g/mL}$  and 100  $\mu\text{g/mL}$ , respectively (Figure 43H).

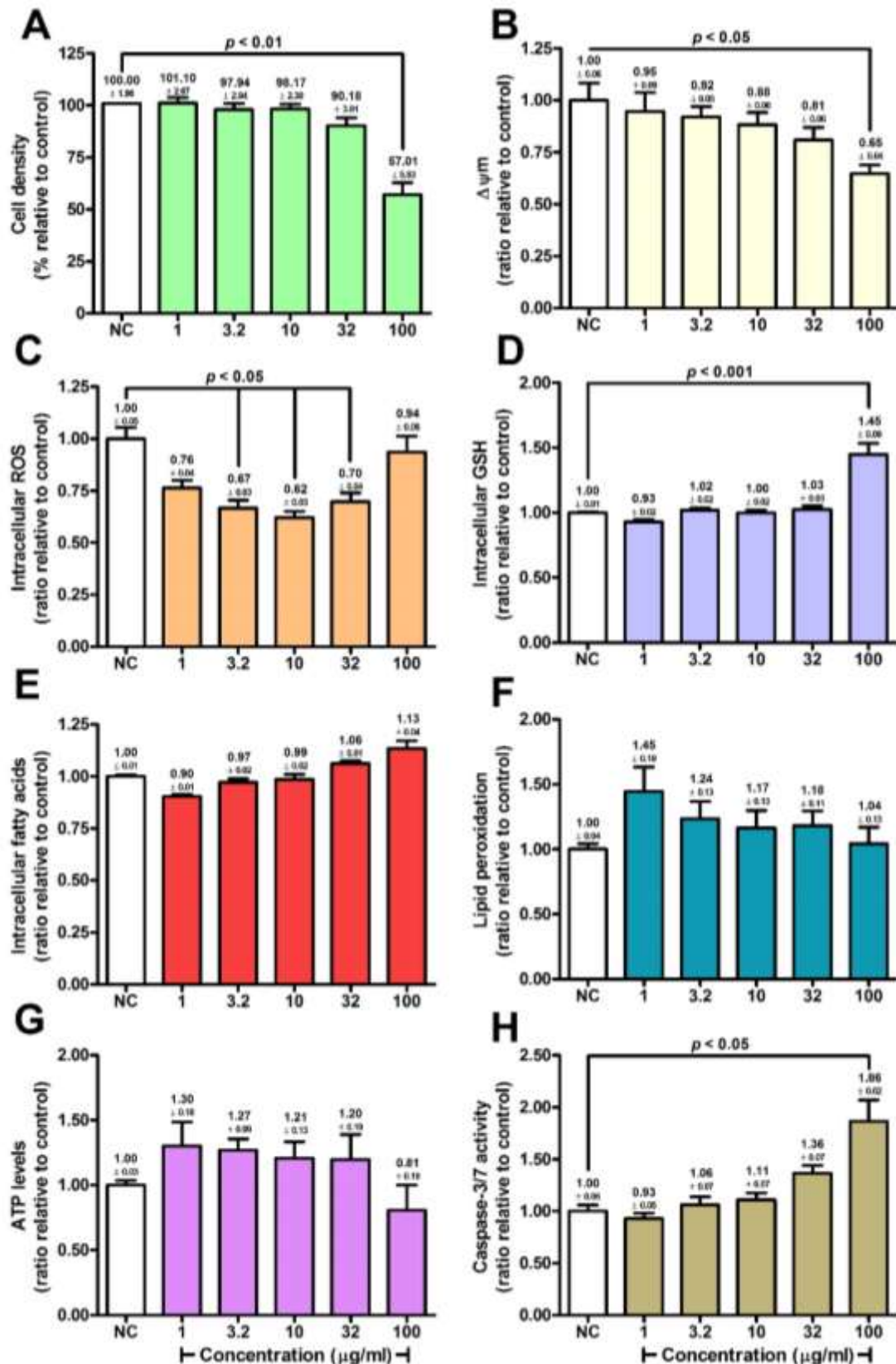


**Figure 43:** The effect of the crude hot water extract of *T. elegans* in HepG2 cells; A) cell density, B)  $\Delta\Psi_m$ , C) ROS concentration, D) GSH concentration, E) fatty acid concentration, F) lipid peroxidation, G) ATP levels and H) caspase-3/7 activity.

The methanol extract displayed high cytotoxicity with reduction of cell density at all concentrations ranging from 45.51% to 91.27%, and an  $IC_{50}$  of 3.07  $\mu\text{g/mL}$  (Figure 44A).  $\Delta\Psi_m$  reduced dose-dependently by 0.68-fold at 100  $\mu\text{g/mL}$ , with significant ( $p < 0.01$ ) reduction at concentrations  $\geq 10$   $\mu\text{g/mL}$  (Figure 44B). ROS concentrations were increased non-significantly from 1  $\mu\text{g/mL}$  to 32  $\mu\text{g/mL}$  by 1.85-fold, but was abolished at 100  $\mu\text{g/mL}$  (Figure 44C). GSH was depleted between 1  $\mu\text{g/mL}$  and 3.2  $\mu\text{g/mL}$  by approximately 0.15-fold, and increased dose-dependently by 4.56-fold at 100  $\mu\text{g/mL}$  ( $p < 0.001$ ) (Figure 44D). Fatty acid accumulation was significant ( $p < 0.001$ ) at 3.2  $\mu\text{g/mL}$  and higher, with a sharp increase of 5.80-fold at 100  $\mu\text{g/mL}$  (Figure 44E). Lipid peroxidation was slightly elevated at all concentrations, but did not follow an expected dose-dependent trend (Figure 44F). At 3.2  $\mu\text{g/mL}$ , ATP levels increased by 1.44-fold, but were completely abolished at higher concentrations ( $p < 0.01$ ) (Figure 44G). Caspase-3/7 activity was induced at all concentrations, but this was only significant ( $p < 0.05$ ) at concentrations  $\geq 10$   $\mu\text{g/mL}$ , with an increase of 3.53- to 50.80-fold from 1  $\mu\text{g/mL}$  to 100  $\mu\text{g/mL}$ , respectively (Figure 44H).

The hot water extract increased the percentage of cells in the sub-G1-, G1- and G2/M-phase by 8.30%, 0.07% and 20.93% ( $p < 0.001$ ), respectively, after 24 h, while reducing those in the S-phase by 21.00% ( $p < 0.001$ ) (Figure 45B, Table 22). After 72 h exposure the cells in the sub-G1- and G2/M-phase was increased by 24.77% ( $p < 0.001$ ) and 6.12%, respectively, while being reduced in the G1- and S-phase by 4.47% and 1.65%, respectively (Figure 45E, Table 22). After 24 h the methanol extract increased the sub-G1- and G2/M-phase by 2.53% and 9.24% ( $p < 0.05$ ), respectively, while reducing the cells in the G1- and S-phase by 1.16% and 8.08%, respectively (Figure 45C, Table 22). After 72 h exposure the sub-G1- and G2/M-phase were increased by 4.73% and 5.15%, respectively, and the G1- and S-phase were reduced by 4.98% and 0.18%, respectively (Figure 45F, Table 22).

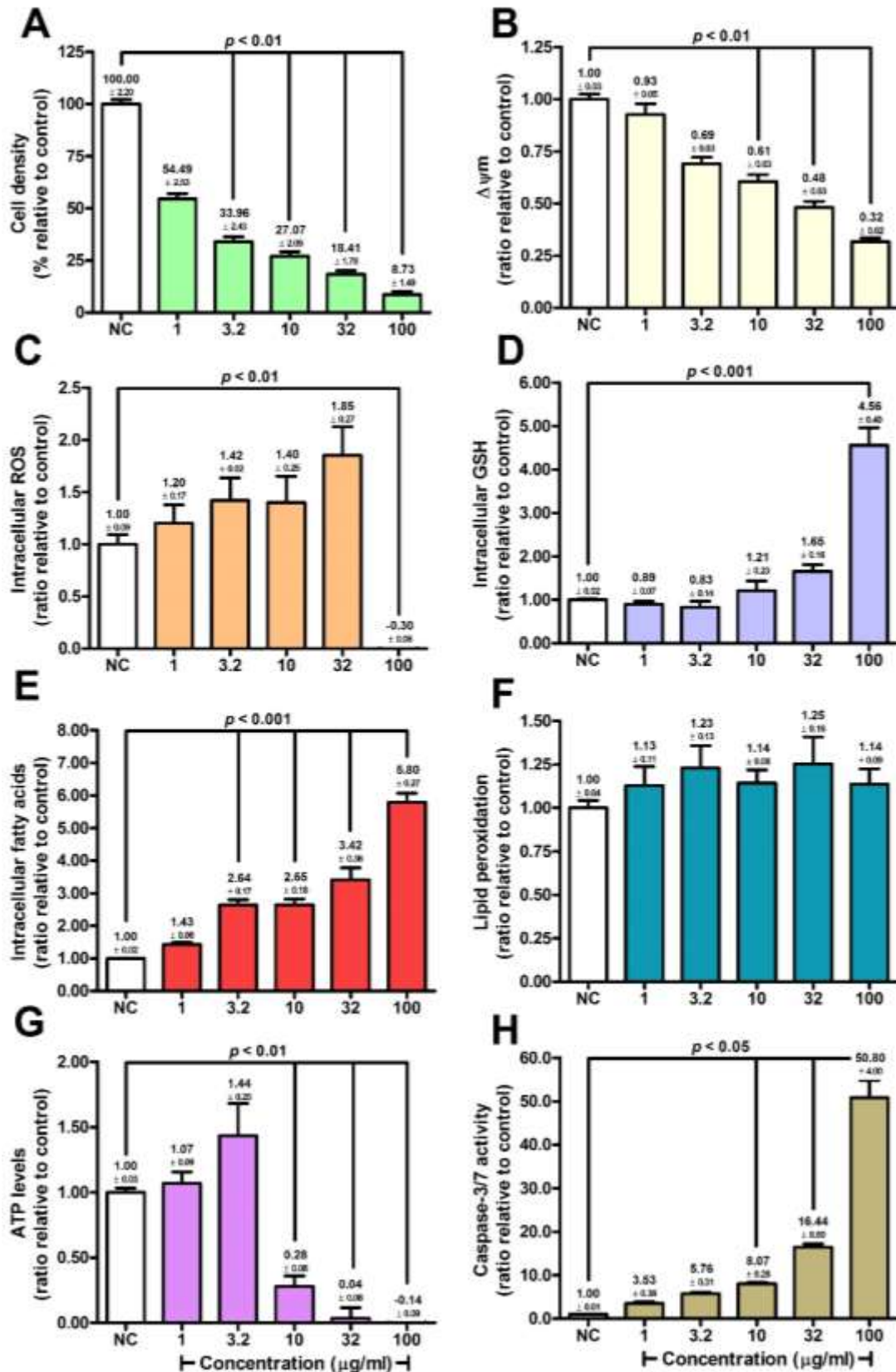


**Figure 44:** The effect of the crude methanol extract of *T. elegans* in HepG2 cells; A) cell density, B)  $\Delta\Psi_m$ , C) ROS concentration, D) GSH concentration, E) fatty acid concentration, F) lipid peroxidation, G) ATP levels and H) caspase-3/7 activity.

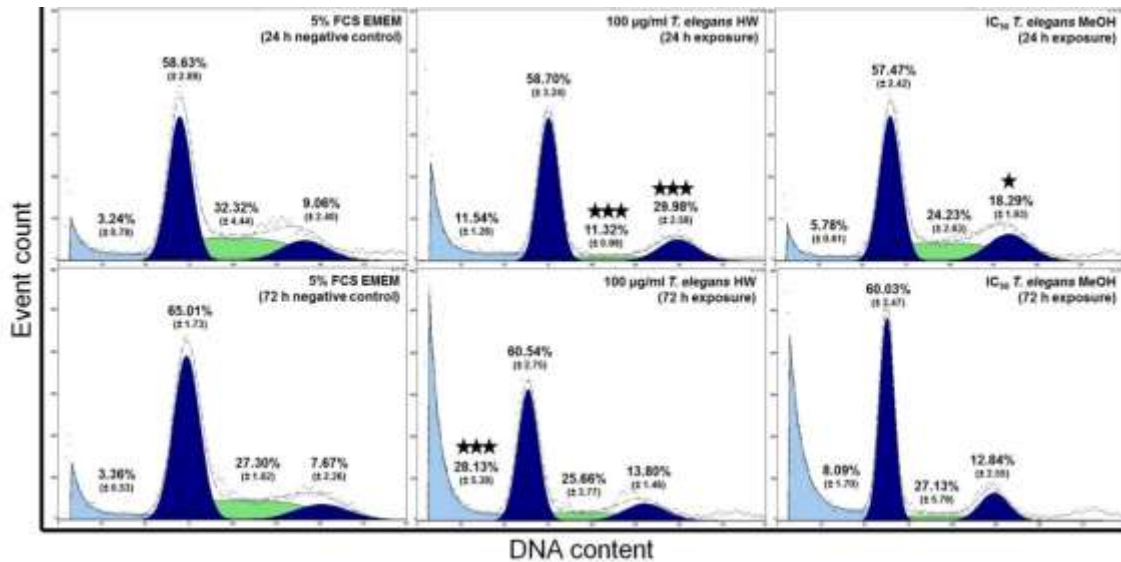


**Figure 45:** The effect of 100 µg/mL and the IC<sub>50</sub> of the hot water and methanol extract of *T. elegans*, respectively, on cellular kinetics in HepG2 cells exposed for 24 h and 72 h; A) negative control (24 h), B) hot water extract (24 h), C) methanol extract (24 h), D) negative control (72 h), E) hot water extract (72 h), F) methanol extract (72 h). Significant difference relative to the respective time points of the negative control: ★  $p < 0.05$  and ★★★  $p < 0.001$ .

**Table 22:** The effect of 100 µg/mL and the IC<sub>50</sub> of the hot water and methanol extract of *T. elegans*, respectively, on cellular kinetics in HepG2 cells exposed for 24 h and 72 h summarized as the shift in phase from the respective negative control.

Phase of cell cycle	Shift in cell cycle phase after exposure to <i>T. elegans</i> (%)			
	Hot water extract		Methanol extract	
	24 h	72 h	24 h	72 h
Sub-G1	↑ 8.30	↑ 24.77***	↑ 2.53	↑ 4.73
G1	↑ 0.07	↓ 4.47	↓ 1.16	↓ 4.98
S	↓ 21.00***	↓ 1.65	↓ 8.08	↓ 0.18
G2/M	↑ 20.93***	↑ 6.12	↑ 9.24*	↑ 5.15

Significant difference relative to the respective time points of the negative control: ★  $p < 0.05$  and ★★★  $p < 0.001$ .

After 24 h the hot water extract decreased cell viability by 4.63%, with an increase of early apoptotic, late apoptotic and necrotic cells by 1.47%, 0.19% and 2.98%, respectively (Figure 46B, Table 23). After 72 h exposure, cell viability was reduced by 27.10% ( $p < 0.001$ ), and early apoptotic, late apoptotic and necrotic cells increased by 2.50%, 0.81% and 23.79% ( $p < 0.001$ ), respectively (Figure 46E, Table 23). The methanol extract reduced cell viability by 6.92% after 24 h exposure, while early apoptotic, late apoptotic and necrotic cells were increased by 5.08%, 0.58% and 1.25%, respectively (Figure 46C, Table 23). After 72 h exposure cell viability was decreased by 21.12% ( $p < 0.001$ ), and an increase of 5.67%, 0.94% and 13.92% ( $p < 0.05$ ) was observed for early apoptotic, late apoptotic and necrotic cells, respectively (Figure 46F, Table 23).

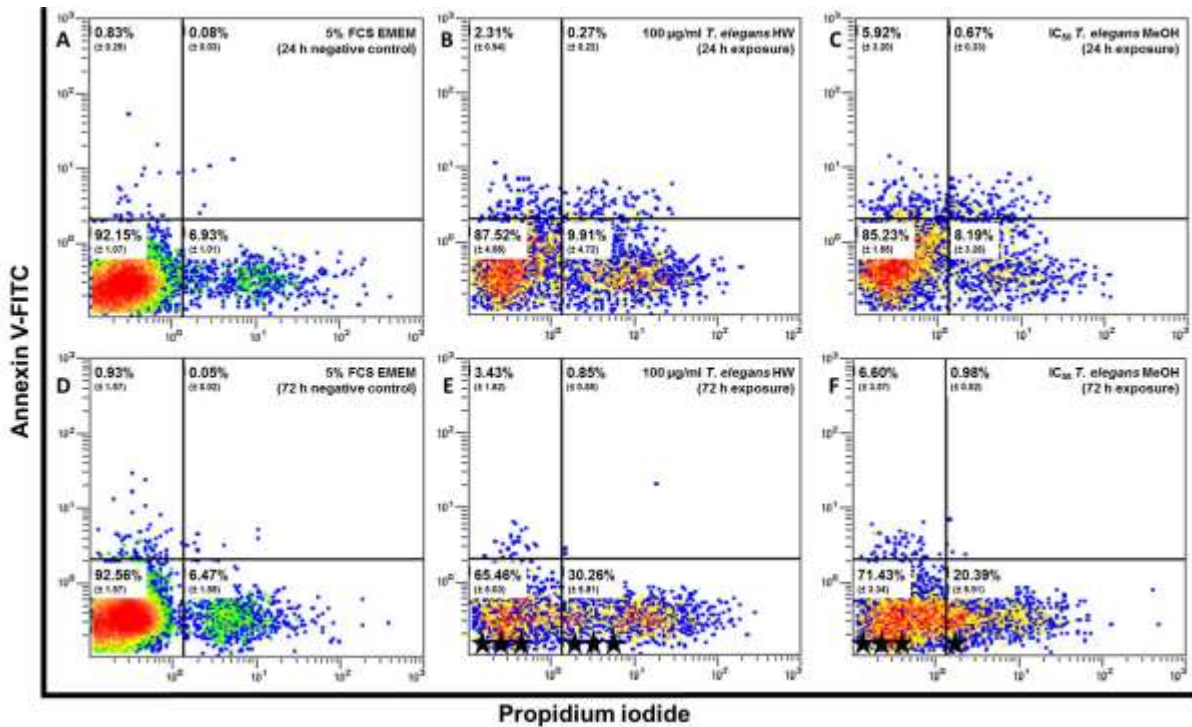


**Figure 46:** The effect of 100 µg/mL and the IC<sub>50</sub> of the hot water and methanol extract of *T. elegans*, respectively, on cellular viability in HepG2 cells exposed for 24 h and 72 h; A) negative control (24 h), B) hot water extract (24 h), C) methanol extract (24 h), D) negative control (72 h), E) hot water extract (72 h), F) methanol extract (72 h). Significant difference relative to the respective time points of the negative control: ★  $p < 0.05$  and ★★ ★  $p < 0.001$ .

**Table 23:** The effect of 100 µg/mL and the IC<sub>50</sub> of the hot water and methanol extract of *T. elegans*, respectively, on cellular viability in HepG2 cells exposed for 24 h and 72 h summarized as the shift in phase from the respective negative control.

State of viability	Shift in viability after exposure to <i>T. elegans</i> (%)			
	Hot water extract		Methanol extract	
	24 h	72 h	24 h	72 h
Viable	↓ 4.63	↓ 27.1***	↓ 6.92	↓ 21.12***
Early apoptosis	↑ 1.47	↑ 2.5	↑ 5.08	↑ 5.67
Late apoptosis	↑ 0.19	↑ 0.81	↑ 0.58	↑ 0.94
Necrosis	↑ 2.98	↑ 23.79***	↑ 1.25	↑ 13.92*

Significant difference relative to the respective time points of the negative control: ★  $p < 0.05$  and ★★ ★  $p < 0.001$ .

Hepatotoxicity screening displayed a similar trend for both extracts, except for ROS concentrations, where the effects were more pronounced after exposure to the methanol extract. While ROS concentrations were decreased for the hot water extract, a dose-dependent increase was displayed by the methanol extract until complete abolishment at the highest concentration tested was achieved. Lipid peroxidation was slightly increased at all concentrations. ATP levels initially increased at lower concentrations, though paralleled the reduction in cell density at higher concentrations.

Both extracts induced an increase in the cells in the sub-G1- and G2/M-phase, although this was more pronounced with the hot water extract. Although hepatotoxicity screening indicated that the methanol extract was more detrimental towards cellular viability, Annexin V-FITC staining displayed a gradual reduction of cell viability with increased necrosis for both extracts, with the effect being more pronounced for the hot water extract.

#### 4.3.3.6. *Terminalia sericea*

The hot water extract of *T. sericea* presented with a slight reduction of cellular viability (Figure 47A), of up to 37.30% at 100 µg/mL.  $\Delta\Psi_m$  decreased dose-dependently (Figure 47B), and was statistically significant ( $p < 0.01$ ) at  $\geq 32$  µg/mL (up to 0.74-fold at 100 µg/mL). ROS concentrations remained stable (Figure 47C), except for a marginal, statistically significant ( $p < 0.05$ ) increase of 1.19-fold at 10 µg/mL. Intracellular GSH concentrations did not change (Figure 47D). A significant ( $p < 0.01$ ) increase in fatty acid concentration was observed (1.54-fold at 100 µg/mL) (Figure 47E), while lipid peroxidation was slightly elevated, although this was not statistically significant (Figure 47F). ATP levels were significantly ( $p < 0.05$ ) reduced in a dose-dependent manner at 100 µg/mL (0.40-fold) (Figure 47G), and caspase-3/7 activity was diminished by 0.35-fold at 100 µg/mL (Figure 47H).

The methanol extract of *T. sericea* induced marginally higher reduction of cell viability by 48.81% at 100 µg/mL (Figure 48A).  $\Delta\Psi_m$  decreased dose-dependently and reached a plateau at  $\geq 32$  µg/mL (approximately 0.82-fold) (Figure 48B). ROS concentrations remained below baseline, which was only significant ( $p < 0.001$ ) at  $\geq 10$  µg/mL where a plateau was reached (approximately 0.50-fold reduction) (Figure 48C). GSH concentrations reduced dose-dependently and significantly ( $p < 0.001$ ) up to 0.52-fold at 100 µg/mL (Figure 48D). Fatty acid content remained unaffected (Figure 48E), while lipid peroxidation tended to increase insignificantly (Figure 48F). ATP levels decreased dose-dependently by a maximum of 0.46-fold at 100 µg/mL (Figure 48G). Caspase-3/7 activity was similarly decreased and significant ( $p < 0.05$ ) at  $\geq 32$  µg/mL (up to complete abolishment at 100 µg/mL) (Figure 48H).

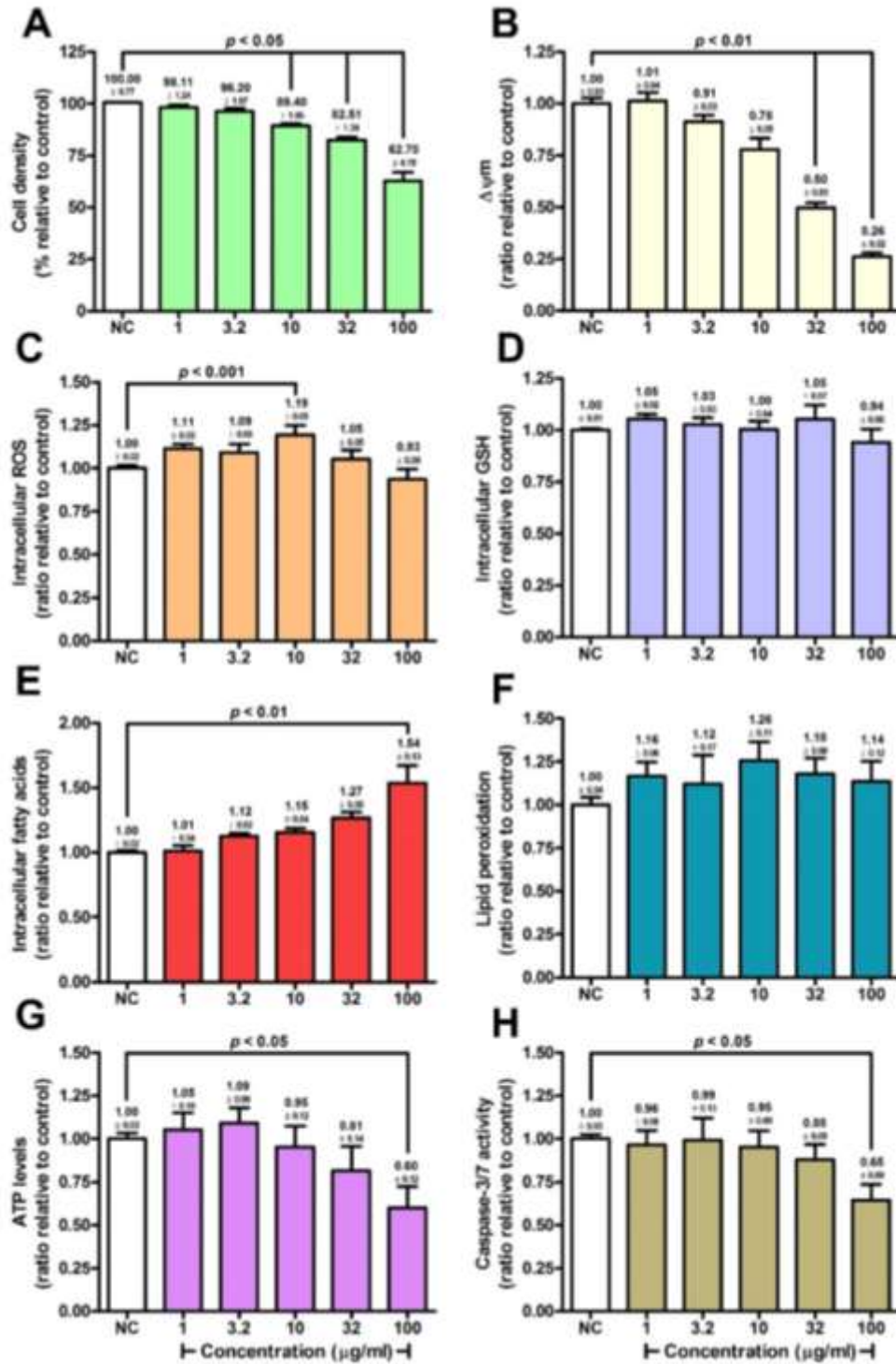


**Figure 47:** The effect of the crude hot water extract of *T. sericea* in HepG2 cells; A) cell density, B)  $\Delta\Psi_m$ , C) ROS concentration, D) GSH concentration, E) fatty acid concentration, F) lipid peroxidation, G) ATP levels and H) caspase-3/7 activity.

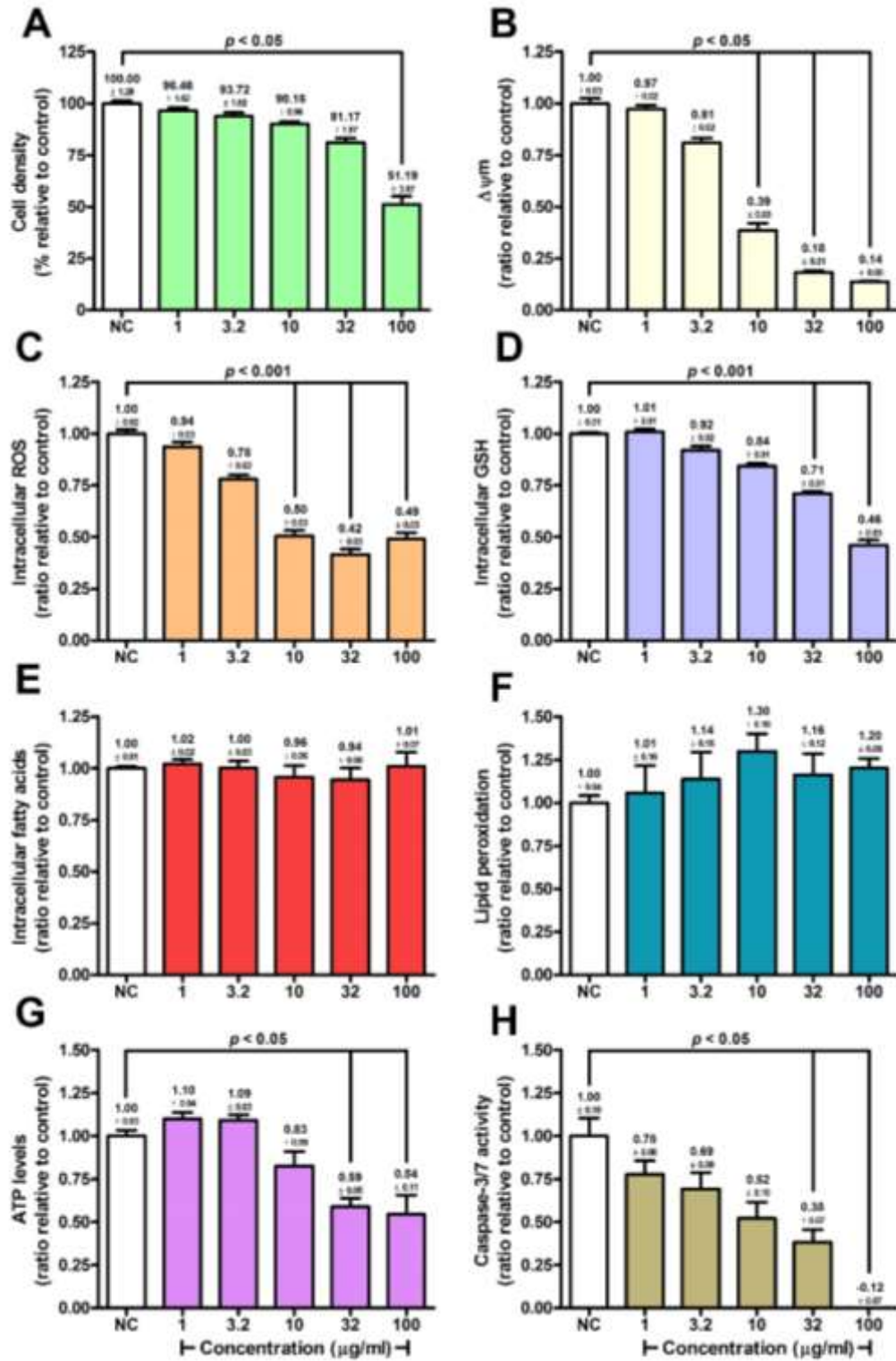


**Figure 48:** The effect of the crude methanol extract of *T. sericea* in HepG2 cells; A) cell density, B)  $\Delta\Psi_m$ , C) ROS concentration, D) GSH concentration, E) fatty acid concentration, F) lipid peroxidation, G) ATP levels and H) caspase-3/7 activity.

After 24 h the hot water extract increased the cells in the sub-G1-, G1- and G2/M-phase by 2.91%, 3.5% and 2.69%, respectively, while it reduced those in the S-phase by 6.19% (Figure 49B, Table 24). After 72 h the cells in the sub-G1- and S-phase were increased by 1.38% and 9.67%, respectively, and reduced in the G1- and G2/M-phase by 7.21% and 3.09%, respectively (Figure 49E, Table 24). Exposure to the methanol extract for 24 h increased the sub-G1- and S-phase by 6.67% and 2.73%, respectively, whereas the G1- and G2/M-phase were reduced by 0.35% and 2.38%, respectively (Figure 49C, Table 24). After 72 h the sub-G1-phase was increased by 9.84% as well as the S-phase by 11.85% ( $p < 0.05$ ), while the G1- and G2/M-phase were reduced by 8.41% and 3.44%, respectively (Figure 49F, Table 24).

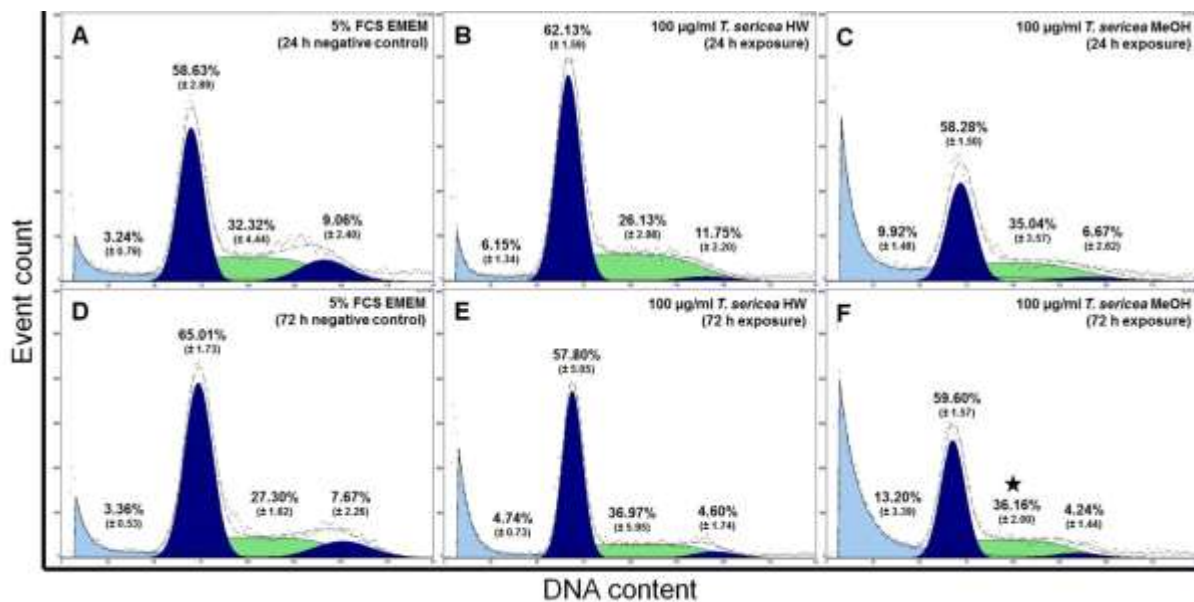


**Figure 49:** The effect of the 100 µg/mL *T. sericea* on cellular kinetics in HepG2 cells exposed for 24 h and 72 h; A) negative control (24 h), B) hot water extract (24 h), C) methanol extract (24 h), D) negative control (72 h), E) hot water extract (72 h), F) methanol extract (72 h) . Significant difference relative to the respective time points of the negative control: ★  $p < 0.05$ .

**Table 24:** The effect of the 100 µg/mL *T. sericea* on cellular kinetics in HepG2 cells exposed for 24 h and 72 h summarized as the shift in phase from the respective negative control.

Phase of cell cycle	Shift in cell cycle phase after exposure to <i>T. sericea</i> (%)			
	Hot water extract		Methanol extract	
	24 h	72 h	24 h	72 h
Sub-G1	↑ 2.91	↑ 1.38	↑ 6.67	↑ 9.84
G1	↑ 3.5	↓ 7.21	↓ 0.35	↓ 8.41
S	↓ 6.19	↑ 9.67	↑ 2.73	↑ 11.85★
G2/M	↑ 2.69	↓ 3.09	↓ 2.38	↓ 3.44

Significant difference relative to the respective time points of the negative control: ★  $p < 0.05$ .

Exposure to the hot water extract for 24 h decreased cell viability by 9.85%, while necrotic cells were increased by 9.89% (Figure 50B, Table 25). After 72 h cell viability was reduced by 14.96%, while early apoptotic, late apoptotic and necrotic cells were increased by 7.57%, 0.38% and 7.01%, respectively (Figure 50E, Table 25). At 24 h exposure the methanol extract decreased cell viability by 40.14% ( $p < 0.001$ ), and increased early apoptotic, late apoptotic and necrotic cells by 3.22%, 2.08% and 34.89% ( $p < 0.001$ ), respectively (Figure 50C, Table 25). After 72 h the cell viability was decreased by 30.56% ( $p < 0.001$ ), and early apoptotic, late apoptotic and necrotic cells by 3.41%, 0.18% and 29.96% ( $p < 0.001$ ), respectively (Figure 50F, Table 25).

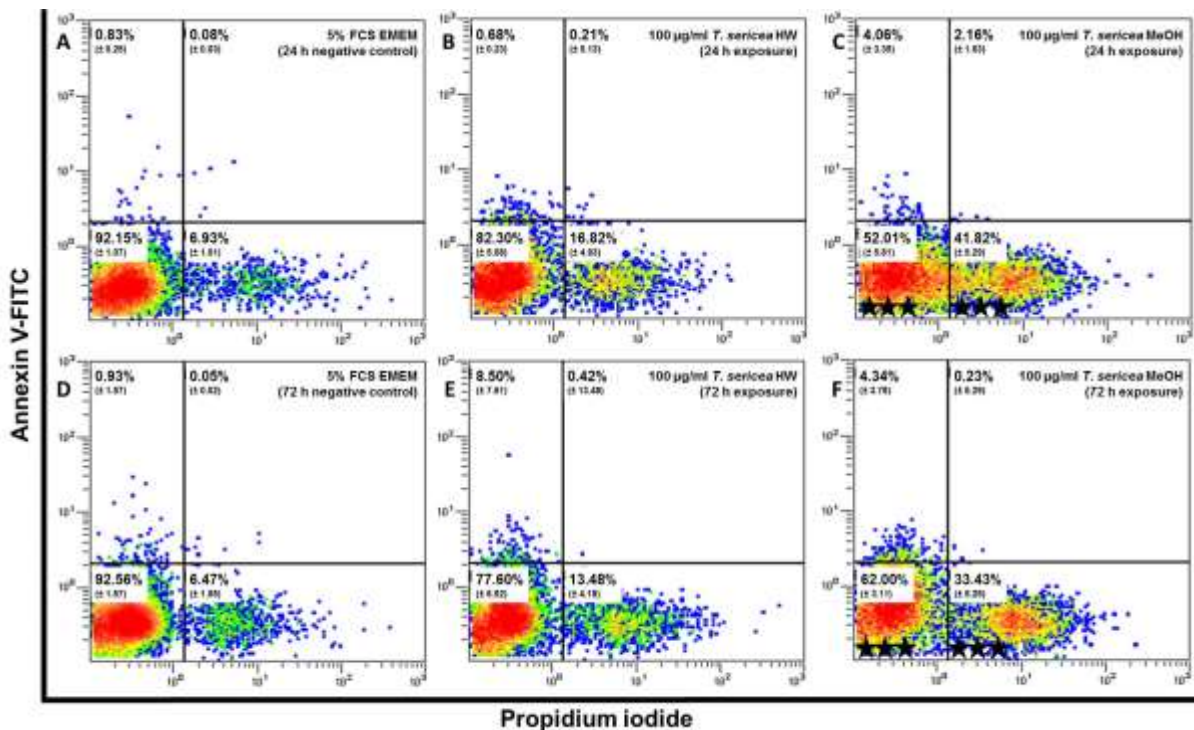


**Figure 50:** The effect of the 100 µg/mL *T. sericea* on cellular viability in HepG2 cells exposed for 24 h and 72 h; A) negative control (24 h), B) hot water extract (24 h), C) methanol extract (24 h), D) negative control (72 h), E) hot water extract (72 h), F) methanol extract (72 h). Significant difference relative to the respective time points of the negative control: ★★★  $p < 0.001$ .

**Table 25:** The effect of the 100 µg/mL *T. sericea* on cellular viability in HepG2 cells exposed for 24 h and 72 h summarized as the shift in phase from the respective negative control.

State of viability	Shift in viability after exposure to <i>T. sericea</i> (%)			
	Hot water extract		Methanol extract	
	24 h	72 h	24 h	72 h
<b>Viable</b>	↓ 9.85	↓ 14.96	↓ 40.14***	↓ 30.56***
<b>Early apoptosis</b>	↓ 0.16	↑ 7.57	↑ 3.22	↑ 3.41
<b>Late apoptosis</b>	↑ 0.13	↑ 0.38	↑ 2.08	↑ 0.18
<b>Necrosis</b>	↑ 9.89	↑ 7.01	↑ 34.89***	↑ 26.96***

Significant difference relative to the respective time points of the negative control: ★★★  $p < 0.001$ .

While the hot water extract reduced cell density,  $\Delta\Psi_m$  and caspase-3/7 activity, and increased the fatty acid concentrations, the methanol extract had a greater effect on reducing ROS and GSH concentrations, without altering fatty acid concentrations. Both extracts increased cells in the S-phase of the cell cycle, with a more pronounced effect by the methanol extract. While the hot water extract increased apoptotic and necrotic cells (primarily), the methanol extract increased necrotic cells by a much greater degree.

#### 4.3.3.7. *Ziziphus mucronata*

The hot water extract of *Z. mucronata* induced a dose-dependent decrease in cell density at concentrations  $\geq 32$   $\mu\text{g/mL}$  (Figure 51A), with a maximum inhibition of 43.91% attained at 100  $\mu\text{g/mL}$ .  $\Delta\Psi_m$  decreased dose-dependently, with a maximal significant ( $p < 0.001$ ) reduction of 0.67-fold at 100  $\mu\text{g/mL}$  (Figure 51B). ROS concentrations were marginally reduced at  $\geq 32$   $\mu\text{g/mL}$  (0.26-fold at 100  $\mu\text{g/mL}$ ) (Figure 51C). GSH concentrations remained constant, except for a small, insignificant increase of 1.10-fold at 10  $\mu\text{g/mL}$  (Figure 51D). Fatty acid accumulation occurred at  $\geq 10$   $\mu\text{g/mL}$ , with a significant increase of 1.35-fold at 100  $\mu\text{g/mL}$  (Figure 51E). Lipid peroxidation (Figure 51F) and ATP levels (Figure 51G) remained largely unaltered. Decreased caspase-3/7 activity was observed at  $\geq 10$   $\mu\text{g/mL}$ , which was not dose-dependent (maximal reduction of 0.55-fold at 100  $\mu\text{g/mL}$ ) (Figure 51H).

The methanol extract was found to display dose-dependent cytotoxicity, with an  $\text{IC}_{50}$  of 36.29  $\mu\text{g/mL}$  and maximum cell density reduction of 81.39% at 100  $\mu\text{g/mL}$  (Figure 52A).  $\Delta\Psi_m$  was reduced dose-dependently by a maximum of 0.78-fold at 100  $\mu\text{g/mL}$  (Figure 52B). ROS concentrations decreased dose-dependently from  $\geq 1$   $\mu\text{g/mL}$ , with a maximal reduction of 0.92-fold observed at 100  $\mu\text{g/mL}$  (Figure 52C). GSH concentrations remained unaltered (Figure 52D). An increase of 3.43-fold occurred with regards to fatty acid concentrations (Figure 52E), however no change occurred for lipid peroxidation (Figure 52F). ATP levels increased by 1.57-fold at 32  $\mu\text{g/mL}$ , but decreased by 0.14-fold at 100  $\mu\text{g/mL}$  (Figure 52G). Caspase-3/7 activity was dose-dependently decreased, and ultimately abolished at 100  $\mu\text{g/mL}$  (Figure 52H).

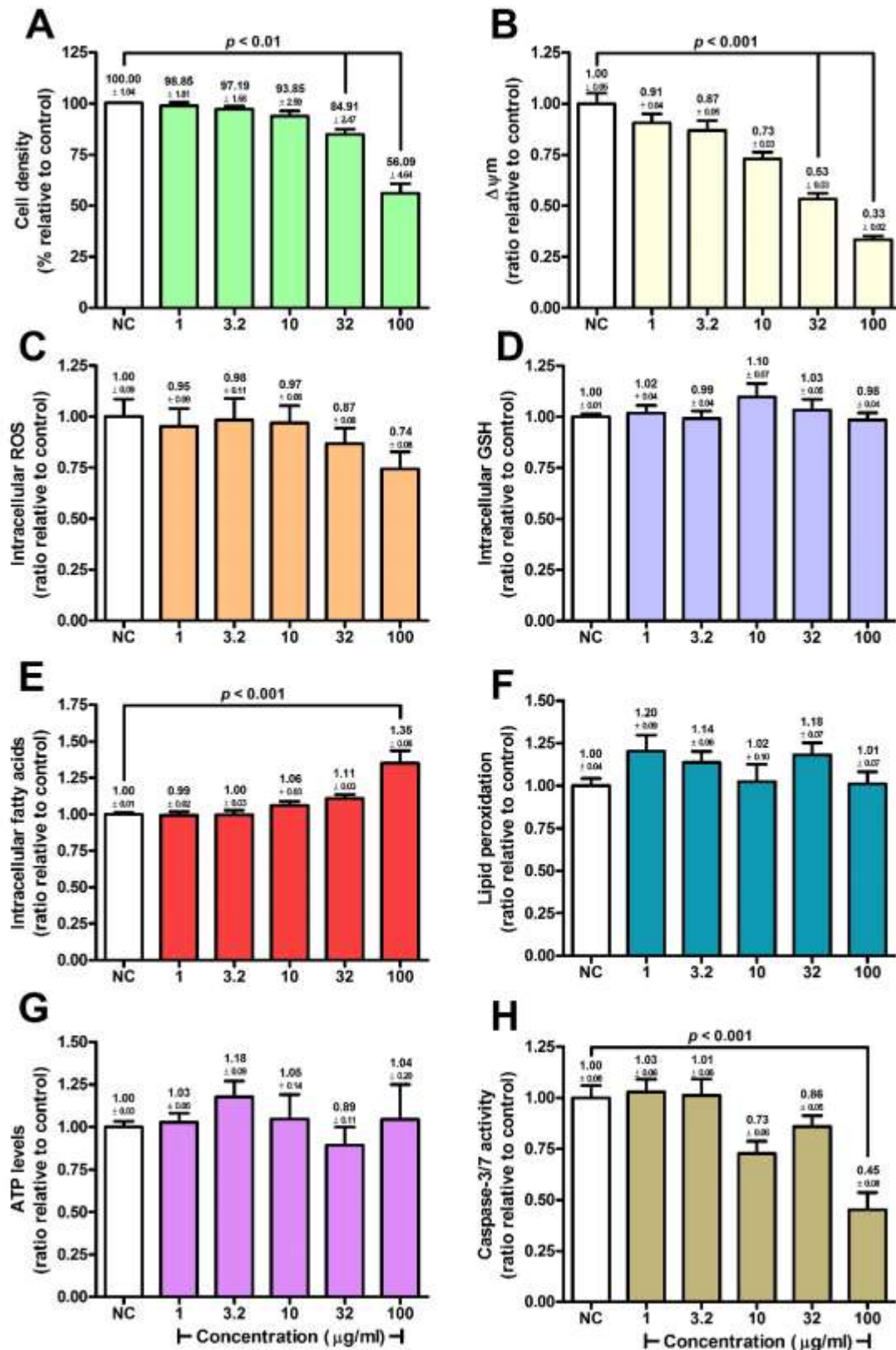


**Figure 51:** The effect of the crude methanol extract of *Z. mucronata* in HepG2 cells; A) cell density, B)  $\Delta\Psi_m$ , C) ROS concentration, D) GSH concentration, E) fatty acid concentration, F) lipid peroxidation, G) ATP levels and H) caspase-3/7 activity.

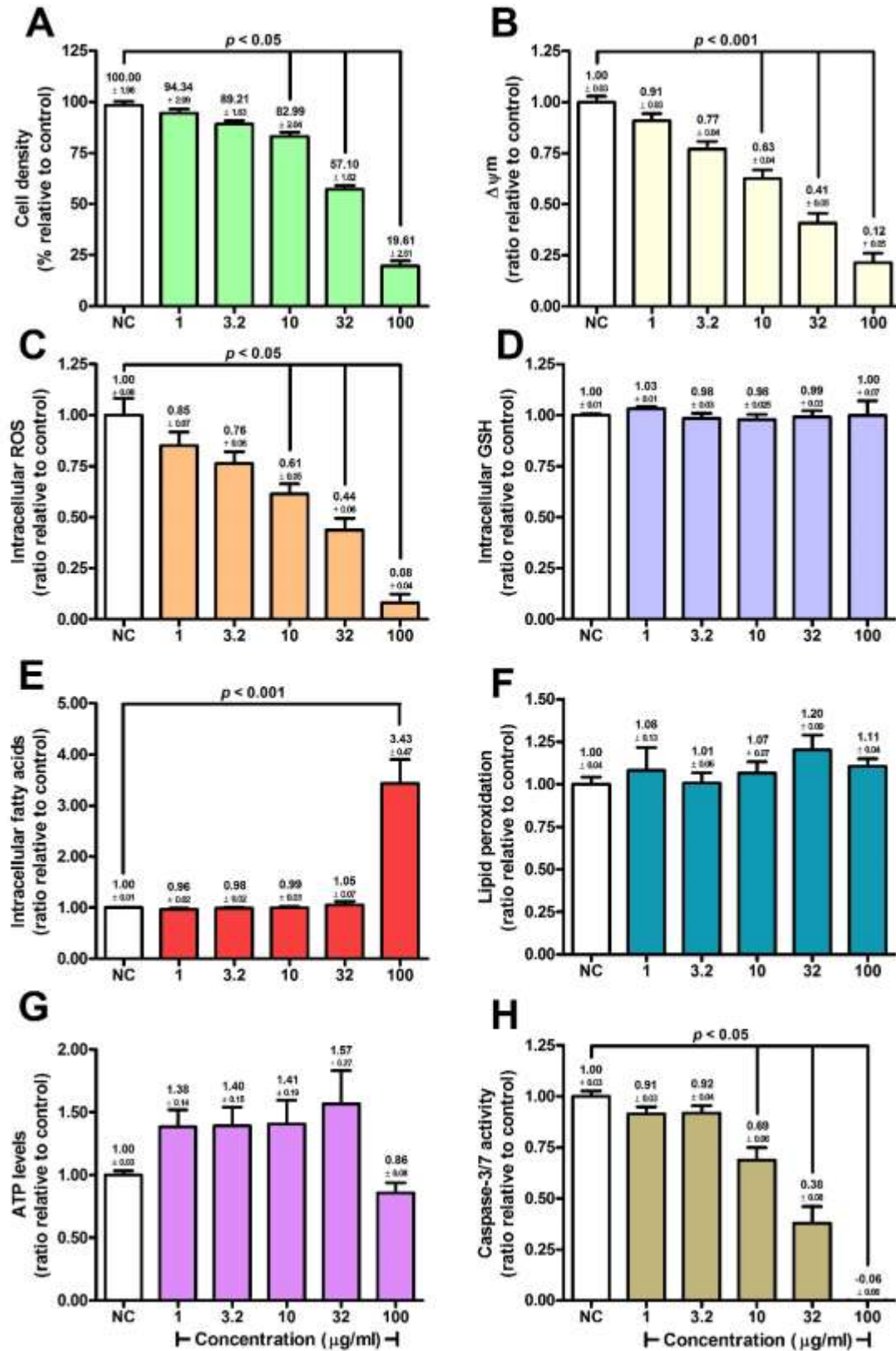


**Figure 52:** The effect of the crude methanol extract of *Z. mucronata* in HepG2 cells; A) cell density, B)  $\Delta\Psi_m$ , C) ROS concentration, D) GSH concentration, E) fatty acid concentration, F) lipid peroxidation, G) ATP levels and H) caspase-3/7 activity.

After 24 h the hot water extract increased the cells in the sub-G1-, G1- and G2/M-phase by 2.97%, 7.29% and 4.44%, respectively, while cells in the S-phase were reduced by 11.73% ( $p < 0.01$ ) (Figure 53B, Table 26). After 72 h exposure there was a 0.29% and 4.62% increase in the sub-G1- and G1-phase, respectively, while the S-phase and G2/M-phase were decreased by 3.44% and 1.18%, respectively (Figure 53E, Table 26). At 24 h, the methanol extract increased the sub-G1-, G1- and G2/M-phase by 0.04%, 9.96% ( $p < 0.05$ ) and 5.09%, respectively, while the S-phase was reduced by 15.05% ( $p < 0.001$ ) (Figure 53C, Table 26). After 72 h exposure the sub-G1-, G1- and G2/M-phase were increased by 0.39%, 5.29% and 2.13%, respectively, and the S-phase reduced by 7.42% (Figure 53F, Table 26).

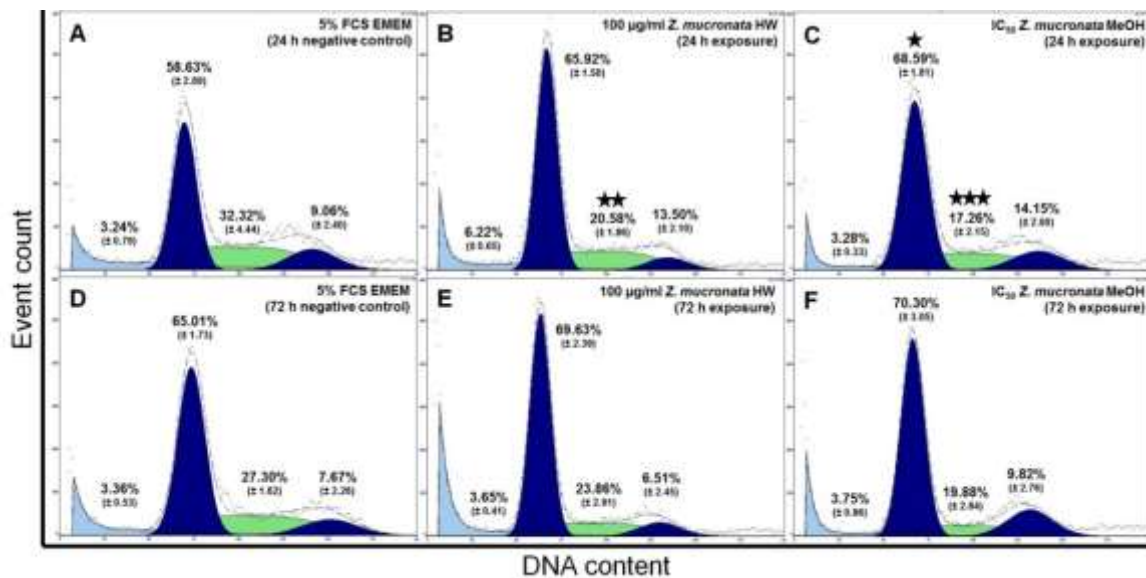


**Figure 53:** The effect of 100 µg/mL and the IC<sub>50</sub> of the hot water and methanol extract of *Z. mucronata*, respectively, on cellular kinetics in HepG2 cells exposed for 24 h and 72 h; A) negative control (24 h), B) hot water extract (24 h), C) methanol extract (24 h), D) negative control (72 h), E) hot water extract (72 h), F) methanol extract (72 h). Significant difference relative to the respective time points of the negative control: ★  $p < 0.05$ , ★★  $p < 0.01$  and ★★★  $p < 0.001$ .

**Table 26:** The effect of 100 µg/mL and the IC<sub>50</sub> of the hot water and methanol extract of *Z. mucronata*, respectively, on cellular kinetics in HepG2 cells exposed for 24 h and 72 h summarized as the shift in phase from the respective negative control.

Phase of cell cycle	Shift in cell cycle phase after exposure to <i>Z. mucronata</i> (%)			
	Hot water extract		Methanol extract	
	24 h	72 h	24 h	72 h
Sub-G1	↑ 2.97	↑ 0.29	↑ 0.04	↑ 0.39
G1	↑ 7.29	↑ 4.62	↑ 9.96★	↑ 5.29
S	↓ 11.73★★	↓ 3.44	↓ 15.05★★★	↓ 7.42
G2/M	↑ 4.44	↓ 1.18	↑ 5.09	↑ 2.13

Significant difference relative to the respective time points of the negative control: ★  $p < 0.05$ , ★★  $p < 0.01$  and ★★★  $p < 0.001$ .

After 24 h exposure the hot water extract reduced cell viability by 21.61% ( $p < 0.001$ ), while early apoptotic, late apoptotic and necrotic cells were increased 5.86%, 1.59% and 14.17% ( $p < 0.05$ ), respectively (Figure 54B, Table 27). After 72 h there was a reduction of 21.21% ( $p < 0.001$ ), and increase of 6.24%, 0.03% and 14.93% ( $p < 0.05$ ) in early apoptotic, late apoptotic and necrotic cells, respectively (Figure 54E, Table 27). After 24 h exposure there was a 21.72% ( $p < 0.001$ ) reduction of cell viability, and 4.03%, 1.56% and 16.13% ( $p < 0.01$ ) increase in early apoptotic, late apoptotic and necrotic cells, respectively (Figure 54C, Table 27). After 72 h exposure cell viability was reduced by 17.95% ( $p < 0.01$ ), while early apoptotic, late apoptotic and necrotic cells were increased by 2.75%, 0.02% and 15.17% ( $p < 0.05$ ), respectively (Figure 54F, Table 27).

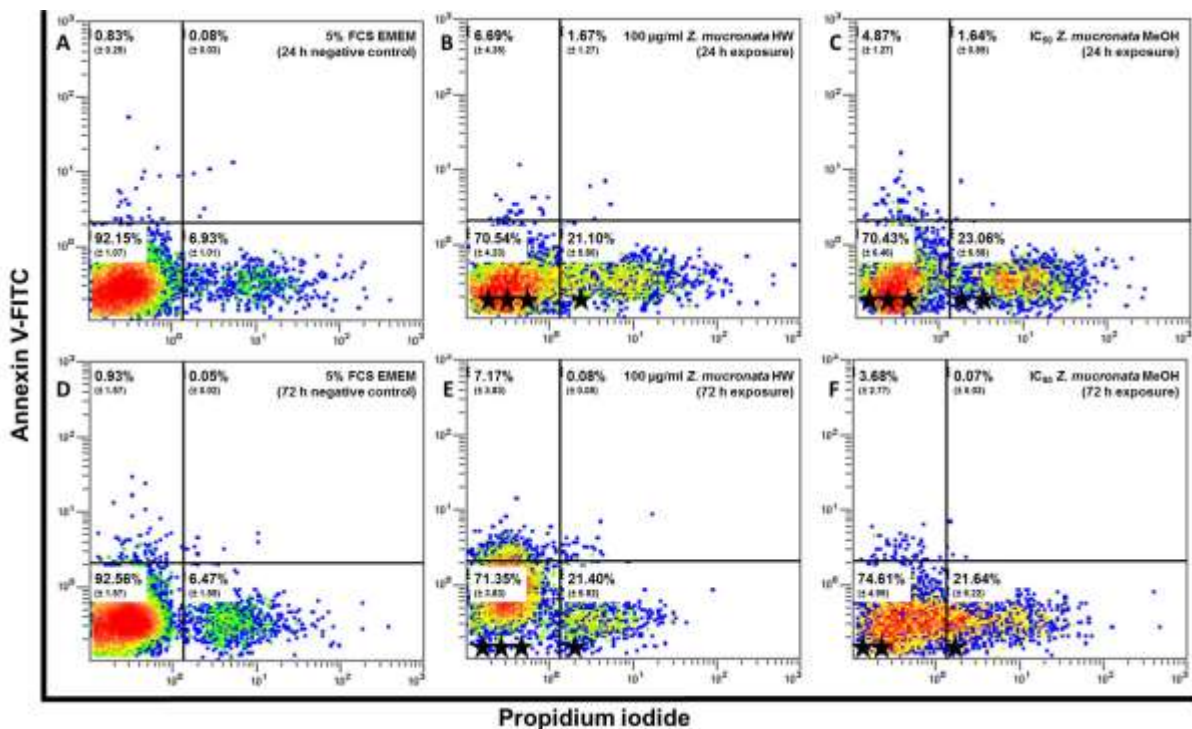


**Figure 54:** The effect of 100 µg/mL and the IC<sub>50</sub> of the hot water and methanol extract of *Z. mucronata*, respectively, on cellular viability in HepG2 cells exposed for 24 h and 72 h; A) negative control (24 h), B) hot water extract (24 h), C) methanol extract (24 h), D) negative control (72 h), E) hot water extract (72 h), F) methanol extract (72 h). Significant difference relative to the respective time points of the negative control: ★  $p < 0.05$ , ★★  $p < 0.01$  and ★★★  $p < 0.001$ .

**Table 27:** The effect of 100 µg/mL and the IC<sub>50</sub> of the hot water and methanol extract of *Z. mucronata*, respectively, on cellular viability in HepG2 cells exposed for 24 h and 72 h summarized as the shift in phase from the respective negative control.

State of viability	Shift in viability after exposure to <i>Z. mucronata</i> (%)			
	Hot water extract		Methanol extract	
	24 h	72 h	24 h	72 h
<b>Viable</b>	↓ 21.61***	↓ 21.21***	↓ 21.72***	↓ 17.95**
<b>Early apoptosis</b>	↑ 5.86	↑ 6.24	↑ 4.03	↑ 2.75
<b>Late apoptosis</b>	↑ 1.59	↑ 0.03	↑ 1.56	↑ 0.02
<b>Necrosis</b>	↑ 14.17*	↑ 14.93*	↑ 16.13**	↑ 15.17*

Significant difference relative to the respective time points of the negative control: ★  $p < 0.05$ , ★★  $p < 0.01$  and ★★★  $p < 0.001$ .

Both extracts presented with similar trends to all hepatotoxic parameters, but the methanol extract had a larger detrimental effect to cell status. Although both extracts increased the percentage of cells in the G1- and G2/M-phases after 24 h, these effects dissipated after 72 h. Both extracts reduced cellular viability and increased early apoptotic and necrotic cells to the same degree.

A summary of the hepatotoxicity results are presented in Table 28.

## 4.4. Discussion

### 4.4.1. *Acokanthera oppositifolia*

Of all crude extracts tested, *A. oppositifolia* was the only sample to show slightly higher cytotoxicity induced by the hot water extract than the methanol extract. Although data on the root-bark is scarce, the cytotoxicity of *Acokanthera* as a whole is supported. Dichloromethane extracts of the roots and stems have been reported to display moderate to high cytotoxicity against TK10 renal carcinoma, MCF-7 breast carcinoma and UACC62 melanoma cells with total growth inhibition at  $\leq 15$  µg/mL.<sup>6</sup> In-house studies have shown that *A. oppositifolia* induces cytotoxicity in a variety of cell lines (SK-Br-3, MDA-MB-231 and MCF-7 breast carcinoma), with IC<sub>50</sub>'s between 1.29 µg/mL and 15.76 µg/mL (Appendix IV). Similar to the present study, the hot water extract displayed greater activity than the methanol extract (Appendix IV).

**Table 28:** Summary of the hepatotoxicity of the selected crude extracts.

Plant	Extract	Hepatotoxic parameter assessed									
		Cell density (IC <sub>50</sub> )	Oxidative stress	$\Delta\Psi_m$	Fatty acid content	Caspase-3/7 activity	ATP levels	Cellular kinetics		Mode of cell death	
								Effect	Time-dependence	Effect	Time-dependence
<i>A. oppositifolia</i>	HW	Dose-dependent ↓ (24.26 µg/mL)	Slight ROS ↓ Dose-dependent GSH ↓, plateau at 32 µg/mL No peroxides	Dose-dependent ↓	Dose-dependent ↑ ≥32 µg/mL	Slight ↓ ≤3.2 µg/mL, ↑ ≥10 µg/mL	Dose-dependent ↓ ≥1 µg/mL	S- (primary) and G2/M block (secondary) with increased DNA fragmentation	Effect present at 24 h, but more prominent at 72 h	Necrosis (primary), slight apoptosis (secondary)	Effect more prominent at 24 h than 72 h
	MeOH	Dose-dependent ↓ (26.16 µg/mL)	ROS ↓ GSH ↓ ≤32 µg/mL, GSH ↑ 100 µg/mL No peroxides	Dose-dependent ↓	Dose-dependent ↑	Dose-dependent ↑ ≥32 µg/mL	Dose-dependent ↓ ≥1 µg/mL, plateaus at 10 µg/mL	G2/M-block, DNA fragmentation	Effect present at 24 h, but more prominent at 72 h	Necrosis (primary), slight apoptosis (secondary)	Effect more prominent at 24 h than 72 h
<i>B. disticha</i>	HW	Dose-dependent ↓ (51.39 µg/mL)	Dose-dependent ROS ↓, reaches plateau at 32 µg/mL Dose-dependent GSH ↓ ≤32 µg/mL No peroxides	Dose-dependent ↓	Dose-dependent ↑	Dose-dependent ↓ ≤32 µg/mL, slight ↓ 100 µg/mL	↑ ≥10 µg/mL	Slight G2/M-block, which later shifts to slight G1-block	G2/M-block at 24 h, which becomes G1-block at 72 h	Early apoptosis	Effect more prominent at 24 h than 72 h
	MeOH	Dose-dependent ↓ (35.11 µg/mL)	Dose-dependent ROS ↓ Dose-dependent GSH ↓ ≤10 µg/mL, ↑ 100 µg/mL Slight ↑ peroxides	Slight ↓	Dose-dependent ↑	Dose-dependent ↓ ≤32 µg/mL, slight ↓ 100 µg/mL	↑ ≥3.2 µg/mL, reduces to baseline at 100 µg/mL	Slight G2/M-block	Effect similar at 24 h and 72 h	Early apoptosis	Effect more prominent at 24 h than 72 h
<i>M. oleifera</i>	HW	= (>100 µg/mL)	Slight ROS ↓, sharp increase at 100 µg/mL Dose-dependent GSH ↓ No peroxides	Dose-dependent ↓	No change	Dose-dependent ↓	Dose-dependent ↓	Slight G1-block	Effect present at 72 h	Slight early apoptosis and slight necrosis	Early apoptosis prominent at 24 h, while necrosis more prominent at 72 h

Plant	Extract	Hepatotoxic parameter assessed									
		Cell density (IC <sub>50</sub> )	Oxidative stress	$\Delta\Psi_m$	Fatty acid content	Caspase-3/7 activity	ATP levels	Cellular kinetics		Mode of cell death	
								Effect	Time-dependence	Effect	Time-dependence
<i>M. oleifera</i>	MeOH	Slight ↑ (>100 µg/mL)	Dose-dependent ROS ↓ Dose-dependent GSH ↓ Slight peroxide ↑	Slight ↓	Slight ↓, plateaus at ≥3.2 µg/mL	Slight fluctuations	No change	Slight G1-block, which later shifts to a slight G2/M-block	G1-block at 24 h, which becomes G2/M-block at 72 h	Slight early apoptosis and necrosis	Effect more prominent at 24 h than 72 h
<i>S. aculeastrum</i>	HW	Dose-dependent, sharp ↓ (67.83 µg/mL)	Dose-dependent ROS ↓ GSH ↑ at 100 µg/mL No peroxides	Dose-dependent ↓	Sharp dose-dependent ↑ ≥10 µg/mL	Dose-dependent ↑ ≥32 µg/mL	Slight ↑ at 10 µg/mL, ↓ ≥32 µg/mL	S-block with increased DNA fragmentation	S-block present at 24 h, but more prominent at 72 h with DNA fragmentation	Necrosis (primary), slight apoptosis (secondary)	Necrosis similar at 24 and 72 h, apoptosis more prominent at 72 h
	MeOH	Dose-dependent, sharp ↓, reaches plateau (17.91 µg/mL)	ROS ↓ GSH ↓ at 32 µg/mL, ↑ at 100 µg/mL Slight peroxide ↑	Dose-dependent ↓	Sharp dose-dependent ↑ ≥32 µg/mL	↑ 10 µg/mL, sharp ↓ ≥32 µg/mL	Sharp decrease ≥32 µg/mL	G2/M-block, which becomes slight S-block with DNA fragmentation	G2/M-block at 24 h, which becomes S-block at 72 h with DNA fragmentation	Necrosis (primary), slight apoptosis (secondary)	Apoptosis more prominent at 24 h than 72 h, and necrosis more prominent at 72 h
<i>T. elegans</i>	HW	Dose-dependent ↓ (>100 µg/mL)	ROS ↓ ≤32 mg/mL, slight ↓ at 100 µg/mL ↑ at 100 µg/mL ↑ peroxides ≤100 µg/mL	Slight dose-dependent ↓	Dose-dependent ↑	Dose-dependent ↑ ≥10 µg/mL	↑ ≤32 µg/mL, ↓ at 100 µg/mL	G2/M-block with DNA fragmentation	Block more prominent at 24 h than 72 h, while DNA fragmentation occurs at 72 h	Necrosis (primary), slight early apoptosis (secondary)	Effect more prominent at 72 h than at 24 h
	MeOH	Dose-dependent ↓ (3.07 µg/mL)	Dose-dependent ROS ↑ ≤32 µg/mL, ↓ at 100 µg/mL Dose-dependent GSH ↑ ≥10 µg/mL Peroxide fluctuations	Dose-dependent ↓	Dose-dependent ≥1 µg/mL	Sharp dose-dependent ↑ ≥1 µg/mL	↑ at 3.2 µg/mL, sharp ↓ ≥10 µg/mL	G2/M-block with DNA fragmentation	Effect more prominent at 24 h than 72 h	Necrosis (primary), slight early apoptosis (secondary)	Effect more prominent at 72 h than at 24 h

Plant	Extract	Hepatotoxic parameter assessed									
		Cell density (IC <sub>50</sub> )	Oxidative stress	$\Delta\Psi_m$	Fatty acid content	Caspase-3/7 activity	ATP levels	Cellular kinetics		Mode of cell death	
								Effect	Time-dependence	Effect	Time-dependence
<i>T. sericea</i>	HW	Dose-dependent ↓ (>100 µg/mL)	Slight fluctuations in ROS No GSH change Slight peroxide fluctuations	Dose-dependent ↓	Slight dose-dependent ↑ ≥3.2 µg/mL	Slight ↓ at 100 µg/mL	Slight dose-dependent ↓ ≥32 µg/mL	Slight G1- and G2/M-block, which shifts to S-block	G1- and G2/M-block at 24 h, which becomes S-block at 72 h	Necrosis (primary), slight early apoptosis (secondary)	Early apoptosis more prominent at 72 h, while necrosis present at 24 h and 72 h
	MeOH	Dose-dependent ↓ (>100 µg/mL)	Dose-dependent ROS ↓ <10 µg/mL, reaches plateau Dose-dependent GSH ↓ Slight peroxide fluctuations	Dose-dependent ↓	No change	Dose-dependent ↓ ≥10 µg/mL, plateaus at 32 µg/mL	Dose-dependent ↓ ≥1 µg/mL	S-block with increased DNA fragmentation	S-block and DNA fragmentation present at 24 h, but more prominent at 72 h	Necrosis (primary), slight early apoptosis (secondary)	Early apoptosis more prominent at 72 h, while necrosis present at 24 h and 72 h
<i>Z. mucronata</i>	HW	Dose-dependent ↓ (>100 µg/mL)	Slight ROS ↓ No GSH change Slight peroxide fluctuations	Dose-dependent ↓	Slight ↑ at 100 µg/mL	↓ ≥10 µg/mL	Slight fluctuations	G1- (primary) and slight G2/M-block (secondary), which shifts to G1-block	G1- and G2/M-block at 24 h, which becomes G1-block at 72 h	Necrosis (primary), slight early apoptosis (secondary)	Effect similar at 24 h and 72 h
	MeOH	Dose-dependent ↓ (36.29 µg/mL)	Dose-dependent ROS ↓ No GSH change Slight peroxide fluctuations	Dose-dependent ↓	Sharp ↑ at 100 µg/mL	Dose-dependent ↓ ≥10 µg/mL	↑ ≤32 µg/mL, ↓ at 100 µg/mL	G1- (primary) and slight G2/M-block (secondary), which shifts to G1-block	Effect more prominent at 24 h than 72 h	Necrosis (primary), slight early apoptosis (secondary)	Effect similar at 24 h and 72 h

HW – hot water extract; MeOH – methanol extract.

Both extracts induced a mixture of cytostatic (Figure 29) and cytotoxic (Figure 30) effects, with the hot water extract being slightly more active towards the hepatocarcinoma cells. Necrotic cell death was evident as early as 24 h. Necrosis has been linked to deleterious effects on physiological systems due to widespread toxicity and downstream inflammatory responses.<sup>294</sup> These effects may result in inflammatory liver diseases and acute liver failure. Taking into consideration the fatty acid accumulation observed (Figures 27E and 28E), a risk of steatosis is also present.<sup>244</sup> Whether or not the steatosis is a side effect of or contributor to the necrotic cell death observed is unknown. Cytostatic effects were also identified, which appears to be mediated primarily through G2/M-arrest. The hot water extract reduced cell numbers in the G0/G1-phase as early as 24 h, which resulted in a systematic increase in the S- and G2/M-phases over the 72 h period. The methanol extract, however, merely increased G2/M-phase cells while reducing other phase cells. The hot water extract appears to induce a multi-potent blockade, resulting in slower cellular cycling and ultimate arrest in the G2/M-phase. The G2/M-phase cell blockade would suggest that cells were inhibited prior to the induction of mitosis, most likely due to the presence of damaged DNA that had been replicated during the S-phase. As the cell cycle is a tightly controlled system, several mechanisms may be at play in the induction of this arrest, such as DNA damage.<sup>330</sup>

Mitochondrial depolarisation was evident (Figures 27B and 28B), however, this did not result in the expected generation of ROS (Figures 27C and 28C). Depolarisation is often linked to increased ROS levels.<sup>247,277</sup> ROS levels remained stable after exposure to the hot water extract, and depleted significantly with methanol extract exposure. Although antioxidant activity was detected in the extracts, it is unlikely that this would have contributed to this depletory effect. Taking into account the attenuation of GSH (Figures 27D and 28D) levels and lack of ROS generation, it appears that oxidative stress was not involved. Phase II GSH conjugation, aimed at the removal of phytochemical components from the intracellular compartment for detoxification<sup>276</sup> may be the reason for GSH depletion. This reduction has been implicated in a number of hepatotoxic pathologies, and seems to favour necrotic cell death in hepatocytes rather than apoptotic pathways,<sup>281</sup> supporting the results of the present study. The slight increase in GSH concentrations at 100 µg/mL methanol extract exposure suggests an adaptive *de novo* response. GSH synthesis would be required to

accommodate higher levels of detoxification.<sup>282</sup> ROS has been implicated as a mediator of several physiological pathways,<sup>282</sup> the effect of which correlates with the concentration thereof.<sup>280</sup> ROS modulates the mitogen-activated protein kinase (MAPK) pathways, which in turn activates cell proliferation, differentiation, survival and apoptosis.<sup>280</sup> ROS depletion may have caused the observed cytostatic effects. Redox status is an important propagator of cellular cycling.<sup>282</sup> Compounding this, ATP loss is detrimental to proliferation<sup>332,333</sup> and has been linked to G2/M-phase arrest if unavailable.<sup>332</sup> Acute, potent opening of the MPTP has been shown to render the mitochondria unable to function,<sup>277</sup> and as such leads to inhibition of the respiratory chain, with depletion of ATP, induction of necrosis and reduced  $\beta$ -oxidation.<sup>250</sup> Inhibition of mitochondrial respiration in hepatocytes has been shown to activate adenosine monophosphate-activated kinase (AMPK) pathways, with subsequent inhibition of ATP-consuming pathways and induction of ATP-production pathways. This increases fatty acid accumulation, which under normal circumstances would be metabolised, but if mitochondrial  $\beta$ -oxidation is impaired it may cause steatosis.<sup>250</sup> Reduced  $\beta$ -oxidation as a consequence of mitochondrial toxicity<sup>244,276</sup> would explain the fatty acid accumulation observed. This accumulation could in turn have also contributed to ATP depletion (Figures 27G and 28G). Hepatocytes exposed to fatty acids have been shown to induce ATP leakage.<sup>241</sup> As ROS generation did not occur, it is not surprising that lipid peroxidation was not detected. Although ATP levels were decreased, caspase-3/7 activation was still observed (Figures 27H and 28H), especially after exposure to the methanol extract. As apoptosis is an energy-dependent process,<sup>247</sup> one would assume that caspases would not be activated. Taking into consideration the mitochondrial toxicity and ATP depletion, it is unlikely that caspase-3 activation would have occurred via the intrinsic apoptotic pathway. This pathway requires ATP-mediated apoptosome activation,<sup>247</sup> thus it is rather suggested that the extrinsic pathway was involved. The extrinsic apoptotic pathway takes place via activation of death receptors on the cellular surface, with subsequent activation of caspase-8. Caspase-8 functions as an initiator caspase, and may promote caspase-3 activation either directly or through secondary mediators such as Bid cleavage or ceramide production.<sup>273,300</sup> Ceramide, which is produced from fatty acids,<sup>284</sup> has been linked to necrosis should the apoptotic pathway be insufficiently activated, as well as mitochondrial dysfunction and hindered ATP synthesis.<sup>334</sup> Non-selective release of soluble intermembrane proteins from the mitochondrial space, such as apoptosis-

inducing factor (AIF),<sup>273</sup> would contribute to cell death. As AIF does not require ATP to elicit DNA fragmentation,<sup>273</sup> it would explain the DNA fragmentation observed in the sub-G1-phase in the absence of apoptotic cell death. It is thus proposed that although the extrinsic apoptotic pathway was activated, necrosis was preferred due to compounded mitochondrial dysfunction and impaired energetics. The transition of apoptotic to necrotic cell death during ATP deficiency is described in literature.<sup>281</sup>

As stated earlier, the Apocynaceae family contains potent cardiac glycosides,<sup>99</sup> thus it was suspected that high cytotoxicity would be present in plants from this family. The most likely toxic phytochemicals contributing to the effects seen are ouabain and acovenoside A.<sup>57,102</sup> As ouabain is a hydrophilic molecule due to hydroxyl groups,<sup>102</sup> it is likely to be better extracted in aqueous extracts, such as the hot water extract. This would explain the greater cytotoxicity observed for the hot water extract, though the combined effect of the phytochemical matrix cannot be excluded. Ouabain has been shown to decrease the viability of HepG2 cells<sup>335-337</sup> through, amongst others, down-regulation of MAPK1.<sup>336</sup> This effect is more pronounced under glucose deprivation.<sup>337</sup> Cell death has been shown to vary amongst cell type and concentration ranges, inducing both apoptosis,<sup>335</sup> necrosis<sup>338</sup> or a mixture thereof.<sup>339</sup> Ouabain has been described to increase ROS concentrations, cause intracellular calcium influx,<sup>340</sup> elevate caspase-3 activity and depolarise the mitochondrial membrane.<sup>339</sup> Calcium influx has been implicated in both necrosis and apoptosis.<sup>336,339</sup> Alternatively, nitric oxide is known to prevent mitochondrial ATP generation,<sup>341</sup> which may be increased due to ouabain's action as a nitric oxide synthase inducer.<sup>99</sup> This may further contribute to its deleterious effects on bioenergetic processes, leading to cell death and reduced fatty acid usage. The potential of phytochemicals to induce necrotic cell death, even in the presence of activated pro-apoptotic mediators is known. Antiproliferative effects have been attributed to ouabain exposure as well, primarily as arrest in the S-phase<sup>335,336</sup> or G0/G1-phase.<sup>338</sup> As a large depletion of ATP occurred, it is possible that the phytochemical mixture opted for blockade in a later phase. It has been reported that ouabain increases HepG2 mitochondrial DNA damage.<sup>342</sup> The latter may result in the reduced cycling and ultimate cessation at the G2/M-checkpoint for repair. Apart from cardiac glycosides, saponins were also identified during phytochemical screening. These compounds are well-known membrane

permeabilising agents, which would incur necrotic cell death due to rupturing of the cell membrane and leakage of intracellular components.<sup>51</sup>

#### 4.4.2. *Boophane disticha*

The methanol extract of *B. disticha* presented with greater cytotoxicity than the hot water extract. Ethanol extracts of the inner scales of the bulb have been shown to decrease ATP production in human neutrophils (most likely due to cytotoxic effects), while hot water extracts of the inner and outer scales, and the ethanol extract of the outer scales were inactive.<sup>45</sup> The latter study did not normalise ATP to the number of cells present, and thus it may account for the differences in findings between the latter and present study. Furthermore, as differentiation wasn't made between the scales of the bulbs, it is possible that this may explain the increased ATP observed (Figures 31G and 32G). The hot water and methanol extracts displayed varying cytotoxicity in SK-Br-3, MCF-7 and MDA-MB-231 cell lines ( $IC_{50}$ 's = 7.29  $\mu$ g/mL to 36.44  $\mu$ g/mL). Surprisingly, the hot water extract had greater cytotoxicity in the MCF-7 and SK-Br-3 cell lines (Appendix IV), indicating a potential for cell-specificity between the extracts. A methanol extract of the roots displayed similar cytotoxicity, with an  $IC_{50}$  of ~25.5  $\mu$ g/mL in the SH-SY5Y neuroblastoma cell line.<sup>90</sup> In an animal study an increase in liver weight of rats after acute treatment with a hydroethanolic extract of *B. disticha* bulbs was noted. This occurred in the absence of histological alterations, and was theorised to have been adaptive *de novo* synthesis of liver enzymes to counteract the burden of phytotoxins.<sup>343</sup>

Both crude extracts of *B. disticha* displayed a similar trend in hepatotoxicity, with the methanol extract being more active. Cytostatic events (Figure 33) were observed instead of cytotoxicity (Figure 34). This was evident by the reduction of cell density, with negligible decrease in cell viability. Although a slight decrease in cell viability occurred after 24 h, this did not persist or worsen, and was paralleled by a slight, but insignificant, increase in early apoptotic cells. Interestingly cellular kinetics was mostly unaltered, apart from a small increase in the amount of cells in the G2/M-phase. Taking into account the lack of cell death, reduction of cell viability and unperturbed cycling, it is suggested that a transition of proliferative cells to a quiescent G0-state likely took place. Since the propidium iodide stains DNA content, and both the G0- and G1-phase

is diploid,<sup>287</sup> differentiation between these phases will not occur. It is thus suggested that the cells were hidden in the G<sub>0</sub>-quiescent phase, and appeared as G<sub>1</sub>-phase cells due to method non-specificity. This assumption, however, needs to be ascertained using proliferative assays, such as a marker for proliferation (e.g. Ki-67).<sup>238</sup> If this holds true, cells are still metabolically active, though do not actively cycle,<sup>285</sup> and thus will give insight into the reduced cellular parameters. Diminished proliferation may lead to impaired hepatic regeneration and healing. Quiescence may have been induced through a downregulation of cyclin D, or induction of p27,<sup>333</sup> possibly as a consequence of MAPK-attenuation.<sup>280</sup>

Mechanistically, both extracts displayed a similar effect, and thus hepatotoxicity most likely follows the same modality. Weak mitochondrial depolarisation occurred (Figures 31B and 32B). This may indicate a gradual or low-level opening of the MPTP.<sup>247</sup> Low-level mitochondrial effects would explain the lack of ATP depletion, as functionality may still be largely unhindered. Interestingly enough, ATP levels increased at higher concentrations (which paralleled the reduction of cell density), suggesting a higher need for energetic systems, possibly as adaptation for the detoxification and efflux of phytotoxins. The methanol extract at 100 µg/mL displayed baseline ATP levels compared to the lower concentrations, which could relate to a high enough concentration to interfere with ATP production. ROS concentrations decreased (Figures 31C and 32C) in a similar fashion to *A. oppositifolia*, suggesting a loss of functionality of the signalling cascades.<sup>282</sup> As a state of oxidation is required for transition from the G<sub>1</sub>- to S-phase of the cell cycle,<sup>282</sup> this may be a component of the antiproliferative effect observed. Hot water and methanol extracts have been shown to inhibit superoxide production in neutrophils,<sup>45</sup> which gives credence to the results obtained. The concurrent reduction in GSH levels (Figures 31D and 32D) is most likely due to detoxification of phytotoxins<sup>245</sup> rather than an antioxidant effect. The increase of GSH at 100 µg/mL methanol extract exposure may be a similar adaptive *de novo* synthesis response.<sup>282</sup> Although mitochondrial functionality did not appear perturbed, fatty acid systems were evidently interrupted, as a dose-dependent increase was observed (Figures 31E and 32E). This may be through the inhibition of enzymes involved in β-oxidation (such as acyl-CoA synthases), cofactor depletion,<sup>250,274</sup> reduced fatty acid efflux or promotion of fatty acid synthesis/uptake.<sup>250</sup> Lipid peroxidation was not present (Figures 31F and 32F), which is conceivable due to the

lack of ROS generation. However, a slight increasing trend was seen for the methanol extract, but this was not significant. Both extracts reduced caspase-3/7 activity (Figures 31H and 32H), proposing an anti-apoptotic effect. However, a small increase in early apoptotic cells was observed, indicating that apoptotic processes may have been induced via caspase-independent means, such as non-caspase proteases.<sup>344</sup> At 100 µg/mL of both extracts, caspase-3/7 activity returned to approximate baseline levels, suggesting a possible switch to caspase-mediated apoptotic cell death at high enough concentrations.

As with *C. bulbispermum* and *S. puniceus*, *B. disticha* belongs to the Amaryllidaceae family, and thus certain isoquinoline-alkaloids are suspected to be responsible for the cytotoxic effects that were observed. However, alkaloids were only identified in the methanol extract, thus some other common phytochemical between the two extracts most probably elicited the antiproliferative effects seen. Anthrones and saponins have both been shown to decrease cell growth. Derivatives of anthralin, an antiproliferative anthrone,<sup>345,346</sup> have been reported to display growth inhibitory effects in the absence of cytotoxicity.<sup>346</sup> This most probably is mediated through DNA damage that prevents proper replication of cells.<sup>345</sup> Saponins have been shown to reduce proliferation in the HepG2 cell line, although pro-apoptotic activity was reported.<sup>347–349</sup> Due to the low saponin content, which was nearly undetected in the methanol extract, anthrones are more likely responsible for the effects observed. It is suggested that certain phytochemical(s) may have induced cell cycle exiting into the quiescent state through cell cycle arrest. Furthermore, this activity occurs devoid of induction of significant levels of cell death at the IC<sub>50</sub>. It has been suggested that the alkaloids buphanadrine,<sup>217</sup> buphanamine and buphansine<sup>212</sup> are not highly cytotoxic. The latter two have only been assessed up to 10 µM, but it is theorised that the β-ethano bridge contributes to its inactivity.<sup>212</sup> 6-Hydroxycrinamine has been shown to induce cytotoxicity in the SH-SY5Y neuroblastoma cell line (IC<sub>50</sub> ~58.1 µM), existing as the A-form in an epimeric ratio of 3:1.<sup>89</sup> It is present at very low concentrations though, as it is estimated to constitute 2.5%<sup>89</sup> of the ~0.31% alkaloidal fraction of the bulb.<sup>87</sup> This would render 6-hydroxycrinamine at possibly sub-toxic levels, though one cannot be sure if cell-specificity or matrix effects might not contribute even at a low concentration. Distichamine<sup>217</sup> and lycorine<sup>211–215</sup> are likely contributors to the cytotoxicity seen in the methanol extract. As described in Chapter 3, lycorine acts as both an

antiproliferative<sup>212–214</sup> and pro-apoptotic agent.<sup>211</sup> Furthermore, distichamine has also been shown to exert strong antiproliferative effects in the low micromolar range.<sup>217</sup> This may explain the slightly higher antiproliferative effect displayed by the methanol extract, but ultimately it appears as if an unidentified agent is responsible.

#### 4.4.3. *Moringa oleifera*

The crude extracts did not display a reduction of cell density, and thus were considered as non-cytotoxic in this model. Literature, although scarce, appears to support the low cytotoxicity of leaf extracts. Both an aqueous (2 µg protein) and hydroethanolic (150 µg/mL) extract resulted in low cytotoxicity, with only 21.1% and 27.9% cell death, respectively.<sup>350</sup> A methanol extract displayed no cytotoxicity, while an aqueous extract displayed an IC<sub>50</sub> of 6 mg/mL (wet weight).<sup>351</sup> Extracts were found to not display cytotoxicity in a panel of cancerous cell lines during in-house experimentation (Appendix IV). Furthermore, leaf extracts were reported to possess low cytotoxicity in non-cancerous cells, including Vero green monkey kidney cells,<sup>352</sup> primary lymphocytes<sup>353</sup> and peripheral mononuclear blood cells.<sup>354</sup> One study contradicted the safety above, reporting an IC<sub>50</sub> of 3.89 µg/mL and 6.20 µg/mL for a hot water and ethanol extract of the leaves.<sup>355</sup> This effect may be highly dependent on the geographical variation of the plant extracts. Data from animal studies support non-toxicity in acute<sup>356–360</sup> and chronic<sup>305,359,360</sup> rat and murine models for leaf extracts. Histopathologically, the liver appeared unaffected,<sup>305</sup> apart from slight congestion of hepatocytes which was deemed non-toxic.<sup>305</sup> Thus extracts are considered low risk for the induction of cytotoxic responses.

Both crude extracts reduced cell viability slightly (~10%) after 24 h incubation at 100 µg/mL (Figure 38). Cell death occurred via a mixture of apoptotic and necrotic cell death for the hot water extract, while the methanol extract appeared to predominantly induce necrosis. As cytotoxicity did not increase with time, low cytotoxicity appears to be the norm. Pro-apoptotic activity has been described for an aqueous extract, though this was only present at high concentrations.<sup>361</sup> Furthermore, cellular kinetics were largely unaltered (Figure 37), with slightly increased G<sub>0</sub>/G<sub>1</sub>- and G<sub>2</sub>/M-phases occurring over 72 h for the hot water and methanol extracts, respectively. Although no reduction in cell density was observed (Figures 35A and 36A), cell death was evident.

This may have been undetected with the SRB assay, but observed due to the higher sensitivity of flow cytometric assays. A hydroethanolic extract was found to arrest cells in the G0/G1 phase,<sup>362</sup> similar to what was observed in the present study. However, negligible apoptotic activity was described.<sup>362</sup> It would appear as if activity is related to cell type and collection parameters, though most support non-toxic effects.

Both extracts displayed dose-dependent mitochondrial depolarisation (Figures 35B and 36B), though this did not appear to translate to cytotoxicity at 72 h (apart from the slight reduction in cell viability observed at 100 µg/mL). These effects appear to suggest a potential for later cytotoxicity should exposure remain constant. Alternatively, the depolarisation noted may rather indicate an increase in mitochondrial respiration,<sup>272</sup> rather than cytotoxicity. This in turn would explain the decrease in fatty acid levels (Figures 35E and 36E). An increase in respiration would result in higher  $\beta$ -oxidation for bioenergetics purposes.<sup>247,274,275</sup> Important to note though is that the hot water extract resulted in greater depolarisation, however with less fatty acid decline than the methanol extract. The high levels of depolarisation may cause higher respiration, and some dysfunction. A more subtle depolarisation may describe why the methanol extract presented with higher fatty acid reduction, as functionality would not have been perturbed. Apart from mitochondrial activity, this reduction may also be due to increased fatty acid efflux, or decreased fatty acid synthesis.<sup>250,274</sup> ATP levels would be expected to increase with cellular respiration, though this effect was not observed. The depletory effect of the hot water extract may indicate low level cytotoxicity that occurs at longer exposure times, and thus may indicate a risk of chronic toxicity. The hot water extract induced significant generation of ROS at 100 µg/mL (Figure 35C), supported by the effects seen in the KB HeLa-contaminant carcinoma cell line treated with an aqueous leaf extract at  $\geq 50$  µg/mL.<sup>361</sup> In Chapter 2 it was shown that *M. oleifera* does contain antioxidant activity ascribed to its polyphenolic content. It has been reported that certain polyphenols can generate high levels of ROS in cancerous cell lines through pro-oxidant activity,<sup>52</sup> which may be attributed to the flavonoid content. Due to the low polyphenolic content, high concentrations may be required to elicit this, explaining the lack of activity at lower concentrations. Conversely, the methanol extract resulted in a dose-dependent decrease of intracellular ROS even at low concentrations (Figure 36C), which may indicate loss of functional signalling.<sup>282</sup> The latter did not appear to translate to any significant cellular detriment apart from the

highest concentration tested. This effect is likely a product of the differential phytochemical matrix between the two crude extracts. GSH concentrations displayed a slight trend to increase dose-dependently with hot water extract exposure, but remained stable with the methanol extract (Figures 35D and 36D). It is known that GSH increases in cells exposed to *M. oleifera* extracts,<sup>160</sup> which may once again be a *de novo* response.<sup>282</sup> Although no ROS were formed, lipid peroxidation appeared to increase slightly with methanol extract exposure, thus a different free radical source, such as reactive nitrogen species, may be responsible for this effect. Caspase-3/7 activity was reduced after hot water extract exposure, though remained stable when treated with the methanol extract (Figures 35H and 36H). Various potent protease inhibitors have been isolated from *M. oleifera*,<sup>155,156</sup> thus it is likely that these may exert an inhibitory activity on caspases. The decrease in ATP levels and caspase-3/7 activity seen with the hot water extract (Figure 35G,H) may support the slight necrotic effect noted at 100 µg/mL. Although this may support necrosis,<sup>281</sup> caspase-independent apoptosis cannot be ruled out.<sup>344</sup> The methanol extract however had stable ATP levels and caspase-3/7 activity (Figure 36G,H), thus membrane destabilisation may be responsible for the necrosis observed.<sup>51</sup>

Compounds such as niazirin and niazicin appear non-cytotoxic.<sup>363</sup> Trigonelline has displayed antiproliferative activity at low concentrations, incurring a G0/G1-arrest,<sup>364</sup> as observed in the present study. Polyphenols, such as kaempferol, quercetin and gallic acid, may further contribute to the antiproliferative effects observed.<sup>365,366</sup> Trigonelline does not alter fatty acid uptake in Caco-2 cells,<sup>367</sup> however it does reduce lipid accumulation and inhibits fatty acid synthase in 3T3-L1 cells.<sup>368</sup> Effects may thus be a consequence of inhibition of  $\beta$ -oxidation enzymes or reduced lipid metabolism.<sup>250,274</sup> Furthermore, trigonelline, and to a larger extent its thermal degradation product N-methylpyridinium, promotes cellular respiration and fatty acid usage in HepG2 cells, most likely due to depolarisation of the mitochondria.<sup>369</sup> Boiling results in thermal decomposition of trigonelline to N-methylpyridinium, therefore it is likely that the latter would be present in the hot water extract, giving credence to the mitochondrial effects and reduced fatty acid concentrations observed. This would also be likely for the methanol extract, as rotary evaporation during extract concentration occurs under reduced pressure and heating. Although not tested *in vitro*, moringine has also been shown to reduce fatty acid concentrations in rats.<sup>370</sup>

#### 4.4.4. *Solanum aculeastrum*

Both solvent extracts displayed cytotoxic activity, though the methanol extract was much more potent. A narrow cytotoxicity index was observed, which had no effect at low concentrations albeit a sudden large decrease in cell density at higher concentrations (Figures 39A and 40A). A similar narrow cytotoxicity index was induced by aqueous and methanol extracts in HeLa cervical, MCF-7 breast and HT29 colonic carcinoma cells.<sup>65</sup> Furthermore, the cytotoxicity of the methanol extract at 32 and 100 µg/mL was similar indicating a plateau of ~85% cell death. This could indicate a ceiling effect of cytotoxicity or an induction of cytostasis. This plateau was also described by Koduru *et al.*<sup>65</sup> The IC<sub>50</sub>'s obtained for the methanol extract in the HepG2 and Caco-2 cell lines were similar to those found for MCF7 and HT29 cell lines.<sup>65</sup> Comparable IC<sub>50</sub>'s were observed in the SK-Br-3 and MCF-7 cell lines, with more prominent cytotoxicity present with methanol extract exposure. Greater cytotoxicity was apparent in the MDA-MB-231 (1.3 – 2.0-fold increase) cell line, with the methanol extract once again being more active (Appendix IV). An alkaloidal-enriched fraction of *S. lycocarpum*,<sup>371</sup> and a polyphenolic-enriched fraction of *S. nigrum*<sup>372</sup> were found to display prominent cytotoxicity in various cell lines, with potent effects in HepG2 cells.<sup>371</sup> From animal studies, a lack of severe hepatotoxic effects with acute treatment, though sub-acute toxicity dosing increased body weight, with decreased liver size have been described.<sup>373</sup>

Both extracts displayed cytostatic (Figure 41) and cytotoxic (Figure 42) activity as early as 24 h, though interestingly enough the effect of the hot water extract was much more detrimental at the IC<sub>50</sub> than the methanol extract, regardless of whether the concentration was higher. Although a maximum of 50% cell death was expected, 75% of cells were necrotic after hot water extract exposure, compared to 20% with the methanol extract. Combined with the reduction in cell density, this could indicate that membrane integrity was compromised without necessarily resulting in cellular detachment from the culture surface. Extracts have been shown to induce haemolytic activity in erythrocytes, indicating membrane rupturing,<sup>60</sup> lending support to the necrosis observed. Cell death was seen in conjunction with reduced cellular cycling, although this was dependent on extract-type. While the hot water extract displayed persistent S-phase arrest as early as 24 h, the methanol extract progressed from G2/M- to S-phase arrest from 24 h to 72 h, respectively. The latter may be in response

to a more gradual cell cycle blockade, hence the change as time progresses. Improper DNA replication or chromosomal replication is considered a likely contributor to the blockage seen.<sup>290</sup> Both extracts increased the sub-G1-phase, suggesting DNA fragmentation. Based on the large spread of fluorescence observed in the sub-G1-phase, a more random degradation of DNA due to necrosis is supported, opposed to systematic cleavage. Literature regarding the mechanism of cell death after exposure to *S. aculeastrum* is unfortunately lacking, though a polyphenolic extract of *S. nigrum* has been shown to reduce cellular cycling through G2/M-arrest.<sup>372</sup>

Mechanistically a similar approach was followed by both crude extracts to induce hepatotoxicity, although effects were much more prominent with the methanol extract. A sudden drop in  $\Delta\Psi_m$  occurred parallel to the reduction in cell density (Figures 39B and 40B). As with *A. oppositifolia*, this is most likely due to a severe opening of the MPTP, with subsequent cessation of the respiratory chain, inability to produce ATP and leakage of mitochondrial mediators of cell death.<sup>250</sup> ROS levels decreased (Figures 39C and 40C), contrary to what would be expected,<sup>282</sup> and was completely abolished at 100  $\mu\text{g/mL}$  methanol extract exposure. This would most likely explain the detrimental effects observed, as cellular signalling pathways would be rendered dysfunctional, leading to decreased proliferation and cell survival modalities.<sup>282</sup> The hot water extract increased GSH significantly at concentrations paralleling cytotoxicity, suggesting increased *de novo* synthesis (Figures 39D and 40D). This is expected in an effort to combat cellular strain and aid detoxification.<sup>282</sup> The methanol extract had a similar effect at 100  $\mu\text{g/mL}$ , though a sharp drop occurred at 32  $\mu\text{g/mL}$ . The fatty acid accumulation observed (Figures 39E and 40E) is most likely due to the inability of mitochondria to properly catabolise it through  $\beta$ -oxidation.<sup>250</sup> Both extracts had a slight tendency to increase lipid peroxidation (Figures 39F and 40F), though this did not correlate to the reduced levels of ROS, suggesting another free radical source as oxidiser. Lipid peroxidation products, such as 4-HNE, down-regulate cell cycle accelerators.<sup>283</sup> High concentrations of 4-HNE have been shown to activate necrotic cell death as opposed to apoptosis.<sup>283</sup> Caspase-3/7 activity increased dose-dependently with hot water extract exposure, though this did not result in the expected apoptotic cell death (Figure 39H). It is suggested that the extrinsic apoptotic pathway was activated through modulation of death receptors,<sup>273,300</sup> which would not necessarily require ATP for caspase-3 activation. A lack of ATP would, however, shift

cell death to necrotic means<sup>281</sup> and debilitate proper cellular cycling.<sup>332,333</sup> As with *A. oppositifolia*, the involvement of ceramide cannot be excluded in this pathway.<sup>273,300,334</sup> The methanol extract resulted in a slight increase of caspase-3/7 activity (Figure 40H), which may have been an induction of pro-apoptotic activity, though this was abolished at higher concentrations. This would suggest that a threshold effect could be present, as was found for the narrow cytotoxicity. Once a certain concentration is reached a 'point of no return' is seen where necrotic activity dominates. The complete abolishment of caspase-3/7 could be due to a complete bypassing of the caspase systems and incurring full rupturing of the plasma membrane.

The Solanaceae family is known to contain steroidal glucosaponins and glucoalkaloids,<sup>173</sup> which are usually present as glycosides<sup>177</sup> and most likely responsible for the effects observed. Solasonine,<sup>374</sup> solasodine<sup>374,375</sup> and solamargine<sup>375,376</sup> induce potent cytotoxicity in various cell lines. Solamargine and solasonine have been reported to display activity towards the HepG2<sup>371,376</sup> and Hep3B hepatoma cell lines,<sup>375</sup> which correlates to the activity found in the present study. Important to note though is that solamargine induced lower cytotoxicity in primary liver cells than cancerous counterparts,<sup>376</sup> suggesting a potential for lower cytotoxicity than expected due to the cancerous nature of the HepG2 cell line. Solasonine appears to be more active than solasodine, indicating the importance of the sugar moiety in inducing detrimental effects.<sup>374</sup> Solamargine has been shown to increase Fas expression on cells, which allows for greater activation of the extrinsic apoptotic pathway,<sup>377</sup> lending some credence to the pathway suggested. It is possible that death receptor expression was increased on HepG2 cells, allowing for activation of the extrinsic pathway. However, due to severe cytotoxic advances, such as mitochondrial rupturing or membrane destabilisation, necrosis was opted for. This may have occurred post-induction of cell cycle arrest, which has also been ascribed to solamargine in hepatoma cell lines.<sup>378</sup> Whereas solamargine induced apoptotic cell death, solasodine did not, which can be ascribed to the former's rhamnose moiety.<sup>375</sup> However, cytotoxicity, DNA fragmentation (possible apoptosis indicator) and G0/G1-arrest has been attributed to solasodine as well,<sup>379</sup> suggesting a cell-type specific effect. Solasodine and tomatodine have been found to induce moderate cytotoxicity in the MCF-7, HT29 and HeLa cell lines at concentrations  $\geq 100$   $\mu\text{M}$ . Viability was decreased due to a G0/G1-phase arrest, which ultimately led to slight necrosis, but no

apoptosis. Research has shown that glycoalkaloids obtained from *Solanum* spp.<sup>176</sup> and saponins<sup>380</sup> promotes cell membrane disruption and necrotic cell death, which supports the necrosis observed. Although a different cell cycle blockade was observed in the present study, the mixture of steroidal alkaloids may cause preferential necrotic cell death as described by the latter study. Solanine was found to induce cytotoxicity in the HepG2 cell line at low concentrations<sup>381</sup> and induce mitochondrial depolarisation with concomitant increase of intracellular calcium concentrations and induction of apoptosis.<sup>277,382</sup> Furthermore, solanine decreased ATP in the SMMC7721 hepatoma cell line.<sup>383</sup> Solanine treatment reduced membrane integrity, allowing for lactate dehydrogenase leakage.<sup>384</sup> This may in turn also promote necrotic cell death, as shown with other glycoalkaloids as well.<sup>384</sup> Saponin content was much higher in the methanol extract, thus one would assume higher necrotic activity to be exerted by it. However, this was evident in the hot water extract. It is possible that the differential phytochemical matrix and their respective ratios may shift biological activity towards a different spectrum of effect. Various glycoalkaloids, such as solanine, possess long half-lives (21 – 44 h),<sup>384</sup> and may thus be bioaccumulated with chronic administration.

#### **4.4.5. *Tabernaemontana elegans***

The methanol crude extract was found to display greater reduction in cell density at a very low concentration, indicating a high potential for cytotoxic advances. The hot water extract on the other hand displayed low cytotoxicity (Figures 43A and 44A), which is supported by previous findings of aqueous extracts<sup>61</sup> (Appendix IV). Alcohol extracts have been found to display potent cytotoxicity with IC<sub>50</sub>'s ranging from 0.35 µg/mL to 19.27 µg/mL<sup>106,387</sup> (Appendix IV). Cytotoxicity seemed to effect metabolic conversion and lysosomal integrity, which increased with alkaloid-enrichment.<sup>106</sup> These effects appear to be independent of cell type, thus non-selective killing seems possible. Research into the cytotoxicity of *T. elegans* remains scarce, however data is available on other *Tabernaemontana* spp. Mixed cytotoxicity profiles have been reported, but it appears that aqueous extracts have low activity,<sup>388,389</sup> while some organic extracts display greater potential for reducing cell growth or survival.<sup>388,390,391</sup> Some organic extracts possess low cytotoxicity,<sup>392–395</sup> which appears to be dependent on cell type, species or extraction methodology.

Both crude extracts exerted a similar mechanism of hepatotoxicity, with a mixture of antiproliferative (Figure 45) and pro-necrotic activity (Figure 46). As with *S. aculeastrum*, the hot water extract exerted a more detrimental effect than the methanol extract. Cell death appeared to be time-dependent, only occurring after 72 h, while anti-proliferative effects were observed as early as 24 h. Both extracts induced an increase of cells in the G2/M-phase after 24 h, although this gradually decreased at 72 h. This would suggest that the initial arrest induced is not strongly maintained, and cellular cycling does tend to normalise after the effect has subsided. Furthermore, the hot water extract seemed to elicit DNA fragmentation, which would coincide with the random DNA degradation seen during necrosis. Following the reduced proliferation, cells undergo necrosis, most likely due to sufficient damage to cellular organelles and membranes. The methanol extract did display slight apoptotic activity, though this was subtle in comparison to the necrotic effect.

While the hot water extract only reduced cell density to a moderate degree at the highest concentration tested, this was achieved at low concentrations with exposure to the methanol extract. This was in combination with mitochondrial depolarisation, although the greatest effect was observed with the methanol extract (Figures 43B and 44AB). The hot water extract appeared to offer a low level of depolarisation. This suggests a gradual opening of the MPTP.<sup>276</sup> The methanol extract depolarised the mitochondrial membrane to a much higher degree. Important to note is that a prominent reduction of cell density was already evident at 1 µg/mL, while mitochondrial effects only occurred at higher concentrations. This suggests that the effects elicited by the methanol extract may be independent of mitochondrial dysfunction. The hot water extract decreased ROS levels initially, but as the concentration increased, ROS levels returned to baseline (Figure 43C). This effect was observed in the absence of mitochondrial depolarisation, thus the reason for this effect is unknown. Although antioxidant activity was present, it would require a much higher concentration to elicit such a ROS-depletory effect. The return to baseline may suggest that the hot water extract started increasing ROS levels >100 µg/mL. Worryingly though is that low levels of lipid peroxidation occurred at 1 µg/mL (Figure 43F), even though this steadily decreased as the concentration increased. Another free radical source may thus be used to oxidise lipids. The methanol extract induced a dose-dependent increase in ROS levels, with concurrent slight lipid peroxidation (Figure 44C,F), as expected from

mitochondrial depolarisation.<sup>250</sup> Both crude extracts increased GSH levels (Figures 43D and 44D), though this effect was more prominent with the methanol extract. The hot water extract only increased GSH levels at 100 µg/mL, while the methanol extract did so in a dose-dependent fashion. Whether or not this is an adaptive *de novo* synthesis to counteract high levels of detoxification is unknown. However, due to the effect seen it is suggested that GSH synthesis pathways remain unperturbed.<sup>282</sup> The hot water extract decreased fatty acid concentrations to below baseline at low concentrations (Figure 43E), which may suggest an increased usage of fatty acids to assist in the prevention of cytotoxicity through hormetic means.<sup>250</sup> This is supported by the increase in ATP levels at lower concentrations (Figure 43G), which is a consequence of  $\beta$ -oxidation. Fatty acid levels steadily increased as cytotoxicity was observed. The latter may have occurred due to the subsequent mitochondrial effects observed, shifting to fatty acid accumulation due to disruption of  $\beta$ -oxidation or altered synthesis/catabolism pathways.<sup>250</sup> The methanol extract's increase in fatty acid accumulation occurred from 1 µg/mL (Figure 44E), indicating that  $\beta$ -oxidation or fatty acid synthesis pathways are altered<sup>250</sup> at a low concentration, and thus steatotic changes may occur early on in dosing. While ATP levels were initially increased, possibly through usage of excess fatty acids, this declined as cytotoxicity increased (Figure 44G). Due to the large depolarisation observed, it is likely that disruption of mitochondrial respiration occurred,<sup>247</sup> inhibiting ATP synthase and ultimately leading to reduced bioenergetic pathways.<sup>250</sup> Caspase-3/7 activation was observed for both extracts (Figures 43H and 44H), with an immense increase evident by the methanol extract. Due to the increased levels of ATP and mitochondrial depolarisation observed, it is likely that the intrinsic apoptotic pathway<sup>299</sup> could have been followed, though the involvement of the extrinsic pathway cannot be excluded. Although the methanol extract displayed a subtle increase in apoptosis, both extracts primarily induced necrotic cell death. Although caspase activation may have occurred, an overwhelming pro-necrotic effect may have allowed for cell death to rather be followed.

The indole alkaloids have been described as the bioactive constituents of *T. elegans*, and thus focus has been placed on them. The effects of these alkaloids have been assessed on various cell lines, and these appear to be dependent on cell line origin (Table 29). Apparacine,<sup>396</sup> dregamine,<sup>108,110,396-399</sup> 16-epidregamine,<sup>110</sup> tabernaemontanine,<sup>108,110,397-399</sup> and tubotaiwine<sup>396</sup> do not appear to be highly

**Table 29:** Summary of the effects of indole/bisindole alkaloids that have been isolated from *T. elegans* on cellular cultures.

Indole/Bisindole alkaloid	Cell line	Assay	Time	IC <sub>50</sub> (µM)	Additional comments	References
Alosmontamine A	HL-60 leukaemia	N/S	N/S	31.7		109
Apparacine	HepG2 hepatocarcinoma	MTT	24 h	41	-	404
	P-338 murine leukaemia	MTT / SRB	N/S	N/D	Inactive	396
	A-549 lung carcinoma					
Coronaridine	HeLa cervical carcinoma	MTT	48 h	146.32	-	405
	B-16 murine skin cells			<125		
	Hep-2 laryngeal carcinoma			54.47	Apoptosis and DNA damage. No membrane damage	
	3T3 murine fibroblasts			89.28		
	KB/S vincristine-sensitive epidermoid carcinoma	72 h	11.5	-	402	
	KB/VJ300 vincristine-resistant epidermoid carcinoma		2.6			
	A2780 ovarian carcinoma	N/S	N/S	9.9		401
Dregamine	HCT116 colon carcinoma	MTS	72 h	N/D	Low levels of apoptosis, caspase-3/7 activation	399
Dregamine	HepG2 hepatocarcinoma	MTS	72 h	N/D	Low levels of apoptosis, caspase-3/7 activation	399
	KB/S vincristine-sensitive epidermoid carcinoma	MTT		>25	-	398
Dregamine	KB/VJ300 vincristine-resistant epidermoid carcinoma	MTT	72 h	>25	-	398
	HCT116 colon carcinoma	MTS	48 h	>50		110
	MRC-5 lung cells and L-6 myoblasts	MTT	72 h	N/D	Inactive	397



Indole/Bisindole alkaloid	Cell line	Assay	Time	IC <sub>50</sub> (µM)	Additional comments	References
Dregamine	HuH-7 hepatoma cells	Trypan blue	24 h	N/D	~2.7-fold increased cell death through apoptosis (no caspase-3)	108
	P-338 murine leukaemia	MTT / SRB	N/S		Inactive	396
	A-549 lung carcinoma					
16-Epidregamine	HCT116 colon carcinoma	MTS	48 h	>50	-	110
Isositsirikine	BGM monkey kidney cells	MTT	24 h	28		406
	HepG2 hepatocarcinoma			34		
Isovoacangine	KB/S vincristine-sensitive epidermoid carcinoma		72 h	>25		402
	A2780 ovarian carcinoma	N/S	N/S	9.40	401	
Tabernaemontanine	HCT116 colon carcinoma	MTS	72 h	N/D	Low levels of apoptosis and caspase-3/7 activation	399
	HepG2 hepatocarcinoma					
	KB/S vincristine-sensitive epidermoid carcinoma	MTT		>25	-	398
Tabernaemontanine	KB/VJ300 vincristine-resistant epidermoid carcinoma	MTT	72 h	>25	-	398
	HCT116 colon carcinoma	MTS	48 h	>50		108
	MRC-5 lung cells and L-6 myoblasts	MTT	72 h	5.20-8.40		397
Tabernaemontanine	HuH-7 hepatoma cells	Trypan blue	24 h	N/D	~2-fold increased cell death through apoptosis (caspase-3 activated)	108
Tabernaelegantine B	HCT116 colon carcinoma	MTS	48 h	Between 0.5 – 1	Pro-apoptotic	110
Tabernaelegantine C				Between 20 – 50	Pro-apoptotic	
Tabernine A	PAR-L5178 parenteral murine lymphoma	MTT	72 h	45.90	-	108



Indole/Bisindole alkaloid	Cell line	Assay	Time	IC <sub>50</sub> (µM)	Additional comments	References
Tabernine A	MDR-L5178 multidrug resistant murine lymphoma	MTT	72 h	37.50	-	
	HuH-7 hepatoma cells	Trypan blue	24 h	N/D	~3.2-fold increased cell death through necrosis (no caspase-3)	
Tabernine B	PAR-L5178 parenteral murine lymphoma	MTT	72 h	46.60	-	108
	MDR-L5178 multidrug resistant murine lymphoma			39.70		
	HuH-7 hepatoma cells	Trypan blue	24 h	N/D	~3.2-fold increased cell death through necrosis (no caspase-3)	
Tabernine C	PAR-L5178 parenteral murine lymphoma	MTT	72 h	70.60	-	
	MDR-L5178 multidrug resistant murine lymphoma			51.50		
Tabernine C	HuH-7 hepatoma cells	Trypan blue	24 h	N/D	~2.6-fold increased cell death through apoptosis (no caspase-3)	108
Tubotaiwine	P-338 murine leukaemia	MTT / SRB	N/S	N/D	Inactive	396
	A-549 lung carcinoma					
Voacangine	HepG2 hepatocarcinoma	MTT	72 h	10	-	403
	A375 melanoma			14		
	MDA-MB-231 breast carcinoma			8		
	SH-SY5Y neuroblastoma			7.60		
	CT26 murine colon carcinoma			11		
	HCT116 colon carcinoma	MTS	48 h	>50	108	
	HeLa cervical carcinoma	MTT	48 h	271.97	405	
	B-16 murine skin cells			439.16		



Indole/Bisindole alkaloid	Cell line	Assay	Time	IC <sub>50</sub> (µM)	Additional comments	References
Voacangine	Hep-2 laryngeal carcinoma	MTT	48 h	159.33	-	405
	3T3 murine fibroblasts			104.16		
	KB/S vincristine-sensitive epidermoid carcinoma		72 h	>25		
	KB/VJ300 vincristine-resistant epidermoid carcinoma		72 h	>25		
	KB/VJ300 vincristine-resistant epidermoid carcinoma		72 h	>25		
	A2780 ovarian carcinoma	N/S	N/S	10.40		401
Vobasine	HepG2 hepatocarcinoma	MTT	72 h	19.30	-	403
	A375 melanoma			19.50		
	MDA-MB-231 breast carcinoma			25		
	SH-SY5Y neuroblastoma			19		
	CT26 murine colon carcinoma			20		
	KB/S vincristine-sensitive epidermoid carcinoma			>25		398
	KB/VJ300 vincristine-resistant epidermoid carcinoma			>25		
Vobasine	HCT116 colon carcinoma	MTS	48 h	>50	-	110
	HuH-7 hepatoma cells	Trypan blue	24 h	N/D	~2.2-fold increased cell death through apoptosis (caspase-3 activated)	108

MTS - 3-(4,5-dimethylthiazol-2-yl)-5-(3-carboxymethoxyphenyl)-2-(4-sulfophenyl)-2H-tetrazolium conversion assay; MTT - 3-(4,5-dimethylthiazol-2-yl)-2,5-diphenyltetrazolium bromide conversion assay; N/D – not determined; N/S – not stated; SRB – sulforhodamine B staining

cytotoxic, and thus are not likely the primary hepatotoxic contributors. Dregamine has been found to increase apoptotic cell death in hepatoma cell lines,<sup>108,399</sup> although

caspase-3/7 activation was not always a contributing factor.<sup>108</sup> Tabernaemontanine is known to induce low levels of apoptosis in hepatoma cell lines through the activation of caspase-3.<sup>108</sup> Moderate levels of activity have been described for alosmontamine A,<sup>109</sup> isositsirikine<sup>109</sup> and tabernines A-C.<sup>400</sup> Tabernine A and B have been reported to induce necrotic cell death, while tabernine C causes caspase-3-independent apoptosis.<sup>108</sup> The most likely candidates for cytotoxicity are coronaridine,<sup>401,402</sup> isovoacangine,<sup>401</sup> tabernaelegantine B-C,<sup>110</sup> voacangine<sup>401,403</sup> and vobasine.<sup>403</sup> The latter two have been shown to induce cytotoxicity in the HepG2 cell line,<sup>403</sup> although it has shown that the latter six compound's cytotoxicity is cell-type-dependent.<sup>108,110,402,405,407</sup> Literature is scarce with regards to their mechanistic activity, and thus no real inferences can be made to their involvement in mitochondrial toxicity. However, it is suggested that as these indole/bisindole alkaloids have presented with a mixture of necrotic and apoptotic activity. Their concomitant involvement may have activated the intrinsic apoptotic pathway, with membrane destabilisation resulting in a switch to necrotic cell death. Due to the appreciable levels of saponins identified in the extracts, it is a possibility that loss of plasma membrane integrity may have resulted in cytolysis.<sup>51</sup> Taking into account the low concentration of the methanol extract, it would explain the greater effect elicited by saponins in the hot water extract, as concentrations would be much more dilute.

#### **4.4.6. *Terminalia sericea***

Both crude extracts of *T. sericea* displayed low cytotoxic potential (Figures 47A and 48A), only inducing moderate activity at 100 µg/mL, with the methanol extract exhibiting slightly higher activity. This is supported in literature for various cell lines,<sup>127,314,408,409</sup> as well as in brine shrimp.<sup>313,410</sup> However, it appears as if cytotoxicity may be determined by cell type, as moderate<sup>314,409,411,412</sup> to high cytotoxicity<sup>314</sup> has also been reported. The majority of references support that higher cytotoxicity of organic extracts compared to aqueous or hot water extracts.

The crude extracts exhibited a similar cell death modality. The accumulation of cells in the S-phase after 72 h is suggestive of a slight antiproliferative effect (Figure 49), which appeared to slow proliferation of cells, leading to reduced growth. However, induction of cell death as early as 24 h after exposure appears to be the main

mechanism of hepatotoxicity (Figure 50). The hot water extract induced necrosis after 24 h, however, after 72 h an increase in early apoptotic cells was also evident. Although an initial rupturing of cells occurred, the mixed effect is most likely due to a delayed pro-apoptotic effect. Hepatic cell death frequently appears as a mixture of apoptotic and necrotic events.<sup>296</sup> The methanol extract induced necrosis within 24 h, which persisted over the 72 h period without apoptotic involvement. Literature is not available with regards to the antiproliferative, pro-apoptotic or pro-necrotic effects of *T. sericea* extracts except for standard cytotoxicity assays. An ethyl acetate has been shown to inhibit topoisomerase I.<sup>413</sup> Topoisomerase I poisons have been shown to reduce S-phase cycling to due to diminished DNA synthesis,<sup>414</sup> giving basis for the potential antiproliferative mechanism of *T. sericea*.

Mechanistically both crude extracts induced detrimental changes to cellular function, though oxidative status differed between them. Mitochondrial depolarisation was found for both extracts, with the methanol extract being more active (Figures 47B and 48B). The large effect observed here might indicate that high frequency opening of the MPTP had taken place,<sup>277</sup> resulting in ATP depletion and subsequent infliction of necrotic cell death.<sup>250</sup> Although the hot water extract had no prominent effect on oxidative homeostasis, the methanol extract decreased both ROS and GSH in a dose-dependent manner (Figures 47C,D,F and 48C,D,F). Phytotoxin-detoxification through GSH-conjugation is a likely explanation for the latter,<sup>245</sup> though the effect behind ROS depletion is unknown. It is possible that the high antioxidant activity displayed by the methanol extract may incur a detrimental effect, reducing baseline ROS levels and eliciting further functional impairment.<sup>250</sup> Mitochondrial depolarisation many times indicates a loss of functionality of the bioenergetics system, giving rise to reduced  $\beta$ -oxidation with subsequent fatty acid accumulation,<sup>250</sup> as observed. Due to lack of synthesis systems, ATP levels would not be maintained and subsequent loss would occur.<sup>250</sup> Although ROS levels were not increased, lipid peroxidation was slightly elevated, thus the involvement of a separate free radical source cannot be excluded. Caspase-3/7 activity was reduced (Figures 47H and 48H), suggesting an inhibition of the caspase-system. As ATP levels were reduced (Figures 47G and 48G), it gives credence to a lack of caspase-3/7 activation due to the need of energy in the intrinsic apoptotic pathway.<sup>299</sup> The apoptotic cell death observed for the hot water extract is thus likely caspase-independent, via non-caspase proteases.<sup>344</sup>

Phytochemicals (Table 30) such as  $\beta$ -sitosterol,<sup>121,415,416</sup> arjungenin,<sup>417–419</sup> epicatechin-catechin, epigallocatechin-gallocatechin<sup>121</sup> and sericic acid<sup>418</sup> do not offer much in terms of cytotoxic effects. Likely contributors include arjunic acid,<sup>417–420</sup> gallic acid<sup>419</sup> and lupeol.<sup>121,415,416,423–425</sup> Arjunic acid has been shown to inflict variable levels of cytotoxicity in several different cancer cell lines, including HepG2 cells.<sup>417–420</sup> However, contradictory evidence of non-cytotoxicity has been described as well in the latter.<sup>417–420</sup> Although contradictory evidence is present on the cytotoxicity of lupeol,<sup>416,422</sup> noteworthy activity has been described in literature. In hepatoma cells (including HepG2 cells) it was described that lupeol induced an S-phase block, and induced apoptosis through caspase-3.<sup>424</sup> A similar S-phase block was observed in the present study. Furthermore, it has been described that lupeol induces mitochondrial depolarisation in MCF-7 cells with concomitant induction of DNA damage.<sup>426</sup> Taking all this in account, it is possible that the combination of lupeol and arjunic acid may be incurring mitochondrial stress and inducing non-caspase dependent pathways involved with apoptosis and necrosis. Furthermore, fatty acid accumulation may be due to lupeol, which induced steatosis at concentrations as low as 1  $\mu$ M.<sup>427</sup>

**Table 30:** Summary of the effects of phytochemicals that have been isolated from *T. sericea* on cellular cultures.

Phytochemical	Cell line	Assay	Time	IC <sub>50</sub> ( $\mu$ M)	Additional comments	References
$\beta$ -Sitosterol	Vero kidney cells	N/S	N/S	197.72		121
	HEK293 human embryonic kidney cells	MTT	48 h	>300		416
	HepG2 hepatocarcinoma			>300		415
	Primary murine splenocytes		72 h	>100		
$\beta$ -Sitosterol-acetate	Vero kidney cells	N/S	N/S	482.25		121
Arjungenin	MDA-MB-231 breast carcinoma	MTT	72 h	>200	-	418
	PC3 prostatic carcinoma			>200		
	HCT116 colon carcinoma			>200		
	T98G glioblastoma			>200		
	KB Hela contaminant cells		48 h	>198		417
	PA-1 ovarian carcinoma			79.26		



Phytochemical	Cell line	Assay	Time	IC <sub>50</sub> (µM)	Additional comments	References	
Arjungenin	HepG2 hepatocarcinoma	MTT	48 h	>198	-	417	
	WRL-68 Hela derivative			>198			
	HL-60 leukaemia		N/S	>100		419	
	A549 lung carcinoma			>100			
	AZ521 gastric carcinoma			>100			
	Sk-Br-3 breast carcinoma			>100			
Arjunic acid	MDA-MB-231 breast carcinoma		72 h	32.1		418	
	PC3 prostatic carcinoma			>200			
	HCT116 colon carcinoma			12.6			
	T98G glioblastoma			32.8			
	KB Hela contaminant cells		48 h	10.23		417	
	PA-1 ovarian carcinoma			15.35			
	HepG2 hepatocarcinoma			1.43			
	WRL-68 Hela derivative		48 h	15.35		417	
	HL-60 leukaemia		N/S	45.3		419	
	A549 lung carcinoma			>100			
	AZ521 gastric carcinoma		N/S	>100		419	
	Sk-Br-3 breast carcinoma			73.20			
	MCF-7 breast carcinoma	72 h	>100	421			
	NCI-H460 lung carcinoma		>100				
	HepG2 hepatocarcinoma		>100				
		A549 lung carcinoma		24 h	~50	Activation of c-Jun N-terminal kinase-dependent endoplasmic reticulum stress pathway with subsequent apoptotic induction	420



Phytochemical	Cell line	Assay	Time	IC <sub>50</sub> (µM)	Additional comments	References
Arjunic acid	NCI-H460 lung carcinoma	MTT	24 h	~50	Activation of c-Jun N-terminal kinase-dependent endoplasmic reticulum stress pathway with subsequent apoptotic induction	420
Epicatechin-catechin mixture	Vero kidney cells	N/S	N/S	689.00	-	121
				653.02		
Gallic acid	HL-60 leukaemia	MTT	N/S	13.9	-	419
	A549 lung carcinoma			>100		
	AZ521 gastric carcinoma			29.10		
	Sk-Br-3 breast carcinoma			54.70		
Lupeol	Vero kidney cells	N/S		705.14		121
Lupeol	CCRF-CEM lymphoblastic leukaemia	RZN	72 h	4.53	-	422
	CEM/ADR5000 adriomycin-resistant lymphoblastic leukaemia	RZN	72 h	78.93	-	422
	MDA-MB-231- <i>pcDNA</i> breast carcinoma			>82.75		
	MDA-MB-231- <i>BCRP</i> breast carcinoma			>82.75		
	HCT116 (p53+/+) colon carcinoma			>82.75		
	HCT116 (p53-/-) colon carcinoma			>82.75		
	U87MG glioblastoma			>82.75		
	UG87MG.Δ <i>EGFR</i> glioblastoma			>82.75		
	HepG2 hepatocarcinoma			56.89		
	AML12 murine hepatocytes			>82.75		
	HEK293 human embryonic kidney cells			MTT		



Phytochemical	Cell line	Assay	Time	IC50 (µM)	Additional comments	References
Lupeol	HepG2 hepatocarcinoma	MTT	48 h	289.40	-	416
	MCF-7 breast carcinoma		72 h	25.02		423
	HeLa cervical carcinoma			13.09		
	HT-29 colorectal carcinoma			>30		
	SMMC7721 hepatocarcinoma		48 h	45	S-phase cell cycle arrest and pro-apoptotic activity mediated by caspase-3	424
	HepG2 hepatocarcinoma			48.50		
	Primary murine splenocytes			45		
Sericic acid	MDA-MB-231 breast carcinoma	72 h	>200	-	418	
	PC3 prostatic carcinoma		>200			
	HCT116 colon carcinoma		>200			
	T98G glioblastoma		>200			

MTT - 3-(4,5-dimethylthiazol-2-yl)-2,5-diphenyltetrazolium bromide conversion assay; N/S – not stated; RZN – resazurin conversion assay

#### 4.4.7. *Ziziphus mucronata*

The methanol extract induced noteworthy cytotoxicity (Figure 52A), albeit not as high as some of the previously mentioned extracts. The higher cytotoxicity for the methanol extract compared to that reported in Chapter 3 may be as a result of phenotypic shift of the HepG2 cell line as the study progressed. The hot water extract was relatively absent of this, apart from the highest concentration tested (Figure 51A). Findings from other studies seem to concur that extracts do not present with high levels of cytotoxicity,<sup>199,429,430</sup> though methanol extracts do appear to offer more effects than aqueous extracts.<sup>199,430</sup> While leaves have been shown to promote genotoxicity upon metabolic activation,<sup>431</sup> cytotoxicity of the leaves<sup>201,432</sup> and roots appears to be poor.<sup>169</sup> Potent cytotoxic effects have been reported at 2.7 µg/mL in Vero cells exposed to bark extracts.<sup>433</sup> Other species of *Ziziphus*, such as *Z. spina-christi*<sup>434</sup> and *Z. multiflora*<sup>435</sup> have been shown to possess little cytotoxic activity, whereas *Z. jujube*<sup>436,437</sup> and *Z.*

*mauritiana*<sup>438</sup> induced cytotoxic effects at concentrations within the range of that observed in the present study. The cytotoxicity of the methanol extract seen in the present study may be a factor of geographical or seasonal variation.

With regards to the mode of cell death, a slight antiproliferative effect in the G1-phase appeared to be induced by both extracts (Figure 53). The largest contributor was necrotic cell death (Figure 54). This appeared within 24 h of incubation, and persisted up to 72 h of exposure. It thus seems likely that within 24 h a reduction of cellular cycling occurred, with subsequent dismantling of the cellular membrane and cytolysis ensues. Although literature pertaining to *Z. mucronata* could not be obtained, *Z. jujube*<sup>436,437</sup> and *Z. mauritiana*<sup>438</sup> extracts have been shown to induce cytotoxicity through induction of apoptosis.

Although both extracts induced cytotoxic responses, the hot water extract tended to have a less prominent effect than the methanol extract. Mitochondrial toxicity was apparent (Figures 51B and 52B), though ROS levels were not raised (Figures 51C and 52C), it did decrease in a dose-dependent manner. This was most prominent with the methanol extract, while little effect was shown with the hot water extract. This reduction was not coupled to alterations to GSH levels (Figures 51D and 52D). It is suggested that ROS-attenuation decreased cell functionality, and thus incurred a cytotoxic effect.<sup>282</sup> While the hot water extract increased fatty acid levels slightly, the methanol extract only had a notable effect at the highest concentration (Figures 51E and 52E). This increase was not paralleled by lipid peroxidation (Figures 51F and 52F). As mitochondrial toxicity was observed, one can thus assume that bioenergetics pathways were altered reducing ATP (Figures 51G and 52G) due to inhibition of  $\beta$ -oxidation.<sup>247,274,275</sup> Caspase-3/7 activity was decreased (Figures 51H and 52H), and even abolished at the highest concentration of the methanol extract, suggesting that the apoptotic activity observed was due to a non-caspase-dependent mechanism.<sup>344</sup>

Only one reference to the cytotoxic properties of the isolated constituents of *Z. mucronata* could be found, thus very little can be presumed with regards to possible contributors. Mucronine E and abyssenine A have been shown to induce cell death, primarily by non-necrotic means, though these results were only obtained at 1 mM.<sup>439</sup> Necrotic cell death may be due to saponins, which was found to be concentrated in the extracts (Chapter 2).

#### 4.5. Conclusion

The objectives of the chapter were met. An all-encompassing conclusion is provided in Chapter 6. This is one of the first studies to evaluate the hepatotoxic effects of various African herbal remedies that have yet to be classified as potential hepatotoxins. Of the seven plants selected for hepatotoxicity screening, all presented with associated risks, albeit to varying degrees. Of note is the prominent effects that hot water extracts had in inducing detrimental effects, even if a higher concentration was required compared to the respective methanol extracts. The methanol extract of *T. elegans* presented with the most potent hepatotoxic effects, while crude extracts of *M. oleifera* displayed low hepatotoxic potential. Regardless of this, the latter still altered mitochondrial functioning, which may be a sign of low-level cytotoxic activity, which may have downstream effects. The risk of mitochondrial toxicity, steatotic effects and necrotic cell death was evident with the majority of extracts, and thus further emphasis must be placed on determining their exact mechanisms and contributing phytochemicals. As necrotic cell death was the norm, emphasis should be placed on the detrimental outcomes thereof. Although the degree of systemic absorption was not determined in the present study, it would be best to be cautious in their use as pre-clinical results suggest a present danger in use.

## Chapter 5

### ***In vitro* effect of herbal remedies on absorption and metabolism**

#### **5.1. Literature review**

##### **5.1.1. Intestinal drug transport**

Absorption primarily takes place in the intestines of the gastrointestinal tract, more specifically via the microanatomical structures known as villi and microvilli which increase the absorptive surface area.<sup>440</sup> Intestinal transport is mediated through these structures, amongst others via transporters and enzymes.<sup>440</sup> Transportation from the apical surface of the intestines may occur via passive or active mechanisms. Efflux transporters may diminish absorption into the systemic circulation due to extrusion.<sup>440</sup> Compounds with a high cellular permeability are presumed to not require active transport mechanisms.<sup>441</sup>

Transport of compounds, solutes, ions and nutrients across biological membranes form an integral part of physiological processes. It is estimated that approximately 15% to 30% of membrane proteins are transporting units, and that 60% of energy usage is earmarked for facilitating transportation of molecules.<sup>442</sup> Transport proteins are found in large quantities throughout the body. Their importance is further elucidated by the fact that many are involved in disease progression.<sup>442</sup> Various transporters and enzymes have been identified in the intestinal canal, and their distribution is dependent on the intestinal sections involved (Table 31) (Figure 55).

##### **5.1.2. P-glycoprotein transporters**

The majority of transporters in the ATP-binding cassette (ABC) family act as active efflux transporters that require energy from ATP hydrolysis to extrude molecules from the intracellular compartment.<sup>443,444</sup> P-gp belongs to the ABC superfamily of transporters.<sup>443–445</sup> It was first discovered as the protein implicated in multidrug resistance of cancerous cells due to its ability to actively efflux chemotherapeutics from

**Table 31:** Distribution of transporters and enzymes in the gastrointestinal tract (reproduced from Pang, 2003<sup>440</sup> with permission).

Transporter	Segmental distribution
Apical sodium dependent bile acid transporter	Distal > proximal
Peptide transporter 1	Jejunum > ileum > duodenum
Monocarboxylic acid transporter 1	Duodenum > jejunum > ileum
Organic anion transporting polypeptide 3	Highest in jejunum
Concentrative nucleoside transporter	Highest in jejunum
Multidrug resistance-associated protein 2	Duodenum ~ jejunum > ileum
P-gp	Jejunum ~ ileum > duodenum
Multidrug resistance-associated protein 3 (basolateral)	Ileum > jejunum > duodenum
<b>Enzymes</b>	
CYP3A	Duodenum ~ jejunum > ileum
Uridine 5'-diphospho-glucuronosyltransferase	Duodenum ~ jejunum > ileum
Phenol sulfotransferase	Duodenum ~ jejunum > ileum
Glutathione S-transferase	Duodenum ~ jejunum > ileum
Estrone sulfatase	Proximal > distal

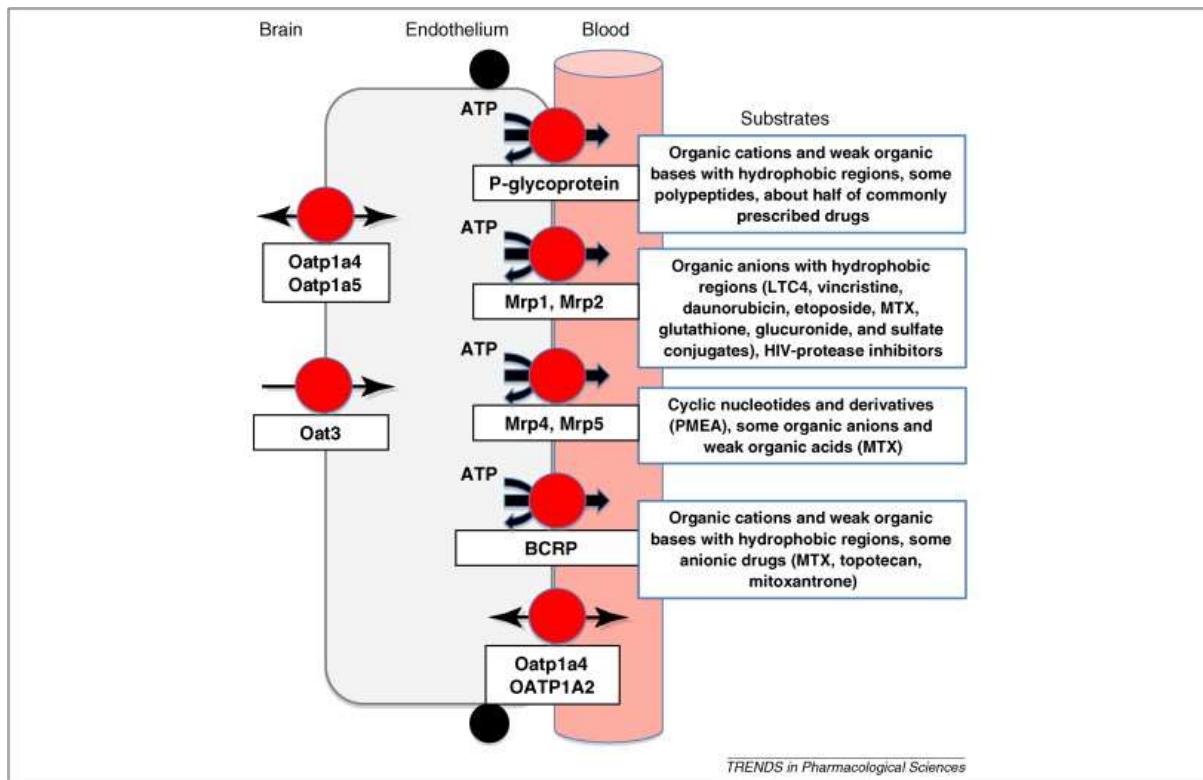


**Figure 55:** Graphical representation of P-glycoprotein and other membrane transporters in the blood-brain barrier allowing for efflux of chemicals to protect the brain (as reproduced by Miller<sup>446</sup> with permission).

the intracellular space.<sup>442</sup> P-gp is a 170 kDa glycoprotein<sup>443</sup> consisting of 1 280 amino acids<sup>447,448</sup> and is encoded by the multi-drug resistance-1 (MDR-1) gene.<sup>444,445</sup> The functional unit of P-gp consist of four domains: two nucleotide-binding domains (NBD) and two transmembrane domains (TMD).<sup>445,448</sup> The NBD is a cytoplasmic domain necessary for energy production through the binding and hydrolysis of ATP.<sup>442</sup> Each TMD consists of six transmembrane helices<sup>442</sup> which forms a hydrophobic membrane-crossing pathway for substrates.<sup>448</sup>

Efflux of compounds through P-gp is energy-dependent and requires conformational change of the transporter domains.<sup>442</sup> It is proposed that transportation involves four processes: i) binding of ATP and/or drug to respective domains, ii) NBD conformation change due to ATP binding and/or hydrolysis, iii) TMD conformational change from high-affinity to low-affinity binding due to changes in NBD, and iv) resetting of conformational changes after drug release.<sup>442</sup>

Binding of ATP results in NBD dimerisation due to alterations in the electrostatic charges of ATPase, with subsequent association of the NBD sites.<sup>442</sup> This binding is not direct, and occurs through the nucleotide.<sup>442</sup> It is suggested that drug-binding does not influence the affinity of ATP for the NBD, nor does it reduce activation energy.<sup>442</sup> The TMDs form a channel into the intracellular compartment, but once ATP binds to the NBD a conformational change occurs. A cavity containing the various drug-binding sites is found within the P-gp structure which allows for binding through hydrophobic interactions.<sup>448</sup> This closes the intracellular channel and opens a pore to the extracellular compartment, resulting in the efflux of bound substrates.<sup>448</sup> This is a result of high-affinity cytoplasmic drug-binding sites, which after a conformational change to a low-affinity site releases the drug at an extracellular site.<sup>442</sup> It would appear that there are multiple binding sites, which appear to have overlapping substrate specificity.<sup>443</sup> P-gp is often dependent on the surrounding lipid membrane characteristics, and as such can be altered through membrane disturbances or disruptions.<sup>443</sup>

P-gp is present on numerous tissue types, including the apical surface of mature enterocytes, canicular membranes of hepatocytes, and endothelial cells of the brain and kidney.<sup>443,444</sup> Its high expression in organ systems containing endothelial/epithelial borders, as well as those involved in metabolism and clearance, gives insight into its primary function.<sup>449</sup> P-gp counteracts the absorption and transport of toxic compounds,

thus decreases the exposure of organs, such as the liver, brain and kidney, to potential cytotoxins.<sup>276,448</sup> P-gp localisation is generally on apical membranes of tissues facing an excretory compartment, which would increase elimination of potential cytotoxins. A high abundance is found in the lower gastrointestinal tract, which indicates the importance of direct extrusion into the gastric lumen as a method for detoxification and excretion. P-gp functioning in the gastrointestinal tract thus prevents absorption of orally-administered molecules, and reduces bioavailability.<sup>445</sup> It has been suggested that P-gp in the blood-brain barrier could explain the low brain bioavailability of several larger hydrophobic molecules, which further illustrates its function in the body.<sup>447</sup>

P-gp accommodates a very broad range of substrates and inhibitors due to its number of available binding sites (up to five). This allows it to transport hydrophobic, amphipathic, cationic and neutral molecules. It is commonly accepted that most P-gp substrates or inhibitors display a matter of hydrophobicity and amphipathic characteristics, and as most inhibitors are also substrates, competition arises.<sup>447</sup> Its broad range however makes it an ideal candidate for drug-drug or drug-herb interactions.<sup>444</sup> Although metabolism has always been a major factor in drug-drug interactions, the importance of transporter interactions have come to light.<sup>444</sup>

P-gp-mediated drug-drug interactions are well-described in literature, though many do not pose severe clinical implications due to unaltered metabolism profiles. As many P-gp substrates are metabolised through the CYP450 system, inhibition of transportation may not be enough to alter the pharmacokinetic profile of the drug significantly.<sup>449</sup> Some of these interactions may be beneficial though. It has been shown that various types of cancers express high levels of P-gp,<sup>450</sup> resulting in an inherent resistance to many chemotherapeutics due to low intracellular accumulation.<sup>443,450</sup> If P-gp is inhibited, higher levels of the chemotherapeutics can be accumulated, resulting in greater therapeutic concentrations and higher efficacy.<sup>450</sup>

Except for P-gp, several other transporters have been implicated in drug transport. These include multidrug resistance-associated protein (MRP) and organic cation transporters.<sup>441</sup> MRP is also a member of the ABC-superfamily. Although there is some overlapping substrate specificity between P-gp and MRP, there are distinct differences. While MRP tends to prefer anionic substrates and inhibitors, P-gp prefers cationic substrates. MRP has been shown to contribute to intestinal transport.<sup>441</sup>

### 5.1.3. Metabolism

Xenobiotic metabolism forms a critical step in the removal of foreign chemical entities from the body, and thus has an important protective function. Drug metabolism aims to detoxify xenobiotic molecules to aid in their removal, however activation into toxic metabolites may also occur.<sup>246</sup> Metabolism has been classified as a phase I (bioactivation) or phase II (detoxification) metabolic process, often, but not always, working in conjunction with one another.<sup>246</sup> Regulation of drug-metabolising enzymes, as well as some transporters, are mediated by aryl hydrocarbon receptor (AhR), constitutive androstane receptor (CAR), pregnane X receptor (PXR), peroxisome proliferator-activated receptor-alpha (PPAR $\alpha$ ) and nuclear factor erythroid 2-related factor 2 (Nrf2).<sup>451</sup>

Phase I metabolic systems, primarily mediated by the CYP450 enzyme system<sup>452</sup> induces parent molecule biotransformation with addition of hydroxyl, carboxyl, amino or thiol groups to increase hydrophilicity of the xenobiotic.<sup>246,453</sup> Phase II metabolism increases hydrophilicity further through conjugation reactions with small endogenous molecules. These occur with glucuronic acid, acetate and GSH via glucuronosyltransferases, *N*-acetyltransferase 2 and glutathione *S*-transferase, respectively.<sup>246,454</sup> Phase II metabolites are generally transferred to the intestines in bile, or to sinusoidal circulation for renal excretion.<sup>246</sup> As CYP450 enzymes are most often involved in drug interactions, this part of the study will focus primarily on phase I metabolism with regards to enzymes, more specifically CYP2B6, CYP2D6 and CYP3A4 as models. Important to note is that drug-drug or drug-herb interactions may occur by either inducing or inhibiting enzyme activity. This may be beneficial or detrimental depending on the clinical consequence. For example, in antiviral therapy, lopinavir is used to decrease viral load, however, it undergoes high CYP3A4-mediated metabolism which reduces its bioavailability. The addition of ritonavir leads to CYP3A4 inhibition, allowing for higher plasma concentrations of lopinavir and better therapy.<sup>455</sup>

The CYP450 monooxygenase enzyme system is an ubiquitous protein family of heme-thiolate enzymes,<sup>456,457</sup> that is highly conserved between families.<sup>458</sup> Standard categorisation of CYP450 occurs following sequence homology, which allows for distinction between families.<sup>456,458</sup> CYP450 enzymes may also be classified according to their type of redox partner used for monooxygenation.<sup>456</sup> Conserved entities allow

for conformational stability and function, while variable regions allow for substrate-directed bioactivity (Figure 56).<sup>456,458</sup> A conserved structural fold is thus apparent, even with sequence homology <20%.<sup>459</sup> The catalytic site is contained around the porphyrin-heme complex.<sup>457</sup> All CYP450 enzymes have a conserved heme-binding region comprised out of  $\alpha$ D-,  $\alpha$ E-,  $\alpha$ I-,  $\alpha$ L-,  $\alpha$ J- and  $\alpha$ K- structures, and a Cys-pocket for the thiolate heme ligand.<sup>458</sup> While the structure of all CYP450 enzymes may be quite similar, the diverse groups allow for substrate-specificity and differing bioactivity profiles, however substrate overlap does often occur.<sup>453,458</sup> Six substrate-recognition and –binding regions have been identified.<sup>458</sup> Between  $\alpha$ K and the Cys-pocket a meander-loop is formed that is involved with heme-binding and stabilisation.<sup>458</sup> Efflux transporters, such as P-gp, and CYP450 enzymes work in conjunction to decrease xenobiotic exposure through a constant metabolism-and-efflux cycle coupled to absorption, metabolism and extrusion processes.<sup>460</sup> Furthermore, CYP450 enzymes are expressed at different abundances throughout the body (Table 32). Polymorphic differences also allow for a wide distribution of alleles, each with varying bioactivity.<sup>461</sup> Thus inter-individual differences result in unexpected therapeutic or adverse outcomes.<sup>461</sup> While poor metabolisers are more likely to experience decreased metabolism of drugs with subsequent increased adverse effects, ultra-rapid metabolisers may not reach therapeutic efficacy due to metabolic clearance.<sup>461</sup>

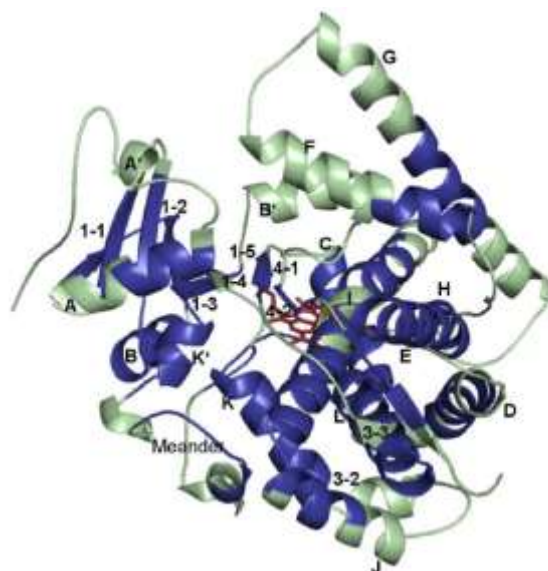


**Figure 56:** Structurally-conserved regions of CYP450 enzymes in a structural overview (reproduced from Sirim *et al.*<sup>458</sup> with permission). The reference structure of CYP450 BM-3 is from *Bacillus megaterium*. The blue regions indicate structurally conserved regions, while the grey-green indicate variable regions.

**Table 32:** Relative expression of CYP1, CYP2 and CYP3 subfamilies in different tissues (reproduced from Pavek & Dvorak<sup>452</sup> with permission).

Enzyme	Small intestines	Kidney	Lung	Placenta	Liver
CYP1A1	+	+	+++ <sup>c</sup> /±	++/+	++
CYP1A2	-	-	±	+/- <sup>a</sup>	+++
CYP1B1	+	++/+	++/+	+	+
CYP2A6	-	-	++/+	±	+++
CYP2A13	±	±	+	-	+++
CYP2B6	++/+	++/+	+++	±	+++
CYP2C8	+	±	±	± <sup>ab</sup>	+++
CYP2C9	++	±	±	± <sup>ab</sup>	+++
CYP2C19	++	±	±	± <sup>ab</sup>	+++
CYP2D6	++/+	+	+	++/+ <sup>a</sup>	+++
CYP2E1	++/+	+	+++/>++/+	+	+++
CYP2F1	-	-	+++/>++	±	-
CYP2J2	++/+	+	+	++	++
CYP2R1	+	+	+	+	+
CYP2S1	++/+	±	+	+	-
CYP3A4	+++	+	±	±	+++
CYP3A5	+++/>++	++	+++/>++	+	+++/>++
CYP3A7	±	+	±	± <sup>a</sup>	+ <sup>d</sup>
CYP3A43	-	±	-	-	+++

+++ = organ with high expression; ++ = organ with moderate expression; + = low expression; - = undetectable expression; ± = controversial results; a = expressed in first trimester; b = CYP2C2 expression reported in first trimester; c = smokers, ± in non-smokers; d = foetal liver expresses highest level.

The CYP1A subfamily is primarily comprised of CYP1A1, CYP1A2 and CYP1B1. CYP1A1 and CYP1B1 are mostly located in extrahepatic tissues, with CYP1A1 not being constitutively expressed at high concentrations, unless induced by xenobiotic exposure.<sup>452</sup> CYP1A2 is primarily hepatic, and is induced in a similar fashion to CYP1A1 and CYP1B1, however its substrate specificity differs.<sup>452</sup> CYP1 enzymes, such as CYP1A2, are known to metabolise drugs such as clozapine and theophylline, endogenous compounds such as steroids, as well as to activate procarcinogens.<sup>462</sup>

The most important CYP2 (Table 33) enzymes include CYP2A6, CYP2B6, CYP2C8, CYP2C9, CYP2C19, CYP2D6, CYP2E1 and CYP2F1.<sup>452</sup> CYP2C9 is expressed in high levels in the liver and intestines, and is described as the second most abundant enzyme of the CYP450 family after CYP3A4.<sup>452</sup> CYP2D6 metabolises approximately 25% of known drugs, even though it contributes to a small percentage of hepatic CYP450 enzymes.<sup>461</sup> Although not as highly expressed as CYP3A4, CYP2B6<sup>452</sup> and CYP2D6 is involved to an appreciable level in intestinal metabolism.<sup>463</sup>

**Table 33:** A brief summary of substrates and polymorphisms for CYP2B6 and CYP2D6.

Enzyme	Drug substrates	Polymorphisms	Alteration to enzyme activity	Frequency
CYP2B6	Efavirenz <sup>464,465</sup> Nevirapine <sup>466</sup> Bupropion <sup>465,466</sup> Cyclophosphamide <sup>466</sup> Methobarbital <sup>466</sup> Cyclophosphamide <sup>465</sup> Ketamine <sup>465</sup> Propofol <sup>465</sup> Artemisinin <sup>465</sup>	<i>CYP2B6*6</i> 464,465,467–470	Reduced 464,465,467–470	Black Africans (23%) <sup>464</sup> Ghanians (50%) <sup>467</sup> Nigerians (17-21%) <sup>465</sup> Tanzanians (36%) <sup>470</sup> West Africans (42%) <sup>466</sup> Zanzibar (9.7%) <sup>468</sup> Zimbabweans (49%) <sup>469</sup>
CYP2D6	Alprenol <sup>461</sup> Atenolol <sup>461</sup> Clozapine <sup>461</sup> Codeine <sup>461</sup> Dextromethorphan <sup>461</sup> Haloperidol <sup>461</sup> Imipramine <sup>461</sup> Ondansetron <sup>461</sup> Propranolol <sup>461</sup> Quinidine <sup>461</sup> Risperidone <sup>461</sup>	<i>CYP2D6*1</i> <sup>471</sup>	Functional <sup>471</sup>	Black Africans (20%) <sup>471</sup>
		<i>CYP2D6*2</i> <sup>471</sup>	Functional <sup>471</sup>	Black Africans (22%) <sup>471</sup>
		<i>CYP2D6*3</i> <sup>471</sup>	Functional <sup>471</sup>	Black Africans (4%) <sup>471</sup>
		<i>CYP2D6*1xn</i> 471,472	Increased 471,472	Black Africans (<1%) <sup>471</sup> Caucasians (<1%) <sup>472</sup> Coloureds (2%) <sup>472</sup>
		<i>CYP2D6*2xn</i> 461,472	Increased 461,472	Black Africans (<1-2%) <sup>461,472</sup> Caucasians (<1-5%) <sup>461,472</sup> Coloureds (1%) <sup>472</sup> Ethiopians and Saudi-Arabians (10-16%) <sup>461</sup>
		<i>CYP2D6*3</i> <sup>461,472</sup>	Inactivated <sup>472</sup>	Caucasians (1%) <sup>472</sup> Coloureds (0%) <sup>472</sup>



Enzyme	Drug substrates	Polymorphisms	Alteration to enzyme activity	Frequency
CYP2D6	Alprenol <sup>461</sup> Atenolol <sup>461</sup> Clozapine <sup>461</sup> Codeine <sup>461</sup> Dextromethorphan <sup>461</sup> Haloperidol <sup>461</sup> Imipramine <sup>461</sup> Ondansetron <sup>461</sup> Propranolol <sup>461</sup> Quinidine <sup>461</sup> Risperidone <sup>461</sup>	<i>CYP2D6</i> *4 461,471,472	Inactivated 461,471,472	Black Africans (2-7%) <sup>461,471</sup> Caucasians (12-21%) <sup>461,472</sup> Coloureds (7%) <sup>472</sup> Ethiopians and Saudi-Arabians (1-4%) <sup>461</sup>
		<i>CYP2D6</i> *5 <sup>461,471,472</sup>	Inactivated 468,471,472	Black Africans (4%) <sup>461,471</sup> Caucasians (2-7%) <sup>461,472</sup> Coloureds (18%) <sup>472</sup> Ethiopians and Saudi-Arabians (1-3%) <sup>461</sup>
		<i>CYP2D6</i> *6 <sup>471,472</sup>	Inactivated 471,472	Black Africans (2%) <sup>471</sup> Caucasians (1%) <sup>472</sup> Coloureds (0%) <sup>472</sup>
		<i>CYP2D6</i> *9 <sup>471,472</sup>	Reduced 471,472	Black Africans (1%) <sup>471</sup> Caucasians (35%) <sup>472</sup> Coloureds (0%) <sup>472</sup>
		<i>CYP2D6</i> *10 461,471,472	Reduced 461,471,472	Black Africans (2-6%) <sup>461,471</sup> Caucasians (1-2%) <sup>461</sup> Ethiopians and Saudi-Arabians (3-9%) <sup>461</sup> Coloureds (3%) <sup>472</sup>
		<i>CYP2D6</i> *17 461,471,472	Reduced 461,471	Black Africans (9-35%) <sup>461,471</sup> Caucasians (0-<1%) <sup>461,472</sup> Coloureds (13%) <sup>472</sup> Ethiopians and Saudi-Arabians (3-9%) <sup>461</sup>
		<i>CYP2D6</i> *41 471,472	Reduced 471,472	Black Africans (5%) <sup>471</sup> Caucasians (8%) <sup>472</sup> Coloureds (4%) <sup>472</sup>

The CYP3A subfamily are the primary drug metabolising enzymes in the body. It is estimated that 50 to 70% of drugs on the market are metabolised to some extent by CYP3A,<sup>460</sup> and thus it proves to be an important target for drug interactions. CYP3A contributes approximately 30% and 70% to hepatic and intestinal CYP450 enzyme

systems, respectively.<sup>460</sup> The major CYP3A isoform is CYP3A4 (Table 34).<sup>452,460</sup> CYP3A4 levels and activity increases from the duodenum to the jejunum, while gradually decreasing from the ileum to the colon.<sup>460</sup> Several other CYP3A isoforms contribute to drug metabolism, such as CYP3A5 and CYP3A7, however their frequency and activity spectrum are generally much lower than that of CYP3A4.<sup>460</sup>

**Table 34:** A brief summary of substrates and polymorphisms for CYP3A4.

Drug substrates	Polymorphisms	Alteration to enzyme activity	Frequency
Alprazolam <sup>473</sup> Amlodipine <sup>473</sup> Artemether <sup>470</sup> Atorvastatin <sup>473</sup> Cyclosporine <sup>473</sup> Diazepam <sup>473</sup> Estradiol <sup>473</sup> Lumefantrine <sup>470</sup> Simvastatin <sup>473</sup> Sildenafil <sup>473</sup> Quinine <sup>470</sup> Verapamil <sup>473</sup> Zolpidem <sup>473</sup>	<i>CYP3A4*1B</i> <sup>468 470 474</sup>	Reduced <sup>468 470 474</sup>	Caucasians (84) <sup>474</sup> Khoisan (77%) <sup>475</sup> Mixed ancestry (46%) <sup>475</sup> Malawians (77%) <sup>476</sup> Tanzanians (78%) <sup>470</sup> Xhosa (73%) <sup>475</sup> Zanzibar (49.5%) <sup>468</sup>
	<i>CYP3A4*1G</i> <sup>475</sup>	Reduced <sup>477</sup>	Khoisan (91%) <sup>475</sup> Mixed ancestry (60%) <sup>475</sup> Xhosa (84%) <sup>475</sup>

Two primary sites that affect the metabolism of drugs administered orally during the first-pass effect are the small intestines and liver. Enterocytes are the first site of CYP-mediated metabolism that orally-administered drugs reach, which mostly consists of CYP3A4 (80%) and CYP2C9 (15%) in relation to total intestinal CYP450.<sup>452,478</sup> However, CYP1A1, CYP2C8, CYP2C10, CYP2B6, CYP2D6, CYP2E1 and CYP3A5<sup>452,454</sup> also contribute to intestinal metabolism. Intestinal CYP3A4 metabolism has been suggested to play a significant effect on orally-administered drugs' first-pass effect, however this is a controversial topic. Many accept hepatic CYP450-mediated metabolism as the primary driver for first-pass effect.<sup>452</sup>

#### 5.1.4. Nevirapine absorption and metabolism

Successful anti-HIV treatment using HAART requires plasma concentration levels within a defined range to ensure proper control over viral load. As such, the permeability and metabolism of one of the commonly-used NNRTIs, nevirapine, needs to be taken into account. Nevirapine displays bioavailability >90% in healthy

individuals, which suggests that solubility and permeability does not limit oral absorption.<sup>441</sup> This has been substantiated by high intestinal permeability and ultimately extensive metabolism.<sup>479</sup> Physicochemical properties indicate a logD of 1.8, cross-sectional area of 52 Å<sup>2</sup>,<sup>480</sup> logP value of 2.5, low water solubility (0.1 mg/mL), and pKa of 2.8, thus the molecule itself is lipophilic.<sup>481</sup> Taking the former into account, the deduction is that transport would mostly entail passive influx,<sup>480,482</sup> however, several reports indicate the involvement of active transport mechanisms for drug efflux.<sup>13,483,484</sup> Nevirapine has been shown to act as a MRP-inhibitor, thus may function as a substrate thereof.<sup>484</sup> Furthermore, nevirapine displays a higher basolateral-to-apical transport in Caco-2 cell monolayers. This, however, is decreased in the presence of a P-gp inhibitor (verapamil), suggesting that active extrusion is involved.<sup>13</sup> Haas *et al.*<sup>483</sup> reported that altered nevirapine accumulation is associated with *MDR1*-variants, suggesting an involvement of P-gp. Nevirapine does not appear to be a substrate for organic cation transporter 1 and 2 (OCT1 and OCT2)<sup>485</sup> or breast cancer resistance protein (BCRP).<sup>480</sup>

Nevirapine is primarily metabolised by CYP3A isoforms,<sup>486</sup> specifically CYP3A4, as well as CYP2B6.<sup>487</sup> CYP2B6 is primarily found in the liver, and contributes to a large amount of nevirapine's metabolism.<sup>482</sup> This may result in the formation of 3- and 8-hydroxy metabolites.<sup>482</sup> Nevirapine is known to induce CYP2C9, CYP2B6 and CYP3A4 enzymes,<sup>486,487</sup> and undergoes enterohepatic recycling.<sup>488</sup>

#### **5.1.5. Aim of testing the crude extracts on pharmacokinetic parameters**

The aim of testing the effect of crude extracts on pharmacokinetic parameters was to determine their risk of inducing herb-drug interactions. The objectives were to:

- Determine the effect of crude extracts on P-gp activity.
- Determine the effect of selected crude extracts on nevirapine permeability.
- Determine the effect of crude extracts on CYP2B6, CYP2D6 and CYP3A4 activity.

## 5.2. Materials and Methods

A detailed list of all reagents used in the study, as well as the preparation thereof, is provided (Appendix III).

### 5.2.1. Effect of herbal remedies on rhodamine-123 accumulation

Various assays are available for the determination of P-gp inhibitory activity. The presence of multiple binding sites may complicate the determination of P-gp activity,<sup>443</sup> and thus selection of an appropriate model is imperative to identify if a potential exists for drug-herb interactions. Typically employed *in vitro* models include the drug-stimulated ATPase activity, Rh-123, calcein-AM and bidirectional permeability assays. The drug-stimulated ATPase activity assay employs a colorimetric change that occurs when inorganic phosphates are released due to energy-dependent transportation of P-gp substrates.<sup>443</sup> Fluorometric models include the Rh-123 and calcein-AM accumulation assays, in which the fluorescent dye acting as a P-gp substrate accumulates intracellularly when P-gp is inhibited. In the presence of a P-gp inhibitor the dye cannot be actively pumped out into the extracellular space, and thus fluorescent intensity is increased.<sup>443</sup> The Rh-123 accumulation assay is well-described in literature<sup>443</sup> and has been shown to correlate well with other assays.<sup>443</sup> Furthermore, it has been recommended as an initial step in drug discovery of P-gp inhibitors and substrates.<sup>443</sup>

The effect of crude extracts on P-gp function was determined according to the Rh-123 accumulation assay as described by Jia and Wasan<sup>184</sup> with minor modifications. Cells (100  $\mu$ L) were seeded into sterile, white 96-well plates at  $2 \times 10^4$  cells/well and  $1 \times 10^4$  cells/well for HepG2 and Caco-2 cells, respectively. Plates were incubated for 48 h at 37°C and 5% CO<sub>2</sub> in a humidified incubator, after which they were exposed to 100  $\mu$ L PBS (negative control), 0.8% DMSO (vehicle control), verapamil (1 000  $\mu$ M, positive control) or crude extracts (6.4, 20 and 64  $\mu$ g/mL) for 1 h. Cells were exposed to 20  $\mu$ L Rh-123 (10  $\mu$ M in PBS), agitated for 1 min and incubated for a further 1 h. Plates were washed thrice with PBS to remove effluxed dye, and the fluorescence of the reaction mixture (100  $\mu$ L) measured at  $\lambda_{\text{ex}} = 485$  nm and  $\lambda_{\text{em}} = 520$  nm (gain 500). Cell density was determined according to the SRB assay as described in Chapter 3 and used to

standardise fluorescent data. The percentage Rh-123 accumulation was expressed using the following equation:

$$\text{Rh} - 123 \text{ accumulation (\%)} = \frac{\text{Fls}}{\text{Flc}} \times 100$$

where, Fls = the standardized, fluorescent intensity of the sample, and Flc = the standardized, average fluorescent intensity of the negative control.

## 5.2.2. Effect of herbal remedies on transport of nevirapine

### 5.2.2.1. Caco-2 bidirectional permeability assay

The Caco-2 bidirectional permeability assay is dependent on differentiation of Caco-2 cells into a monolayer simulating the epithelium of the human small intestine. Differentiation allows for the expression of all major digestive enzymes and transporters, as well as the presentation of tight junctions and brush border characteristics. Transport of different chemical entities between this *in vitro* model and *in vivo* reports display positive correlations.<sup>489</sup> By measuring the amount of chemical entity transported across the Caco-2 monolayer in both an apical-to-basolateral and basolateral-to-apical direction an estimation of the permeability characteristics, in terms of the permeability coefficients ( $P_{app}$ ), can be calculated (Figure 57).<sup>489</sup> This measurement is generally done based on liquid chromatography tandem mass spectrometry (LC-MS/MS). Assessment of Caco-2 monolayer integrity needs to be ascertained, which commonly is done through the measurement of trans-epithelial electrical resistance (TEER),<sup>490</sup> or the rejection of large, impermeable compounds (e.g. Lucifer Yellow or mannitol).<sup>489,491</sup> The Federal Drug Administration recommends that an efflux ratio be used to express functionality, defined as the permeability from basolateral to apical relative to the permeability from apical to basolateral.<sup>492</sup>

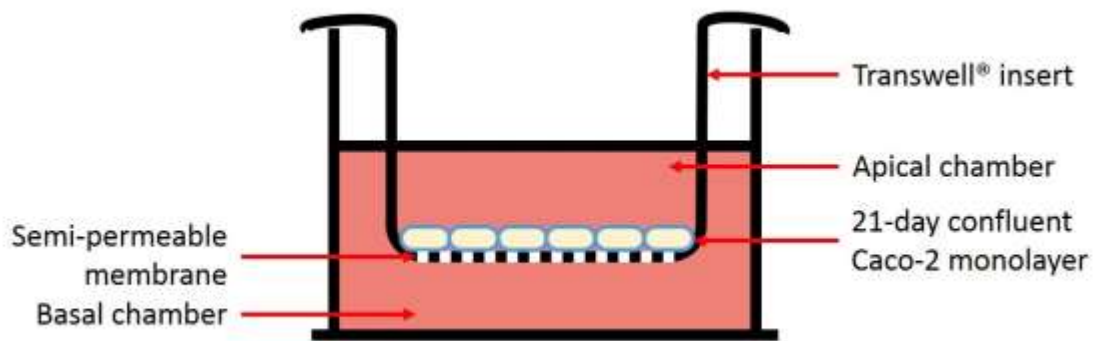


**Figure 57:** Graphical representation of the structure of the Caco-2 bidirectional permeability assay supports that are implemented.

The effect of crude extracts on the transport of nevirapine was assessed using the Caco-2 bidirectional permeability assay as described by Corning Incorporated Life Sciences<sup>491</sup> with minor modifications to volumes used. Culturing of Caco-2 cells was in 10% FCS-fortified EMEM. Transwell® permeable support inserts (6.5 mm, 0.4  $\mu$ m porosity) were fitted into sterile 24-well plates, and conditioned with 50  $\mu$ L medium in the insert, and 600  $\mu$ L medium in the reservoir for 1 h. Caco-2 cells (50  $\mu$ L,  $2 \times 10^5$  cells/mL) were pipetted into each insert, and incubated at 37°C for 21 days. On day 3, 6 and 9 of culture, 30  $\mu$ L additional medium was added to the insert, while the medium in the reservoir was completely replaced. On day 12, 15, 18 and 20 of culture, medium was replaced in both the insert and reservoir. On day 21, apical-to-basolateral and basolateral-to-apical transport was assessed by removing all medium from the insert and reservoir, and preparing all dilutions in Hank's Balanced Saline Solution (HBSS). To pre-treat cells, 75  $\mu$ L HBSS (0.1% DMSO, vehicle control), verapamil (200  $\mu$ M, positive control), or crude extracts (20 and 64  $\mu$ g/mL) was added to the insert, and 235  $\mu$ L HBSS to the reservoir for 1 h. For apical-to-basolateral transport, 75  $\mu$ L nevirapine (320  $\mu$ M) was added to all inserts, and 235  $\mu$ L to the reservoir for 1 h. For basolateral-to-apical transport, 235  $\mu$ L nevirapine (320  $\mu$ M) was added to the reservoir, and 75  $\mu$ L to the insert for 1 h. The full aliquot was removed separately from both the insert and reservoir, and stored separately at -80°C until analysis.

### 5.2.2.2. Lucifer yellow rejection assay

To assess the membrane integrity of the Caco-2 cell monolayer grown on the Transwell® insert, the Lucifer yellow rejection assay was performed as described by Corning Incorporated Life Sciences<sup>491</sup> with minor modifications to volumes used. A 235 µL aliquot of HBBS was added to the reservoir, while 75 µL Lucifer yellow (60 µM) was added to the insert for 1 h. Aliquots of the reservoir (200 µL) and insert (50 µL diluted with 50 µL HBSS) was pipetted into a white 96-well plate, and the fluorescence intensity measured at  $\lambda_{\text{ex}} = 485 \text{ nm}$  and  $\lambda_{\text{em}} = 520 \text{ nm}$  (gain 750). The percentage Lucifer yellow rejection was expressed using the following equation:

$$\text{Lucifer yellow rejection (\%)} = 100 - \left( \frac{\text{FI}(\text{basolateral})}{\text{FI}(\text{apical})} \right)$$

where, FI(basolateral) = the fluorescent intensity of the basolateral side, and FI(apical) = the fluorescent intensity of the apical side.

### 5.2.2.3. LC-MS/MS determination of nevirapine concentrations

To determine the concentration of nevirapine that was transported across the Caco-2 monolayer, LC-MS/MS quantification was used. A standard curve of nevirapine was prepared ranging from 12.5 nM to 10 µM. An aliquot of each sample underwent protein-precipitation using a triple-crash method with acetonitrile:methanol (1:1) as precipitant solution. The aliquot (100 µL) was diluted with 50 µL, 50 µL and 200 µL precipitant solution sequentially, with 5 min sonication between each step. The mixture was centrifuged at 10 000g for 10 min, after which exactly 100 µL of the solution was diluted with 100 µL zidovudine (20 µM, internal standard) and transferred to chromatography vials. Chromatographic separation (Table 35) was achieved using Agilent 1100 series HPLC system (Agilent Technologies, Waldbronn, Germany) equipped with a well-plate autosampler, mobile phase degasser, binary pump and column thermostat unit. Quantitation (Table 36) was done using an AB Sciex Series 4000 QTrap triple-quadrupole mass spectrometer (Applied Biosystems MSD/SCIEX, Concord, Canada) equipped with a TurboV electrospray ionisation source operated in positive mode and multiple reaction monitoring (MRM) mode. Data processing was carried out using Analyst 1.5.2 software to determine nevirapine concentrations in both the apical-to-basolateral and basolateral-to-apical samples.

**Table 35:** Chromatographic conditions of nevirapine quantitation

<b>Guard column</b>	Sentry Guard Column with XBridge C18 2.5 µm 4.6x20 mm guard inserts
<b>Analytical column</b>	XBridge™ BEH C18 2.5 µm, 4.6x100 mm column
<b>Mobile phase</b>	10 mM ammonium formate in deionised water and methanol (45:55)
<b>Flow rate</b>	600 µL/min
<b>Injection volume</b>	15 µL
<b>Run-time</b>	5 min isocratic
<b>Column temperature</b>	30°C

**Table 36:** Mass spectrometry conditions of nevirapine quantitation

	<b>Nevirapine</b>	<b>Zidovudine</b>
<b>Precursor ion</b>	267.4 m/z	268.4 m/z
<b>Product ions</b>	226.4 m/z and 198.3 m/z	127.4 m/z and 142.3 m/z
<b>Declustering potential</b>	70	70
<b>Collision energy</b>	15	15

Nevirapine concentrations were used to determine the apical-to-basolateral and basolateral-to-apical  $P_{app}$  using the following equation:

$$P_{app}(10^{-6} \text{ cm/s}) = \frac{V_r \times C_f}{C(0) \times A \times t}$$

where,  $V_r$  = volume of receiving chamber (mL),  $C_f$  = final concentration in receiving chamber (mM),  $C(0)$  = initial concentration (mM),  $A$  = surface area (cm<sup>2</sup>),  $t$  = time of assay (s).

Efflux ratio was determined using the following equation:

$$\text{Efflux ratio} = \frac{P(\text{appB} \rightarrow \text{A})}{P(\text{appA} \rightarrow \text{B})}$$

where,  $P(\text{appB} \rightarrow \text{A})$  = the  $P_{app}$  in a basolateral-to-apical direction, and  $P(\text{appA} \rightarrow \text{B})$  = the  $P_{app}$  in an apical-to-basolateral direction.

### 5.2.3. Effect of herbal remedies on CYP450 enzyme systems

The effect of crude extracts on cDNA-expressed recombinant human CYP450 enzyme activity was measured using a commercially-available fluorescence kit.<sup>493–495</sup> Substrates and positive controls were prepared as per the manufacturer's instructions

and used at 37°C (Table 37). Into white 96-well plates were pipetted 100 µL NADPH-cofactor mixture containing either nothing additional (negative control and blank), 0.8% DMSO (vehicle control), positive control or the extracts (one-third serial dilutions of 200 µg/mL). After 10 min incubation at 37°C, 100 µL enzyme-substrate mixture was added to all wells except for the blank, and incubated for 30 min. Thereafter, stop solution (75 µL) was added to all wells, as well as 100 µL enzyme-substrate mixture to the blank wells. Fluorescent intensity was measured immediately and the percentage enzyme activity relative to the negative control was expressed using the following equation:

$$\text{Enzyme activity (\%)} = \frac{\text{FIs}}{\text{Flc}} \times 100$$

where, FIs = the blank-adjusted fluorescence of the sample, and Flc = the blank-adjusted average fluorescence of the negative control.

**Table 37:** Substrates and positive controls used to assess CYP450 enzyme inhibitory activity

CYP isoform	Substrate (in-reaction concentration)	Positive control (in-reaction concentration)
CYP2B6	7-Ethoxy-4-trifluoromethylcoumarin (EFC) (2.5 µM)	Tranlycypromine (100 µM)
CYP2D6	3-[2-(N,N-diethyl-N-methylamino)ethyl]-7-methoxy-4-methylcoumarin (AMMC) (1.5 µM)	Quinidine (100 nM)
CYP3A4	7-Benzyl-trifluoromethylcoumarin (BFC) (50 µM)	Ketoconazole (1 µM)

#### 5.2.4. Statistics

P-gp inhibition and Caco-2 bidirectional permeability assays were performed using two technical and four biological replicates, while the CYP450 inhibition assays were performed using two technical and biological replicates. The CYP450 enzyme IC<sub>50</sub> was determined using non-linear regression (normalized, variable slope). Significant differences were determined between the negative control and treated cells using Kruskal-Wallis and a post-hoc Dunns test. Significance was defined as  $p < 0.05$ .

## 5.3. Results

### 5.3.1. P-glycoprotein inhibitory activity

The positive control, verapamil, induced significant ( $p < 0.001$ ) accumulation of Rh-123 in both HepG2 (24.4%) and Caco-2 (40.7%) cells (Figure 58).

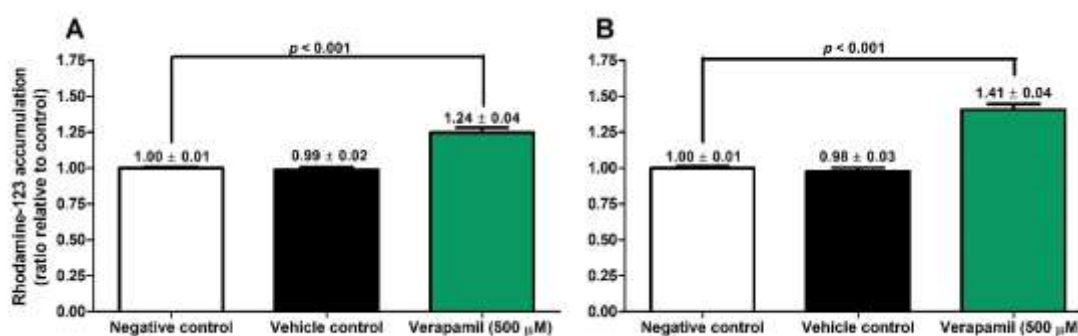


**Figure 58:** Effect of verapamil on Rh-123 accumulation in A) HepG2 and B) Caco-2 cells. Significance was determined against the negative control.

Only seven of the thirty-four crude extracts assessed had a significant ( $p < 0.05$ ) effect on Rh-123 accumulation in either the Caco-2 (four extracts) or HepG2 (three extracts) cell lines (Figure 60 and Figure 59). This effect was only present at the highest concentration tested (32 µg/mL). Only the methanol extract of *S. aculeastrum* displayed activity in both cell lines, resulting in a significant ( $p < 0.05$ ) increase in Rh-123 accumulation (HepG2 = 28.8%; Caco-2 = 192.4%). The methanol extract of *M. sericea* also resulted in significant ( $p < 0.05$ ) Rh-123 accumulation in the HepG2 cell line (11.3%). All other extracts resulted in a significant ( $p < 0.05$ ) decrease in Rh-123 accumulation: the methanol extract of *P. capense* (7.9%) in the HepG2 cell line; the hot water extract of *B. africana* (9.3%) and methanol extracts of *R. caffra* (9.9%) and *S. latifolius* (9.3%) in the Caco-2 cell line.

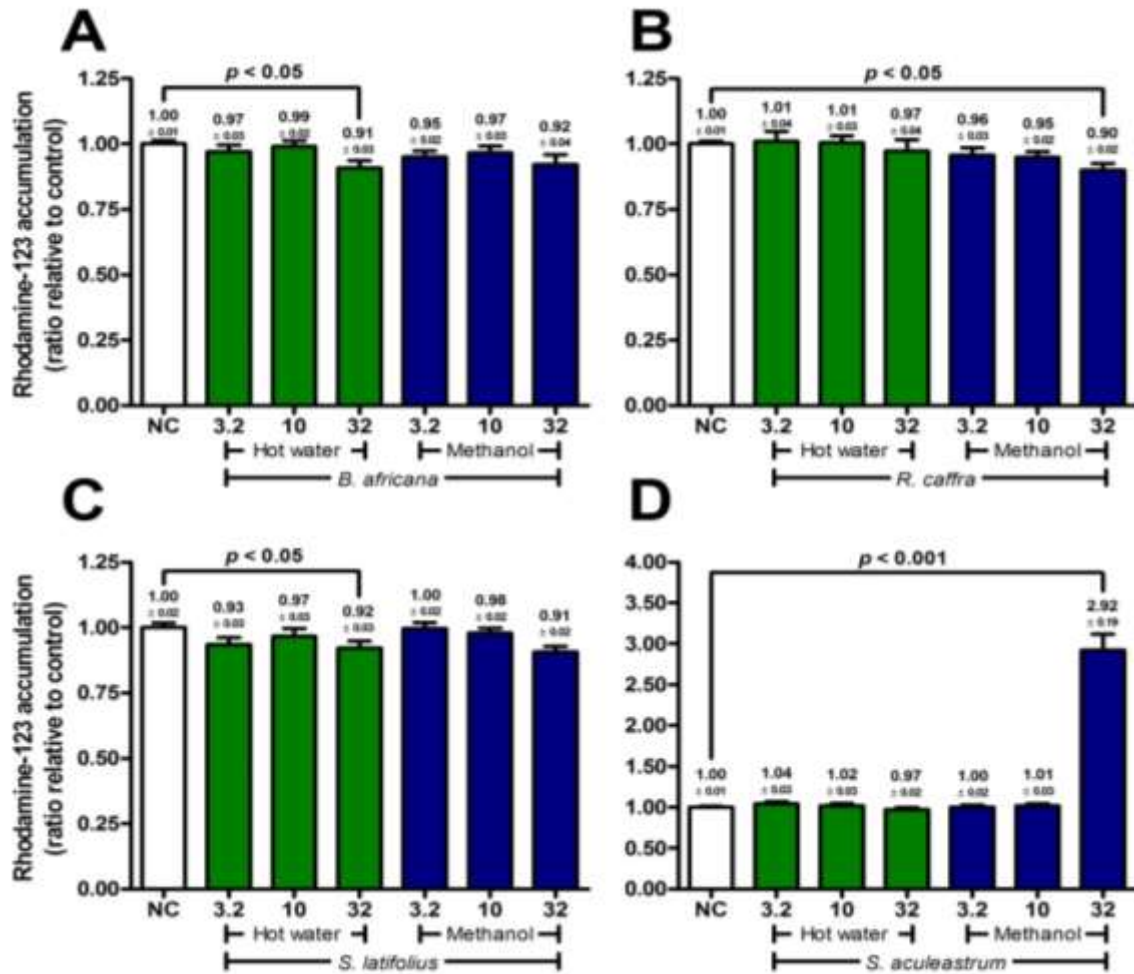


**Figure 59:** Effect of crude extracts of A) *B. africana*, B) *R. caffra*, C) *S. latifolius* and D) *S. aculeastrum* on Rh-123 accumulation in Caco-2 cells. Significance was determined against the negative control.

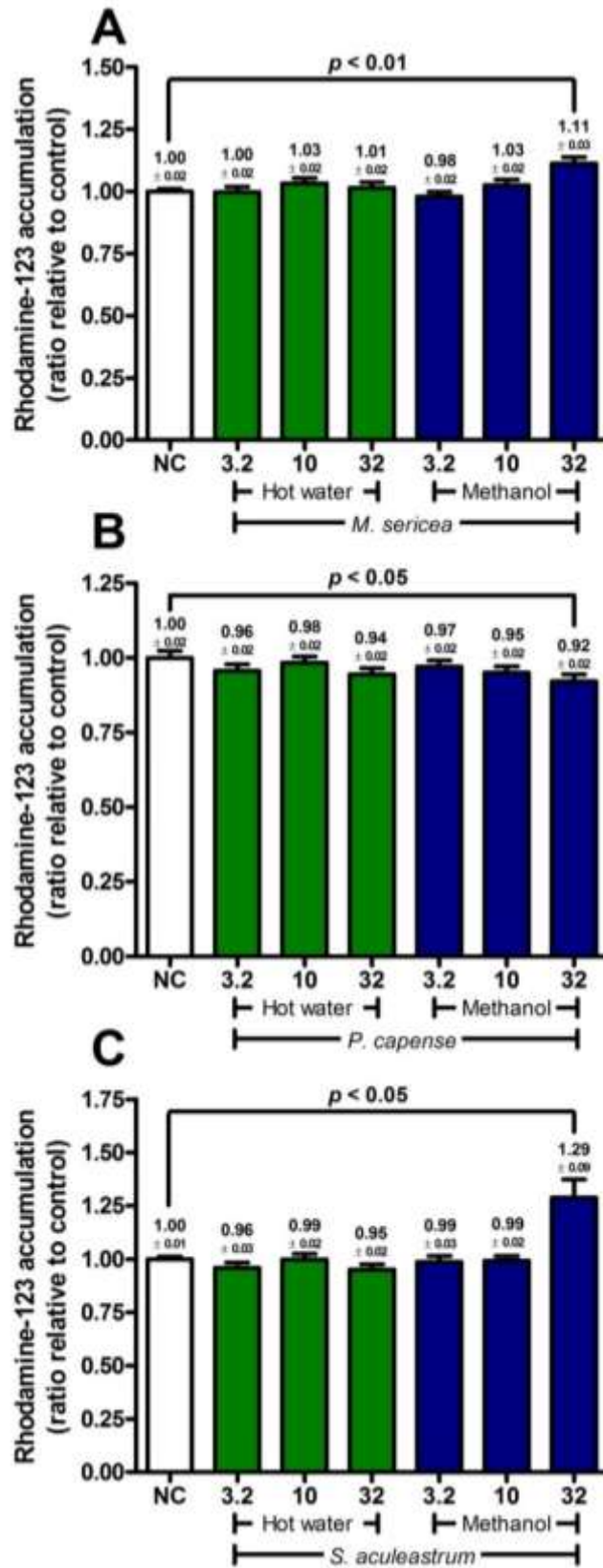


**Figure 60:** Effect of crude extracts of A) *M. sericea*, B) *P. capense* and C) *S. aculeastrum* on Rh-123 accumulation in HepG2 cells. Significance was determined against the negative control.

The crude extracts that resulted in a significant change in P-gp activity were evaluated for their effects on nevirapine transport across a Caco-2 cell monolayer using the bi-directional permeability assay. Analysis was performed using a LC-MS/MS quantitative method on apical-to-basolateral and basolateral-to-apical samples. These samples were taken from cells displaying a Lucifer yellow rejection  $\geq 98\%$ , indicating intact monolayer qualities. A 5 min chromatographical run was used to assess samples (Figure 61) in comparison to a six-point calibration curve ( $r^2 = 0.9968$ ) (Figure 62). Intra- and interday variability, as well as recovery, was in acceptable ranges ( $\pm 15 - 20\%$ ). The signal-to-noise ratio was  $\geq 13$  at the lowest concentration tested (12.5 nM).

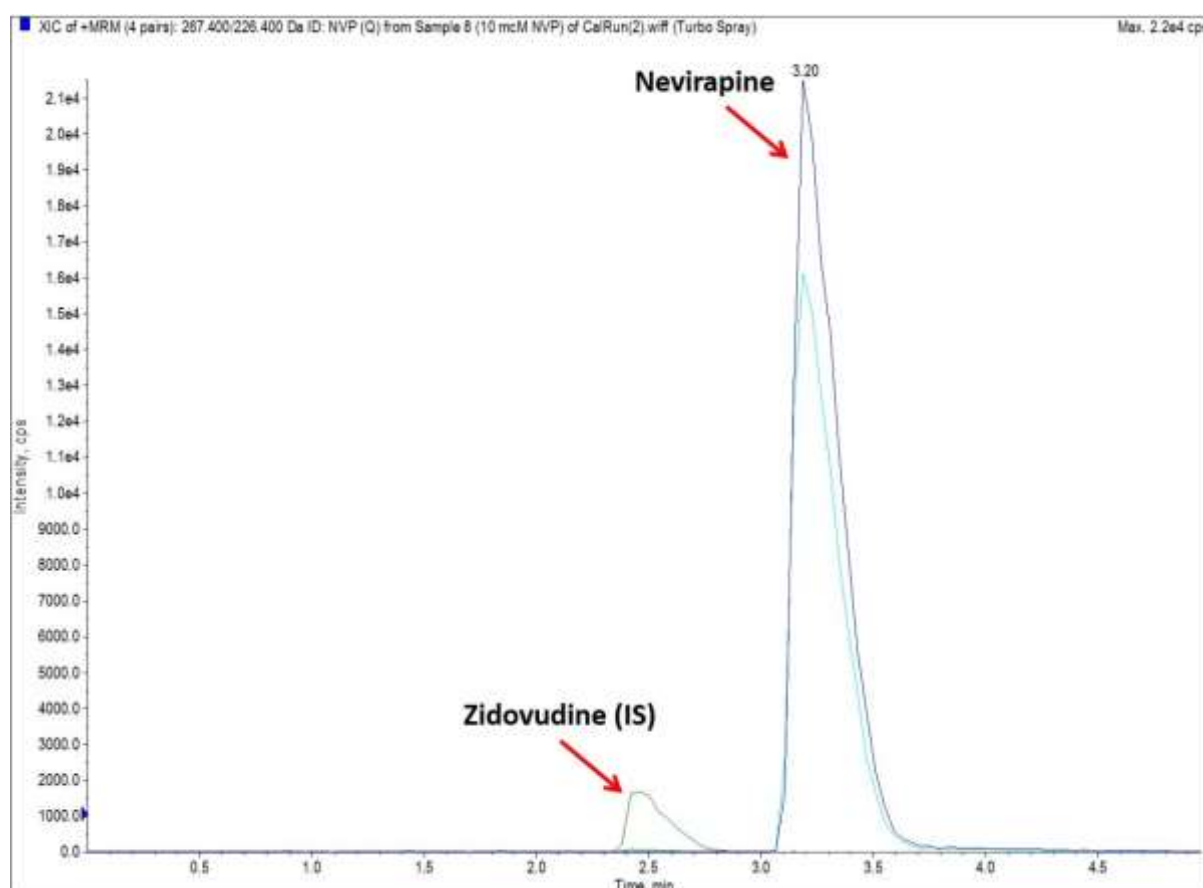


**Figure 61:** Chromatogram of nevirapine (10  $\mu\text{M}$ )

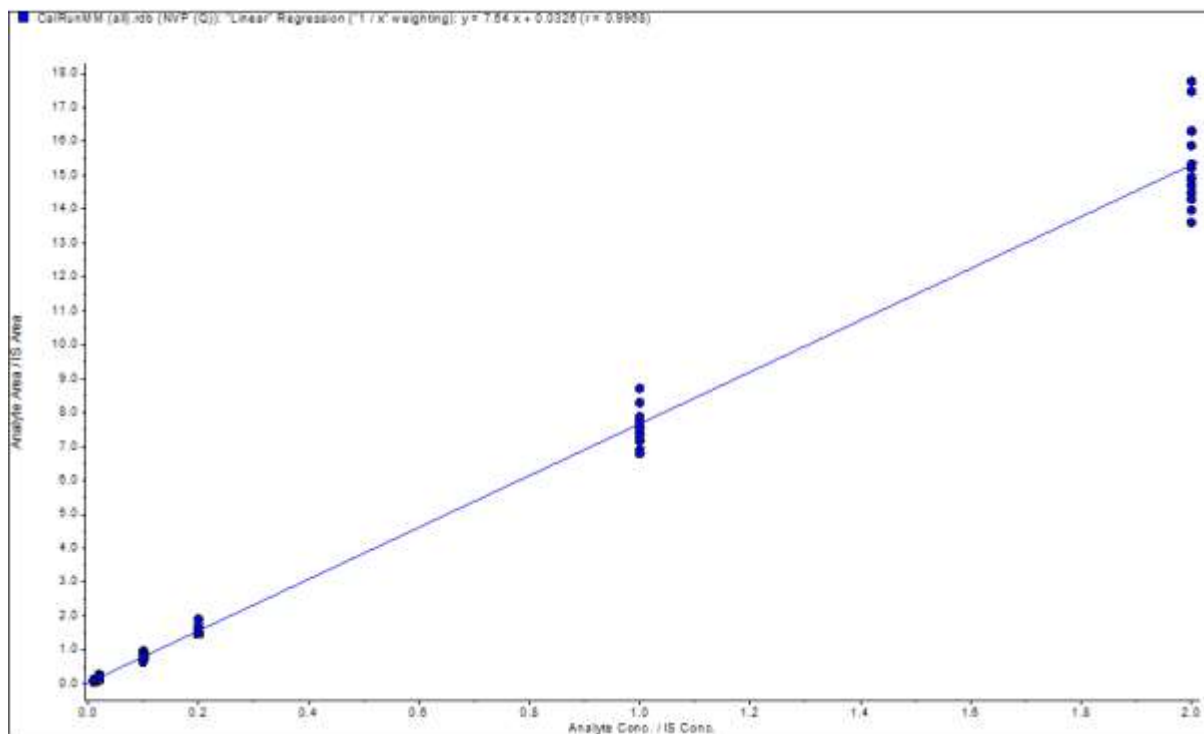
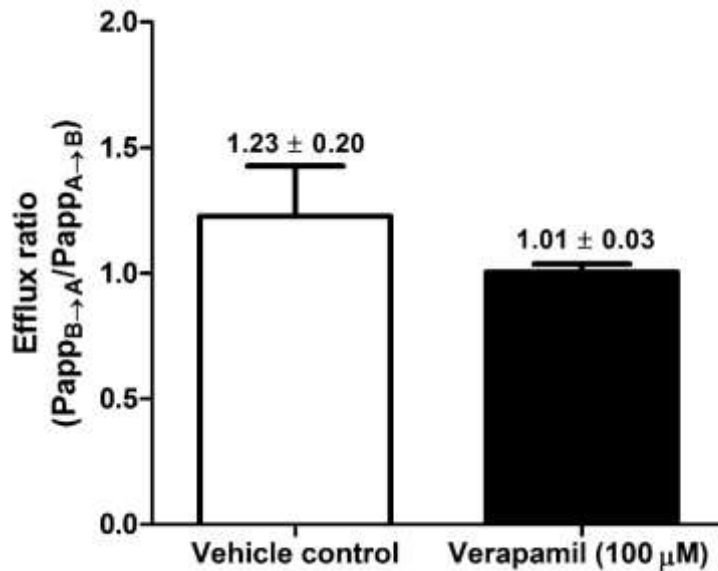


Figure 62: Calibration curve of nevirapine

### 5.3.2. Alteration to nevirapine efflux in Caco-2 bidirectional assay

Although not statistically significant, nevirapine efflux (1.23) was reduced after exposure to verapamil-pretreated cells (1.01, Figure 63). The hot water extract of *B. africana* and *S. latifolius*, as well as the methanol extracts of *R. caffra* and *S. aculeastrum* displayed a dose-dependent decrease in nevirapine efflux. *S. aculeastrum* at 32  $\mu\text{g}/\text{mL}$  induced the most prominent effect (0.64) ( $p < 0.05$ , Figure 64). At 10  $\mu\text{g}/\text{mL}$ , these extracts did not display any effect compared to the vehicle control. The methanol extract of *M. sericea*, however, reduced efflux at both 10  $\mu\text{g}/\text{mL}$  (0.94) and 32  $\mu\text{g}/\text{mL}$  (1.06), though the effect was more pronounced at the lower concentration.



**Figure 63:** Nevirapine efflux ratio in verapamil-pretreated cells

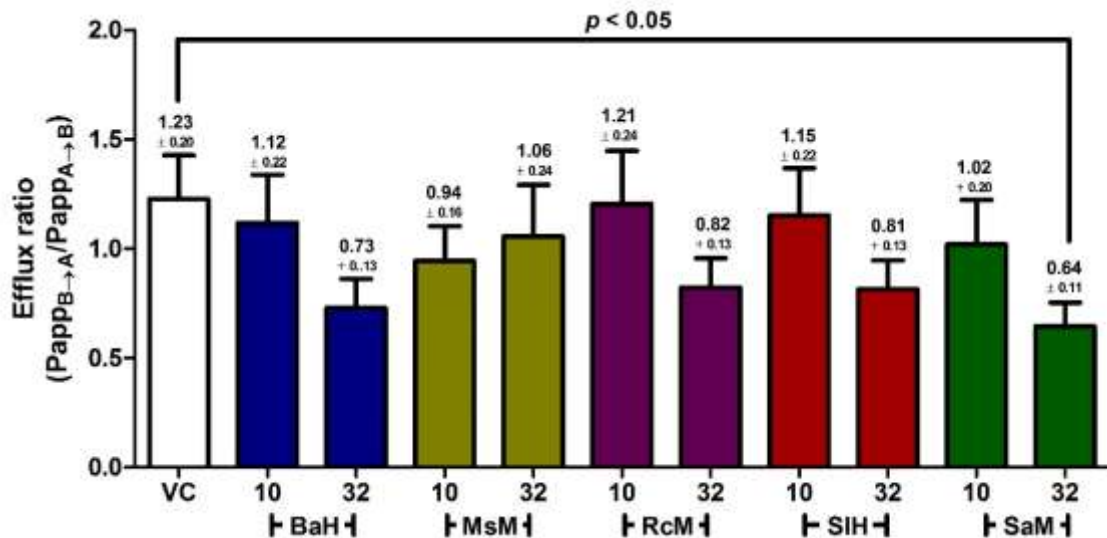


**Figure 64:** Nevirapine efflux ratio in crude extract-pretreated cells; VC: vehicle control; BaH: *B. africana* hot water extract, MsM: *M. sericea* methanol extract, RcM: *R. caffra* methanol extract, SIH: *S. latifolius* hot water extract, and SoM: *S. aculeastrum* methanol extract.

### 5.3.3. CYP450 inhibitory activity

The positive controls for inhibitors of CYP450 activity, tranlycypromine, quinidine and ketoconazole inhibited CYP2B6, CYP2D6 and CYP3A4 by 86.78%, 95.43% and

95.45%, respectively (Figure 65). Furthermore, IC<sub>50</sub> values for tranylcypromine, quinidine and ketoconazole were 8.00 μM (1.07 μg/mL), 18.71 nM (6.07 ng/mL) and 30.00 nM (1.59 ng/mL), respectively (Table 38). Vehicle controls altered CYP450 activity, inhibiting CYP2B6 and CYP3A4 by 16.24% and 35.66%, respectively. CYP2D6 activity was increased by 12.70% (Figure 65).

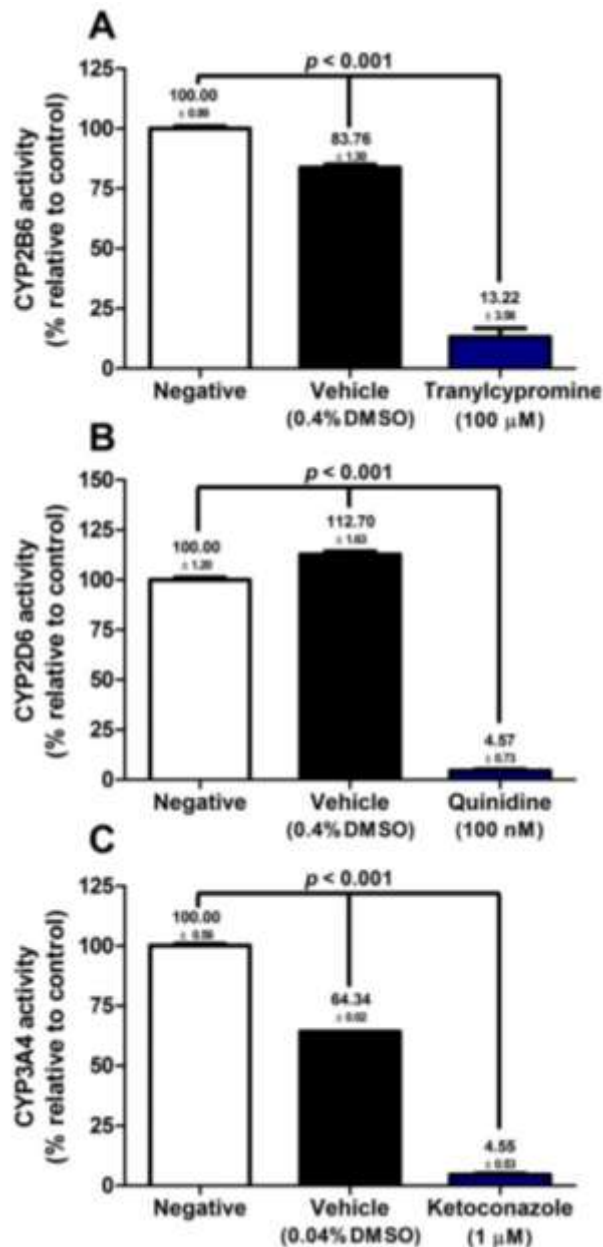


**Figure 65:** Controls for the CYP450 inhibitory activity assay indicating A) CYP2B6, B) CYP2D6 and C) CYP3A4 activity.

Crude extracts displayed variability in their potency against CYP450 enzymes (Table 38). Ten extracts displayed inhibitory activity greater than 50% against CYP2B6, and nine against CYP2D6. Of the ten crude extracts, six displayed prominent CYP2B6 inhibitory activity in the low microgram per milliliter range ( $IC_{50}$  between 3  $\mu\text{g}/\text{mL}$  and 6  $\mu\text{g}/\text{mL}$ ): both extracts of *B. africana*, the hot water extract of *T. sericea* and methanol extracts of *P. capense*, *T. elegans* and *Z. mucronata*. Of the nine extracts that were shown to possess activity against CYP2D6, six had noteworthy activity ( $IC_{50} \leq 30$   $\mu\text{g}/\text{mL}$ ), with five presenting with  $IC_{50}$ 's  $\leq 15$   $\mu\text{g}/\text{mL}$ : both extracts of *B. africana*, the hot water extract of *T. sericea* and methanol extracts of *T. elegans* and *Z. mucronata*. Furthermore, the extracts of *B. africana* and methanol extract of *T. elegans* displayed half-maximal activity between 3  $\mu\text{g}/\text{mL}$  and 5  $\mu\text{g}/\text{mL}$ . Due to the significant ( $p < 0.001$ ) interference induced by the vehicle control against CYP3A4, methanol extracts were not tested above 11.11  $\mu\text{g}/\text{mL}$ . Twenty six extracts displayed noteworthy inhibitory activity (defined as an  $IC_{50} < 30$   $\mu\text{g}/\text{mL}$ , or activity  $> 40\%$  at 11.11  $\mu\text{g}/\text{mL}$ ) against CYP3A4, with *T. elegans* presenting with an  $IC_{50}$  below  $< 1.2$   $\mu\text{g}/\text{mL}$  (55.21% inhibition at 1.2  $\mu\text{g}/\text{mL}$ ). Across all three enzyme systems, both extracts of *B. africana*, the hot water extract of *T. sericea* and the methanol extracts of *T. elegans* and *Z. mucronata* displayed prominent inhibitory activity. Inhibitory activity tended to follow a trend of CYP3A4  $>$  CYP2B6  $>$  CYP2D6. Methanol extracts were more active than hot water extracts against CYP2B6 and CYP3A4, though hot water tended to display greater activity than the methanol extracts against CYP2D6 activity.

## 5.4. Discussion

### 5.4.1. P-glycoprotein inhibitory activity and altered nevirapine permeation

Accumulation of Rh-123 in cells in the presence of a xenobiotic is characteristic of P-gp efflux inhibitors (Figure 58), such as verapamil.<sup>496,497</sup> As verapamil induced an increase in Rh-123 fluorescence, the assay was deemed to perform as expected. Verapamil also reduced the efflux of nevirapine slightly, indicating a possible involvement of P-gp. It has been suggested that nevirapine absorption occurs via passive diffusion,<sup>480,482</sup> though active efflux transporters, such as P-gp and MRP, may hinder accumulation in unaffected physiological systems.<sup>13,483,484</sup> Taking into account

**Table 38:** CYP450 inhibitory activity of crude extracts expressed as the IC<sub>50</sub> values, and percentage inhibition of the methanol extracts against CYP3A4.

Plant	Extract	IC <sub>50</sub> ± SEM (µg/mL)			CYP3A4 inhibition at 11.11 µg/mL methanol extract (%)
		CYP2B6	CYP2D6	CYP3A4	
<i>A. oppositifolia</i>	Hot water	>100	>100	<b>24.69 ± 1.13</b>	N/A
	Methanol	>100	>100	<b>9.15 ± 1.38</b>	59.15 ± 1.05
<i>B. disticha</i>	Hot water	>100	56.00 ± 1.36	95.41 ± 1.15	N/A
	Methanol	>100	>100	<b>11.48 ± 1.27</b>	52.3 ± 1.58
<i>B. africana</i>	Hot water	<b>4.03 ± 1.17</b>	<b>4.71 ± 1.08</b>	<b>3.66 ± 1.2</b>	N/A
	Methanol	<b>3.51*</b>	<b>3.39*</b>	<b>2.72 ± 1.76</b>	90.83 ± 1.8
<i>C. lauroleola</i>	Hot water	>100	>100	36.92 ± 1.08	N/A
	Methanol	48.24 ± 1.08	77.61 ± 1.49	>12	43.3 ± 2.2
<i>C. bulbispermum</i>	Hot water	>100	>100	<b>12.21 ± 1.63</b>	N/A
	Methanol	>100	>100	<b>7.08 ± 2.22</b>	69.37 ± 10.65
<i>L. leonurus</i>	Hot water	>100	>100	<b>9.74 ± 1.85</b>	N/A
	Methanol	39.44 ± 1.85	>100	<b>5.93 ± 1.02</b>	73.06 ± 0.19
<i>M. oleifera</i>	Hot water	>100	>100	<b>12.33 ± 1.77</b>	N/A
	Methanol	>100	>100	<b>7.06 ± 3.21</b>	69.61 ± 13.95
<i>M. sericea</i>	Hot water	>100	>100	>100	N/A
	Methanol	<b>2.29*</b>	>100	<b>1.98 ± 2.23</b>	90.8 ± 0.02
<i>P. capense</i>	Hot water	>100	>100	<b>14.60 ± 1.13</b>	N/A
	Methanol	<b>3.29 ± 2.53</b>	<b>29.58 ± 1.09</b>	<b>5.28 ± 1.14</b>	75.85 ± 1.33
<i>R. caffra</i>	Hot water	>100	>100	<b>3.70 ± 1.82</b>	N/A
	Methanol	>100	>100	<b>6.73 ± 1.39</b>	59.82 ± 1.51
<i>R. lancea</i>	Hot water	>100	65.18 ± 1.13	38.30 ± 1.09	N/A
	Methanol	38.24 ± 1.06	>100	<b>9.43 ± 1.22</b>	57.96 ± 1.75
<i>S. puniceus</i>	Hot water	>100	>100	>100	N/A
	Methanol	>100	>100	>12	35.33 ± 0.93
<i>S. latifolius</i>	Hot water	>100	>100	53.72 ± 1.16	N/A
	Methanol	>100	>100	>12	41.92 ± 1.46
<i>S. aculeastrum</i>	Hot water	>100	>100	<b>17.70 ± 1.10</b>	N/A
	Methanol	>100	>100	>12	35.75 ± 0.78
<i>T. elegans</i>	Hot water	>100	>100	38.46 ± 1.09	N/A
	Methanol	<b>3.45*</b>	<b>5.06 ± 1.10</b>	<b>&lt;1.2</b>	87.72 ± 1.12
<i>T. sericea</i>	Hot water	<b>4.78 ± 1.08</b>	<b>12.47 ± 1.07</b>	<b>9.35 ± 1.12</b>	N/A
	Methanol	>100	>100	<b>6.72 ± 1.64</b>	67.82 ± 2.47
<i>Z. mucronata</i>	Hot water	32.97 ± 1.24	>100	<b>13.67 ± 1.31</b>	N/A
	Methanol	<b>6.04 ± 1.98</b>	<b>14.88 ± 1.63</b>	<b>4.07 ± 1.19</b>	88.75 ± 1.17
Tranlycypromine (µM)		<b>8.00 ± 1.10</b>	N/A	N/A	N/A
Quinidine (nM)		N/A	<b>18.71 ± 1.09</b>	N/A	N/A
Ketoconazole (nM)		N/A	N/A	<b>30.00 ± 1.08</b>	N/A

\* – Ambiguous data fit; N/A – not applicable

the results of the P-gp inhibitory and bidirectional permeability assays it is suggested that P-gp-mediated efflux may not be a primary contributor to reduced nevirapine accumulation. A substrate with greater efflux ratio (>2), such as digoxin or quinidine, would have been more appropriate for assessment of bidirectional permeability. However, it does provide a risk that is apparent with nevirapine.

Only six extracts affected P-gp functioning in the Caco-2 and HepG2 cell lines, with the methanol extract of *S. aculeastrum* displaying activity in both cell lines (Figure 59). The effects on Rh-123 accumulation was only significant at 32 µg/mL. To confirm whether this effect would alter drug absorption, nevirapine apical-to-basolateral flux was assessed using these extracts, excluding *P. capense* as it did not show activity in the Caco-2 cell line. Contrary to what was expected, the hot water extracts of *B. africana* and *S. latifolius*, as well as the methanol extracts of *M. sericea*, *R. caffra* and *S. aculeastrum*, all increased nevirapine accumulation (Figure 64). It is important to note that except for *M. sericea* and *S. aculeastrum*, all other extracts increased P-gp-mediated efflux of Rh-123, thus an increase in nevirapine efflux was expected. At 32 µg/mL, the hot water extracts of *B. africana* and *S. latifolius*, and the methanol extracts of *R. caffra* and *S. aculeastrum*, reduced nevirapine efflux. The greatest effect was induced by *S. aculeastrum*, similar to the pronounced inhibition displayed in the P-gp inhibitory assay. The methanol extract of *M. sericea* had slightly greater activity in increasing nevirapine accumulation at 10 µg/mL compared to 32 µg/mL.

To the best of the authors' knowledge very little information is available on the effect of crude extracts of African herbal remedies on P-gp function in cells. Due to the short incubation time used for this assay, alterations in P-gp expression was not considered as a potential mechanism. The hot water extracts of *B. africana* and *S. latifolius*, and methanol extracts of *R. caffra* and *P. capense* increased P-gp-mediated Rh-123 efflux, suggesting an induction of transporter functioning. It has been reported that inhibition of protein kinase C promotes P-gp activity,<sup>498</sup> and thus this may be a likely route of activation. The methanol extracts of *S. aculeastrum* and *M. sericea* inhibited P-gp function. This may most likely be via diminished ATPase activity<sup>499</sup> or structural instability due to alterations in membrane viscosity.<sup>484</sup> Membrane fluidity influences drug permeation due to changes to membrane-bound transporters and creation of porosities.<sup>284,500</sup> Altering membrane fluidics have severe implications on membrane transporters, enzyme and receptor functioning, endocytosis, and may alter susceptibility to cytotoxins.<sup>501</sup> Increasing membrane fluidity has been shown to have differential effects on intracellular absorption of molecules, such as increasing permeation and accumulation.<sup>501</sup> It is thus likely that *S. aculeastrum* and *M. sericea* increased intracellular Rh-123 accumulation due to an increased uptake and/or inhibition of active efflux following changes to membrane fluidics or transporter activity.

No information is available on the P-gp modulatory activity of *B. africana*, however a myriad of literature was obtained concerning its phytochemicals contradicting the effects observed. Flavonoids have been shown to induce membrane stabilisation,<sup>502–504</sup> while inhibiting P-gp,<sup>505–507</sup> suggesting that intracellular Rh-123 accumulation should have occurred. It is of course prudent to suggest that the phytochemical matrix may be producing differential effects, thereby antagonising the inhibitory activity. Similar to *B. africana*, literature does not indicate P-gp stimulatory activity induced by *P. capense* and *R. caffra*. Piperine (present in *P. capense*)<sup>508</sup> and yohimbine-analogues (similar to those identified in *R. caffra*)<sup>509</sup> have been described to increase P-gp expression, though this would not take place within the short incubation time of the present study. Although these compounds have been shown to inhibit P-gp, it may cause upregulation through a feedback mechanism.<sup>508</sup> Literature on the P-gp modulatory activity of *S. latifolius* could not be found, however retrorsine has been shown to be a weak substrate of P-gp, although it does not inhibit it.<sup>510</sup>

P-gp inhibitory activity of plants containing steroidal alkaloids, such as those from the Solanaceae family, has been reported. A methanol extract of *S. aculeastrum* reduced P-gp function in both cancerous and non-cancerous cell lines, though only at  $\geq 32$   $\mu\text{g/mL}$ .<sup>511</sup> An ethanol extract of *S. trilobatum* was found to decrease P-gp activity by 55% in the Caco-2 cell line, although this occurred at 300  $\mu\text{g/mL}$ ,<sup>496</sup> which would be considered unfeasible. In an *in vivo* case report, ivermectin toxicosis was described in horses fed *S. eleagnifolium*- and *S. dimidatum*-contaminated hay. This was thought to be mediated by P-gp inhibition, leading to ivermectin accumulation, confirmed by experimentation.<sup>512</sup> Steroidal alkaloids, such as solamargine, offer some insight in the activity of these plants. Solamargine, which was identified in *S. aculeastrum* fractions prepared from the same plant material in-house, reduced P-gp activity *in vitro*.<sup>511</sup> Furthermore, solamargine is capable of reducing expression of P-gp through down-regulation of *MDR-1* genes and actin disruption.<sup>450</sup> It is likely that solamargine is the primary contributor of P-gp inhibitory activity of the methanol extract of *S. aculeastrum*. This inhibition of P-gp activity is most likely the reason for the observed increase in intracellular nevirapine concentrations. This may potentially be via diminished ATPase activity<sup>499</sup> or shutting down of transporter function due to altered membrane fluidics<sup>484</sup> inducing conformational changes in protein or binding site structures.<sup>499</sup> Phytochemicals may directly inhibit ATPase activity, or act competitively as substrates

for P-gp, reducing the efflux of lower-affinity substrates.<sup>513</sup> As *S. aculeastrum* was shown to reduce ATP levels (Chapter 4), it is possible that depletion of cellular energy reduces the functionality of P-gp, however as the incubation time was short this mechanism may be unlikely as an acute contributor. Although only measured after 24 h, *S. aculeastrum* resulted in high levels of necrosis in HepG2 cells (Chapter 4), thus it is conceivable that alterations to membranes, such as increased fluidity, porosity and ultimate cytolysis, may have been incurred. Reductions of membrane viscosity would explain the increase of nevirapine accumulation by facilitating passive diffusion or inhibition of extrusion.<sup>500</sup> As stated earlier, solamargine is the most likely contributor to P-gp inhibitory activity, however, the potential activity of other phytochemicals cannot be disregarded. Saponins act as surfactants by complexing with cholesterol in the plasma membrane, thus inducing aggregation, pore-formation, membrane fluidisation and permeabilisation. Surface-activity is modulated by their amphiphilic nature due to a lipophilic aglycone and hydrophilic sugar chain.<sup>56,219</sup> Effects are largely dependent on the size of the porosities formed.<sup>514</sup> Surfactant-like molecules are known to interfere with membrane stability and the cytoskeleton, and thus may cause membrane lysis and solubilisation.<sup>515,516</sup> Saponins may thus aid in increasing the permeation of molecules into the intracellular compartment<sup>219</sup> through ease of passive diffusion, opening of tight junctions and inhibition of active efflux.<sup>481,517–519</sup> These effects are however dependent on the nature of the chemical entities.<sup>520</sup>

*M. sericea* produced a slight reduction in efflux potential at 10 µg/mL, however the P-gp inhibitory activity was only present at 32 µg/mL. This suggests that the effect was not mediated by P-gp, and rather that a separate mechanism is at play. As nevirapine is a substrate of MRP,<sup>484</sup> it is possible that non-P-gp efflux transporters may have been inhibited which would normally assist in extrusion thereof. A paradoxical effect was seen at 32 µg/mL, where activity was slightly decreased at higher concentrations. No literature could be found supporting the inhibitory activity of phytochemicals identified from *M. sericea*, however one study has supported the ability of certain rotenoids to inhibit BCRP.<sup>521</sup> Nevirapine, however, is not recognised as such a substrate, and thus it is unlikely that BCRP function was involved.

All other extracts tested reduced efflux at 32 µg/mL, through increased P-gp activity in the Rh-123 assay. Taking this into account it is possible that separate mechanisms of action may be interfering with the efflux of nevirapine or increasing the permeation

across the apical border, regardless of whether activity is stimulated. Altered membrane fluidics will increase nevirapine's passive diffusion rate, and will not necessarily reduce P-gp functionality depending on the level of alteration.<sup>516</sup> Alternative efflux pumps, such as MRP, may be inhibited, reducing the extrusion of nevirapine.<sup>484</sup>

Only one study could be found assessing the effect of herbal remedies on nevirapine absorption. Hot water extracts of *Hypoxis hemerocallidea* and *Sutherlandia frutescens* were found to increase the intestinal absorption of nevirapine in the Caco-2 bidirectional permeability assay. These extracts, as well as L-canavanine (a compound isolated from *S. frutescens*), reduced the P-gp-mediated efflux of nevirapine as indicated by an increase in apical-to-basal transport, which was higher than basal-to-apical transport.<sup>13</sup> This study is thus one of the few to add to the list of potentially interfering phytochemical mixtures with nevirapine.

#### 5.4.2. Inhibition of CYP450 enzymes

Positive controls for the three CYP450 enzymes assessed during the present study all resulted in the expected inhibitory activity. Unfortunately, vehicle controls altered enzyme activity, especially in the case of CYP3A4, however cognisance was taken of the implications of DMSO-mediated enzyme inhibition during analysis and interpretation. Methanol extracts were not soluble in acetonitrile and could not be concentrated beyond 25 mg/mL stock in DMSO. As such, for the CYP3A4 inhibitory assay, methanol extracts were capped at a maximum of 11.11 µg/mL, while hot water extracts could be assayed at higher concentrations due to their reconstitution in PBS.

Inhibition of the CYP450 enzyme system followed a trend of CYP3A4>CYP2B6>CYP2D6, suggesting that phytochemicals have higher binding affinity to CYP3A4. However, three cases of non-selective inhibition were observed, resulting in IC<sub>50</sub>'s in close range from one another: both extracts of *B. africana*, the hot water extract of *T. sericea* and methanol extract of *Z. mucronata*. This would suggest a structural commonality between the three enzyme systems that may be targeted by phytochemicals present in these extracts. This may be at a structurally-conserved site, such as the core, supporting the integrity of the enzyme.<sup>456,458</sup> Furthermore, the similar

activity between the hot water and methanol extract of *B. africana* suggests that extraction of a polar phytochemical matrix occurred in similar levels between the extraction solvent systems.

The high frequency of inhibition, as well as the potency of the extracts, against the CYP3A4 enzyme system is a cause for concern. CYP3A4 is known to contribute to the largest extent of xenobiotic metabolism, and as such may result in a clinically-significant drug-herb interaction should adequate concentration ranges be achieved. This effect was most prominent with the methanol extract of *T. elegans*, where as little as 6 mg extract (assuming full absorption and systemic fluid volume of 5 L) would be required to reach inhibitory concentrations. Taking into account the extraction yield, this would be achieved with an alcoholic tincture of 81.5 mg starting plant material.

To determine whether there was a risk for intestinal or systemic cytotoxicity, the same principle as described in Chapter 3 was used. Calculations were based on the volume of the gastrointestinal and systemic compartments, concentrations required and the extraction yields. Similar to before, it should be noted that these are based on the assumption of full dissolution and absorption, and they may not present with the most likely scenario *in vivo*. CYP3A4 is the most abundant CYP450 isoform in the gastrointestinal tract compared to CYP2B6 and CYP2D6,<sup>452</sup> and thus carries a high risk of being inhibited. Importantly, as CYP450's are highly different between individuals, although retaining a similar basic structure, it should be expected that degree of inhibitory activity between them would also be subject to whether it is related to binding of a common element.

Eleven (three hot water and eight methanol) and seven (two hot water and five methanol) extracts appear to carry a risk of inhibiting intestinal and hepatic CYP2B6 enzymes, respectively (Table 39). Decreased metabolism in the gut may increase bioavailability of drugs such as efavirenz, nevirapine, bupropion and ketamine, which will increase plasma concentrations due to reduced hepatic conversion. This in turn may likely increase the occurrence of adverse effects. Important to note is the ability of the hot water extract of *B. africana* and methanol extract of *M. sericea* to also reduce nevirapine efflux at higher concentrations of the extract. This will further compound the increasing plasma concentration and increase the associated risk.

**Table 39:** Plants that carry a risk of inhibiting intestinal or hepatic CYP2B6, including amount of extract and plant material required (assuming full dissolution and absorption).

Extracts with a risk of inhibiting intestinal and hepatic CYP2B6 enzymes							
Intestinal enzymes				Hepatic enzymes			
Crude extract		Extract needed to reach IC <sub>50</sub> (mg)	Plant material required to reach mass (mg)	Crude extract		Extract needed to reach IC <sub>50</sub> (mg)	Plant material required to reach mass (mg)
<i>B. africana</i>	HW	0.60	3.80	<i>B. africana</i>	HW	20.15	126.73
	MeOH	0.53	1.63		MeOH	17.55	54.25
<i>C. laureola</i>	MeOH	724	27.19	<i>M. sericea</i>	MeOH	11.45	46.81
<i>L. leonurus</i>	MeOH	5.92	49.34	<i>P. capense</i>	MeOH	16.45	189.30
<i>M. sericea</i>	MeOH	0.34	1.40	<i>T. elegans</i>	MeOH	17.25	234.38
<i>P. capense</i>	MeOH	0.49	5.68	<i>T. sericea</i>	HW	23.90	314.89
<i>R. lancea</i>	MeOH	5.74	103.35	<i>Z. mucronata</i>	MeOH	30.20	439.59
<i>T. elegans</i>	MeOH	0.52	7.03				
<i>T. sericea</i>	HW	0.72	9.45				
<i>Z. mucronata</i>	HW	4.95	104.12				
	MeOH	0.91	13.19				

HW – hot water; MeOH – methanol.

Nine (four hot water and five methanol) and six (two hot water and four methanol) extracts carry a risk of inhibiting intestinal and hepatic CYP2D6 enzymes, respectively (Table 40). Decreased metabolism in the gut and liver may increase plasma concentrations and adverse effects of drugs such as codeine and haloperidol.

**Table 40:** Plants that carry a risk of inhibiting intestinal or hepatic CYP2D6, including amount of extract and plant material required (assuming full dissolution and absorption)

Extracts with a risk of inhibiting intestinal and hepatic CYP2D6 enzymes							
Intestinal enzymes				Hepatic enzymes			
Crude extract		Extract needed to reach IC <sub>50</sub> (mg)	Plant material required to reach mass (mg)	Crude extract		Extract needed to reach IC <sub>50</sub> (mg)	Plant material required to reach mass (mg)
<i>B. disticha</i>	HW	8.40	54.12	<i>B. africana</i>	HW	23.55	148.11
<i>B. africana</i>	HW	0.71	4.44		MeOH	16.95	52.40
	MeOH	0.51	1.57	<i>P. capense</i>	MeOH	147.90	1701.96
<i>C. laureola</i>	MeOH	11.64	43.75	<i>T. elegans</i>	MeOH	25.30	343.75
<i>P. capense</i>	MeOH	4.44	51.06	<i>T. sericea</i>	HW	62.35	821.48
<i>R. lancea</i>	HW	9.78	130.71	<i>Z. mucronata</i>	MeOH	74.40	1082.97
<i>T. elegans</i>	MeOH	0.76	10.31				
<i>T. sericea</i>	HW	1.87	24.64				
<i>Z. mucronata</i>	MeOH	2.23	32.49				

Twenty-eight (fifteen hot water and thirteen methanol) and twenty-three (ten hot water and thirteen methanol) extracts carry a risk of inhibiting intestinal and hepatic CYP3A4 enzymes, respectively (Table 41). CYP3A4 enzyme inhibition carries a great risk of reducing the metabolic profiles of most of the drugs used concurrently, and thus may increase the adverse effect profiles of compounds such as artemether, lumefantrine and quinine.<sup>470</sup> As with CYP2B6, the hot water extract of *B. africana*, and methanol extracts of *M. sericea* and *R. caffra*, may increase the bioavailability of nevirapine by both inhibiting metabolism and efflux. As two enzymes systems are affected, extracts of *B. africana* and *M. sericea* carry a dual risk of affecting nevirapine.

The mechanism of inhibition was not deduced in the current project, and thus inferences cannot be made with regards to competitive, non-competitive, mixed or irreversible-inhibition. Enzyme inhibition may occur at any number of sites on the CYP450 enzyme, such as the substrate-binding sites or structurally-conserved sites, such as the heme core.<sup>456,458,522</sup> Taking pharmacogenetic data into account it is evident that large proportions of the African communities are at risk of possessing an allele of CYP2B6, CYP2D6 (Table 33) or CYP3A4 (Table 34) with reduced functionality. If these extracts were to be administered to individuals with already reduced CYP450 enzyme activity, further inhibition may exacerbate their pharmacokinetic profiles and lead to higher prevalence of adverse effects.

Literature concerning the CYP450 inhibitory activity of *A. oppositifolia*, *B. disticha*, *B. africana*, *C. laureola*, *C. bulbispermum*, *L. leonurus*, *M. sericea*, *R. caffra*, *S. puniceus*, *S. latifolius* and *T. elegans* could not be found, including species related to the genus.

#### 5.4.2.1. Amaryllidaceae

Appreciable activity was observed for the methanol extract of *B. disticha* and both extracts of *C. bulbispermum*, with IC<sub>50</sub>'s < 12 µg/mL. No literature could be found on species of *Boophane*, *Crinum* and *Scadoxus* relating to CYP450 modulatory activity, and neither could their isolated compounds. Other Amaryllidaceae-derived isoquinoline-alkaloids have been shown to inhibit CYP450 enzymes, however the greatest inhibitory activity was towards CYP2D6 and CYP3A4.<sup>523</sup> The results obtained in the present study are similar to that described by Salminen *et al.*<sup>523</sup>

**Table 41:** Plants that carry a risk of inhibiting intestinal or hepatic CYP3A4, including amount of extract and plant material required (assuming full dissolution and absorption).

Extracts with a risk of inhibiting intestinal and hepatic CYP3A4 enzymes							
Intestinal enzymes				Hepatic enzymes			
Crude extract		Extract needed to reach IC <sub>50</sub> (mg)	Plant material required to reach mass (mg)	Crude extract		Extract needed to reach IC <sub>50</sub> (mg)	Plant material required to reach mass (mg)
<i>A. oppositifolia</i>	HW	3.70	61.01	<i>A. oppositifolia</i>	HW	123.45	2033.77
	MeOH	1.37	16.92		MeOH	45.75	564.12
<i>B. disticha</i>	HW	14.31	92.21	<i>B. disticha</i>	MeOH	57.40	604.85
	MeOH	1.72	18.15	<i>B. africana</i>	HW	18.30	115.09
<i>B. africana</i>	HW	0.55	3.45		MeOH	13.60	42.04
	<i>C. laureola</i>	MeOH	0.41	1.26	<i>C. bulbispermum</i>	HW	61.05
HW		5.54	24.08	MeOH		35.40	550.54
<i>C. bulbispermum</i>	HW	1.83	27.54	<i>L. leonurus</i>	HW	48.70	375.48
	MeOH	1.06	16.52		MeOH	29.65	247.29
<i>L. leonurus</i>	HW	1.46	11.26	<i>M. oleifera</i>	HW	61.65	273.27
	MeOH	0.89	7.42		MeOH	35.30	135.40
<i>M. oleifera</i>	HW	1.85	8.20	<i>M. sericea</i>	MeOH	9.90	40.47
	MeOH	1.06	4.06	<i>P. capense</i>	HW	73.00	1508.26
<i>M. sericea</i>	MeOH	0.30	1.21		MeOH	26.40	303.80
<i>P. capense</i>	HW	2.19	45.25	<i>R. caffra</i>	HW	18.50	315.70
	MeOH	0.79	9.11		MeOH	33.65	505.26
<i>R. caffra</i>	HW	0.56	9.47	<i>R. lancea</i>	MeOH	47.15	849.55
	MeOH	1.01	15.16	<i>S. aculeastrum</i>	HW	88.50	641.30
<i>R. lancea</i>	HW	5.75	76.80	<i>T. elegans</i>	MeOH	<6.00	<81.52
	MeOH	1.41	25.49	<i>T. sericea</i>	HW	46.75	615.94
<i>S. latifolius</i>	HW	5.64	62.81		MeOH	33.60	253.39
<i>S. aculeastrum</i>	HW	2.66	19.24	<i>Z. mucronata</i>	HW	68.35	1438.95
<i>T. elegans</i>	HW	5.77	52.93		MeOH	20.35	296.22
	MeOH	<0.18	<2.45				
<i>T. sericea</i>	HW	1.40	18.48				
	MeOH	1.01	7.60				
<i>Z. mucronata</i>	HW	2.05	43.17				
	MeOH	0.61	8.89				

HW – hot water; MeOH – methanol. As the methanol extracts of *C. laureola*, *S. puniceus*, *S. latifolius* and *S. aculeastrum* could not be tested at concentrations higher than 12 µg/mL, estimations were not done. It should however be taken as a potential risk when comparing these with the respective hot water extract's activity.

#### 5.4.2.2. Anacardiaceae

Extracts of *R. lancea* displayed an alternative inhibitory profile depending on the extract-type and CYP450 isoform. Although the inhibitory effects were not regarded as potent, the methanol extract inhibited CYP2B6 activity, but not CYP2D6 activity. Conversely, the hot water extract displayed activity against CYP2D6, though not CYP2B6. This effect appears to indicate that a different phytochemical matrix is present in each extract, and therefore selectivity is different. CYP3A4 was notably affected by the methanol extract, with the hot water extract presenting with lower activity. An aqueous *R. verniciflua* extract was described as a potent inhibitor of CYP1A2, CYP2C9 and CYP2C19, with negligible inhibition of CYP2D6 or CYP3A4.<sup>524</sup> Flavonoids, such as myricetin, kaempferol and quercetin are known to inhibit CYP450 activity. Myricetin displays noteworthy activity against CYP3A4,<sup>525</sup> which may be due to non-competitive inhibition,<sup>526</sup> however the latter was determined at concentrations which are most likely non-physiological. Kaempferol has been found to decrease CYP2D6<sup>527</sup> and CYP3A4 activity.<sup>527,528</sup> Quercetin has been shown to inhibit CYP2D6 and CYP3A4 in a competitive fashion.<sup>529</sup> Varying levels and ratios of these phytochemicals may result in a mixture of inhibitory profiles between the two extracts.

#### 5.4.2.3. Apocynaceae

While the hot water extract of *A. oppositifolia* had a moderate inhibitory activity towards CYP3A4 ( $IC_{50} = 25 \mu\text{g/mL}$ ), the methanol extract was a more potent inhibitor. Although no literature could be found to support the inhibitory pattern, it is suggested that alcohol-soluble phytochemicals may be contributing to the greater activity seen in the methanol extract.

The hot water extract of *R. caffra* presented with potent inhibitory activity against CYP3A4, with the methanol extract being slightly less active. Polar, hydrophilic molecules may be contributing towards the activity spectrum noted. Yohimbine,<sup>530</sup> ajmaline<sup>531</sup> and ajmalicine<sup>532</sup> are potent inhibitors of CYP2D6, while the ajmalicine is less active against CYP3A4.<sup>532</sup> As no inhibition against CYP2D6 was observed, it may be that phytochemical concentrations were too low to induce these effects, or alternatively antagonistic effects between chemical entities could have reduced

inhibitory potential. The compounds responsible for CYP3A4 inhibition are thus unknown.

The methanol extract of *T. elegans* had a potent, non-selective inhibitory profile against all three CYP450 isoforms tested, with the greatest effect against the CYP3A4 isoform. No literature supporting this effect could be found, however one can argue that a similar structural moiety between these three CYP450 isoforms were targeted.

#### 5.4.2.4. Asteraceae

*C. laureola* did not present with high inhibitory potential, and no literature could be obtained to corroborate this. A risk of CYP2B6 and CYP3A4 inhibitory activity is evident for the methanol and hot water extract, respectively.

No prominent inhibitory activity was displayed for *S. latifolius*. Retrorsine<sup>533,534</sup> and senecionine<sup>533</sup> have been described as being substrates for CYP2B6, CYP2D6 and CYP3A4. It is possible that concentrations were not sufficient to induce any noteworthy competitive inhibitory activity.

#### 5.4.2.5. Combretaceae

The hot water extract of *T. sericea* displayed non-selective inhibition of all three CYP isoforms investigated, with activity between 4.78 µg/mL and 12.47 µg/mL and potency increasing from CYP2B6>CYP3A4>CYP2D6. It is possible that the phytochemicals in the extracts may be affecting a site common between all three isoforms (such as a structural core), or that the phytochemical matrix may be structurally-variable enough to elicit activity in these isoforms.<sup>456,458</sup> The methanol extract, however, was inactive against both the CYP2B6 and CYP2D6 isoforms, only eliciting activity (greater than the hot water extract) against the CYP3A4 isoform. The methanol extract displayed higher selectivity than that of the hot water extract. Different *Terminalia* spp. have been found to display a mixed panel of inhibition. *T. chebula*<sup>535,536</sup> and *T. bellerica*<sup>536</sup> have poor CYP450 inhibitory activity, whereas *T. arjuna* has been found to inhibit CYP2C9, CYP2D6 and CYP3A4 activity (IC<sub>50</sub>'s ranging between 16.6 µg/mL and 34.52 µg/mL).<sup>537</sup> The three main phytochemicals present in the plant; arjunic acid, arjunetin

and arjungenin, do not appear to be the bioactive molecules contributing to the inhibitory effect.<sup>537</sup> CYP3A4 expression profiles were not altered in mice administered a methylene chloride extract of *T. superba*.<sup>538</sup> The inhibitory potential may be attributed to the catechin constituents of the extract, which are known to inhibit CYP2B6, CYP2D6 and CYP3A4 isoforms.<sup>539</sup>

#### 5.4.2.6. Fabaceae

Both extracts of *B. africana* displayed potent inhibitory activity against the three CYP450 isoforms (IC<sub>50</sub>'s <5 µg/mL), indicating a broad, non-selective effect. Very little difference was found between the hot water and methanol extract, suggesting a similar phytochemical extraction profile. The candidates for inhibition may be an interplay between the high saponin<sup>56</sup> and flavonoid content.<sup>529</sup> Saponins are known protein-complexing agents, which form structural bonds to enzymes and result in altered activity.<sup>56</sup>

No literature could be found regarding the CYP450 inhibitory potential of *M. sericea*, or its isolated compounds. Activity was directed against CYP2B6 and CYP3A4 by the methanol extract, which produced potent inhibition (IC<sub>50</sub>'s <2.5 µg/mL). The high saponin content is a potential candidate for further assessment in this case.<sup>56</sup>

#### 5.4.2.7. Lamiaceae

Both extracts of *L. leonurus* displayed prominent activity against CYP3A4 (IC<sub>50</sub>'s <10 µg/mL). Moderate activity (39 µg/mL) against CYP2B6 was induced by the methanol extract. Activity has been ascribed to apigenin and luteolin. Apigenin<sup>540–542</sup> and luteolin<sup>540,542,543</sup> have been shown to inhibit CYP3A isoforms. It is thus likely that the potent inhibitory activity expressed by both extracts could be ascribed to apigenin and luteolin, both of which would be extracted by aqueous and alcoholic extraction solvents.

#### 5.4.2.8. Moringaceae

*M. oleifera* did not display any activity towards CYP2B6 or CYP2D6, however prominent inhibition was observed against CYP3A4. Extracts thus appear to offer selectivity towards the CYP3A4 isoform. The lack of activity towards CYP2D6 is supported by literature.<sup>544</sup> A chlorogenic-standardised extract did not display any prominent activity against CYP3A4, with chlorogenic acid presenting with poor activity.<sup>544</sup> Trigonelline was not found to inhibit either CYP3A4 or CYP2D6.<sup>545</sup>

#### 5.4.2.9. Piperaceae

The potent, non-selective inhibitory activity of the methanol extract of *P. capense* is thought to be due to alkaloids. As the hot water extract was devoid of alkaloids, it may explain the reason for the lack of activity. Low inhibitory potential has been described for *P. hispidum*,<sup>546</sup> *P. nigrum*<sup>547</sup> and *P. methysticum*,<sup>548</sup>. The isolated compound piperine has been found to display selective inhibitory activity towards CYP3A4,<sup>549,550</sup> but not against CYP2B6 or CYP2D6.<sup>550</sup> Although the involvement of piperine cannot be discounted, the broad spectrum of activity would suggest an alternative alcohol-soluble phytochemical contributing to the inhibition.

#### 5.4.2.10. Rhamnaceae

Both extracts of *Z. mucronata* displayed appreciable activity against all three CYP450 isoforms, except for inactivity of the hot water extract against CYP2D6. The hot water extract was more active against CYP3A4, while the methanol extract displayed a trend towards non-selective inhibition (potency CYP3A4>CYP2B6>CYP2D6). No literature could be found to support this effect in the three enzyme systems, however an aqueous and ethanol extract of *Z. jujuba* were described to increase CYP1A2-mediated conversion of phenacetin to acetaminophen.<sup>551</sup> Although no literature could be obtained on the inhibitory potential of mucronines, inhibitory potential may be attributed to the high saponin<sup>56</sup> and flavonoid content.<sup>529</sup>

#### 5.4.2.11. Solanaceae

The only extract of *S. aculeastrum* that displayed inhibitory activity was the hot water extract against CYP3A4, while the methanol extract did not produce any effect. The activity of the hot water extract was highly selective against CYP3A4. *S. lyratum* decreased CYP2C9, CYP2D6 and CYP3A4 activity in rats, but did not have any effect on CYP1A2 and CYP2C19.<sup>552</sup> No other literature could be obtained on the effects of isolated steroidal alkaloids, and thus no inferences could be made on potential contributing phytochemicals apart from saponins<sup>56</sup> and flavonoids.<sup>529</sup>

### 5.5. Conclusion

The objectives of the chapter were met. An all-encompassing conclusion is provided in Chapter 6. This is one of the few studies to determine the risk of African herbal remedies to elicit herb-drug interactions. Apart from the methanol extract of *S. aculeastrum*, P-gp modulatory activity was not prominent in any of the extracts. Nevirapine permeability was influenced by the selected extracts, though effects appeared to be mediated by activities other than P-gp alone. Nevirapine efflux was not high in the bidirectional permeability model, indicating a lack of specificity towards the assay. As such the model would be more apt using a more appropriate substrate, such as digoxin. Regardless of this, the observed alterations induced by all extracts assayed in this model suggest a possible risk with concomitant use. CYP450 inhibitory activity was displayed by the majority of extracts, especially towards CYP3A4. As CYP3A4 accounts for the metabolism of numerous xenobiotics, it is recommended that concomitant use be avoided, or if not possible staggered, to ensure risks are decreased. Compounding this risk is the low amount of extract that would be required to elicit potential inhibition either in the gastrointestinal tract or systemic circulation. Although risk was calculated as the possibility of reaching concentrations within the gastrointestinal and systemic compartments, it should be noted that bioavailability of phytochemicals were not assessed, and thus *in vivo* results are highly dependent on the potential of active phytochemicals to cross dissolve and be absorbed across biological barriers.

## Chapter 6

### Conclusion

#### 6.1. Concluding remarks

This *in vitro* study aimed to investigate the potential hepatotoxicity and drug-herb interactions of a panel of South African herbal remedies. These fields are quite under-researched in Africa, and thus this study forms an important foundation for further assessments. Extracts were prepared as both an ethnomedicinal (hot water extract) and a pharmaceutically-relevant (methanol extract) simulant. These two methods are seen as commonly-used extraction methods in herbal remedy preparation. All extracts were successfully prepared, and a broad phytochemical overview was established. This aided in mechanistic elucidation later on in the study. Overall the phytochemical classes detected for the majority of extracts correlated well with what has been described in literature. Although in some instances differences were observed in relation to other studies, these may be attributed to the variations in extraction procedure, seasonal collection, geographical location and storage conditions. Specific phytochemicals were not isolated or detected, and thus only speculation and inferences can be made based on literature and the phytochemical classes detected.

Extracts of *B. africana*, *T. sericea* and *Z. mucronata* were most abundant in flavonoids, phenolic acids and saponins, and presented with the highest antioxidant activity. Phytochemical concentration varied greatly between different extracts, albeit the methanol extracts generally appeared to be more enriched in phytochemical classes. Alcohol extractions are generally regarded as a broader extraction modality than aqueous solutions. The most potent antioxidant activity was observed in the methanol extract of *T. sericea*, which exceeded that of the positive control (Trolox).

Preliminary results indicated that the resazurin conversion assay was not suitable for the assessment of cytotoxic effects of the crude extracts due to interactions with the dye. The most suitable screening assay was deemed to be the SRB assay. Of the seventeen plants assessed, ten displayed the potential for cytotoxicity in cells of either liver or intestinal origin. Intestinal cells (Caco-2) appeared to be more susceptible to

the deleterious effects of the phytochemical matrices, while in general the methanol extracts displayed higher cytotoxicity than the hot water extracts. Of note was the seemingly proliferative effect of four extracts in the Caco-2 cell line: both extracts of *B. africana*, and the methanol extracts of *C. laureola* and *R. caffra*. Of these only *C. laureola* displayed a dose-dependent increase, which should be subjected to further scrutiny to determine the extent of its action and whether true proliferation had taken place and the effect was not an experimental artefact. Of note are the extracts of *A. oppositifolia*, *M. sericea* and *T. elegans*, which presented with the highest cytotoxic activity. The cytotoxic potential of the majority of the plant species selected is supported by literature. This encompasses a wide variety of mechanisms, including amongst others pro-apoptotic activity, disturbance of redox homeostasis and perturbation of cellular kinetics. The hot water extracts of *A. oppositifolia*, *B. disticha* and *M. sericea* displayed prominent cytotoxicity in at least one cell line, which highlights the caution of use of the ethnomedicinal extracts.

Seven plants in total were selected for mechanistic screening, which comprised of high cytotoxicity (*A. oppositifolia*, *S. aculeastrum* and *T. elegans*), moderate cytotoxicity (*B. disticha*) and low cytotoxicity (*M. oleifera*, *T. sericea* and *Z. mucronata*) risks. Of the fourteen extracts that were assessed for hepatotoxicity on a mechanistic scale, it was evident differential mechanisms were followed to decreased cell viability. Worryingly, the majority of hepatotoxic extracts resulted in necrotic cell death and involved mitochondrial membrane destabilisation, which may compound detrimental effects by the induction of inflammatory responses. Although apoptosis was never induced at high levels, it appears that most extracts did induce a pro-apoptotic mechanism, however, this was ultimately abolished upon cell death. Antiproliferative activity was observed as well, and may be a consequence of the altered bioenergetic pathways and inhibitory activity of cyclin-Cdk complexes.

*A. oppositifolia* exerted both a cytostatic and cytotoxic effect, related mitochondrial toxicity with resultant deficient bioenergetics processes. Improper cellular functioning due to alterations of redox status may have attenuated cellular cycling. Necrotic cell death, perhaps as a result of extrinsic death receptor pathway-linked formation of necroptosomes, DNA fragmentation and damage, or permeation of the cell membrane, appears to be the ultimate consequence. Inflammatory liver toxicity, combined with steatotic changes, appears a possible risk upon exposure.

*B. disticha* appeared to exhibit cytostatic hepatotoxicity, rather than cytotoxicity. This may be mediated by an undescribed phytochemical entity or entities. A lack of cytotoxicity and prominent cellular alterations were found. Steatosis is considered a potential risk as fatty acid accumulation occurred in high levels. As neurological symptoms are described at much higher frequency, low level chronic administration may need to be present to offer a substantial effect to be noticed in the absence of the more severe hallucinogenic effects.

*M. oleifera* did not induce highly detrimental effects, and rather would seem useful for the treatment of excessive fatty acid production or hepatosteatosis. However, the decrease of ATP paralleled to reduced fatty acid levels may present with a key interruption of the bioenergetics process. As the effects on the majority of parameters, apart from mitochondrial depolarisation, were quite subtle, hepatotoxicity is not presumed to be a high risk. Over-administration cannot be excluded thus the effects of chronic use cannot be excluded, especially in the case of a plant considered highly nutritious.

The crude extracts of *S. aculeastrum* demonstrated both antiproliferative and pro-necrotic activity, however the most detrimental effect appeared to be due to the hot water extract, albeit at a higher concentration. It is likely that the primary phytotoxin eliciting activity here is solamargine. Antiproliferative activity may be a consequence of altered DNA replication. A definite risk exists during use, which may result in necrotic hepatotoxicity and increased fatty acid levels. Mechanistically it is possible that acute mitochondrial rupturing through large-scale MPTP opening resulted in disruption of bioenergetics, release of necrotic mediators and interruption of pro-apoptotic activities. The likelihood of membrane destabilisation with subsequent cytolysis cannot be disregarded. These effects appear consistent with literature. Bioaccumulation may result in toxic physiological concentrations being reached, with subsequent hepatotoxicity.

*T. elegans* presents with a high risk of hepatotoxicity, including the involvement of steatotic changes. Both extracts appeared to inflict an antiproliferative effect, giving way to necrotic death. The hot water extract was not highly cytotoxic at low concentrations, though the pronounced necrotic effect at higher concentrations may be dangerous if over-administered, or bioaccumulation occurs. Mitochondrial toxicity

was evident, with subsequent oxidation in the absence of GSH depletion. Depolarisation of the mitochondria appeared to activate caspase systems, with ultimate cell death being achieved through necrotic means, thus a possible inhibitor of the final execution is present.

*T. sericea* holds a risk of hepatotoxicity, although this is not as prominent as with some or the other crude extracts. The methanol extract caused the most damage, primarily through mitochondrial toxicity, as well as depletion of ROS and GSH. This ultimately resulted in an S-phase block, which may be subject to topoisomerase II inhibitory activity, and subsequent cell necrotic cell death. However, slight involvement of apoptosis was noted, which appears to be through a non-caspase dependent mechanism, such as non-caspase proteases or cathepsins. There is a prominent risk for steatotic changes with exposure to the hot water extract, making it imperative that the community be aware of this risk.

*Z. mucronata* resulted in a mixture of necrotic and apoptotic cell death, though much higher activity was seen with the former. A slight propensity for cell cycle arrest was observed, though this did not appear to be the greatest contributor to the reduced cell density. It is suggested that *Z. mucronata* acts as a hepatotoxin through mitochondrial toxicity and interruption of bioenergetic synthesis, without oxidative stress contributing to this effect. The compounds responsible for this activity are not yet known.

It was observed that few extracts had prominent effects on P-gp activity, where *S. aculeastrum* was the only extract to have a large inhibitory action. These inhibitory activities were however only present at 32 µg/mL, and thus may be at a concentration not likely to be reached in the system circulation. However, this may be achieved easily within the gastrointestinal tract where a smaller volume is present. Due to this finding, it was decided to assess the possible interference with nevirapine uptake across the intestinal monolayers. Nevirapine accumulation from apical to basolateral compartments was increased by five extracts, however, *B. africana*, *R. caffra* and *S. latifolius* were found to increase P-gp activity. Thus it is apparent that a mixed mechanism of inhibition was increasing nevirapine accumulation, which was necessarily dependent on P-gp functioning. It is suggested that a combination of P-gp and similar efflux transporters may be inhibited, or membrane fluidity may be increased to allow for greater absorption of nevirapine through passive diffusion.

Three CYP450 isoforms were assessed for interactions with the crude extracts selected for this study. It was observed that inhibition increased from CYP2D6<CYP2B6<CYP3A4. Both extracts of *B. africana*, the hot water extract of *T. sericea* and the methanol extracts of *P. capense*, *T. elegans* and *Z. mucronata*, could inhibit all three CYP450 enzymes tested, and thus presents with the highest potential of interaction with intestinal and hepatic enzymes. The greatest inhibitory potential was achieved by *T. elegans* against CYP3A4. Important to note is that most extracts have the potential of inhibiting intestinal enzymes due to the higher concentrations that may be reached in the gastrointestinal tract. The majority of extracts indicated the potential of interfering with CYP3A4-mediated metabolism, which may thus increase plasma concentrations of more than half of clinically-used medications to toxic levels. Due to the reduced efflux of nevirapine, as well as a concurrent inhibition of CYP2B6 and CYP3A4, the hot water extract of *B. africana* and methanol extract of *M. sericea* may cause a risk of increased nevirapine levels.

Of the seventeen plants, the majority were involved in the induction of either cytotoxicity in the liver, or alteration of pharmacokinetic parameters *in vitro*. Great caution is recommended during use, as cytotoxicity was invoked through necrotic means, which may lead to severe inflammatory hepatotoxicity. Furthermore, steatotic changes were evident, which may further compound hepatotoxic effects and reduce quality of life. Although not necessarily through alteration of P-gp, five of the extracts increased accumulation of nevirapine, and may thus increase the adverse effects profile thereof. The majority of extracts displayed some CYP450 inhibitory activity, primarily against CYP3A4. This is worrying due to its involvement in the metabolism of more than 50% of clinically-used medications. As inhibition was prevalent at low concentrations, the risk thereof is high as gastrointestinal metabolism may already be attenuated, leading to an increase in bioavailability of various drug classes. Although crude extrapolations to risk was done using activity and extraction yields, it must be stressed that these are speculative in nature. Extrapolation from *in vitro* to *in vivo* situations require a full understanding of the bioavailability profiles of phytochemicals extracted, and thus can only be used as a potential guideline.

It is recommended that caution be used for all the plants assessed in the study, and all other herbal remedies as a whole. Due to the lack of safety assessment and

regulation, herbal remedies may pose significant threats to human health if used without careful scrutiny of their interactions with the liver and other medications.

## 6.2. Executive summary

This *in vitro* study aimed to evaluate the risk of a number of commonly-used African herbal remedies to elicit hepatotoxic and drug-herb interactions. It is one of the few studies to determine the risks involved with African herbal remedies. It was observed that selected African herbal remedies elicit a mixture of mechanisms to induce cytotoxic effects, though mainly through induction of necrotic cell death. This may in turn propagate inflammatory liver disease, and coupled to the steatotic changes noted, may lead to reduced quality of life. Drug-herb interactions were evident, as was observed with the accumulation of nevirapine in the intestinal model, and the high CYP450 enzyme inhibitory activity. The former effect appears to be independent, or poorly linked, to P-glycoprotein activity. CYP3A4 activity was the most susceptible to herbal remedies' inhibitory properties. The plant with the highest risk of hepatotoxicity was determined to be *T. elegans* extracted with methanol as solvent. As there is limited scientific background to prove their efficacy and safety, it is thus recommended that herbal remedies be subjected to the same in-depth scrutiny that is applied to allopathic medications.

## 6.3. Limitations of the study and recommendations

The HepG2 cell line was chosen due to its well-described use as a hepatotoxic model, though it does suffer from several limitations. These would include its cancerous origin, and its metabolic incompetence. Due to the latter it is likely that metabolic influences were not taken into consideration during induction of cytotoxicity. Further research utilising primary hepatocytes (which are considered the gold standard) or hepatic spheroids may shed more light on the risk involved. The majority of all hepatotoxic parameters were only assessed at 72 h, which is a late stage in cytotoxicity determination. Although this allows for identification of the hepatotoxic effect, closer scrutiny would need to be done at shorter intervals to more accurately describe the mechanistic processes involved. Induction of oxidative systems may be evident at

earlier time-points, and thus the contribution thereof may have not been fully taken into account. Although a broad mechanistic overview has been established for seven of the seventeen plants that were assessed, no specific pathways could be identified, and only inferences can be made. Proteomic assessment is recommended to scrutinise the involvement of several key pathways in cell death and proliferation, such as the MAPK, extracellular signal regulated kinases (ERK) and JNK pathways. The involvement of cellular arrest in hepatotoxicity may be researched by assessing changes in Cdk-cyclin complexes and proliferative markers (Ki-67). As phytochemicals were not individually detected or identified, the primary contributors to biological activity are not known, and thus discussion is speculative and based off of literature and comparison to phytochemical classes detected in TLC methodologies. Ultimately it would be best to isolate and identify the main contributors of each extracts hepatotoxic properties to avoid speculation on possible hepatotoxic phytochemicals.

With specific mention to *B. disticha*, the quiescence discussed is largely speculative, and thus needs to be confirmed via proliferative markers to ascertain its validity. Although *M. oleifera* appears to offer negligible cytotoxic effects, the decreased levels of ATP as a potential consequence of interrupted bioenergetics pathways must also be further examined.

Only nevirapine was used to determine the potential of African herbal remedies to influence drug accumulation, and thus a broader range of substrates would be ideal, including those that are isolated to active or passive transport mechanism. As suggestions were made to the membrane destabilisation properties of the extracts, further investigation into the membrane fluidisation activities would be suggested. This may be accomplished through fluorescence polarisation or inclusion of membrane solidifiers or fluidisers. The involvement of other membrane transporters, such as BCRP and OAT, should also be determined.

Only three CYP450 isoforms were included in this study, and thus further research would need to determine the possibility of extracts to inhibit CYP1A, CYP2C9 and CYP3A4, which are also involved in xenobiotic metabolism. Furthermore, the assessment of enzyme activity using Federal Drug Administration recommended guidelines (LC-MS/MS substrate specific cleavage in microsomes) would offer more accuracy into their inhibitory activities. As with hepatotoxicity, isolation of the active

components would be necessary to determine the main contributor of these interactions. Through use of Michaelis-Menton kinetics one would be able to determine the mechanism by which these inhibitory activities take place in the selected CYP450 isoforms.

Overall, a greater emphasis could be placed on further statistical analyses to determine correlation between different parameters. As a large panel of mechanistic assays were conducted, it would be prudent to assess relationship between them and the final outcome of reduced cell viability through the use of principal component or multivariate analysis. Efforts in these may elucidate potential mechanistic responses and serve as a basis for further scrutiny of pathways.

Although the abovementioned is recommended, it should be noted that this study formed the basis for future work, and is thus serves as a foundation where very little is currently known.

## References

1. Binswanger HC, Smith KR. Paracelsus and Goethe: founding fathers of environmental health. *Bull World Health Organ.* 2000;78:1162–4.
2. Werneke U, Earl J, Seydel C, Horn O, Crichton P, Fannon D. Potential health risks of complementary alternative medicines in cancer patients. *Br J Cancer.* 2004;90:408–13.
3. Cohen PA, Ernst E. Safety of Herbal Supplements : A Guide for Cardiologists. *Cardiovasc Ther.* 2010;28:246–53.
4. Rosecrans R, Dohnal JC. The effect of complimentary and alternative medicine products on laboratory testing. *Semin Diagn Pathol.* 2009;26:38–48.
5. Louw C, Regnier T, Korsten L. Medicinal bulbous plants of South Africa and their traditional relevance in the control of infectious diseases. *J Ethnopharmacol.* 2002;82:147–54.
6. Fouche G, Cragg G, Pillay P, Kolesnikova N, Maharaj V, Senabe J. *In vitro* anticancer screening of South African plants. *J Ethnopharmacol.* 2008;119:455–61.
7. Aremu A, Ndhlala A, Fawole O, Light M, Finnie J, Van Staden J. *In vitro* pharmacological evaluation and phenolic content of ten South African medicinal plants used as anthelmintics. *South African J Bot.* 2010;76:558–66.
8. Stafford G, Pedersen M, van Staden J, Jäger A. Review on plants with CNS-effects used in traditional South African medicine against mental diseases. *J Ethnopharmacol.* 2008;119:513–37.
9. Wintola O, Afolayan A. Ethnobotanical survey of plants used for the treatment of constipation within Nkonkobe Municipality of South Africa. *African J Biotechnol.* 2010;9:7767–70.
10. Aithal GP. When is a herb a drug? *Eur J Gastroenterol Hepatol.* 2005;17:391–3.
11. Izzo AA, Di Carlo G, Borrelli F, Ernst E. Cardiovascular pharmacotherapy and herbal medicines: the risk of drug interaction. *Int J Cardiol.* 2005;98:1–14.
12. Aithal GP. When is a herb a drug? *Eur J Gastroenterol Hepatol.* 2005;17:391–3.
13. Brown L, Heyneke O, Brown D, van Wyk JPH, Hamman JH. Impact of traditional medicinal plant extracts on antiretroviral drug absorption. *J Ethnopharmacol.* 2008;119:588–92.
14. Cordier W, Steenkamp V. Drug interactions in African herbal remedies. *Drug Metabol Drug Interact.* 2011;26:53–63.
15. Reynolds C, de Koning CB, Pelly SC, van Otterlo WAL, Bode ML. In search of a treatment for HIV – current therapies and the role of non-nucleoside reverse transcriptase inhibitors (NNRTIs). *Chem Soc Rev.* 2012;41:4657–70.
16. Antoniou T, Tseng AL. Interactions between antiretrovirals and antineoplastic drug therapy. *Clin Pharmacokinet.* 2005;44:111–45.
17. Penzak SR, Kabuye G, Mugenyi P, Mbamanya F, Natarajan V, Alfaro RM, *et al.* Cytochrome P450 2B6 (CYP2B6) G516T influences nevirapine plasma concentrations in HIV-infected patients in Uganda. *HIV Med.* 2007;8:86–91.

18. Parathyras J, Gebhardt S, Hillermann-Rebello R, Grobbelaar N, Venter M, Warnich L. A pharmacogenetic study of CD4 recovery in response to HIV antiretroviral therapy in two South African population groups. *J Hum Genet.* 2009;54:261–5.
19. Núñez M, Soriano S. Hepatotoxicity of antiretrovirals: incidence, mechanisms and management. *Drug Saf.* 2005;28:53–66.
20. Van den Bout-van den Beukel C, Koopmans P, van der Ven A, De Smet P, Burger D. Possible drug-metabolism interactions of medicinal herbs with antiretroviral agents. *Metab Metab Rev.* 2006;38:477–514.
21. Van Tonder JJ, Cromarty AD, Gulumian M, Steenkamp V. Development of an *in vitro* mechanistic toxicity screening model using cultured hepatocytes. 2011.
22. Wai C-T, Tan B-H, Chan C-L, Sutedja DS, Lee Y-M, Khor C, *et al.* Drug-induced liver injury at an Asian center: a prospective study. *Liver Int.* 2007;27:465–74.
23. Su Y-W, Chen X, Jiang Z-Z, Wang T, Wang C, Zhang Y, *et al.* A panel of serum microRNAs as specific biomarkers for diagnosis of compound- and herb-induced liver injury in rats. *PLoS One.* 2012;7:e37395.
24. Jung KA, Min HJ, Yoo SS, Kim HJ, Choi SN, Ha CY, *et al.* Drug-induced liver injury: Twenty five cases of acute hepatitis following ingestion of *Polygonum multiflorum* Thunb. *Gut Liver.* 2011;5:493–9.
25. Nin CT, Cheung WI, Ngan T, Lin J, Lee KWS, Tat Poon W, *et al.* Causality assessment of herb-induced liver injury using multidisciplinary approach and Roussel Uclaf Causality Assessment Method (RUCAM). *Clin Toxicol (Phila).* 2011;49:34–9.
26. Teschke R, Qiu SX, Lebot V. Herbal hepatotoxicity by kava: update on pipermethystine, flavokavain B, and mould hepatotoxins as primarily assumed culprits. *Dig Liver Dis.* 2011;43:676–81.
27. Chalasani N, Fontana RJ, Bonkovsky HL, Watkins PB, Davern T, Serrano J, *et al.* Causes, clinical features, and outcomes from a prospective study of drug-induced liver injury in the United States. *Gastroenterology.* 2008;135:1924–34.
28. Stickel F, Schuppan D. Herbal medicine in the treatment of liver diseases. *Dig Liver Dis.* 2007;39:293–304.
29. Teschke R, Glass X, Schulze J. Herbal hepatotoxicity by Greater Celandine (*Chelidonium majus*): causality assessment of 22 spontaneous reports. *Regul Toxicol Pharmacol.* 2011;61:282–91.
30. Neuman MG, Jia AY, Steenkamp V. *Senecio latifolius* induces *in vitro* hepatocytotoxicity in a human cell line. *Can J Physiol Pharmacol.* 2007;85:1063–75.
31. Wainwright J, Schonland M, Candy H. Toxicity of *Callilepis laureola*. *S Afr Med J.* 1977;52:313–5.
32. Neuman M, Jia A, Steenkamp V. *Senecio latifolius* induces *in vitro* hepatocytotoxicity in a human cell line. *Can J Physiol Pharmacol.* 2007;85:1063–75.
33. Radler DG. Dietary supplements: clinical implications for dentistry. *J Am Dent Assoc.* 2008;139:451–5.

34. Deferme S, Kamuhabwa A, Nshimo C, Witte P De, Augustijns P. Screening of Tanzanian plant extracts for their potential inhibitory effect on P-glycoprotein mediated efflux. *Pharm Biol.* 2003;464:459–64.
35. De Maat MMR, Ekhardt GC, Huitema AD., Koks CHW, Mulder JW, Beijnen JH. Drug interactions between antiretroviral drugs and comedicated agents. *Clin Pharmacokinet.* 2003;42:223–82.
36. Pal D, Mitra AK. MDR- and CYP3A4-mediated drug-herbal interactions. *Life Sci.* 2006;78:2131–45.
37. Muscatello MR, Spina E, Bandelow B, Baldwin DS. Clinically relevant drug interactions in anxiety disorders. *Hum Psychopharmacol Clin Exp.* 2012;27:239–53.
38. Thummel KE, Wilkinson GR. *In vitro* and *in vivo* drug interactions involving human CYP3A. *Annu Rev Pharmacol Toxicol.* 1998;38:389–430.
39. Markovsky E, Baabur-Cohen H, Eldar-Boock A, Omer L, Tiram G, Ferber S, *et al.* Administration, distribution, metabolism and elimination of polymer therapeutics. *J Control Release.* 2011;161:446–60.
40. Hines LE, Murphy JE. Potentially harmful drug-drug interactions in the elderly: a review. *Am J Geriatr Pharmacother.* 2011;9:364–77.
41. Charbit B, Becquemont L, Lepère B, Peytavin G, Funck-Brentano C. Pharmacokinetic and pharmacodynamic interaction between grapefruit juice and halofantrine. *Clin Pharmacol Ther.* 2002;72:514–23.
42. Shaw D, Leon C, Koley S, Murray V. Traditional remedies and food supplements. A 5-year toxicological study (1991 – 1995). *Drug Saf.* 1997;17:870–6.
43. Tannergren C, Engman H, Knutson L, Hedeland M, Bondesson U, Lennernäs H. St John's wort decreases the bioavailability of R- and S-verapamil through the induction of the first-pass metabolism. *Clin Pharmacol Ther.* 2004;75:298–309.
44. Arnold H, Gulumian M. Pharmacopoeia of traditional medicine in Venda. *J Ethnopharmacol.* 1984;12:35–74.
45. Botha EW, Kahler CP, Plooy WJ, Plooy SH, Mathibe L. Effect of *Boophone disticha* on human neutrophils. *J Ethnopharmacol.* 2005;96:385–8.
46. Koch A, Tamez P, Pezzuto J, Soejarto D. Evaluation of plants used for antimalarial treatment by the Maasai of Kenya. *J Ethnopharmacol.* 2005;101:95–9.
47. Suffness M, Pezzuto J. Assays for bioactivity. In: *Methods in Plant Biochemistry Vol 6.* Academic Press, London; 1991. pp 71–134.
48. Wink M. Functions of plant secondary metabolites and their exploitation in biotechnology (Annual Plant Reviews, Volume 3). Blackwell Publishing. 1999.
49. Krief S, Hladik CM, Haxaire C. Ethnomedicinal and bioactive properties of plants ingested by wild chimpanzees in Uganda. *J Ethnopharmacol.* 2005;101:1–15.
50. Croteau R, Kutchan TM, Lewis NG. Natural products (secondary metabolites). In: *Biochemistry & Molecular Biology of Plants.* 2000.
51. Crozier A, Clifford MN, Ashihara H. *Plant Secondary Metabolites: Occurrence, Structure and Role in the Human Diet.* Blackwell Publishing. 2006.

52. Yordi E, Pérez E, Matos M, Villares E. Antioxidant and pro-oxidant effects of polyphenolic compounds and structure-activity relationship evidence. In: Nutrition, Well-Being and Health [Internet]. 2012. p. 23–48.
53. Scalbert A, Johnson IT, Saltmarsh M. Polyphenols: Antioxidants and beyond. *Am J Clin Nutr.* 2005;81:215S – 7S.
54. Valko M, Leibfritz D, Moncol J, Cronin MT, Mazur M, Telser J. Free radicals and antioxidants in normal physiological functions and human disease. *Int J Biochem Cell Biol.* 2007;39:44–84.
55. Venugopala KN, Rashmi V, Odhav B. Review on natural coumarin lead compounds for their pharmacological activity. *Biomed Res Int.* 2013;2013;1–14.
56. Makkar H, Siddhuraju P, Becker K. Plant secondary metabolites. In: *Methods in Molecular Biology.* Humana Press. 2007. pp 93–100.
57. Van Wyk B-E, van Heerden F, van Oudtshoorn B. *Poisonous plants of South Africa.* Briza Publications, South Africa; 2002.
58. Adedapo A, Jimoh F, Afolayan A, Masika P. Antioxidant activities and phenolic contents of the methanol extracts of the stems of *Acokanthera oppositifolia* and *Adenia gummifera*. *BMC Complement Altern Med.* 2008;8:54.
59. Cordier W, Gulumian M, Cromarty A, Steenkamp V. Attenuation of oxidative stress in U937 cells by polyphenolic-rich bark fractions of *Burkea africana* and *Syzygium cordatum*. *BMC Complement Altern Med.* 2013;13:116–27.
60. Cordier W, Cromarty AD, Botha E, Steenkamp V. Effects of selected South African plant extracts on haemolysis and coagulation. *Hum Exp Toxicol.* 2012;31:250–7.
61. Pallant C, Steenkamp V. In-vitro bioactivity of Venda medicinal plants used in the treatment of respiratory conditions. *Hum Exp Toxicol.* 2008;27):859–66.
62. Cordier W, du Toit E, Steenkamp V. *Moringa oleifera*: Benefits in Nutrition and Health. In: *Plant Extracts: Role in Agriculture, Health Effects and Medical Applications.* Nova Publishers. 2013. pp 87–118.
63. Chen T-B, Green T, Wiemer D. Capentin: A novel sesquiterpene from the roots of *Piper capense*. *Tetrahedron Lett.* 1992;33:5673–6.
64. Barboni L, Gariboldi P, Torregiani E, Verotta L. Cyclopeptide alkaloids from *Ziziphus mucronata*. *Phytochemistry.* 1994;35:1579–82.
65. Koduru S, Grierson D, van de Venter M, Afolayan A. *In vitro* antitumour activity of Solanum aculeastrum berries on three carcinoma cells. *Intl J Cancer Res.* 2006;2:397–402.
66. PlantzAfrica.com. *Acokanthera oppositifolia*. 2001. Accessed on 2 February 2016 from <http://www.plantzafrica.com/plantab/acokantheroposit.htm>.
67. PlantzAfrica.com. *Boopbane disticha*. 2005. Accessed on 2 February 2016 from from <http://www.plantzafrica.com/plantab/boophdist.htm>
68. PlantzAfrica.com. *Burkea africana*. 2010. Accessed on 2 February 2016 from <http://www.plantzafrica.com/plantab/burkeaafricana.htm>
69. PlantzAfrica.com. *Callilepis laureola*. 2008. Accessed on 2 February 2016 from <http://www.plantzafrica.com/plantcd/callilepislaur.htm>

70. PlantzAfrica.com. *Crinum bulbispermum*. 2001. Accessed on 2 February 2016 from <http://www.plantzafrica.com/plantcd/crinumbulbisp.htm>
71. PlantzAfrica.com. *Leonotis leonurus*. 2001. Accessed on 2 February 2016 from <http://www.plantzafrica.com/plantklm/leonotisleon.htm>
72. PBCGOV.com. *Moringa oleifera*. 2012. Accessed on 2 February 2016 from [http://www.pbcgov.com/newsroom/0812/08-24-12\\_moringa.htm](http://www.pbcgov.com/newsroom/0812/08-24-12_moringa.htm)
73. PlantzAfrica.com. *Mundulea sericea*. 2008. Accessed on 2 February 2016 from <http://www.plantzafrica.com/plantklm/munduleasericea.htm>
74. ZimbabweFlora.co.zw. *Piper capense*. 2002. Accessed on 2 February 2016 from [http://www.zimbabweflora.co.zw/speciesdata/species.php?species\\_id=119880](http://www.zimbabweflora.co.zw/speciesdata/species.php?species_id=119880)
75. PlantzAfrica.com. *Rauvolfia caffra*. 2011. Accessed on 2 February 2016 from <http://www.plantzafrica.com/plantqrs/rauvolfiacaffra.htm>
76. PlantzAfrica.com. *Rhus lancea*. 2008. Accessed on 2 February 2016 from <http://www.plantzafrica.com/plantqrs/rhuslancea.htm>
77. PlantzAfrica.com. *Scadoxus puniceus*. 2001. Accessed on 2 February 2016 from <http://www.plantzafrica.com/plantqrs/scadoxuspuniceus.htm>
78. ZimbabweFlora.co.zw. *Senecio latifolius*. 2002. Accessed on 2 February 2016 from [http://www.zimbabweflora.co.zw/speciesdata/species.php?species\\_id=161230](http://www.zimbabweflora.co.zw/speciesdata/species.php?species_id=161230)
79. PlantzAfrica.com. *Solanum aculeastrum*. 2004. Accessed on 2 February 2016 from <http://www.plantzafrica.com/plantqrs/solanacul.htm>
80. PlantzAfrica.com. *Tabernaemontana elegans*. 2010. Accessed on 2 February 2016 from <http://www.plantzafrica.com/planttuv/taberelegans.htm>
81. PlantzAfrica.com. *Terminalia sericea*. 2012. Accessed on 2 February 2016 from <http://www.plantzafrica.com/planttuv/terminaliasericea.htm>
82. PlantzAfrica.com. *Ziziphus mucronata*. 2007. Accessed on 2 February 2016 from <http://www.plantzafrica.com/plantwxyz/zizimucro.htm>
83. Bolliger H, Brenner M, Ganshirt H, Mangold H, Seiler H, Stahl E, Waldi D. Thin-layer chromatography: A Laboratory Handbook. Springer-Verlag; 1965.
84. Dewanto V, Wu X, Adom K, Liu R. Thermal processing enhances the nutritional value of tomatoes by increasing total antioxidant activity. *J Agric Food Chem*. 2002;8:3010–4.
85. Slinkard K, Singleton V. Total phenol analysis: Automation and comparison with manual methods. *Am J Enol Vitic*. 1977;28:49–55.
86. Re R, Pellegrini N, Proteggente A, Pannala A, Yang M, Rice-Evans C. Antioxidant activity applying an improved ABTS radical cation decolorization assay. *Free Radic Biol Med*. 1999;26:1231–7.
87. De Smet P. Some ethnopharmacological notes on African hallucinogens. *J Ethnopharmacol*. 1996;50:141–6.
88. Cheesman L. Micropropagation and pharmacological evaluation of *Boophane disticha*. PhD thesis, University of KwaZulu Natal, Pietermaritzburg. 2013.

89. Adewusi E, Fouche G, Steenkamp V. Cytotoxicity and acetylcholinesterase inhibitory activity of an isolated crinine alkaloid from *Boophane disticha* (Amaryllidaceae). *J Ethnopharmacol.* 2012;143:572–28.
90. Adewusi E, Fouche G, Steenkamp V. Antioxidant, acetylcholinesterase inhibitory activity and cytotoxicity assessment of the crude extracts of *Boophane disticha*. *African J Pharmacol Ther.* 2012;1:78–83.
91. Nair JJ, Van Staden J. Traditional usage, phytochemistry and pharmacology of the South African medicinal plant *Boophane disticha* (L.f.) Herb. (Amaryllidaceae). *J Ethnopharmacol.* 2014;151:12–26.
92. Aboul-Ela M, El-Lakany A, Hammoda H. Alkaloids from the bulbs of *Crinum bulbispermum*. *Pharmazie.* 2004;59:894–6.
93. Cortes N, Alvarez R, Osorio EH, Alzate F, Berkov S, Osorio E. Alkaloid metabolite profiles by GC/MS and acetylcholinesterase inhibitory activities with binding-mode predictions of five Amaryllidaceae plants. *J Pharm Biomed Anal.* 2015;102:222–8.
94. Adewusi E, Steenkamp V. *In vitro* screening for acetylcholinesterase inhibition and antioxidant activity of medicinal plants from southern Africa. *Asian Pac J Trop Med.* 2011;4:829–35.
95. Nair JJ, van Staden J. Pharmacological and toxicological insights to the South African Amaryllidaceae. *Food Chem Toxicol.* 2013;62:262–75.
96. Nair A, Kotiyal J, Bhardwaj D. Myricetin 7,4'-dimethyl ether and its 3-galactoside from *Rhus lancea*. *Phytochemistry.* 1983;22:318–9.
97. Gundidza M, Gweru N, Mmbengwa V, Ramalivhana NJ, Magwa Z, Samie A. Phytoconstituents and biological activities of essential oil from *Rhus lancea* L. F. *Afr J Biol.* 2008;7:2787–9.
98. Mulaudzi RB, Ndhkala AR, Kulkarni MG, Van Staden J. Pharmacological properties and protein binding capacity of phenolic extracts of some Venda medicinal plants used against cough and fever. *J Ethnopharmacol.* 2012;143:185–93.
99. Philippe G, Angenot L. Recent developments in the field of arrow and dart poisons. *J Ethnopharmacol.* 2005;100:85–91.
100. Adebayo SA, Dzoyem JP, Shai LJ, Elof JN. The anti-inflammatory and antioxidant activity of 25 plant species used traditionally to treat pain in southern African. *BMC Complement Altern Med.* 2015;15:159.
101. De Wet B. Medicinal plants and human health. *South African Pharmacol J.* 2011;78(6):38–40.
102. Kingdon J, Agwanda B, Kinnaird M, Brien TO, Holland C, Gheysens T, *et al.* A poisonous surprise under the coat of the African crested rat. *Proc R Soc B.* 2012;279:675–80.
103. Sharma P, Chaurasia S. Evaluation of total phenolic, flavonoid contents and antioxidant activity of *Acokanthera oppositifolia* and *Leucaena leucocephala*. *Int J Pharmacogn Phytochem Res.* 2015;7:175–80.
104. Milugo T, Omosa L, Ochanda J, Owuor B, Wamunyokoli F, Oyugi J, *et al.* Antagonistic effect of alkaloids and saponins on bioactivity in the quinine tree (*Rauvolfia caffra* sond.): further evidence to support biotechnology in traditional medicinal plants. *BMC Complement Altern Med.* 2013;13:285–90.

105. Nasses A, Court W. Stem bark alkaloids of *Rauvolfia caffra*. J Ethnopharmacol. 1984;11:99–117.
106. Pallant C, Cromarty A, Steenkamp V. Effect of an alkaloidal fraction of *Tabernaemontana elegans* (Stapf.) on selected micro-organisms. J Ethnopharmacol. 2012;140:398–404.
107. Van der Heijden R, Brouwer R, Verpoorte R, Wijnsma R, van Beek T, Harkes P, *et al.* Indole alkaloids from a callus culture of *Tabernaemontana elegans*. Phytochemistry. 1986;25:843–6.
108. Mansoor T, Ramalho R, Mulhovo S, Rodrigues C, Ferreira M. Induction of apoptosis in HuH-7 cancer cells by monoterpene and beta-carboline indole alkaloids isolated from the leaves of *Tabernaemontana elegans*. Bioorg Med Chem Lett. 2009;19:4255–8.
109. Hirasawa Y, Miyama S, Hosoya T, Koyama K, Rahman A, Kusumawati I, *et al.* Alasmontamine A, a first tetrakis monoterpene indole alkaloid from *Tabernaemontana elegans*. Org Lett. 2009;11:5718–21.
110. Mansoor TA., Borralho PM, Dewanjee S, Mulhovo S, Rodrigues CMP, Ferreira MJU. Monoterpene bisindole alkaloids, from the African medicinal plant *Tabernaemontana elegans*, induce apoptosis in HCT116 human colon carcinoma cells. J Ethnopharmacol. 2013;149:463–70.
111. Popat A, Shear N, Malkiewicz I, Stewart M, Steenkamp V, Thomson S, *et al.* The toxicity of *Callilepis laureola*, a South African traditional herbal medicine. Clin Biochem. 2001;34:229–36.
112. Molefe-Khamanga DM, Mbandezelo M. Qualitative phytochemical studies and thin layer chromatography analysis of solvent extracts from *Callilepis laureola*. Int J Med Plant Altern Med. 2013;1.
113. Steenkamp V, Grimmer H, Semano M, Gulumian M. Antioxidant and genotoxic properties of South African herbal extracts. Mutat Res. 2005;581:35–42.
114. Bredenkamp M, Wiechers A, van Rooyen P. A new pyrrolizidine alkaloid from *Senecio latifolius* DC. Tetrahedron Lett. 1985;26:929–32.
115. Watt H. LIX.- The alkaloids of *Senecio latifolius*. J Chem Soc Trans. 1909;95:466–77.
116. Fyhrquist P, Laakso I, Garcia Marco S, Julkunen-Tiitto R, Hiltunen R. Antimycobacterial activity of ellagitannin and ellagic acid derivate rich crude extracts and fractions of five selected species of *Terminalia* used for treatment of infectious diseases in African traditional medicine. South African J Bot. 2014;90:1–16.
117. Joseph C, Moshi M, Innocent E, Nkunya M. Isolation of a stilbene glycoside and other constituents of *Terminalia sericeae*. African J Tradit Complement Altern Med. 2007;4:383–6.
118. Bombardelli E, Martinelli E, Mustich G. A new hydroxystilbene glycoside from *Terminalia sericea*. Fitoterapia. 1975;46:199–201.
119. Eldeen IMS, Elgorashi EE, Mulholland DA, van Staden J. Anolignan B: a bioactive compound from the roots of *Terminalia sericea*. J Ethnopharmacol. 2006;103:135–8.
120. Eldeen I, van Heerden F, van Staden J. Isolation and biological activities of termilignan B and arjunic acid from *Terminalia sericea* roots. Planta Med. 2008;74:411–3.
121. Nkobole N. Antidiabetic activity of pentacyclic triterpenes and flavonoids isolated from stem bark of *Terminalia sericea* Burch.Ex DC. MSc dissertation, University of Pretoria, Pretoria. 2011.

122. Bombardelli E, Bonati A, Gabetta B, Mustich G. Triterpenoids of *Terminalia sericea*. *Phytochemistry*. 1974;13:2559–62.
123. Kruger J. Isolation, chemical characterization and clinical application of an antimicrobial compound from *Terminalia sericea*. DPhil thesis, University of Pretoria, Pretoria. 2004.
124. Masoko P, Picard J, Eloff JN. Antifungal activities of six South African *Terminalia* species (Combretaceae). *J Ethnopharmacol*. 2005;99:301–8.
125. Masoko P, Eloff J. Screening of twenty-four South African Combretum and six *Terminalia* species (Combretaceae) for antioxidant activities. *Afr J Tradit Complement Altern Med*. 2007;4:231–9.
126. Anokwuru CP, Ramaite IDI, Bessong P. Phenolic content distribution and antioxidant activities of *Terminalia sericea* Burch. *Afr J Tradit Complement Altern Med*. 2015;12:21–7.
127. Steenkamp V, Mathivha E, Gouws M, van Rensburg C. Studies on antibacterial, antioxidant and fibroblast growth stimulation of wound healing remedies from South Africa. *J Ethnopharmacol*. 2004;95:353–7.
128. Tanko Y, Iliya B, Mohammed A, Mahdi M, Musa K. Modulatory effect of ethanol stem bark extract of *Burkea africana* on castrol oil induced diarrhoeal on experimental animals. *Arch Appl Sci Res*. 2011;3:122–30.
129. Mathisen E, Diallo D, Anderson Ø, Malterud K. Antioxidants from the bark of *Burkea africana*, an African medicinal plant. *Phyther Res*. 2002;16:148–53.
130. Diallo D, Marston A, Terreaux C, Touré Y, Paulsen B, Hostettman K. Screening of Malian medicinal plants for antifungal, larvicidal, molluscicidal, antioxidant and radical scavenging activities. *Phyther Res*. 2001;15:401–6.
131. Sharma S, Shukla Y, Tandon J. Constituents of *Colocasia formicata*, *Sagittaria sagittiflora*, *Arnebia nobilis*, *Ipomoea paniculata*, *Rhododendrom niveum*, *Paspalum scrobiculatum*, *Mundulea sericea* and *Duabanga sonneratiodes*. *Phytochemistry*. 1972;11:2621–3.
132. Luyengi L, Lee I-S, Fong H, Pezzuto J, Kinghorn A. Rotenoids and chalcones from *Mundulea sericea* that inhibit phorbol ester-induced ornithine decarboxylase activity. *Phytochemistry*. 1994;36:1523–6.
133. El-Ansari MA., Aboutabl EA., Farrag ARH, Sharaf M, Hawas UW, Soliman GM, *et al*. Phytochemical and pharmacological studies on *Leonotis leonurus*. *Pharm Biol*. 2009;47:894–902.
134. Bienvenu E, Amabeoku GJ, Eagles PK, Scott G, Springfield EP. Anticonvulsant activity of aqueous extract of *Leonotis leonurus*. *Phytomedicine*. 2002;9:217–23.
135. Oyedemi SO, Yakubu MT, Afolayan AJ. Antidiabetic activities of aqueous leaves extract of *Leonotis leonurus* in streptozotocin induced diabetic rats. 2011;5:119–25.
136. Oyedemi S, Afolayan A. *In vitro* and *in vivo* antioxidant activity of aqueous leaves extract of *Leonotis leonurus*. *Int J Pharmacol*. 2011;7:248–56.
137. Madureira AM, Ramalheite C, Mulhovo S, Duarte A, Ferreira M-JU. Antibacterial activity of some African medicinal plants used traditionally against infectious diseases. *Pharm Biol*. 2012;5:481–9.

138. Naidoo D, Maharaj V, Crouch NR, Ngwane A. New labdane-type diterpenoids from *Leonotis leonurus* support circumscription of Lamiaceae s.l. *Biochem Syst Ecol.* 2011;39:216–9.
139. Mckenzie J, Green I, Mugabo P. Leonurun , a novel labdane diterpenoid from *Leonotis leonurus*. *South African J Chem.* 2006;25:114–6.
140. He F, Lindqvist C, Harding W. Leonurenones A-C: Labdane diterpenes from *Leonotis leonurus*. *Phytochemistry.* 2012;83:168–72.
141. Frum Y. *In vitro* 5-lipoxygenase and anti-oxidant activities of South African medicinal plants commonly used topically for skin diseases. MSc dissertation, University of Witwatersrand, Johannesburg. 2006.
142. Hurinanthan V. Immune modulatory effect of *Dichrostachys cinerea*, *Carpobrotus dimidiatus*, *Capparis tomentosa* and *Leonotis leonurus*. MTech dissertation, University of Technology, Durban. 2009.
143. Makkar HP., Becker K. Nutrients and antiquality factors in different morphological parts of the *Moringa oleifera* tree. *J Agric Sci.* 1997;128:311–22.
144. Bukar A, Uba A, Oyeyi TI. Antimicrobial profile of *Moringa oleifera* Lam. extracts against some food-borne microorganisms. *Bayero J Pure Appl Sci.* 2010;3:43–8.
145. Arun T, Rao CHP. Phytochemical screening and antibacterial activity of *Moringa oleifera* Lam. against *Proteus mirabilis* from urinary tract infected patients. *Int J PharmTech Res.* 2011;3:2118–23.
146. Srinivasa U, Amrutia JN, Katharotiya R, Rajan MS. Preliminary phytochemical investigation and anthelmintic activity of *Moringa oleifera* leaves. *Int Res J Pharm.* 2011;2:130–1.
147. Adejumo OE, Kolapo AL, Folarin AO. *Moringa oleifera* Lam. (Moringaceae) grown in Nigeria: *In vitro* antisickling activity on deoxygenated erythrocyte cells. *J Pharm Bioallied Sci.* 2012;4:118–22.
148. Dholvitayakhun A, Cushnie TPT, Trachoo N. Antibacterial activity of three medicinal Thai plants against *Campylobacter jejuni* and other foodborne pathogens. *Nat Prod Res.* 2012;26:356–63.
149. Ndong M, Uehara M, Katsumata S-I, Suzuki K. Effects of oral administration of *Moringa oleifera* Lam on glucose tolerance in Goto-Kakizaki and Wistar rats. *J Clin Biochem Nutr.* 2007;40:229–33.
150. Verma AR, Vijayakumar M, Mathela CS, Rao C V. *In vitro* and *in vivo* antioxidant properties of different fractions of *Moringa oleifera* leaves. *Food Chem Toxicol.* Elsevier Ltd; 2009;47:2196–201.
151. Sinha M, Das DK, Datta S, Ghosh S, Dey S. Amelioration of ionizing radiation induced lipid peroxidation in mouse liver by *Moringa oleifera* Lam. leaf extract. *Indian J Exp Biol.* 2012;50:209–15.
152. Mathur M, Kamal R. Studies on trigonelline from *Moringa oleifera* and its *in vitro* regulation by feeding precursor in cell cultures. *Brazilian J Pharmacogn.* 2012;22:994–1001.
153. Chen K-H, Chen Y-J, Yang C-H, Liu K-W, Chang J-L, Pan S-F, *et al.* Attenuation of the extract from *Moringa oleifera* on monocrotaline-induced pulmonary hypertension in rats. *Chin J Physiol.* 2012;55:22–30.

154. Sahakitpichan P, Mahidol C, Disadee W, Ruchirawat S, Kanchanapoom T. Unusual glycosides of pyrrole alkaloid and 4'-hydroxyphenylethanamide from leaves of *Moringa oleifera*. *Phytochemistry*. 2011;72:791–5.
155. Bijina B, Chellappan S, Basheer SM, Elyas KK, Bahkali AH, Chandrasekaran M. Protease inhibitor from *Moringa oleifera* leaves: Isolation, purification, and characterization. *Process Biochem*. 2011;46:2291–300.
156. Bijina B, Chellappan S, Krishna JG, Basheer SM, Elyas KK, Bahkali AH, *et al*. Protease inhibitor from *Moringa oleifera* with potential for use as therapeutic drug and as seafood preservative. *Saudi J Biol Sci*. 2011;18:273–81.
157. Khalafalla MM, Abdellatef E, Dafalla HM, Nassrallah AA, Aboul-enein KM, Lightfoot DA, *et al*. Active principle from *Moringa oleifera* Lam leaves effective against two leukemias and a hepatocarcinoma. *African J Biotechnol*. 2010;9:8467–71.
158. Moyo B, Oyedemi S, Masika PJ, Muchenje V. Polyphenolic content and antioxidant properties of *Moringa oleifera* leaf extracts and enzymatic activity of liver from goats supplemented with *Moringa oleifera* leaves/sunflower seed cake. *Meat Sci*. 2012;91:441–7.
159. Singh BN, Singh BR, Singh RL, Prakash D, Dhakarey R, Upadhyay G, *et al*. Oxidative DNA damage protective activity, antioxidant and anti-quorum sensing potentials of *Moringa oleifera*. *Food Chem Toxicol*. 2009;47:1109–16.
160. Luqman S, Kaushik S, Srivastava S, Kumar R, Bawankule DU, Pal A, *et al*. Protective effect of medicinal plant extracts on biomarkers of oxidative stress in erythrocytes. *Pharm Biol*. 2009;47:483–90.
161. Green TP, Wiemer DF. Four neolignan ketones from *Piper capense*. *Phytochemistry*. 1991;30:3759–62.
162. Green T, Galinis D, Wiemer D. Three neolignans from the roots of *Piper capense*. *Phytochemistry*. 1991;30:1649–52.
163. Tchoumboungang F, Jazet D, Sameza M, Ndifor F, Wouatsa N, Amvam Z, *et al*. Comparative essential oils composition and insecticidal effect of different tissues of *Piper capense* L., *Piper guineense* Schum. et Thonn, *Piper nigrum* L. and *Piper umbellatum* L. grown in Cameroon. *African J Biotechnol*. 2009;8:424–31.
164. Pedersen ME, Metzler B, Stafford GI, van Staden J, Jäger AK, Rasmussen HB. Amides from *Piper capense* with CNS activity - A preliminary SAR analysis. *Molecules*. 2009;14:3833–43.
165. Matasyoh JC, Wathuta EM, Kariuki ST, Chepkorir R. Chemical composition and larvicidal activity of *Piper capense* essential oil against the malaria vector, *Anopheles gambiae*. *J Asia Pac Entomol*. 2011;14:26–8.
166. Thorburn A. Phytochemical analysis and antimicrobial activity of *Piper capensis* L.f. MSc dissertation, University of Pretoria, Pretoria. 2010.
167. Olajuyigbe O, Afolayan A. Phenolic content and antioxidant property of the bark extracts of *Ziziphus mucronata* Willd. subsp. *mucronata* Willd. *BMC Complement Altern Med*. 2011;11:130.

168. Ibrahim MA, Koorbanally NA, Kiplimo JJ, Islam S. Anti-oxidative activities of the various extracts of stem bark, root and leaves of *Ziziphus mucronata* (Rhamnaceae) *in vitro*. J Med Plants Res. 2011;6:4176–84.
169. Tafadzwa M. Screening of some traditional medicinal plants from Zimbabwe for biological and anti-microbial activity. MPhil dissertation, University of Zimbabwe, Zimbabwe. 2012.
170. Auvin C, Lezenven F, Blond A, Augeven-Bour I, Pousset JL, Bodo B, *et al.* Mucronine J, a 14-membered cyclopeptide alkaloid from *Zizyphus mucronata*. J Nat Prod. 1996;59:676–8.
171. Makkar H, Becker K. Do tannins in leaves of trees and shrubs from African and Himalayan regions differ in level and activity? Agrofor Syst. 1998;40:59–68.
172. Mpiana P, Mudogo V, Tshibangu D, Kitwa E, Kanangila A, Lumbu J, *et al.* Antisickling activity of anthocyanins from *Bombax pentadrum*, *Ficus capensis* and *Ziziphus mucronata*: Photodegradation effect. J Ethnopharmacol. 2008;120:413–8.
173. Wanyonyi A, Chhabra S, Mkoji G, Njue W, Tarus P. Molluscicidal and antimicrobial activity of *Solanum aculeastrum*. Fitoterapia. 2003;74:298–301.
174. Wanyonyi A, Chhabra S, Mkoji G, Eilert U, Njue W. Bioactive steroidal alkaloid glycosides from *Solanum aculeastrum*. Phytochemistry. 2002;59:79–84.
175. Koster M, Price LL. Rwandan female genital modification: elongation of the *Labia minora* and the use of local botanical species. Cult Health Sex. 2008;10:191–204.
176. Koduru S, Grierson D, van de Venter M, Afolayan A. Anticancer activity of steroid alkaloids isolated from *Solanum aculeastrum*. Pharm Biol. 2007;45:613–8.
177. Koduru S, Grierson D, Aderogba M, Eloff J, Afolayan A. Antioxidant activity of *Solanum aculeastrum* (Solanaceae) berries. Int J Pharmacol. 2006;2:262–4.
178. Nannan N, Dorrington R, Laubscher R, Zinyakatira N, Prinsloo M, Darikwa T, *et al.* Under-5 mortality statistics in South Africa: Shedding some light on trends and causes 1997-2007. South African Medical Research Council Report, 2012.
179. Tindimwebwa G, Dambisya Y. When is it herbal intoxication? A retrospective study of children admitted with herbal intoxication at Umtata General Hospital, South Africa. Cent Afr J Med. 2003;49:111–4.
180. De Wet B. Medicinal plants and human health. South African Pharmacol J. 2011;78:38–40.
181. Wink M. Functions and biotechnology of plant secondary metabolites (Annual Plant Reviews, Volume 39). Blackwell Publishing. 2010.
182. American Type Culture Collection. Caco-2 [Caco2] (ATCC® HTB-37™).
183. Pinto M, Robine-Leon S, Appay M-D, Kedingner M, Triadou N, Dussaulx E, *et al.* Enterocyte-like differentiation and polarization of the human colon carcinoma cell line Caco-2 in culture. Biol Cell. 1983;47:323–30.
184. Jia J, Wasan K. Effects of monoglycerides on rhodamine 123 accumulation, estradiol 17-β-D-glucuronide bidirectional transport and MRP2 protein expression within Caco-2 cells. J Pharm Pharm Sci. 2008;11:45–62.
185. American Type Culture Collection. Hep G2 [HEPG2] (ATCC® HB-8065™).

186. Wilkening S, Stahl F, Bader A. Comparison of primary human hepatocytes and hepatoma cell line HepG2 with regard to their biotransformation properties. *Drug Metab Dispos.* 2003;31:1035–42.
187. Riss T, Moravec R, Niles A, Benink H, Worzella T. Cell viability assays. In: *Assay Guidance Manual*. Eli Lilly & Company and the National Center for Advancing Translational Sciences. 2013.
188. Vichai V, Kirtikara K. Sulforhodamine B colorimetric assay for cytotoxicity screening. *Nat Protoc.* 2006;1:1112–6.
189. Repetto G, del Peso A, Zurita J. Neutral red uptake assay for the estimation of cell viability/cytotoxicity. *Nat Protoc.* 2008;3:1125–31.
190. Mosmann T. Rapid colorimetric assay for cellular growth and survival: Application to proliferation and cytotoxicity assays. *J Immunol Methods.* 1983;65:55–63.
191. Rampersad S. Multiple applications of Alamar Blue as an indicator of metabolic function and cellular health in cell viability bioassays. *Sensors.* 2012;12:12347–60.
192. van Tonder A, Joubert A, Cromarty A. Limitations of the 3-(4,5-dimethylthiazol-2-yl)-2,5-diphenyl-2H-tetrazolium bromide (MTT) assay when compared to three commonly used cell enumeration assays. *BMC Res Notes.* 2015;8:47.
193. Collier A, Pritsos C. The mitochondrial uncoupler dicumarol disrupts the MTT assay. *Biochem Pharmacol.* 3AD;66:281–7.
194. Wang P, Henning S, Heber D. Limitations of MTT and MTS-based assays for measurement of antiproliferative activity of green tea polyphenols. *PLoS One.* 2010;5:e10202.
195. Bruggisser R, von Daeniken K, Jundt G, Schaffner W, Tullberg-Reinert H. Interference of plant extracts, phytoestrogens and antioxidants with the MTT tetrazolium assay. *Planta Med.* 2002;68:445–8.
196. Johnston P. Redox cycling compounds generate H<sub>2</sub>O<sub>2</sub> in HTS buffers containing strong reducing reagents – real hits or promiscuous artifacts? *Curr Opin Chem Biol.* 2011;15:174-182:174–82.
197. Monteiro-Riviere N, Inman A, Zhang L. Limitations and relative utility of screening assays to assess engineered nanoparticle toxicity in a human cell line. *Toxicol Appl Pharmacol.* 2009;234:222–35.
198. Seoposengwe K, van Tonder JJ, Steenkamp V. *In vitro* neuroprotective potential of four medicinal plants against rotenone-induced toxicity in SH-SY5Y neuroblastoma cells. *BMC Complement Altern Med.* 2013;13:353.
199. Adewusi E. *In vitro* effect of selected medicinal plants on  $\beta$ -amyloid induced toxicity in neuroblastoma cells. PhD thesis, University of Pretoria, Pretoria. 2012.
200. Adewusi E. *In vitro* effect of selected medicinal plants on  $\beta$ -amyloid induced toxicity in neuroblastoma cells. PhD thesis, University of Pretoria, Pretoria. 2012.
201. McGaw L, Van der Merwe D, Eloff J. *In vitro* anthelmintic, antibacterial and cytotoxic effects of extracts from plants used in South African ethnoveterinary medicine. *Vet J.* 2007;173:366–72.
202. Fouche G, Cragg G, Pillay P, Kolesnikova N, Maharaj V, Senabe J. *In vitro* anticancer screening of South African plants. *J Ethnopharmacol.* 2008;119:455–61.

203. Mokoka T, Zimmermann S, Julianti T, Hata Y, Moodley N, Cal M, *et al.* *In vitro* screening of traditional South African malaria remedies against *Trypanosoma brucei rhodesiense*, *Trypanosoma cruzi*, *Leishmania donovani*, and *Plasmodium falciparum*. *Planta Med.* 2011;77:1663–7.
204. Moshi M, Mbwambo Z, Nondo R, Masimba P, Kamuhabwa A, Kapingu M, *et al.* Evaluation of ethnomedicinal claims and brine shrimp toxicity of some plants used in Tanzania as traditional medicines. *Afr J Trad CAM.* 2006;3:48–58.
205. Kee N, Mnonopi N, Davids H, Naudé R, Frost L. Antithrombotic/anticoagulant and anticancer activities of selected medicinal plants from South Africa. *African J Biotechnol.* 2008;7:217–23.
206. Kaou A, Mahiou-Leddé V, Hutter S, Aïnouddine S, Hassani S, Yahaya I, *et al.* Antimalarial activity of crude extracts from nine African medicinal plants. *J Ethnopharmacol.* 2008;116(1):74–83.
207. Woguem V, Maggi F, Fogang H, Tapondjou L, Womeni H, Quassinti L, *et al.* Volatile oil from the wild pepper *Piper capense* used in Cameroon as a culinary spice. *Nat Prod Commun.* 2013;8:1–6.
208. Kuete V, Sandjo L, Wiench B, Efferth T. Cytotoxicity and modes of action of four Cameroonian dietary spices ethno-medically used to treat cancers: *Echinops giganteus*, *Xylopiya aethiopica*, *Imperata cylindrica* and *Piper capense*. *J Ethnopharmacol.* 2013;149:245–53.
209. Kuete V, Krusche B, Youns M, Voukeng I, Fankam A, Tankeo S, *et al.* Cytotoxicity of some Cameroonian spices and selected medicinal plant extracts. *J Ethnopharmacol.* 2011;134:803–12.
210. Jitsuno M, Yokosuka A, Sakagami H, Mimaki Y. Chemical constituents of the bulbs of *Habranthus brachyandrus* and their cytotoxic activities. *Chem Pharm Bull (Tokyo).* 2009;57:1153–7.
211. Li Y, Liu J, Tang LJ, Shi YW, Ren W, Hu WX. Apoptosis induced by lycorine in KM3 cells is associated with the G0/G1 cell cycle arrest. *OncolRep.* 2007;17:377–84.
212. Van Goietsenoven G, Andolfi A, Lallemand B, Cimmino A, Lamoral-Theys D, Gras T, *et al.* Amaryllidaceae alkaloids belonging to different structural subgroups display activity against apoptosis-resistant cancer cells. *J Nat Prod.* 2010;73:1223–7.
213. Li L, Dai H-J, Ye M, Wang S-L, Xiao X-J, Zheng J, *et al.* Lycorine induces cell-cycle arrest in the G0/G1 phase in K562 cells via HDAC inhibition. *Cancer Cell Int.* 2012;12:49.
214. Cao Z, Yu D, Fu S, Zhang G, Pan Y, Bao M, *et al.* Lycorine hydrochloride selectively inhibits human ovarian cancer cell proliferation and tumor neovascularization with very low toxicity. *Toxicol Lett.* 2013;218:174–85.
215. Doskočil I, Hošťálková A, Šafatová M, Benešová N, Havlík J, Havelek R, *et al.* Cytotoxic activities of Amaryllidaceae alkaloids against gastrointestinal cancer cells. *Phytochem Lett.* 2015;13:394–8
216. Silva AFS, de Andrade JP, Machado KRB, Rocha AB, Apel MA, Sobral MEG, *et al.* Screening for cytotoxic activity of extracts and isolated alkaloids from bulbs of *Hippeastrum vittatum*. *Phytomedicine.* 2008;15:882–5.

217. Nair JJ, Rárová L, Strnad M, Bastida J, van Staden J. Apoptosis-inducing effects of distichamine and narciprimine, rare alkaloids of the plant family Amaryllidaceae. *Bioorg Med Chem Lett.* 2012;22:6195–9.
218. Chan P. Acylation with diangeloyl groups at C21–22 positions in triterpenoid saponins is essential for cytotoxicity towards tumor cells. *Biochem Pharmacol.* 2007;73:341–50.
219. Güçlü-Üstündağ Ö, Mazza G. Saponins: Properties, applications and processing. *Crit Rev Food Sci Nutr.* 2007;47:231–58.
220. McGaw LJ, Van der Merwe D, Eloff JN. In vitro anthelmintic, antibacterial and cytotoxic effects of extracts from plants used in South African ethnoveterinary medicine. *Vet J.* 2007;173:366–72.
221. Popat A, Shear N, Malkiewicz I, Thomson S, Neuman M. Mechanism of *Impila (Callilepis laureola)*-induced cytotoxicity in Hep G2 cells. *Clin Biochem.* 2002;35:57–64.
222. Varga C, Veale D. Isihlambezo: utilization patterns and potential health effects of pregnancy-related traditional herbal medicine. *Soc Sci Med.* 1997;44:911–24.
223. steenkamp V, Stewart M, van der Merwe S, Zuckerman M, Crowther N. The effect of *Senecio latifolius* a plant used as a South African traditional medicine, on a human hepatoma cell line. *J Ethnopharmacol.* 2001;78:51–8.
224. Li YH, Kan WLT, Li N, Lin G. Assessment of pyrrolizidine alkaloid-induced toxicity in an *in vitro* screening model. *J Ethnopharmacol.* 2013;150:560–7.
225. Müller-Tegethoff K, Kersten B, Kasper P, Müller L. Application of the *in vitro* rat hepatocyte micronucleus assay in genetic toxicology testing. *Mutat Res.* 1997;392:125–38.
226. Griffin DS, Segall HJ. Genotoxicity and cytotoxicity of selected pyrrolizidine alkaloids, a possible alkenal metabolite of the alkaloids, and related alkenals. *Toxicol Appl Pharmacol.* 1986;86:227–34.
227. Tu M, Li L, Lei H, Ma Z, Chen Z, Sun S, *et al.* Involvement of organic cation transporter 1 and CYP3A4 in retrorsine-induced toxicity. *Toxicology.* 2014;322:34–42.
228. Neuwinger H. Plants used for poison fishing in tropical Africa. *Toxicon.* 2004;44:417–30.
229. Lee S, Luyengi L, Gerhäuser C, Mar W, Lee K, Mehta R, *et al.* Inhibitory effect of munetone, an isoflavonoid, on 12-O-tetradecanoylphorbol 13-acetate-induced ornithine decarboxylase activity. *Cancer Lett.* 1999;136:59–65.
230. Nair A, Shishodia S, Ahn K, Kunnumakkara A, Sethi G, Bharat B. Deguelin, an Akt inhibitor, suppresses I $\kappa$ B $\alpha$  kinase activation leading to suppression of NF- $\kappa$ B-regulated gene expression, potentiation of apoptosis, and inhibition of cellular invasion. *J Immunol.* 2006;177:5612–22.
231. Thamilselvan V, Menon M, Thamilselvan S. Anticancer efficacy of deguelin in human prostate cancer cells targeting glycogen synthase kinase-3  $\beta$ / $\beta$ -catenin pathway. *Int J Cancer.* 2011;129:2916–27.
232. Baba Y, Fujii M, Maeda T, Suzuki A, Yuzawa S, Kato Y. Deguelin induces apoptosis by targeting both EGFR-Akt and IGF1R-Akt pathways in head and neck squamous cell cancer cell lines. *Biomed Res Int.* 2015;2015:657179.

233. Oyedemi S, Yakubu M, Afolayan a. Effect of aqueous extract of *Leonotis leonurus* (L.) R. Br. leaves in male Wistar rats. *Hum Exp Toxicol*. 2010;29:377–84.
234. Kaou A, Mahiou-Leddet V, Canlet C, Debrauwer L, Hutter S, Azas N, *et al*. New amide alkaloid from the aerial part of *Piper capense* L.f. (Piperaceae). *Fitoterapia*. 2010;81:632–5.
235. Do MT, Kim HG, Choi JH, Khanal T, Park BH, Tran TP, *et al*. Antitumor efficacy of piperine in the treatment of human HER2-overexpressing breast cancer cells. *Food Chem*. 2013;141:2591–9.
236. Motiwala MN, Rangari VD. Combined effect of paclitaxel and piperine on a MCF-7 breast cancer cell line *in vitro*: Evidence of a synergistic interaction. *Synergy*. 2015;2:1–6.
237. Yaffe PB, Power Coombs MR, Doucette CD, Walsh M, Hoskin DW. Piperine, an alkaloid from black pepper, inhibits growth of human colon cancer cells via G1 arrest and apoptosis triggered by endoplasmic reticulum stress. *Mol Carcinog*. 2014;1085:1070–85.
238. Checker R, Gambhir L, Sharma D, Kumar M, Sandur SK. Plumbagin induces apoptosis in lymphoma cells via oxidative stress mediated glutathionylation and inhibition of mitogen-activated protein kinase phosphatases (MKP1/2). *Cancer Lett*. 2015;357:265–78.
239. Khaw AK, Sameni S, Venkatesan S, Kalthur G, Hande MP. Plumbagin alters telomere dynamics, induces DNA damage and cell death in human brain tumour cells. *Mutat Res Toxicol Environ Mutagen*. 2015;793:86–95.
240. Schiller C, Fröhlich C, Giessmann T, Siegmund W, Mönnikes H, Hosten N, *et al*. Intestinal fluid volumes and transit of dosage forms as assessed by magnetic resonance imaging. *Aliment Pharmacol Ther*. 2005;22:971–9.
241. Brenner C, Galluzzi L, Kepp O, Kroemer G. Decoding cell death signals in liver inflammation. *J Hepatol*. 2013;59:583–94.
242. Pandit A, Sachdeva T, Bafna P. Drug-induced hepatotoxicity: A review. *J Appl Pharm Sci*. 2012;02:233–43.
243. Jaeschke H, Gores GJ, Cederbaum AI, Hinson JA, Pessayre D, Lemasters JJ. Mechanisms of hepatotoxicity. *Toxicol Sci*. 2002;65:166–76.
244. Bradbury MW. Lipid Metabolism and Liver Inflammation . I. Hepatic fatty acid uptake: possible role in steatosis. *Am J Physiol Gastrointest Liver Physiol*. 2006;290:G194–8.
245. Zamek-Gliszczyński MJ, Hoffmaster KA., Nezasa KI, Tallman MN, Brouwer KLR. Integration of hepatic drug transporters and phase II metabolizing enzymes: Mechanisms of hepatic excretion of sulfate, glucuronide, and glutathione metabolites. *Eur J Pharm Sci*. 2006;27:447–86.
246. Corsini A, Bortolini M. Drug-induced liver injury: The role of drug metabolism and transport. *J Clin Pharmacol*. 2013;53:463–74.
247. Begriche K, Massart J, Robin M-A, Borgne-Sanchez A, Fromenty B. Drug-induced toxicity on mitochondria and lipid metabolism: mechanistic diversity and deleterious consequences for the liver. *J Hepatol*. 2011;54:773–94.
248. Verma S, Kaplowitz N. Diagnosis , management and prevention of drug-induced liver injury. *Gut*. 2009;58:1555–64.
249. Fontana RJ. Acute liver failure due to drugs. *Semin Liver Dis*. 2008;28:175–87.

250. Pessayre D, Fromenty B, Berson A, Robin M-A, Lettéron P, Moreau R, *et al.* Central role of mitochondria in drug-induced liver injury. *Drug Metab Rev.* 2012;44:34–87.
251. Chalasani N, Fontana R, Bonkovsky H, Watkins P, Davern T, Serrano J, *et al.* Causes, clinical features, and outcomes from a prospective study of drug-induced liver injury in the United States. *Gastroenterology.* 2013;135:1924–34.
252. Hayashi PH, Fontana RJ. Clinical features, diagnosis, and natural history of drug-induced liver injury. *Semin Liver Dis.* 2014;34:134–44.
253. Seeff LB. Herbal hepatotoxicity. *Clin Liver Dis.* 2007;11:577–96.
254. Abdualmjid RJ, Sergi C. Hepatotoxic botanicals - An evidence-based systematic review. *J Pharm Pharm Sci.* 2013;16:376–404.
255. Teschke R, Frenzel C, Schulze J, Eickhoff A. Herbal hepatotoxicity: challenges and pitfalls of causality assessment methods. *World J Gastroenterol.* 2013;19:2864–82.
256. Steenkamp V, Stewart MJ, Zuckerman M. Detection of poisoning by Impila (*Callilepis laureola*) in a mother and child. *Hum Exp Toxicol.* 1999;18:594–7.
257. Steenkamp V, Stewart M, Zuckerman M. Clinical and analytical aspects of pyrrolizidine poisoning caused by South African traditional medicines. *Ther Drug Monit.* 2000;22:302–6.
258. Bottenberg MM, Wall GC, Harvey RL, Habib S. Oral *Aloe vera*-induced hepatitis. *Ann Pharmacother.* 2007;41:1740–3.
259. Tarantino G, Pezzullo MG, di Minno M, Milone F, Pezzullo LS, Milone M, *et al.* Drug-induced liver injury due to “natural products” used for weight loss: A case report. *World J Gastroenterol.* 2009;15:2414–7.
260. Enbom ET, Le MD, Oesterich L, Rutgers J, French SW. Mechanism of hepatotoxicity due to black cohosh (*Cimicifuga racemosa*): Histological, immunohistochemical and electron microscopy analysis of two liver biopsies with clinical correlation. *Exp Mol Pathol.* 2014;96:279–83.
261. Langrand J, Regnault H, Cachet X, Bouzidi C, Villa AF. Phytomedicine toxic hepatitis induced by a herbal medicine: *Tinospora crispa*. *Phytomedicine.* 2014;21:1120–3.
262. Teschke R, Bahre R. Severe hepatotoxicity by Indian Ayurvedic herbal products : A structured causality assessment. *Ann Hepatol.* 2009;8:258–66.
263. Lim TY, Considine A, Quaglia A, Shawcross DL. Subacute liver failure secondary to black cohosh leading to liver transplantation. *BMJ Case Rep.* 2013;1–4.
264. Engels M, Wang C, Matoso A, Maidan E, Wands J. Tea not tincture: hepatotoxicity associated with Rooibos herbal tea. *ACG Case Reports J.* 2013;1:58–60.
265. Jung KA, Min HJ, Yoo SS, Kim HJ, Choi SN, Ha CY, *et al.* Drug-induced liver injury: Twenty five cases of acute hepatitis following ingestion of Polygonum multiflorum Thunb. *Gut Liver.* 2011;5:493–9.
266. Wainwright J, Schonland M. Toxic hepatitis in black patients in Natal. *SA Med J.* 1977;51:571–3.
267. Watson A, Coovadia H, Bhoola K. The clinical syndrome of Impila (*Callilepis laureola*) poisoning in children. *SA Med J.* 1979;55:290–2.

268. Picciotto A, Campo N, Brizzolara R, Giusto R, Guido G, Sinelli N, *et al.* Chronic hepatitis induced by Jin Bu Huan. *J Hepatol.* 1998;28:165–7.
269. Mrzljak A, Kosuta I, Skrtic A, Kanizaj T, Vrhovac R. Drug-induced liver injury associated with Noni (*Moringa citrifolia*) juice and phenobarbital. *Case Rep Gastroenterol.* 2013;7:19–24.
270. Cheung W, Tse M, Ngan T, Lin J, Lee W, Poon W, *et al.* Liver injury associated with the use of *Fructus psoraleae* (Bol-gol-zhee or Bu-gu-zhi) and its related proprietary medicine. *Clin Toxicol.* 2009;47:683–5.
271. Nadir A, Reddy D, van Thiel DH. *Cascara sagrada*-induced intrahepatic cholestasis causing portal hypertension: Case report and review of herbal hepatotoxicity. *Am J Gastroenterol.* 2000;95:3634–7.
272. Wallace K, Starkov A. Mitochondrial targets of drug toxicity. *Annu Rev Pharmacol Toxicol.* 2000;40:353–88.
273. Kroemer G, Reed JC. Mitochondrial control of cell death. *Nat Med.* 2000;6:513–9.
274. Bartlett K, Eaton S. Mitochondrial beta-oxidation. *Eur J Biochem.* 2004;271:462–9.
275. Moreira AC, Machado NG, Bernardo TC, Sardão VA, Oliveira PJ. Mitochondria as a biosensor for drug-induced toxicity – Is it really relevant? In: *Biosensors for Health, Environment and Biosecurity.* InTech Publishing; 2011.
276. Xu J, Diaz D, O'Brien P. Applications of cytotoxicity assays and pre-lethal mechanistic assays for assessment of human hepatotoxicity potential. *Chem Biol Interact.* 2004;150:115–28.
277. Gao S-Y, Wang Q-J, Ji Y-B. Effect of solanine on the membrane potential of mitochondria in HepG2 cells and [Ca<sup>2+</sup>]<sub>i</sub> in the cells. *World J Gastroenterol.* 2006;12:3359–67.
278. Jaeschke H, McGill MR, Ramachandran A. Oxidant stress, mitochondria, and cell death mechanisms in drug-induced liver injury: Lessons learned from acetaminophen hepatotoxicity. *Drug Metab Rev.* 2012;44:88–106.
279. Finkel T, Holbrook NJ. Oxidants, oxidative stress and the biology of ageing. *Nature.* 2000;408:239–47.
280. Son Y, Cheong Y, Kim N, Chung H, Kang DG, Pae H. MAPK pathways. *J Signal Transduct.* 2011;2011.
281. Yuan L, Kaplowitz N. Glutathione in liver diseases and hepatotoxicity. *Mol Aspects Med.* 2009;30:29–41.
282. Vivancos P, Wolff T, Markovic J, Pallardó F, Foyer C. A nuclear glutathione cycle within the cell cycle. *Biochem J.* 2010;431:169–78.
283. Dalleau S, Baradat M, Guéraud F, Huc L. Cell death and diseases related to oxidative stress: 4-hydroxynonenal (HNE) in the balance. *Cell Death Differ.* 2013;20:1615–30.
284. Huang C, Freter C. Lipid metabolism, apoptosis and cancer therapy. *Int J Mol Sci.* 2015;16:924–49.
285. Cooper G. The Cell Cycle. In: *The Cell: A Molecular Approach.* Sinauer Associates. 2000.
286. Pinheiro D, Sunkel C. Mechanisms of cell cycle control. *Canal BQ.* 2012;9:4–17.
287. Darzynkiewicz Z, Crissman H, Jacobberger JW. Cytometry of the cell cycle: cycling through history. *Cytom Part A.* 2004;58A:21–32.

288. Wikipedia. Animal cell cycle. 2012. Accessed on 10 March 2016 from [https://upload.wikimedia.org/wikipedia/commons/thumb/2/2f/Animal\\_cell\\_cycle-en.svg/790px-Animal\\_cell\\_cycle-en.svg.png](https://upload.wikimedia.org/wikipedia/commons/thumb/2/2f/Animal_cell_cycle-en.svg/790px-Animal_cell_cycle-en.svg.png)
289. Bertoli C, Skotheim JM, Bruin RAM De. Control of cell cycle transcription during G1 and S phases. *Nat Rev.* 2013;14:518–28.
290. Novák B, Sible JC, Tyson JJ. Checkpoints in the Cell Cycle. *eLS.* 2003.
291. Bloom J, Cross FR. Multiple levels of cyclin specificity in cell-cycle control. *Nat Rev.* 2007;8:149–60.
292. Patil M, Pabla N, Dong Z. Checkpoint kinase 1 in DNA damage response and cell cycle regulation. *Cell Mol Life Sci.* 2013;70:4009–21.
293. ravinthan A, Scarpini C, Tachtatzis P, Verma S, Penrhyn-low S, Harvey R, *et al.* Hepatocyte senescence predicts progression in non-alcohol-related fatty liver disease. *J Hepatol.* 2013;58:549–56.
294. Kroemer G, Dallaporta B, Resche-Rigon M. The mitochondrial death.life regulator in apoptosis and necrosis. *Annu Rev Physiol.* 1998;60:619–42.
295. Cohen GM. Caspases: the executioners of apoptosis. *Biochem J.* 1997;16:1–16.
296. Wang K. Molecular mechanisms of liver injury: Apoptosis or necrosis. *Exp Toxicol Pathol.* 2014;66:351–6.
297. Wikipedia. Structural changes of cells undergoing necrosis and apoptosis. 2015. Accessed on 15 March 2016 from [https://upload.wikimedia.org/wikipedia/commons/thumb/6/69/Structural\\_changes\\_of\\_cells\\_und ergoing\\_necrosis\\_or\\_apoptosis.png/800px-Structural\\_changes\\_of\\_cells\\_undergoing\\_necrosis\\_or\\_apoptosis.png](https://upload.wikimedia.org/wikipedia/commons/thumb/6/69/Structural_changes_of_cells_und ergoing_necrosis_or_apoptosis.png/800px-Structural_changes_of_cells_undergoing_necrosis_or_apoptosis.png)
298. Tsuji M, Oguchi K. Some findings on apoptosis in hepatocytes. In: *Apoptosis and Medicine.* InTech Publishing. 2012.
299. Hengartner MO. The biochemistry of apoptosis. *Nature.* 2000;407:810–6.
300. Danial NN, Korsmeyer SJ. Cell death: Critical control points. *Cell.* 2004;116:205–19.
301. Wikipedia. Extrinsic and intrinsic pathways to caspase-3 activation. 2008. Accessed on 14 March 2016 from [https://commons.wikimedia.org/wiki/File:Extrinsic\\_and\\_intrinsic\\_pathways\\_to\\_caspase-3\\_activation.jpg](https://commons.wikimedia.org/wiki/File:Extrinsic_and_intrinsic_pathways_to_caspase-3_activation.jpg)
302. Gadaga L, Tagwireyi D, Dzangare J, Nhachi C. Acute oral toxicity and neurobehavioural toxicological effects of hydroethanolic extract of *Boophane disticha* in rats. *Hum Exp Toxicol.* 2011;30:972–80.
303. du Plooy W, Swart L, van Huysteen G. Poisoning with *Boophane disticha*: a forensic case. *Hum Exp Toxicol.* 2001;20:277–8.
304. Bamishaiye EI, Olayemi FF, Awagu EF, Bamshaiye OM. Proximate and phytochemical composition of *Moringa oleifera* leaves at three stages of maturation. *J Food Sci.* 2011;3:233–7.

305. Awodele O, Oreagba IA, Odoma S, da Silva JAT, Osunkalu VO. Toxicological evaluation of the aqueous leaf extract of *Moringa oleifera* Lam. (Moringaceae). J Ethnopharmacol. 2012;139:330–6.
306. National Research Council. Lost Crops of Africa: Volume II: Vegetables. The National Academies Press, Washington. 2006.
307. Oluduro OA, Idowu TO, Aderiye BI, Famurewa O, Omoboye OO. Evaluation of antibacterial potential of crude extract of *Moringa oleifera* seed on orthopaedics wound isolates and characterization of phenylmethanamine and benzyl isothiocyanate derivatives. Res J Med Plant. 2012;6:383–94.
308. Paliwal R, Sharma V, Pracheta, Sharma S, Yadav S. Anti-nephrotoxic effect of administration of *Moringa oleifera* Lam in amelioration of DMBA-induced renal carcinogenesis in Swiss albino mice. Biol Med. 2011;3:27–35.
309. De Saint Sauveur A. Conclusion on the potential of Moringa on the food supplement market in Europe. Moringa News. 2012.
310. Sharma N, Gupta PC, C.V. R. Nutrient content, mineral content and antioxidant activity of *Amaranthus viridus* and *Moringa oleifera* leaves. Res J Med Plant. 2012;6:253–9.
311. Koduru S, Grierson D, Afolayan A. Antimicrobial activity of *Solanum aculeastrum*. Pharm Biol. 2006;44:283–6.
312. Wanyonyi A, Tarus P, Chhabra S. A novel glycosidic steroidal alkaloid from *Solanum aculeastrum*. Bull Chem Soc Ethiop. 2003;17:61–6.
313. Cock IE, van Vuuren SF. Anti-proteus activity of some South African medicinal plants: their potential for the prevention of rheumatoid arthritis. Inflammopharmacology. 2014;22:23–36.
314. Moshi M, Mbwambo Z. Some pharmacological properties of extracts of *Terminalia sericea* roots. J Ethnopharmacol. 2005;97:43–7.
315. Cordier W, Steenkamp V. Evaluation of four assays to determine cytotoxicity of selected crude medicinal plant extracts *in vitro*. Br J Pharm Res. 2015;7:16–21.
316. van Tonder J. Development of an *in vitro* mechanistic toxicity screening model using cultured hepatocytes. PhD thesis, University of Pretoria, Pretoria. 2011.
317. Fernandes AS, Gaspar J, Cabral MF, Rueff J, Castro M, Batinic-Haberle I, *et al*. Protective role of ortho-substituted Mn(III) N-alkylpyridylporphyrins against the oxidative injury induced by tert-butylhydroperoxide. Free Radic Res. 2010;44:430–40.
318. Greenspan P, Mayer EP, Fowler SD. Nile Red: A selective fluorescent stain for intracellular lipid droplets. J Cell Biol. 1985;100:965–73.
319. Kiela PR, Midura AJ, Kuscuoglu N, Jolad SD, Sólyom AM, Besselsen DG, *et al*. Effects of *Boswellia serrata* in mouse models of chemically induced colitis. Am J Physiol Gastrointest Liver Physiol. 2005;288:G798–808.
320. Stern S, Potter T, Neun B. NCL method GTA-4: Hep G2 hepatocyte lipid peroxidation assay. Nanotechnol Charact Lab. 2010.
321. MCL corporation. ApoSENSOR ATP Cell Viability. 2015.

322. Davis PK, Ho A, Dowdy SF. Biological methods for cell-cycle synchronization of mammalian cells. *Biotechniques*. 2001;30:1322–31.
323. Cooper S. Rethinking synchronization of mammalian cells for cell cycle analysis. *Cell Mol Life Sci*. 2003;60:1–9.
324. Rosner M, Schipany K, Hengstschläger M. Merging high-quality biochemical fractionation with a refined flow cytometry approach to monitor nucleocytoplasmic protein expression throughout the unperturbed mammalian cell cycle. *Nat Protoc*. 2013;8:606–26.
325. Chiang P-C, Lin S-C, Pan S-L, Kuo C-H, Tsai I-L, Kuo M-T, *et al*. Antroquinonol displays anticancer potential against human hepatocellular carcinoma cells: A crucial role of AMPK and mTOR pathways. *Biochem Pharmacol*. 2010;79:162–71.
326. Pozarowski P, Darzynkiewicz Z. Analysis of cell cycle by flow cytometry. *Methods Mol Biol*. 2004;281:301–11.
327. Riccardi C, Nicoletti I. Analysis of apoptosis by propidium iodide staining and flow cytometry. *Nat Protoc*. 2006;1:1458–61.
328. Darzynkiewicz Z, Juan G. DNA content measurement for DNA ploidy and cell cycle analysis. *Curr Protoc Cytom*. 2001;7.5:1–24.
329. Hingorani R, Deng J, Elia J, McIntyre C, Mittar D. Detection of apoptosis using the BD Annexin V FITC assay on the BD FACSVerser™ System. Application note, BD Biosci. 2011.
330. DiPaolo R. To arrest or not to G2-M cell-cycle arrest. *Clin Cancer Res*. 2002;8:3512–9.
331. Palanisamy AP, Cheng G, Sutter AG, Evans ZP, Polito CC, Jin L, *et al*. Mitochondrial uncoupling protein 2 induces cell cycle arrest and necrotic cell death. *Metab Syndr Relat Disord*. 2014;12:132–42.
332. Sweet S, Singh G. Accumulation of human promyelocytic leukemic (HL-60) cells at two energetic cell cycle checkpoints. *Cancer Res*. 1995;55:5164–7.
333. Gemin A, Sweet S, Preston TJ, Singh G. Regulation of the cell cycle in response to inhibition of mitochondrial generated energy. *Biochem Biophys Res Commun* [Internet]. 2005;332:1122–32.
334. Hetz CA, Hunn M, Rojas P, Torres V, Leyton L, Quest AFG. Caspase-dependent initiation of apoptosis and necrosis by the Fas receptor in lymphoid cells: onset of necrosis is associated with delayed ceramide increase. *J Cell Sci*. 2002;115:4671–83.
335. Gao M-J, Xu Z, Wang F, Chen X, Hu W, Xu R. The linkage between cell cycle S phase arrest and apoptosis on human hepatocellular carcinoma HepG2 induced by Na<sup>+</sup>/K<sup>+</sup>-ATPase inhibitors via regulating proteins associated with cell cycle. *Chinese Pharmacol Bull*. 2010;26:452–6.
336. Xu Z, Wang F, Xu R, Hu W, Chen X. Effect of Na(+)/K(+)-ATPase α1 siRNA and ouabain upon cell cycle in human hepatoma HepG2 cell and its mechanism. *Zhonghua Yi Xue Za Zhi*. 2010;90:813–7.
337. Ozdemir T, Nar R, Kilinc V, Alacam H, Salis O, Duzgun A, *et al*. Ouabain targets the unfolded protein response for selective killing of HepG2 cells during glucose deprivation. *Cancer Biother Radiopharm*. 2012;27:457–63.
338. Pezzani R, Rubin B, Redaelli M, Radu C, Barollo S, Cicala MV, *et al*. The antiproliferative effects of ouabain and everolimus on adrenocortical tumor cells. *Endocr J*. 2014;61:41–53.

339. Chen D, Song M, Mohamad O, Yu S. Inhibition of Na<sup>+</sup>/K<sup>+</sup>-ATPase induces hybrid cell death and enhanced sensitivity to chemotherapy in human glioblastoma cells. *BMC Cancer*. 2014;14:716.
340. Xu Z-W, Wang F-M, Gao M-J, Chen X-Y, Hu W-L, Xu R-C. Targeting the Na<sup>(+)</sup>/K<sup>(+)</sup>-ATPase  $\alpha$ 1 subunit of hepatoma HepG2 cell line to induce apoptosis and cell cycle arresting. *Biol Pharm Bull*. 2010;33:743–51.
341. Leist M, Single B, Naumann H, Fava E, Simon B, Kühnle S, *et al*. Inhibition of mitochondrial ATP generation by nitric oxide switches apoptosis to necrosis. *Exp Cell Res*. 1999;249:396–403.
342. Nar R, Bedir A, Alacam H, Kilinc V, Avci B, Salis O, *et al*. The effect of ouabain on mitochondrial DNA damage in HepG2 cell lines. *Tumour Biol*. 2012;33:2107–15.
343. Gadaga LL. Investigation of the toxicological and pharmacological activity of a hydroethanolic extract of *Boophone disticha* bulb. Thesis, University of Zimbabwe, Zimbabwe, 2012.
344. Schrader K, Huai J, Jöckel L, Oberle C, Borner C. Non-caspase proteases: Triggers or amplifiers of apoptosis? *Cell Mol Life Sci*. 2010;67:1607–18.
345. Müller K, Leuekl P, Mayer K, Wiegrebbe W. Modification of DNA bases by anthralin and related compounds. *Biochem Pharmacol*. 1995;49:1607–13.
346. Kratz U, Prinz H, Müller K. Synthesis and biological evaluation of novel 10-benzyl-substituted 4,5-dichloro-10H-anthracen-9-ones as inhibitors of keratinocyte hyperproliferation. *Eur J Med Chem*. 2010;45:5278–85.
347. Li Y, Man S, Li J, Chai H, Fan W, Liu Z, *et al*. The antitumor effect of formosanin C on HepG2 cell as revealed by 1H-NMR based metabolic profiling. *Chem Biol Interact*. 2014;220:193–9.
348. Cristina T, Cogliati B, Latorre AO, Akisue G, Nagamine MK, Haraguchi M, *et al*. Pfaffosidic fraction from *Hebanthe paniculata* induces cell cycle arrest and caspase-3-induced apoptosis in HepG2 cells. *Evidence-Based Complement Altern Med*. 2015;1–9.
349. Lu J-J, Lu D-Z, Chen Y-F, Dong Y-T, Zhang J-R, Li T, *et al*. Proteomic analysis of hepatocellular carcinoma HepG2 cells treated with platycodin D. *Chin J Nat Med*. 2015;13:673–9.
350. Waiyaput W, Payungporn S, Issara-Amphorn J, Panjaworayan NT-T. Inhibitory effects of crude extracts from some edible Thai plants against replication of hepatitis B virus and human liver cancer cells. *BMC Complement Altern Med*. 2012;12:246.
351. Monera TG, Wolfe AR, Maponga CC, Benet LZ, Guglielmo J. *Moringa oleifera* leaf extracts inhibit 6 $\beta$ -hydroxylation of testosterone by CYP3A4. *J Infect Dev Ctries*. 2008;2:379–83.
352. Lipipun V, Kurokawa M, Suttisri R, Taweechotipatr P, Pramyothin P, Hattori M, *et al*. Efficacy of Thai medicinal plant extracts against herpes simplex virus type 1 infection *in vitro* and *in vivo*. *Antiviral Res*. 2003;60:175–80.
353. Varalakshmi K, Nair S. Anticancer, cytotoxic potential of *Moringa oleifera* extracts on HeLa cell line. *J Nat Pharm*. 2011;2:138–42.
354. Asare G, Gyan B, Bugyei K, Adjei S, Mahama R, Addo P, *et al*. Toxicity potentials of the nutraceutical *Moringa oleifera* at supra-supplementation levels. *J Ethnopharmacol*. 2012;139:265–72.

355. Khalafalla MM, Abdellatef E, Dafalla HM, Nassrallah AA, Aboul-Enein KM, Lightfoot DA, *et al.* Active principle from *Moringa oleifera* Lam leaves effective against two leukemias and a hepatocarcinoma. *African J Biotechnol.* 2010;9:8467–71.
356. Devaraj VC, Asad M, Prasad S. Effect of leaves and fruits of *Moringa oleifera* on gastric and duodenal ulcers. *Pharm Biol.* 2007;45:332–8.
357. Adedapo AA, Mogbojuri OM, Emikpe BO. Safety evaluations of the aqueous extract of the leaves of *Moringa oleifera* in rats. *J Med Plants Res.* 2009;3:586–91.
358. Sudha P, Asdaq SMB, Dhamingi SS, Chandrakala GK. Immunomodulatory activity of methanolic leaf extract of *Moringa oleifera* in animals. *Indian J Physiol Pharmacol.* 2010;54:133–40.
359. Chivapat S, Sincharoenpokai P, Saktiyasuthorn N, Shuaprom A, Thongsrirak P, Sakpetch A, *et al.* Acute and chronic toxicity of *Moringa oleifera* Linn leaves extracts. *Thai J Vet Med.* 2011;41:417–24.
360. Asare GA, Gyan B, Bugyei K, Adjei S, Mahama R, Addo P, *et al.* Toxicity potentials of the nutraceutical *Moringa oleifera* at supra-supplementation levels. *J Ethnopharmacol.* 2012;139:265–72.
361. Sreelatha S, Jeyachitra A, Padma P. Antiproliferation and induction of apoptosis by *Moringa oleifera* leaf extract on human cancer cells. *Food Chem Toxicol.* 2011;49:1270–5.
362. Diab K, Guru S, Bhushan S, Saxena A. *In vitro* anticancer activities of *Anogeissus latifolia* , *Terminalia bellerica* , *Acacia catechu* and *Moringa oleifera* Indian Plants. *Asian Pacific J Cancer Prev.* 2015;16:6423–8.
363. Francis JA, Jayaprakasam B, Olson LK, Nair MG. Insulin secretagogues from *Moringa oleifera* with cyclooxygenase enzyme and lipid peroxidation inhibitory activities. *Helv Chim Acta.* 2004;87:317–26.
364. Yoo G, Allred CD. The estrogenic effect of trigonelline and 3,3-diindolymethane on cell growth in non-malignant colonocytes. *Food Chem Toxicol.* Elsevier Ltd; 2016;87:23–30.
365. Baliga M. Triphala, Ayurvedic formulation for treating and preventing cancer: a review. *J Altern Complement Med.* 2010;16:1301–8.
366. Kirshanamurthy P, Vardarajulu A, Wadhvani A, Patel V. Identification and characterization of a potent anticancer fraction from the leaf extracts of *Moringa oleifera* L. *Indian J Exp Biol.* 2015;53:98–103.
367. Riedel A, Lang R, Rohm B, Rubach M, Hofmann T, Somoza V. Structure-dependent effects of pyridine derivatives on mechanisms of intestinal fatty acid uptake: Regulation of nicotinic acid receptor and fatty acid transporter expression. *J Nutr Biochem.* 2014;25:750–7.
368. Ilavenil S, Arasu M V, Lee JC, Kim da H, Roh SG, Park HS, *et al.* Trigonelline attenuates the adipocyte differentiation and lipid accumulation in 3T3-L1 cells. *Phytomedicine.* 2014;21:758–65.
369. Riedel A, Hochkogler CM, Lang R, Bytof G, Lantz I, Hofmann T, *et al.* N-methylpyridinium, a degradation product of trigonelline upon coffee roasting, stimulates respiratory activity and promotes glucose utilization in HepG2 cells. *Food Funct.* 2014;5:454–62.

370. Bour S, Visentin V, Prévot D, Daviaud D, Saulnier-Blache J, Guigne C, *et al.* Effects of oral administration of benzylamine on glucose tolerance and lipid metabolism in rats. *J Physiol Biochem.* 2005;61:371–80.
371. Munari CC, de Oliveira PF, Campos JC, Martins Sde P, Da Costa JC, Bastos JK, *et al.* Antiproliferative activity of *Solanum lycocarpum* alkaloidic extract and their constituents, solamargine and solasonine, in tumor cell lines. *J Nat Med.* 2013;68:236-41.
372. Wang H-C, Chung P-J, Wu C-H, Lan K-P, Yang M-Y, Wang C-J. *Solanum nigrum* L. polyphenolic extract inhibits hepatocarcinoma cell growth by inducing G2/M phase arrest and apoptosis. *J Sci Food Agric.* 2011;91:178–85.
373. Aboyade O, Yakubu M, Grierson D, Afolayan A. Safety evaluation of aqueous extract of unripe berries of *Solanum aculeastrum* in male Wistar rats. *African J Pharm Pharmacol.* 2010;4:90–7.
374. Esteves-Souza A, Sarmiento T, Alves C, de Carvalho M, Braz-filho R, Echevarria A. Cytotoxic activities against Ehrlich carcinoma and human K562 leukaemia of alkaloids and flavonoid from two *Solanum* species. *J Braz Chem Soc.* 2002;13:838–42.
375. Chang LC, Tsai TR, Wang JJ, Lin CN, Kuo KW. The rhamnose moiety of solamargine plays a crucial role in triggering cell death by apoptosis. *Biochem Biophys Res Commun.* 1998;242:21–5.
376. Wei G, Wang J, Du Y. Total synthesis of solamargine. *Bioorg Med Chem Lett.* 2011;21:2930–3.
377. Liang C-H, Shiu L-Y, Chang L-C, Sheu H-M, Kuo K-W. Solamargine upregulation of Fas, downregulation of HER2, and enhancement of cytotoxicity using epirubicin in NSCLC cells. *Mol Nutr Food Res.* 2007;51:999–1005.
378. Ding X, Zhu F-S, Li M, Gao S-G. Induction of apoptosis in human hepatoma SMMC-7721 cells by solamargine from *Solanum nigrum* L. *J Ethnopharmacol.* 2012;139:599–604.
379. Trouillas P, Corbière C, Liagre B, Duroux J-L, Beneytout J-L. Structure-function relationship for saponin effects on cell cycle arrest and apoptosis in the human 1547 osteosarcoma cells: a molecular modelling approach of natural molecules structurally close to diosgenin. *Bioorg Med Chem.* 2005;13:1141–9.
380. Gao J, Xia L, Guofeng G, Sun B, Min C, Mei J, *et al.* Efficient synthesis of trisaccharide saponins and their tumor cell killing effects through oncotic necrosis. *Bioorg Med Chem Lett.* 2011;21:622–7.
381. Friedman M, Kee K-R, Kim H-J, Lee I-S, Kozukue N. Anticarcinogenic effects of glycoalkaloids from potatoes against human cervical, liver, lymphoma, and stomach cancer cells. *J Agric Food Chem.* 2005;53:6162–9.
382. Ji Y-B, Gao S-Y. Study on mitochondrion pathway of the apoptosis of HepG2 induced by solanine. *Chinese Pharm J.* 2008;43:272–5.
383. Zhan X, Xu Y, Xie D. Empirical studies on the effect of aromatic turmeric oil for inhibiting proliferation of hepatoma and gastric carcinoma cells using bioluminescence assay. *Chinese J Clin Oncol.* 2007;34:30–3.
384. Mandimika T. Analyzing the effects of single and mixtures of potato glycoalkaloids on gene expression in intestinal epithelial cells. PhD thesis, Cornell University, New York, 2008.

385. Ji Y-B, Gao S-Y, Ji C-F, Zou X. Effects of solanine on kinetic constants of NATase in HepG2 cells. *Chinese Pharmacol Bull.* 2008;24:1187–91.
386. Gao S-Y, Su Y-J, Ji Y-B. Study on the effect of solanine on N-acetyltransferase 1 activity in HepG2 cell. *Chinese Pharm J.* 2011;46:589–94.
387. Luo X, Pires D, Aínsa J, Gracia B, Mulhovo S, Duarte A, *et al.* Antimycobacterial evaluation and preliminary phytochemical investigation of selected medicinal plants traditionally used in Mozambique. *J Ethnopharmacol.* 2011;137:114–20.
388. Lee C, Houghton P. Cytotoxicity of plants from Malaysia and Thailand used traditionally to treat cancer. *J Ethnopharmacol.* 2005;100:237–43.
389. Marathe NP, Rasane MH, Kumar H, Patwardhan A a, Shouche YS, Diwanay SS. *In vitro* antibacterial activity of *Tabernaemontana alternifolia* (Roxb) stem bark aqueous extracts against clinical isolates of methicillin resistant *Staphylococcus aureus*. *Ann Clin Microbiol Antimicrob.* 2013;12:26.
390. Kingston D, Gerhard B, Ionescu F, Mangino M, Sami S. Plant anticancer agents V: New bisindoles alkaloids from *Tabernaemontana johnstonii* stem bark. *J Pharm Sci.* 1978;67:249–51.
391. Thind T, Agrawal S, Saxena A, Arora S. Studies on cytotoxic, hydroxyl radical scavenging and topoisomerase inhibitory activities of extracts of *Tabernaemontana divaricata* (L.) R.Br. ex Roem. and Schult. *Food Chem Tox.* 2008;46:2922–7.
392. Yuo M, Ma X, Mukerjee R, Farnsworth N, Cordell G, Kinghorn A, *et al.* Indole alkaloids from *Peschiera laeta* that enhance vinblastine-mediated cytotoxicity with multidrug-resistant cells. *J Nat Prod.* 1994;57:1517–22.
393. Kuo Y, Sun C, Tsai W, Ou J, Chen W, Lin C. Blocking of cell proliferation, cytokines production and genes expression following administration of Chinese herbs in human mesangial cells. *Life Sci.* 1999;64:2089–99.
394. Weniger B, Robledo S, Arango G, Deharo E, Aragón R, Muñoz V, *et al.* Antiprotozoal activities of Colombial plants. *J Ethnopharmacol.* 2001;78:193–200.
395. Ankli A, Heinrich M, Bork P, Wolfram L, Bauerfeind P, Brun R, *et al.* Yucatec Mayan medicinal plants: evaluation based on indigenous uses. *J Ethnopharmacol.* 2002;79:43–52.
396. Zhang H, Wang X, Lin L, Ding J, Yue J, Chong Z, *et al.* Indole alkaloids from three species of the *Ervatamia* genus: *E. officinalis*, *E. divaricata*, and *E. divaricata* Gouyahua. *J Nat Prod.* 2007;70:54–9.
397. Girardot M, Gadea A, Deregnacourt C, Deville A, Dubost L, Nay B, *et al.* Tabernaelegantinals: Unprecedented cytotoxic bisindole alkaloids from *Munafara sessilifolia*. *European J Org Chem.* 2012;2012:2816–23.
398. Sim DS-Y, Chong K-W, Nge C-E, Low Y-Y, Sim K-S, Kam T. Cytotoxic vobasine, tacaman, and corynanthe-tryptamine bisindole alkaloids from *Tabernaemontana* and structure revision of tronoharine. *J Nat Prod.* 2014;77:2504–12.

399. Paterna A, Borralho PM, Gomes SE, Mulhovo S, Rodrigues CMP, Ferreira M-JU. Monoterpene indole alkaloid hydrazone derivatives with apoptosis inducing activity in human HCT116 colon and HepG2 liver carcinoma cells. *Bioorg Med Chem Lett*. 2015;25:3556–9.
400. Mansoor T, Ramalhete C, Molnár J, Mulhovo S, Ferreira M. Tabernines A-C,  $\beta$ -carbolines from the leaves of *Tabernaemontana elegans*. *J Nat Prod*. 2009;72:1147–50.
401. Prakash Chaturvedula VS, Sprague S, Schilling JK, Kingston DG. New cytotoxic indole alkaloids from *Tabernaemontana calcarea* from the Madagascar rainforest. *J Nat Prod*. 2003;66:528–31.
402. Kam TS, Sim KM, Pang HS, Koyano T, Hayashi M, Komiyama K. Cytotoxic effects and reversal of multidrug resistance by ibogan and related indole alkaloids. *Bioorganic Med Chem Lett*. 2004;14:4487–9.
403. Chen H-M, Yang Y-T, Li H-X, Cao Z-X, Dan X-M, Mei L, *et al*. Cytotoxic monoterpene indole alkaloids isolated from the barks of *Voacanga africana* Staph. *Nat Prod Res*. 2015;6419:1–6.
404. Kam T-S, Pang H-S, Choo Y-M, Komiyama K. Biologically active ibogan and vallesamine derivatives from *Tabernaemontana divaricata*. *Chem Biodivers*. 2004;1:646–56.
405. Rizo WF, Ferreira LE, Colnaghi V, Martins JS, Franchi LP, Takahashi CS, *et al*. Cytotoxicity and genotoxicity of coronaridine from *Tabernaemontana catharinensis* A.DC in a human laryngeal epithelial carcinoma cell line (Hep-2). *Genet Mol Biol*. 2013;36:105–10.
406. Chierrito TPC, Aguiar ACC, de Andrade IM, Ceravolo IP, Goncalves RAC, de Oliveira AJB, *et al*. Anti-malarial activity of indole alkaloids isolated from *Aspidosperma olivaceum*. *Malar J*. 2014;13:142.
407. Aguiar AC, Cunha AC, Ceravolo IP, Gonçalves R a C, Oliveira AJ, Krettl AU. *Aspidosperma* (Apocynaceae) plant cytotoxicity and activity towards malaria parasites. Part II: experimental studies with *Aspidosperma ramiflorum* *in vivo* and *in vitro*. *Mem Inst Oswaldo Cruz*. 2015;110:906–13.
408. Bessong PO, Obi CL, Igumbor E, Andreola M, Litvak S. *In vitro* activity of three selected South African medicinal plants against human immunodeficiency virus type 1 reverse transcriptase. *Afr J Biotechnol*. 2004;3:555–9.
409. Nibret E, Ashour M, Rubanza C, Wink M. Screening of some Tanzanian medicinal plants for their trypanocidal and cytotoxic activities. *Phyther Res*. 2010;24:945–7.
410. Cock IE, van Vuuren SF. South African food and medicinal plant extracts as potential antimicrobial food agents. *J Food Sci Technol*. 2015;52:6879–99.
411. Tshikalange T, Meyer J, Hussein A. Antimicrobial activity, toxicity and the isolation of a bioactive compound from plants used to treat sexually transmitted diseases. *J Ethnopharmacol*. 2005;96:515–9.
412. Fyhrquist P, Mwasumbi L, Vuorela P, Vuorela H, Hiltunen R, Murphy C, *et al*. Preliminary antiproliferative effects of some species of *Terminalia*, *Combretum* and *Pteleopsis* collected in Tanzania on some human cancer cell lines. *Fitoterapia*. 2006;77:358–66.
413. Wall M, Wani M, Brown D, Fullas F, Olwald J, Josephson F, *et al*. Effect of tannins on screening of plant extracts for enzyme inhibitory activity and techniques for their removal. *Phytomedicine*. 1996;3:281–5.

414. Cliby W, Lewis K, Lilliy K, Kaufmann S. S phase and G2 arrests induced by topoisomerase I poisons are dependent on ATR kinase function. *J Biol Chem.* 2002;277:1599–606.
415. Ku CM, Lin JY. Anti-inflammatory effects of 27 selected terpenoid compounds tested through modulating Th1/Th2 cytokine secretion profiles using murine primary splenocytes. *Food Chem.* 2013;141:1104–13.
416. Fadipe V, Mongalo N, Opoku A. *In vitro* evaluation of the comprehensive antimicrobial and antioxidant properties of *Curtisia dentata* (Burm.F) C.A. Sm: Toxicological effect on the human embryonic kidney (HEK239) and human hepatocellular carcinoma (HepG2) cell lines. *EXCLI Journal.* 2015;14:971–83.
417. Saxena M, Faridi U, Mishra R, Gupta M, Darokar M, Srivastava SK, *et al.* Cytotoxic agents from *Terminalia arjuna*. *Planta Med.* 2007;73:1486–90.
418. Ponou B, Teponno R, Ricciutelli M, Nguenefack T, Quassinti L, Bramucci M, *et al.* Novel 3-oxo- and 3,24-dinor-2,4-secooleanane-type triterpenes from *Terminalia ivorensis* A. Chev. *Chem Biodivers.* 2011;8:1301–9.
419. Manosroi A, Jantrawut P, Ogihara E, Yamamoto A, Fukatsu M, Yasukawa K, *et al.* Biological activities of phenolic compounds and triterpenoids from the galls of *Terminalia chebula*. *Chem Biodivers.* 2013;10:1448–63.
420. Joo H, Lee HJ, Shin EA, Kim H, Seo K, Baek N, *et al.* c-Jun N-terminal kinase-dependent endoplasmic reticulum stress pathway is critically involved in arjunic acid induced apoptosis in non-small cell lung cancer cells. *Phytother Res.* 2016;30:596-603.
421. Yan HE, lu FL, Hang LZ, Yan WU, Bo HU, Hang YZ, *et al.* Growth inhibition and apoptosis induced by lupeol, a dietary triterpene, in human hepatocellular carcinoma cells. *Biol Pharm Bull.* 2011;34:517–22.
422. Ahmad S, Sukari MA, Ismail N, Ismail IS, Abdul AB, Abu Bakar MF, *et al.* Phytochemicals from *Mangifera pajang* Kosterm and their biological activities. *BMC Complement Med.* 2015;15:83.
423. Kuete V, Sandjo LP, Mbaveng AT, Zeino M, Efferth T. Cytotoxicity of compounds from *Xylopiya aethiopica* towards multi-factorial drug-resistant cancer cells. *Phytomedicine.* 2015;22:1247–54.
424. Luo Y, Xu QL, Dong LM, Zhou ZY, Chen YC, Zhang WM, *et al.* A new ursane and a new oleanane triterpene acids from the whole plant of *Spermacoce latifolia*. *Phytochem Lett.* 2015;11:127–31.
425. Kuete V, Sandjo LP, Seukep JA, Zeino M, Mbaveng AT, Ngadjui B, *et al.* Cytotoxic compounds from the fruits of *Uapaca togoensis* towards multifactorial drug-resistant cancer cells. *Planta Med.* 2015;81:32–8.
426. Zeng Y-T, Jiang J-M, Lao H-Y, Guo J-W, Lun Y-N, Yang M. Antitumor and apoptotic activities of the chemical constituents from the ethyl acetate extract of *Artemisia indica*. *Mol Med Rep.* 2015;11:2234–40.
427. Choi YJ, Yoon Y, Choi HS, Park S, Oh S, Jeong SM, *et al.* Effects of medicinal herb extracts and their components on steatogenic hepatotoxicity in Sk-hep1 cells. *Toxicol Res.* 2011;27:211–6.

428. Mochizuki M, Hasegawa N. Acceleration of lipid degradation by sericoside of *Terminalia* roots in fully differentiated 3T3-L1 cells. *Phyther Res.* 2006;20:1020–1.
429. Kamuhabwa A, Nshimo C, de Witte P. Cytotoxicity of some medicinal plant extracts used in Tanzanian traditional medicine. *J Ethnopharmacol.* 2000;70:143–9.
430. Da Costa Mousinho N, van Tonder JJ, Steenkamp V. *In vitro* assessment of the anti-diabetic activity of *Sclerocarya birrea* and *Ziziphus mucronata*. *Nat Prod Commun.* 2013;8:1279–84.
431. Elgorashi E, Taylor J, Maes A, van Staden J, De Kimpe N, Verschaeve L. Screening of medicinal plants used in South African traditional medicine for genotoxic effects. *Toxicol Lett.* 2003;143:195–207.
432. Bessong P, Obi C, Andréola M-L, Rojas L, Pouységu L, Igumbor E, *et al.* Evaluation of selected South African medicinal plants for inhibitory properties against human immunodeficiency virus type 1 reverse transcriptase and integrase. *J Ethnopharmacol.* 2005;99:83–91.
433. Mativandela S, Meyer J, Hussein A, Houghton P, Hamilton C, Lall N. Activity against *Mycobacterium smegmatis* and *M. tuberculosis* by extract of South African medicinal plants. *Phyther Res.* 2008;22:841–5.
434. Gadir SA. Assessment of bioactivity of some Sudanese medicinal plants using brine shrimp (*Artemia salina*) lethality assay. *J Chem Pharm Res.* 2012;4:5145–8.
435. Behbahani M. Anti-HIV-1 activity of eight monofloral Iranian honey types. *PLoS One.* 2014;9.
436. Vahedi F, Fathi Najafi M, Bozari K. Evaluation of inhibitory effect and apoptosis induction of *Zyzyphus jujube* on tumor cell lines, an *in vitro* preliminary study. *Cytotechnology.* 2008;56:105–11.
437. Plastina P, Bonofiglio D, Vizza D, Fazio A, Rovito D, Giordano C, *et al.* Identification of bioactive constituents of *Ziziphus jujube* fruit extracts exerting antiproliferative and apoptotic effects in human breast cancer cells. *J Ethnopharmacol.* 2012;140:325–32.
438. Bhatia A, Mishra T, Khullar M. Anticancer potential of aqueous ethanol seed extract of *Ziziphus mauritiana* against cancer cell lines and Ehrlich ascites carcinoma. *Evidence-based Complement Altern Med.* 2011;2011.
439. Toumi M, Rincheval V, Young A, Gergeres D, Turos E, Couty F, *et al.* A general route to cyclopeptide alkaloids: total syntheses and biological evaluation of paliurines E and F, ziziphines N and Q, abyssenine A, mucronine E, and analogues. *European J Org Chem.* 2009:3368–86.
440. Pang KS. Modeling of intestinal drug absorption: Roles of transporters and metabolic enzymes (for the Gillette review series). *Drug Metab Dispos.* 2003;31:1507–19.
441. Aungst BJ. P-glycoprotein, secretory transport, and other barriers to the oral delivery of anti-HIV drugs. *Adv Drug Deliv Rev.* 1999;39:105–16.
442. Sauna Z, Ambudkar S. About a switch: how P-glycoprotein (ABCB1) harnesses the energy of ATP binding and hydrolysis to do mechanical work. *Mol Cancer Ther.* 2007;6:13–23.
443. Schwab D, Fischer H, Tabatabaei A, Poli S, Huwylar J. Comparison of *in vitro* P-glycoprotein screening assays: recommendations for their use in drug discovery. *J Med Chem.* 2003;46:1716–25.
444. Han H-K. Role of transporters in drug interactions. *Arch Pharm Res.* 2011;34:1865–77.

445. Thiebaut F, Tsuruot T, Hamadat H, Gottesman M, Pastan I, Willingham M. Cellular localization of the multidrug-resistance gene product P-glycoprotein in normal human tissues. *Proc Natl Acad Sci USA*. 1987;84:7735–8.
446. Miller D. Regulation of P-glycoprotein and other ABC drug transporters at the blood–brain barrier. *Trends Pharm Sci*. 2010;31:246–54.
447. Schinkel A. P-glycoprotein, a gatekeeper in the blood-brain barrier. *Adv Drug Deliv Rev*. 1999;36:179–94.
448. Li C, Sun B-Q, Gai X-D. Compounds from Chinese herbal medicines as reversal agents for P-glycoprotein-mediated multidrug resistance in tumours. *Clin Transl Oncol*. 2014;16:593-8.
449. Fenner K, Troutman M, Kempshall S, Cook J, Ware J, Smith D, *et al*. Drug-drug interactions mediated through P-glycoprotein: clinical relevance and *in vitro-in vivo* correlation using digoxin as a probe drug. *Clin Pharmacol Ther*. 2009;85:173–81.
450. Li X, Zhao Y, Ji M, Liu S-S, Cui M, Lou H-X. Induction of actin disruption and downregulation of P-glycoprotein expression by solamargine in multidrug-resistant K562/A02 cells. *Chin Med J (Engl)*. 2011;124:2038–44.
451. Aleksunes LM, Klaassen CD. Coordinated regulation of hepatic phase-I and -II drug metabolizing genes and transporters using AhR-, CAR-, PXR-, PPAR $\alpha$ -, and Nrf2-null mice. *Drug Metab Dispos*. 2012;40:1366–79.
452. Pavek P, Dvorak Z. Xenobiotic-induced transcriptional regulation of xenobiotic metabolizing enzymes of the cytochrome P450 superfamily in human extrahepatic tissues. *Curr Drug Metab*. 2008;9:129–43.
453. Hasemann CA, Kurumbail RG, Boddupalli SS, Peterson JA, Deisenhofer J. Structure and function of cytochromes P450: A comparative analysis of three crystal structures. *Structure*. 1995;3:41–62.
454. Wachter VJ, Salphati L, Benet LZ. Active secretion and enterocytic drug metabolism barriers to drug absorption. *Adv Drug Deliv Rev*. 1996;20:99–112.
455. Gorny M, Röhm S, Läer S, Morali N, Niehues T. Pharmacogenomic adaptation of antiretroviral therapy: Overcoming the failure of lopinavir in an African infant with CYP2D6 ultrarapid metabolism. *Eur J Clin Pharmacol*. 2010;66:107–8.
456. Peterson JA, Graham SE. A close family resemblance: The importance of structure in understanding cytochromes P450. *Structure*. 1998;6:1079–85.
457. Mestres J. Structure conservation in cytochromes P450. *Proteins Struct Funct Genet*. 2005;58:596–609.
458. Sirim D, Widmann M, Wagner F, Pleiss J. Prediction and analysis of the modular structure of cytochrome P450 monooxygenases. *BMC Struct Biol*. 2010;10:34.
459. Graham SE, Peterson JA. How similar are P450s and what can their differences teach us? *Arch Biochem Biophys*. 1999;369:24–9.
460. Wachter VJ, Silverman JA, Zhang Y, Benet LZ. Role of P-glycoprotein and cytochrome P450 3A in limiting oral absorption of peptides and peptidomimetics. *J Pharm Sci*. 1998;87:1322–30.

461. Ingelman-Sundberg M. Genetic polymorphisms of cytochrome P450 2D6 (CYP2D6): clinical consequences, evolutionary aspects and functional diversity. *Pharmacogenomics J.* 2005;5:6–13.
462. Zhou S, Wang B, Yang L, Liu J. Structure, function, regulation and polymorphism and the clinical significance of human cytochrome P450 1A2. *Drug Metab Rev.* 2010;42:268–354.
463. Zanger UM, Raimundo S, Eichelbaum M. Cytochrome P450 2D6: Overview and update on pharmacology, genetics, biochemistry. *Naunyn Schmiedebergs Arch Pharmacol.* 2004;369:23–37.
464. Gounden V, van Niekerk C, Snyman T, George JA. Presence of the CYP2B6 516G>T polymorphism, increased plasma efavirenz concentrations and early neuropsychiatric side effects in South African HIV-infected patients. *AIDS Res Ther.* 2010;7:32.
465. Ebeshi BU, Bolaji OO, Masimirembwa CM. Allele and genotype frequencies of cytochrome P450 2B6 and 2C19 genetic polymorphisms in the Nigerian populations : Possible implication on anti-retroviral and anti-malarial therapy. *Int J Med Med Sci.* 2011;3:193–200.
466. Mehlotra R, Ziats M, Zimmerman P. Prevalence of CYP2B6 alleles in malaria-endemic populations of West Africa and Papua New Guinea. *Eur J Clin Pharmacol.* 2006;62:267–75.
467. Klein K, Lang T, Saussele T, Barbosa-Sicard E, Schunck W, Eichelbaum M, *et al.* Genetic variability of CYP2B6 in populations of African and Asian origin: Allele frequencies, novel functional variants, and possible implications for anti-HIV therapy with efavirenz. *Pharmacogenet Genomics.* 2005;15:861–73.
468. Ferreira PE, Veiga MI, Cavaco I, Martins JP, Andersson B, Mushin S, *et al.* Polymorphism of antimalaria drug metabolizing, nuclear receptor, and drug transport genes among malaria patients in Zanzibar, East Africa. *Ther Drug Monit.* 2008;30:10–5.
469. Nyakutira C, Röshammar D, Chigutsa E, Chonzi P, Ashton M, Nhachi C, *et al.* High prevalence of the CYP2B6 516G→T(\*6) variant and effect on the population pharmacokinetics of efavirenz in HIV/AIDS outpatients in Zimbabwe. *Eur J Clin Pharmacol.* 2008;64:357–65.
470. Marwa KJ, Schmidt T, Sjögren M, Minzi OMS, Kamugisha E, Swedberg G. Cytochrome P450 single nucleotide polymorphisms in an indigenous Tanzanian population: a concern about the metabolism of artemisinin-based combinations. *Malar J.* 2014;13:420.
471. Riccardi LN, Bini C, Ceccardi S, Trane R, Luiselli D, Pelotti S. CYP2D6 polymorphism studies: How forensic genetics helps clinical medicine. *Forensic Sci Int Genet Suppl Ser.* 2009;2:485–6.
472. Gaedigk A, Coetsee C. The CYP2D6 gene locus in South African coloureds: Unique allele distributions, novel alleles and gene arrangements. *Eur J Clin Pharmacol.* 2008;64:465–75.
473. Lynch T, Price A. The effect of cytochrome P450 metabolism on drug response, interactions, and adverse effects. *Am Fam Physician.* 2007;76:391–6.
474. Yen-Revollo JL, Van Booven DJ, Peters EJ, Hoskins JM, Engen RM, Kannall HD, *et al.* Influence of ethnicity on pharmacogenetic variation in the Ghanaian population. *Pharmacogenomics J.* 2009;9:373–9.

475. Drögemöller B, Plummer M, Korkie L, Agenbag G, Dunaiski A, Niehaus D, *et al.* Characterization of the genetic variation present in CYP3A4 in three South African populations. *Front Genet.* 2013;4:1–11.
476. Brown K, Hosseinipour MC, Hoskins JM, Thirumaran RK, Tien H-C, Weigel R, *et al.* Exploration of CYP450 and drug transporter genotypes and correlations with nevirapine exposure in Malawians. *Pharmacogenomics.* 2012;13:113–21.
477. Zhang W, Chang Y-Z, Kan Q-C, Zhang L-R, Li Z-S, Lu H, *et al.* CYP3A4\*1G genetic polymorphism influences CYP3A activity and response to fentanyl in Chinese gynecologic patients. *Pharmacogenetics.* 2010;66:61–6.
478. Benet LZ, Izumi T, Zhang Y, Silverman JA., Wachter VJ. Intestinal MDR transport proteins and P-450 enzymes as barriers to oral drug delivery. *J Control Release.* 1999;62:25–31.
479. Chen M-L, Yu L. The use of drug metabolism for prediction of intestinal permeability. *Mol Pharm.* 2009;6:74–81.
480. Marzolini C, Mueller R, Li-Blatter X, Battegay M, Seelig A. The brain entry of HIV-1 protease inhibitors is facilitated when used in combination. *Mol Pharm.* 2013;10:2340–9.
481. Chudasama A, Patel V, Nivsarkar M, Vasu K, Shishoo C. A novel lipid-based oral drug delivery system of nevirapine. *Int J PharmTech Res.* 2011;3:1159–68.
482. Michaud V, Bar-Magen T, Turgeon J, Flockhart D, Desta Z, Wainberg MA. The dual role of pharmacogenetics in HIV treatment: mutations and polymorphisms regulating antiretroviral drug resistance and disposition. *Pharmacol Rev.* 2012;64:803–33.
483. Haas DW, Bartlett JA, Andersen JW, Sanne I, Wilkinson GR, Hinkle J, *et al.* Pharmacogenetics of nevirapine-associated hepatotoxicity: an adult AIDS clinical trials group collaboration. *Clin Infect Dis.* 2006;43:783–6.
484. Weiss J, Theile D, Ketabi-Kiyanvash N, Lindenmaier H, Haefeli W. Inhibition of MRP1/ABCC1, MRP2/ABCC2, and MRP3/ABCC3 by nucleoside, nucleotide, and non-nucleoside reverse transcriptase inhibitors. *Drug Metab Dispos.* 2007;35:340–4.
485. Jung N, Lehmann C, Rubbert A, Knispel M, Hartmann P, Lunzen J Van, *et al.* Relevance of the organic cation transporters 1 and 2 for antiretroviral drug therapy in human immunodeficiency virus infection. *Drug Metab Dispos.* 2008;36:1616–23.
486. Li X, Chan WK. Transport, metabolism and elimination mechanisms of anti-HIV agents. *Adv Drug Deliv Rev.* 1999;39:81–103.
487. Rathbun RC, Liedtke MD. Antiretroviral drug interactions: Overview of interactions involving new and investigational agents and the role of therapeutic drug monitoring for management. *Pharmaceutics.* 2011;3:745–81.
488. Davies NM, Takemoto JK, Brocks DR, Yáñez JA. Multiple peaking phenomena in pharmacokinetic disposition. *Clin Pharmacokinet.* 2010;49:351–77.
489. Bulmer AC, Blanchfield JT, Coombes JS, Toth I. *In vitro* permeability and metabolic stability of bile pigments and the effects of hydrophilic and lipophilic modification of biliverdin. *Bioorganic Med Chem.* 2008;16:3616–25.

490. Mergler BI, Roth E, Bruggaber SFA, Powell JJ, Pereira DIA. Development of the Caco-2 model for assessment of iron absorption and utilisation at supplemental levels. *J Pharm Nutr Sci.* 2012;2:27–34.
491. Corning. Corning® HTS Transwell®-96 permeable support protocols for drug transport. 2007.
492. Balimane P, Marino A, Chong S. P-gp inhibition potential in cell-based models: which “calculation” method is the most accurate? *AAPS J.* 2008;10:577–86501.
493. Corning. CYP2B6/EFC High Throughput Inhibitor Screening Kit. 2013.
494. Corning. CYP2D6/AMMC High Throughput Inhibitor Screening Kit. 2013.
495. Corning. CYP3A4/BFC High Throughput Inhibitor Screening Kit. 2013.
496. Junyaprasert VB, Soonthornchareonnon N, Thongpraditchote S, Murakami T, Takano M. Inhibitory effect of Thai plant extracts on P-glycoprotein mediated efflux. *Phyther Res.* 2006;81:79–81.
497. Ivanova A, Serly J, Christov V, Stamboliyska B, Molnar J. Alkaloids derived from genus *Veratrum* and *Peganum* of Mongolian origin as multidrug resistance inhibitors of cancer cells. *Fitoterapia.* 2011;82:570–5.
498. Thews O, Gassner B, Kelleher DK, Schwerdt G, Gekle M. Impact of extracellular acidity on the activity of P-glycoprotein and the cytotoxicity of chemotherapeutic drugs. *Neoplasia.* 2006;8:143–52.
499. Sharom FJ. Complex interplay between the P-glycoprotein multidrug efflux pump and the membrane: Its role in modulating protein function. *Front Oncol.* 2014;4.
500. Bondar O V., Badeev Y V., Shtyrlin YG, Abdullin TI. Lipid-like trifunctional block copolymers of ethylene oxide and propylene oxide: Effective and cytocompatible modulators of intracellular drug delivery. *Int J Pharm.* 2014;461:97–104.
501. Arispe N, Doh M. Plasma membrane cholesterol controls the cytotoxicity of Alzheimer’s disease A $\beta$ P (1-40) and (1-42) peptides. *FASEB J.* 2002;16:1526–36.
502. Tsuchiya H. Stereospecificity in membrane effects of catechins. *Chem Biol Interact.* 2001;134:41–54.
503. Chen L, Yang X, Jiao H, Zhao B, Al CET. Tea catechins protect against lead-induced cytotoxicity, lipid peroxidation, and membrane fluidity in HepG2 cells. *Toxicol Sci.* 2002;156:149–56.
504. Hendrich A. Flavonoid-membrane interactions: possible consequences for biological effects of some polyphenolic compounds. *Acta Pharmacol Sin.* 2006;27:27–40.
505. Sugihara N, Tsutsui Y, Tagashira T, Choshi T, Hibino S, Kamishikiryu J, *et al.* The ability of gallate and pyrogallol moieties of catechins to inhibit P-glycoprotein function. *J Funct Foods.* 2011;3:298–304.
506. Eichhorn T, Efferth T. P-glycoprotein and its inhibition in tumors by phytochemicals derived from Chinese herbs. *J Ethnopharmacol.* 2012;141:557–70.
507. Knop J, Misaka S, Singer K, Hoier E, Müller F. Inhibitory effects of green tea and (-)-epigallocatechin gallate on transport by OATP1B1, OATP1B3, OCT1, OCT2, MATE1, MATE2-K and P-glycoprotein. *PLoS One.* 2015;1–13.

508. Wang Y-M, Lin W, Chai SC, Wu J, Ong SS, Schuetz EG, *et al.* Piperine activates human pregnane X receptor to induce the expression of cytochrome P450 3A4 and multidrug resistance protein 1. *Toxicol Appl Pharmacol.* 2013;272:96–107.
509. Bhat U, Winter M, Pearce H, Beck W. A structure-function relationship among reserpine and yohimbine analogues in their ability to increase expression of mdr1 and P-glycoprotein in a human colon carcinoma cell line. *Mol Pharmacol.* 1995;48:682–9.
510. Tu M, Li L, Lei H, Ma Z, Chen Z, Sun S, *et al.* Involvement of organic cation transporter 1 and CYP3A4 in retrorsine-induced toxicity. *Toxicology.* 2014;322:34–42.
511. Burger TM. *In vitro* P-glycoprotein activity of alkaloid-enriched fractions from *Solanum aculeastrum* and its synergistic potential with doxorubicin. MSc thesis, University of Pretoria, Pretoria [submitted 2016].
512. Norman T, Chaffin M, Norton P, Coleman M, Stoughton W, Mays T. Concurrent ivermectin and *Solanum* spp. toxicosis in a herd of horses. *J Vet Intern Med.* 2012;26:1439–42.
513. Aurade RM, Akbar S, Goud H, Jayalakshmi SK, Sreeramulu K. Inhibition of P-glycoprotein ATPase and its transport function of *Helicoverpa armigera* by morin, quercetin and phloroglucinol. *Pestic Biochem Physiol.* 2011;101:212–9.
514. Leung YM, Ou YJ, Kwan CY, Loh TT. Specific interaction between tetrandrine and Quillaja saponins in promoting permeabilization of plasma membrane in human leukemic HL-60 cells. *Biochim Biophys Acta.* 1997;1325:318–28.
515. Nazari M, Kurdi M, Heerklotz H. Classifying surfactants with respect to their effect on lipid membrane order. *Biophys J. Biophysical Society;* 2012;102:498–506.
516. Kiss L, Hellinger É, Pilbat AM, Kittel Á, Török Z, Furedi A, *et al.* Sucrose esters increase drug penetration, but do not inhibit P-glycoprotein in Caco-2 intestinal epithelial cells. *J Pharm Sci.* 2014;103:3107–19.
517. Johnson I, Cee J, Price K, Curl C, Fenwick G. Influence of saponins on gut permeability and active nutrient transport in vitro. *J Nutr.* 1986;116:2270–7.
518. Sudji I. Bioactivity of steroid and triterpenoid saponins: Influence on membrane permeability and drug absorption. MSc dissertation 2015.
519. Zhu H, Zhu S, Shakya S, Mao Q, Ding C, Long M, *et al.* Study on the pharmacokinetics profiles of polyphyllin I and its bioavailability enhancement through co-administration with P-glycoprotein inhibitors by LC-MS/MS method. *J Pharm Biomed Anal.* 2015;107:119–24.
520. Felicelli N. Further studies of the effect of saponin on intestinal absorption. MSc dissertation, Loyola University, Chicago, 932.
521. Ahmed-belkacem A, Macalou XS, Borrelli XF, Capasso R, Fattorusso E, Taglialatela-scafati O, *et al.* Nonprenylated rotenoids, a new class of potent breast cancer resistance protein inhibitors. *J Med Chem.* 2007;50:1933–8.
522. DeVore NM, Meneely KM, Bart AG, Stephens ES, Battaile KP, Scott EE. Structural comparison of cytochromes P450 2A6, 2A13, and 2E1 with pilocarpine. *FEBS J.* 2012;279:1621–31.

523. Salminen KA, Meyer A, Jerabkova L, Korhonen LE, Rahnasto M, Juvonen RO, *et al.* Inhibition of human drug metabolizing cytochrome P450 enzymes by plant isoquinoline alkaloids. *Phytomedicine*. 2011;18:533–8.
524. Ramasamy S, Kiew L, Chung L. Inhibition of human cytochrome P450 enzymes by allergen removed *Rhus verniciflua* Stoke standardized extract and constituents. *Evidence-based Complement Altern Med*. 2014;1–5.
525. Li C, Lim SC, Kim J, Choi JS. Effects of myricetin, an anticancer compound, on the bioavailability and pharmacokinetics of tamoxifen and its main metabolite, 4-hydroxytamoxifen, in rats. *Eur J Drug Metab Pharmacokinet*. 2011;36:175–82.
526. Ekstrand B, Rasmussen MK, Woll F, Zlabek V, Zamaratskaia G. *In vitro* gender-dependent inhibition of porcine cytochrome P450 activity by selected flavonoids and phenolic acids. *Biomed Res Int*. 2015;2015.
527. Naramoto K, Kato M, Ichihara K. Effects of an ethanol extract of Brazilian green propolis on human cytochrome P450 enzyme activities *in vitro*. *J Agric Food Chem*. 2014;62:11296–302.
528. Sousa C, Andrade PB, Valentão P. Relationships of *Echium plantagineum* L. bee pollen, dietary flavonoids and their colonic metabolites with cytochrome P450 enzymes and oxidative stress. *RSC Adv*. 2016;6:6084–92.
529. Rastogi H, Jana S. Evaluation of inhibitory effects of caffeic acid and quercetin on human liver cytochrome P450 activities. *Phyther Res*. 2014;28:1873–8.
530. Spaggiari D, Mehl F, Desfontaine V, Grand-Guillaume Perrenoud A, Fekete S, Rudaz S, *et al.* Comparison of liquid chromatography and supercritical fluid chromatography coupled to compact single quadrupole mass spectrometer for targeted *in vitro* metabolism assay. *J Chromatogr A*. 2014;1371:244–56.
531. Delaporte E, Slaughter D, Egan M, Gatto G, Santos A, Shelley J, *et al.* The potential for CYP2D6 inhibition screening using a novel scintillation proximity assay-based approach. *J Biomol Screen*. 2010;6:225–31.
532. Usia T, Watabe T, Kadota S, Tezuka Y. Cytochrome P450 2D6 (CYP2D6) inhibitory constituents of *Catharanthus roseus*. *Biol Pharm Bull*. 2005;28:1021–4.
533. Ruan J, Yang M, Fu P, Ye Y, Lin G. Metabolic activation of pyrrolizidine alkaloids: Insights into the structural and enzymatic basis. *Chem Res Toxicol*. 2014;27:1030–9.
534. Tu M, Li L, Lei H, Ma Z, Chen Z, Sun S, *et al.* Involvement of organic cation transporter 1 and CYP3A4 in retrorsine-induced toxicity. *Toxicology*. 2014;322:34–42.
535. Ponnusankar S, Pandit S, Venkatesh M, Bandyopadhyay A, Mukherjee PK. Cytochrome P450 inhibition assay for standardized extract of *Terminalia chebula* Retz. 2011;154:151–4.
536. Ponnusankar S, Pandit S, Babu R, Bandyopadhyay A, Mukherjee PK. Cytochrome P450 inhibitory potential of Triphala - A Rasayana from Ayurveda. *J Ethnopharmacol*. 2011;133:120–5.
537. Varghese A, Savai J, Pandita N, Gaud R. In vitro modulatory effects of *Terminalia arjuna*, arjunic acid, arjunetin and arjungenin on CYP3A4, CYP2D6 and CYP2C9 enzyme activity in human liver microsomes. *Toxicol Reports*. 2014;2:806–16.

538. Tom ENL, Girard-Thernier C, Martin H, Dimo T, Alvergnas M, Nappey M, *et al.* Treatment with an extract of *Terminalia superba* Engler & Diels decreases blood pressure and improves endothelial function in spontaneously hypertensive rats. *J Ethnopharmacol.* 2014;151:372–9.
539. Misaka S, Kawabe K, Onoue S, Werba JP, Giroli M, Tamaki S, *et al.* Effects of green tea catechins on cytochrome P450 2B6, 2C8, 2C19, 2D6 and 3A activities in human liver and intestinal microsomes. *Drug Metab Pharmacokinet.* 2013;28:244–9.
540. Tsujimoto M, Horie M, Honda H, Takara K, Nishiguchi K. The structure-activity correlation on the inhibitory effects of flavonoids on cytochrome P450 3A activity. *Biol Pharm Bull.* 2009;32:671–6.
541. Choi S-J, Choi J-S. The promotive effects of antioxidative apigenin on the bioavailability of paclitaxel for oral delivery in rats. *Biomol Ther (Seoul).* 2010;18:469–76.
542. Kimura Y, Ito H, Ohnishi R, Hatano T. Inhibitory effects of polyphenols on human cytochrome P450 3A4 and 2C9 activity. *Food Chem Tox.* 2010;48:429–35.
543. Quintieri L, Palatini P, Nassi A, Ruzza P, Floreani M. Flavonoids diosmetin and luteolin inhibit midazolam metabolism by human liver microsomes and recombinant CYP 3A4 and CYP3A5 enzymes. *Biochem Pharmacol.* 2008;75:1426–37.
544. Ahmmed S, Mukherjee P, Bahadur S, Kar A, Al-Dhabi N, Duraipandiyan V. Inhibition potential of *Moringa oleifera* Lam. on drug metabolizing enzymes. *Indian J Tradit Knowl.* 2015;14:614–9.
545. Ahmmed S, Mukherjee P, Bahadur S, Kar A, Mukherjee K, Karmakar S, *et al.* Interaction potential of *Trigonella foenum graecum* through cytochrome P450 mediated inhibition. *Indian J Pharmacol.* 2015;47:530–4.
546. Michel JL, Chen Y, Zhang H, Huang Y, Krunic A, Orjala J, *et al.* Estrogenic and serotonergic butenolides from the leaves of *Piper hispidum* Swingle (Piperaceae). *J Ethnopharmacol.* 2010;129:220–6.
547. Harwansh R, Mekherjee K, Bhadra S, Kar A, Bahadur S, Mitra A, *et al.* Cytochrome P450 inhibitory potential and RP-HPLC standardization of trikatu—A Rasayana from Indian Ayurveda. *J Ethnopharmacol.* 2014;153:674–81.
548. Foster B, Vandenhoeck S, Hana J, Krantis A, Akhtar M, Bryan M, *et al.* *In vitro* inhibition of human cytochrome P450-mediated metabolism of marker substrates by natural products. *Phytomedicine.* 2004;10:334–42.
549. Bhardwaj R, Glaeser H, Bacquemont L, Klotz U, Gupta S, Fromm M. Piperine, a major constituent of black pepper, inhibits human P-glycoprotein and CYP3A4. *J Pharmacol Exp Ther.* 2002;302:645–50.
550. Volak LP, Ghirmai S, Cashman JR, Court MH. Curcuminoids inhibit multiple human cytochrome P 450 (CYP), UDP-glucuronosyltransferase (UGT), and sulfotransferase (SULT) enzymes, while piperine is a relatively selective CYP3A4 inhibitor. *Drug Metab Dispos.* 2008;36:1594–605.
551. Jing X-Y, Peng Y-R, Wang X-M, Duan J-A. Effects of *Ziziphus jujuba* fruit extracts on cytochrome P450 (CYP1A2) activity in rats. *Chin J Nat Med.* 2015;13(8):588–94.
552. Cai J, Lin C, Wang L, Wang Z, Lin G. Effects of *Solanum lyratum* Thunb. on the metabolic ability of CYP450 in rats. *Lat Am J Pharm.* 2014;33:1380–4.



## Appendix I: Publication



*British Journal of Pharmaceutical Research*  
7(1): 16-21, 2015, Article no.BJPR.2015.087  
ISSN: 2231-2919

SCIENCE DOMAIN International  
[www.science domain.org](http://www.science domain.org)



### Evaluation of Four Assays to Determine Cytotoxicity of Selected Crude Medicinal Plant Extracts *In vitro*

Werner Cordier<sup>1\*</sup> and Vanessa Steenkamp<sup>1</sup>

<sup>1</sup>Department of Pharmacology, School of Medicine, Faculty of Health Sciences, University of Pretoria, Pretoria, South Africa.

#### Authors' contributions

This work was carried out in collaboration between both authors. Author WC conducted experimental work and wrote the first draft of the manuscript. Author VS edited the manuscript. Both authors read and approved the final manuscript.

#### Article Information

DOI: 10.9734/BJPR/2015/16906

#### Editor(s):

- (1) Nan Mei, Division of Genetic and Molecular Toxicology, National Center for Toxicological Research (NCTR), U.S. Food and Drug Administration (FDA), USA.
- (2) Yurong Lai, Pharmacokinetics, Dynamics and Metabolism, PGRD, Groton Laboratory, Pfizer, Inc, USA.
- (3) Ali Nolkhodchi, Professor of Pharmaceutics and Drug Delivery, School of Life Sciences, University of Sussex, UK.

#### Reviewers:

- (1) Anonymous, UCSi University, Malaysia.
- (2) Anonymous, International Islamic University, Malaysia.
- (3) Anonymous, Istanbul Yeni Yuzyl University, Turkey.

Complete Peer review History: <http://www.science domain.org/review-history.php?id=1175&id=14&id=9340>

Short Communication

Received 18<sup>th</sup> February 2015  
Accepted 29<sup>th</sup> April 2015  
Published 21<sup>st</sup> May 2015

#### ABSTRACT

**Aims:** Cytotoxic assessment of plant extracts is crucial during the pre-clinical screening of medicinal preparations selected for further development. The aim of this study was to compare four assays used to test the cytotoxicity of eight African plant extracts, as well as to determine whether the antioxidant properties of the extracts potentially diminished the reliability of the resazurin conversion assay.

**Methodology:** HepG2 cells were exposed to hot water or methanol extracts of *Acokanthera oppositifolia*, *Boophae disticha*, *Solanum aculeastrum* and *Tabernaemontana elegans* for 72 h. Cell viability was determined using neutral red uptake, sulphorhodamine B staining, MTT and resazurin conversion assays. Phytochemical interference in the resazurin conversion assay was assessed in a cell-free environment and antioxidant activity of the crude extracts was determined using the Trolox Equivalence Antioxidant Capacity assay.

**Results:** Compared to the other three assays, the resazurin conversion assay failed to detect cytotoxicity, even at the highest concentration tested. The sulphorhodamine B staining assay

\*Corresponding author. Email: [werner.cordier@up.ac.za](mailto:werner.cordier@up.ac.za)



## Appendix II: Ethical approval

The Research Ethics Committee, Faculty Health Sciences, University of Pretoria complies with ICH-GCP guidelines and has US Federal wide Assurance.

- FWA 00002567, Approved dd 22 May 2002 and Expires 20 Oct 2016.
- IRB 0000 2235 IORG0001762 Approved dd 13/04/2011 and Expires 13/04/2014.



UNIVERSITEIT VAN PRETORIA  
UNIVERSITY OF PRETORIA  
YUNIBESITHI YA PRETORIA

Faculty of Health Sciences Research Ethics Committee

21/11/2013

### Approval Certificate New Application

Ethics Reference No.: 276/2013

Title In vitro hepatotoxicity and herb-drug interactions of selected African plant extracts

Dear Mr Werner Cordier

The **New Application** as supported by documents specified in your cover letter for your research received on the 13/11/2013, was approved by the Faculty of Health Sciences Research Ethics Committee on the 20/11/2013.

Please note the following about your ethics approval:

- Ethics Approval is valid for 3 years
- Please remember to use your protocol number (276/2013) on any documents or correspondence with the Research Ethics Committee regarding your research.
- Please note that the Research Ethics Committee may ask further questions, seek additional information, require further modification, or monitor the conduct of your research.

Ethics approval is subject to the following:

- The ethics approval is conditional on the receipt of 6 monthly written Progress Reports, and
- The ethics approval is conditional on the research being conducted as stipulated by the details of all documents submitted to the Committee. In the event that a further need arises to change who the investigators are, the methods or any other aspect, such changes must be submitted as an Amendment for approval by the Committee.

We wish you the best with your research.

Yours sincerely

Dr R Sommers; MBChB; MMed (Int); MPharMed.  
Deputy Chairperson of the Faculty of Health Sciences Research Ethics Committee, University of Pretoria

*The Faculty of Health Sciences Research Ethics Committee complies with the SA National Act 61 of 2003 as it pertains to health research and the United States Code of Federal Regulations Title 45 and 46. This committee abides by the ethical norms and principles for research, established by the Declaration of Helsinki, the South African Medical Research Council Guidelines as well as the Guidelines for Ethical Research: Principles Structures and Processes 2004 (Department of Health).*

◆ Tel: 012-3541330      ◆ Fax: 012-3541367 Fax2Email: 0866515924      ◆ E-Mail: [manda@med.up.ac.za](mailto:manda@med.up.ac.za)  
◆ Web: [www.healthethics-up.co.za](http://www.healthethics-up.co.za)      ◆ H W Snyman Bld (South) Level 2-34      ◆ Private Bag x 323, Arcadia, Pta, S.A., 0007

## Appendix III: Preparation of reagents

### 1. Solvents

#### 1.1. Organic solvents

Acetic acid, acetone, butanol, chloroform, ethanol, methanol and dimethyl sulfoxide were purchased from Merck Chemicals (South Africa) and used undiluted. LC-MS/MS grade acetonitrile, formic acid and methanol was purchased from Sigma-Aldrich (St, Louis, USA) and used undiluted.

### 2. Phytochemical screening

#### 2.1. Phytochemical standards

Ascorbic acid, caffeic acid, catechin, *p*-coumaric acid, curcumin, dicoumarol, digoxigenin, diosgenin, ferulic acid, galanthamine, gallic acid, oleonic acid, quercetin, rutin, sinapic acid, syringic acid, tannic acid and ( $\pm$ )-6-hydroxy-2,5,7,8-tetramethylchromane-2-carboxylic acid (Trolox) were purchased from Sigma-Aldrich (St. Louis, USA). A 20 mg/mL solution was prepared by dissolving 20 mg per 1 mL DMSO (or phosphate-buffered saline for diosgenin) and stored at  $-80^{\circ}\text{C}$  in 20  $\mu\text{L}$  aliquots. Dilutions were prepared in PBS prior to use.

#### 2.2. Thin-layer chromatography

##### 2.1.1. Dragendorff's reagent

Basic bismuth and potassium iodide were purchased from Merck Chemicals (South Africa). Dragendorff's reagent stock solution was prepared by mixing a solution of 0.85 g basic bismuth per 10 mL glacial acetic acid and 40 mL distilled water, and 8 g potassium iodide per 20 mL distilled water in equal ratios. A working dilution was prepared by diluting 1 mL stock solution per 2 mL glacial acetic acid and 10 mL distilled water. The solution was stored at room temperature.

### **2.1.2. Potassium hydroxide**

Potassium hydroxide was purchased from Merck Chemicals (South Africa). A 5% solution was prepared by dissolving 500 mg per 10 mL methanol, and stored at room temperature.

### **2.1.3. Aluminium trichloride**

Aluminium trichloride was purchased from Merck Chemicals (South Africa). A 1% solution was prepared by dissolving 100 mg per 10 mL distilled water, and stored at room temperature.

### **2.1.4. Folin-Ciocalteu**

Folin-Ciocalteu reagent was purchased from Sigma-Aldrich (St. Louis, USA) and used undiluted.

### **2.1.5. Vanillin**

Vanillin was purchased from Sigma-Aldrich (St. Louis, USA). A 1% solution was prepared by dissolving 100 mg per 10 mL hydrochloric acid (4% in methanol), or 100 mg per 8 mL sulphuric acid and 2 mL ethanol, respectively. The solutions were stored at room temperature.

### **2.1.6. Antimony trichloride**

Antimony trichloride was purchased from Sigma-Aldrich (St. Louis, USA). A 20% solution was prepared by dissolving 200 mg per 10 mL chloroform, and stored at room temperature.

## **2.3. Antioxidant activity**

2,2'-azinobis-(3-ethyl benzothiazoline 6-sulfonic acid) (ABTS) and potassium peroxodisulfate were purchased from Sigma-Aldrich (St. Louis, USA). A 7.46 mM ABTS/2.5 mM potassium peroxodisulfate solution was prepared by dissolving 19.2 mg ABTS and 3.31 mg potassium peroxodisulfate per 5 mL distilled water. The solution was incubated for 16 h at 4°C prior to use, and stored at 4°C.

## **2.4. Flavonoid content screening**

### **2.4.1. Aluminium trichloride**

Aluminium trichloride was purchased from Merck Chemicals (South Africa). A 0.4% solution was prepared by dissolving 40 mg per 10 mL distilled water, and stored at 4°C.

### **2.4.2. Sodium hydroxide**

Sodium hydroxide was purchased from Merck Chemicals (South Africa). A 1 M solution was prepared by dissolving 400 mg per 10 mL distilled water, and stored at 4°C.

### **2.4.3. Sodium nitrate**

Sodium nitrate was purchased from Merck Chemicals (South Africa). A 1.25% solution was prepared by dissolving 125 mg per 10 mL distilled water, and stored at 4°C.

## **2.5. Phenolic acid content**

### **2.5.1. Folin-Ciocalteu reagent**

Folin-Ciocalteu reagent was purchased from Sigma-Aldrich (St. Louis, USA). A 10% solution was prepared by diluting 1 mL per 9 mL distilled water, and stored at 4°C in the dark.

### **2.5.2. Sodium carbonate**

Sodium carbonate was purchased from Merck Chemicals (South Africa). A 7% solution was prepared by dissolving 700 mg per 10 mL distilled water, and stored at 4°C.

## **2.6. Saponin content screening**

### **2.6.1. Sulphuric acid**

Sulphuric acid was purchased from Merck Chemicals (South Africa). A 75% solution was prepared by diluting 78.13 mL with 21.87 mL with distilled water and stored at ambient temperature.

### **2.6.2. Vanillin**

Vanillin was purchased from Merck Chemicals (South Africa). A 250 mg/mL solution was prepared by dissolving 2.5 g per 10 mL distilled water, and stored at 4°C.

## **3. Cellular cytotoxicity assays and reagents**

### **3.1. Culture and maintenance**

#### **3.1.1. Dulbecco's Modified Eagle's Medium**

DMEM and sodium bicarbonate was purchased from Sigma-Aldrich (St. Louis, USA). A 1.3% solution was prepared by dissolving 67.35 g medium powder and 18.5 g sodium bicarbonate per 5 L sterile, deionised water. The solution was filter-sterilized (0.22 µm cellulose acetate) twice, supplemented with 1% penicillin/streptomycin mixture and stored at 4°C in 500 mL bottles. A 10% FCS-supplemented medium was prepared, when needed, by adding 50 mL FCS per 450 mL DMEM.

#### **3.1.2. Eagles Minimum Essential Medium**

EMEM and sodium bicarbonate was purchased from Sigma-Aldrich (St. Louis, USA). A 1% solution was prepared by dissolving 48 g medium powder and 11 g sodium bicarbonate per 5 L sterile, deionised water. The solution was filter-sterilized (0.22 µm cellulose acetate) twice, supplemented with 1% penicillin/streptomycin mixture and stored at 4°C in 500 mL bottles. A 10% FCS-supplemented medium was prepared, when needed, by adding 50 mL FCS to 450 mL EMEM.

#### **3.1.3. Foetal calf serum**

FCS was purchased from The Scientific Group (Gauteng, RSA). Solutions were heat-inactivated through heating at 56°C for 45 min and stored at -20°C.

#### **3.1.4. Penicillin/streptomycin**

Penicillin/streptomycin was purchased from BioWhittaker (Walkersville, USA) at 10 000 units penicillin and 10 000 µg streptomycin per 1 mL.

#### **3.1.5. Phosphate-buffered saline**

BBL™ FTA haemagglutination buffer was purchased from BD Biosciences (Sparks, USA). A 0.9% solution was prepared by dissolving 9.23 g per 1 L and stored at 4°C.

#### **3.1.6. Trypsin/Versene**

Trypsin/Versene solution was purchased from The Scientific Group (Gauteng, RSA) and used undiluted. The solution was stored at 4°C.

#### **3.1.7. Trypan blue counting fluid**

Trypan blue was purchased from Sigma-Aldrich (St. Louis, USA). A 0.1% solution was prepared by dissolving 20 mg per 20 mL distilled water, and filtering through a 0.4 µm membrane filter to remove particulate matter. The solution was stored at ambient temperature.

### **3.2. Cytotoxicity assays (cell density, lysosomal integrity, metabolic conversion)**

#### **3.2.1. 3-(4,5-dimethylthiazol-2-yl)-2,5-diphenyltetrazolium bromide**

MTT was purchased from Sigma-Aldrich (St. Louis, USA). A 5 mg/mL solution was prepared by dissolving 50 mg per 10 mL distilled water, and stored at 4°C in the dark.

#### **3.2.2. Acetic acid**

Glacial acetic acid was purchased from Merck Chemicals (South Africa). A 1% solution was prepared by diluting 1 mL to 100 mL with distilled water and stored at ambient temperature.

### 3.2.3. Bradford reagent

Quick-Start Bradford<sup>®</sup> Dye Reagent (1X) was purchased from BioRad Industries (Hercules, RSA) and stored at 4°C. The solution was vacuum-filtered (0.45 µm) prior to use.

### 3.2.4. Neutral red eluent

Glacial acetic acid and ethanol was purchased from Merck Chemicals (South Africa). Neutral red eluent (50:49:1) was prepared by mixing 250 mL distilled water, 245 mL ethanol and 5 mL acetic acid. The solution was stored at 4°C.

### 3.2.5. Neutral red EMEM

Neutral red was purchased from Sigma-Aldrich (St. Louis, USA). A 100 µg/mL solution was prepared by dissolving 25 mg in 250 mL EMEM, and adjusting the pH to 6.4 using glacial acetic acid. The solution was filter-sterilized (0.22 µm) and stored at 4°C.

### 3.2.6. Resazurin

Resazurin sodium salt was purchased from Sigma-Aldrich (St. Louis, USA). A 10 mM stock solution was prepared by dissolving 2.29 mg per 1 mL DMSO and stored at -80°C in 20 µl aliquots. A 10 µM working solution was prepared by diluting 11 µl per 10 990 µl PBS.

### 3.2.7. Sulforhodamine B

Sulphorhodamine B was purchased from Sigma-Aldrich (St. Louis, USA). A 0.057% solution was prepared by dissolving 57 mg per 100 mL acetic acid (1%). The solution was stored at 4°C.

### 3.2.8. Tamoxifen

Tamoxifen was purchased from Sigma-Aldrich (St. Louis, USA) in powder form. A 30 mM stock solution was prepared by dissolving 11.1 mg per 1 mL DMSO and stored at -80°C in 20 µL aliquots. A 10 µM working solution was prepared by diluting 1.3 µL stock solution per 1 999 µL EMEM.

### **3.2.9. Trichloroacetic acid**

TCA was purchased from Merck Chemicals (South Africa). A 50% solution was prepared by dissolving 50 g crystals per 100 mL distilled water and stored at 4°C.

### **3.2.10. Tris-base buffer**

Tris(hydroxymethyl)aminomethane was purchased from Sigma-Aldrich (St. Louis, USA) in powder form. A 10 mM solution was prepared by dissolving 121.1 mg per 100 mL distilled water and the pH adjusted to 10.5 using sodium hydroxide.

## **3.3. Hepatotoxic parameters**

### **3.3.1. Reactive oxygen species content**

#### **3.3.1.1. Dichlorodihydrofluorescein diacetate**

H<sub>2</sub>-DCF-DA was purchased from Sigma-Aldrich (St. Louis, USA). A 2 mM stock solution was prepared by dissolving 4.9 mg per 5 mL DMSO and stored at -80°C in 20 µL aliquots. A 10 µM working solution was prepared by diluting 3 µL stock solution per 1 997 µL PBS.

#### **3.3.1.2. Potassium peroxidisulfate**

Potassium peroxidisulfate was purchased from Sigma-Aldrich (St. Louis, USA). A 30 mM stock solution was prepared by dissolving 8.1 mg per 1 mL DMSO and stored at -80°C in 20 µL aliquots. A 300 µM working solution was prepared by diluting 10 µL stock solution per 990 µL EMEM.

### **3.3.2. Reduced glutathione content**

#### **3.3.2.1. n-Ethylmaleimide**

n-Ethylmaleimide was purchased from Sigma-Aldrich (St. Louis, USA). A 50 mM stock solution was prepared by dissolving 6.3 mg per 1 mL DMSO and stored at -80°C in 10 µL aliquots. A 20 µM working solution was prepared by diluting 0.8 µL stock solution per 1 999 µL EMEM.

### **3.3.2.2. Monochlorobimane**

Monochlorobimane was purchased from Sigma-Aldrich (St. Louis, USA). A 25 mM stock solution was prepared by dissolving 5 mg per 880  $\mu$ L DMSO and stored at  $-80^{\circ}\text{C}$  in 20  $\mu$ L aliquots. A 16  $\mu$ M working solution was prepared by diluting 1  $\mu$ L stock solution per 1 562  $\mu$ L PBS.

### **3.3.3. Mitochondrial membrane potential**

#### **3.3.3.1. Rotenone**

Rotenone was purchased from Sigma-Aldrich (St. Louis, USA). A 30 mM stock solution was prepared by dissolving 11.8 mg per 1 mL DMSO and stored at  $-80^{\circ}\text{C}$  in 20  $\mu$ L aliquots. For the hepatotoxicity model: a 200 nM working solution was prepared by diluting 3.3  $\mu$ L stock solution per 497  $\mu$ L EMEM, of which 1  $\mu$ L was further diluted per 999  $\mu$ L EMEM. For the mode of cell death: a 100 nM working solution was prepared by diluting 3.3  $\mu$ L stock solution per 497  $\mu$ L EMEM, of which 1  $\mu$ L was further diluted per 1 999  $\mu$ L EMEM.

#### **3.3.3.2. 5,5'-6,6'-Tetrachloro-1,1'-3,3'-tetraethylbenzimidazolylcarbocyanine iodide**

JC-1 was purchased from Sigma-Aldrich (St. Louis, USA). A 1.5 mM stock solution was prepared by dissolving 5 mg per 5.11 mL DMSO and stored at  $-80^{\circ}\text{C}$  in 50  $\mu$ L aliquots. A 10  $\mu$ M working solution was prepared by diluting 13.3  $\mu$ L stock solution per 1 987  $\mu$ L PBS.

### **3.3.4. Fatty acid content**

#### **3.3.4.1. Nile red**

Nile red was purchased from Sigma-Aldrich (St. Louis, USA). A 1 mM stock solution was prepared by dissolving 0.3 mg per 1 mL DMSO and stored at  $-80^{\circ}\text{C}$  in 10  $\mu$ L aliquots. A 1  $\mu$ M working solution was prepared by diluting 2  $\mu$ L stock solution per 1 998  $\mu$ L PBS.

### **3.3.4.2. Oleic acid**

Oleic acid was purchased from Sigma-Aldrich (St. Louis, USA). A 20 mM stock solution was prepared by diluting 20  $\mu$ L oil per 3.15 mL DMSO and stored at  $-80^{\circ}\text{C}$  in 20  $\mu$ L aliquots. A 400  $\mu$ M working solution was prepared by diluting 20  $\mu$ L stock solution per 1 980  $\mu$ L EMEM.

### **3.3.5. Caspase-3/7 activity**

#### **3.3.5.1. Acetyl-Asp-Glu-Val-Asp-7-amido-4-methylcoumarin (Ac-DEVD-AMC)**

Ac-DEVD-AMC was purchased from Sigma-Aldrich (St. Louis, USA). A 5 mM stock solution was prepared by dissolving 5 mg per 1.48 mL DMSO and stored at  $-80^{\circ}\text{C}$  in 10  $\mu$ L aliquots.

#### **3.3.5.2. Caspase-3/7 assay buffer**

HEPES, EDTA, phenylmethylsulfonyl fluoride (PMSF) and acetyl-Asp-Glu-Val-Asp-7-amido-4-methylcoumarin (Ac-DEVD-AMC) were purchased from Sigma-Aldrich (St. Louis, USA), while  $\beta$ -mercaptoethanol (14.3 mM) was purchased from Merck Chemicals (South Africa). A solution of 20 mM HEPES, 2 mM EDTA, 0.5 mM PMSF, 4.3 mM  $\beta$ -mercaptoethanol and 5  $\mu$ M Ac-DEVD-AMC was prepared by dissolving 476.6 mg HEPES and 58.4 mg EDTA per 100 mL distilled water. The incomplete buffer was stored at  $4^{\circ}\text{C}$ . Thirty minutes prior to experimentation 50  $\mu$ L PMSF (100 mM), 3  $\mu$ L  $\beta$ -mercaptoethanol (14.3 mM) and 10  $\mu$ L Ac-DEVD-AMC (5 mM) was added per 10 mL cold incomplete assay buffer.

#### **3.3.5.3. Lysis buffer**

HEPES, 3-[(3-cholamidopropyl)-dimethylammonio]-1-propanesulfonate (CHAPS), EDTA and PMSF were purchased from Sigma-Aldrich (St. Louis, USA), while  $\beta$ -mercaptoethanol (14.3 mM) was purchased from Merck Chemicals (South Africa). A solution of 10 mM HEPES, 2 mM CHAPS, 5 mM EDTA, 0.5 mM PMSF and 4.3 mM  $\beta$ -mercaptoethanol was prepared by dissolving 71.5.6 mg HEPES, and 58.4 mg EDTA per 100 mL distilled water. The incomplete buffer was stored at  $4^{\circ}\text{C}$ . Thirty minutes

prior to experimentation 50  $\mu\text{L}$  PMSF (100 mM) and 3  $\mu\text{L}$   $\beta$ -mercaptoethanol (14.3 mM) was added per 10 mL cold incomplete assay buffer.

#### **3.3.5.4. Phenylmethylsulfonyl fluoride**

PMSF was purchased from Sigma-Aldrich (St. Louis, USA). A 100 mM stock solution was prepared by dissolving 17.4 mg per 1 mL DMSO and stored at  $-80^{\circ}\text{C}$  in 50  $\mu\text{L}$  aliquots.

#### **3.3.5.5. Staurosporine**

Staurosporine was purchased from Sigma-Aldrich (St. Louis, USA). A 2.14 mM stock solution was prepared by dissolving 0.5 mg per 500  $\mu\text{L}$  DMSO and stored at  $-80^{\circ}\text{C}$  in 10  $\mu\text{L}$  aliquots. A 20  $\mu\text{M}$  working solution was prepared by diluting 10  $\mu\text{L}$  stock solution per 1 060  $\mu\text{L}$  EMEM.

### **3.3.6. ATP levels**

#### **3.3.6.1. ApoSENSOR™ ATP cell viability chemiluminescence kit**

The ApoSENSOR™ ATP cell viability chemiluminescence kit manufactured by MBL International Corporation was purchased from The Scientific Group (Gauteng, South Africa). The kit was stored at  $-20^{\circ}\text{C}$ . The nucleotide releasing was brought to room temperature prior to experimentation. The ATP monitoring enzyme was dissolved in 2.1 mL enzyme reconstitution buffer and stored on ice.

#### **3.3.6.2. Saponin**

Saponin was purchased from Sigma-Aldrich (St. Louis, USA). A 2% stock solution was prepared by dissolving 100 mg per 10 mL EMEM. The solution was filter-sterilized (0.22  $\mu\text{m}$ ) and stored at  $4^{\circ}\text{C}$ .

### **3.3.7. Lipid peroxidation**

#### **3.3.7.1. 2,2'-azobis(2-amidopropane dihydrochloride)**

2,2'-azinobis-(3-ethyl benzothiazoline 6-sulfonic acid) (AAPH) was purchased from Sigma-Aldrich (St. Louis, USA). A 20 mM stock solution was prepared by dissolving 5.4 mg AAPH per 1 mL DMSO and stored at -80°C in 50 µL aliquots. A 1 mM working solution was prepared by diluting 50 µL stock solution per 950 µL EMEM.

#### **3.3.7.2. Trichloroacetic acid**

TCA was purchased from Merck Chemicals (South Africa). A 16.5% solution was prepared by dissolving 3.3 g crystals per 20 mL distilled water and stored at ambient temperature.

#### **3.3.7.3. Thiobarbituric acid**

Thiobarbituric acid was purchased from Merck Chemicals (South Africa). A 2.5% solution was prepared prior to experimentation by dissolving 0.5 g per 20 mL distilled water containing 80 mg sodium hydroxide and 0.3 mg EDTA.

### **3.3.8. Cell cycle kinetics**

#### **3.3.8.1. Curcumin**

Curcumin was purchased from Sigma-Aldrich (St. Louis, USA). A 25 mM stock solution was prepared by dissolving 9.2 mg per 1 mL DMSO and stored at -80°C in 10 µL aliquots. A 40 µM working solution was prepared by diluting 1.6 µL stock solution per 998 µL EMEM.

#### **3.3.8.2. FCS-supplemented PBS**

A 1%-FCS supplemented solution was prepared by diluting 90 mL sterile PBS with 10 mL FCS. The solution was stored at 4°C.

#### **3.3.8.3. Methotrexate**

Methotrexate was purchased from Sigma-Aldrich (St. Louis, USA). A 25 mM stock solution was prepared by dissolving 11.4 mg per 1 mL DMSO and stored at -80°C in

10  $\mu\text{L}$  aliquots. A 20  $\mu\text{M}$  working solution was prepared by diluting 0.8  $\mu\text{L}$  stock solution per 998  $\mu\text{L}$  EMEM.

#### **3.3.8.4. Propidium iodide staining solution**

DNA-free RNase and Triton X-100 were purchased from Sigma-Aldrich (St. Louis, USA). A solution of 40  $\mu\text{g}/\text{mL}$  propidium iodide, 100  $\mu\text{g}/\text{mL}$  DNA-free RNase and 0.1% Triton X-100 was prepared by dissolving 4 mg propidium iodide and 100  $\mu\text{L}$  Triton X-100 per 99.9 mL distilled water. The incomplete staining solution was stored at 4°C. Five minutes prior to staining 1 mg DNA-free RNase was added per 10 mL incomplete staining solution.

#### **3.3.8.5. Thymidine-fortified EMEM**

Thymidine was purchased from Sigma-Aldrich (St. Louis, USA). A 3.3 mM solution was prepared by dissolving 8 mg per 10 mL FCS-free EMEM medium prior to experimentation. The solution was filter-sterilized (0.22  $\mu\text{m}$ ) and 8.1 mL diluted to 9 mL with 900  $\mu\text{L}$  FCS to obtain a 3 mM thymidine and 10% FCS-fortified EMEM solution.

### **3.3.9. Cell viability**

#### **3.3.9.1. Annexin V-FITC**

Annexin V-FITC was purchased from The Scientific Group (Gauteng, South Africa) and stored at 4°C.

#### **3.3.9.2. Annexin V-FITC binding buffer**

2-[4-(2-hydroxyethyl)piperazin-1-yl] ethanesulfonic acid (HEPES), sodium chloride, potassium chloride, magnesium chloride and calcium chloride was purchased from Merck Chemicals (South Africa). A solution of 10 mM HEPES, 150 mM sodium chloride, 5 mM potassium chloride, 5 mM magnesium chloride and 1.8 mM calcium chloride was prepared by dissolving 238.3 mg HEPES, 876.6 mg sodium chloride, 37.2 mg potassium chloride, 47.6 mg magnesium chloride and 20.0 mg calcium chloride per 100 mL distilled water. The solution was pH adjusted to 7.4 using sodium hydroxide, and stored at 4°C.

### **3.3.9.3. Propidium iodide**

Propidium iodide was purchased from Sigma-Aldrich (St. Louis, USA). A 3 mM solution was prepared by dissolving 2 mg per 1 mL PBS, and stored at 4°C.

## **4. Drug-herb interactions**

### **4.1. P-glycoprotein inhibitory activity**

#### **4.1.1. Rhodamine-123**

Rhodamine-123 was purchased from Sigma-Aldrich (St. Louis, USA). A 2.6 mM stock solution was prepared by dissolving 1 mg per 1 mL and stored at -80°C in 20 µL aliquots. A 10 µM working dilution was prepared by dissolving 27 µL stock solution per 6 973 µL PBS.

#### **4.1.2. Verapamil**

Verapamil was purchased from Sigma-Aldrich (St. Louis, USA). A 25 mM stock solution was prepared by dissolving 11.3 mg per 1 mL DMSO and stored at -80°C in 20 µL aliquots. A 1 mM working dilution was prepared by diluting 40 µL stock solution per 960 µL PBS. A 200 µM working dilution was prepared by diluting 8 µL stock per 992 µL Hank's Buffered Saline Solution (HBSS).

### **4.2. Caco-2 bidirectional permeability assay**

#### **4.2.1. Ammonium formate**

Ammonium formate was purchased from Sigma-Aldrich (St. Louis, USA). A 10 mM solution was prepared by dissolving 630.6 mg per 1 L deionised water.

#### **4.2.2. Hank's Buffered Saline Solution**

HBSS was purchased from Life Technologies (South Africa) and used undiluted. The solution was stored at 4°C.

#### **4.2.3. Lucifer yellow**

Lucifer yellow CH dipotassium salt was purchased from Sigma-Aldrich (St. Louis, USA). A 6 mM stock solution was prepared by dissolving 3.1 mg per 1 mL DMSO and stored at -80°C in 10 µL aliquots. A 60 µM working dilution was prepared by diluting 10 µL stock solution per 990 µL HBSS.

#### **4.2.4. Nevirapine**

Nevirapine was purchased from Sigma-Aldrich (St. Louis, USA). A 25 mM stock solution was prepared by dissolving 6.7 mg per 1 mL DMSO and stored at -80°C in 20 µL aliquots. A 320 µM working dilution was prepared by diluting 12.8 µL stock solution per 997.2 µL PBS.

#### **4.2.5. Zidovudine**

Zidovudine was purchased from Sigma-Aldrich (St. Louis, USA). A 25 mM stock solution was prepared by dissolving 6.7 mg per 1 mL DMSO and stored at -80°C in 20 µL aliquots. A 20 µM working dilution was prepared by diluting 0.8 µL stock solution per 999.2 µL ammonium formate (10 mM).

### **4.3. CYP450 inhibitory assays and reagents**

#### **4.3.1. NADPH-cofactor mix components**

##### **4.3.1.1. Cofactors solution**

A mixture of 1.3 mM NADP<sup>+</sup>, 66 mM magnesium chloride and 66 mM glucose 6-phosphate was purchased from The Scientific Group (Gauteng) as part of the CYP2B6/EFC, CYP2D6/AMMC and CYP3A4/BFC High Throughput Inhibitor Screening Kits (Corning, USA). The cofactor solution was stored at -20°C, thawed prior to use and stored on ice during experimentation.

##### **4.3.1.2. Glucose 6-phosphate dehydrogenase solution**

A 40 units/mL glucose 6-phosphate dehydrogenase solution in 5 mM citrate buffer (pH 7.5) was purchased from The Scientific Group (Gauteng) as part of the CYP2B6/EFC, CYP2D6/AMMC and CYP3A4/BFC High Throughput Inhibitor Screening Kits

(Corning, USA). The glucose 6-phosphate dehydrogenase solution was stored at -20°C, thawed prior to use and stored on ice during experimentation.

#### **4.3.1.3. NADPH-cofactor mix**

A NADPH-cofactor mix was prepared by diluting 1.5 mL cofactors and 1.2 mL glucose 6-phosphate dehydrogenase per 117.8 mL deionized water (37°C) prior to experimentation.

#### **4.3.2. Substrate-enzyme mix**

##### **4.3.2.1. Buffer solution**

A 0.5 M potassium phosphate buffer (pH 7.4) was purchased from The Scientific Group (Gauteng) as part of the CYP2B6/EFC, CYP2D6/AMMC and CYP3A4/BFC High Throughput Inhibitor Screening Kits (Corning, USA). The buffer solution was stored at room temperature, and heated to 37°C prior to use.

##### **4.3.2.2. CYP450 enzyme solutions**

CYP2B6 (containing P450 reductase and cytochrome b5), CYP2D6\*1 (containing CYP2B6 (containing P450 reductase) and CYP3A4 (containing P450 reductase and cytochrome b5) were purchased from The Scientific Group (Gauteng) as part of the CYP2B6/EFC, CYP2D6/AMMC and CYP3A4/BFC High Throughput Inhibitor Screening Kits (Corning, USA). The enzyme solutions were stored at -80°, thawed prior to use and stored on ice during experimentation.

##### **4.3.2.3. 7-Ethoxy-4-trifluoromethylcoumarin-CYP2B6 mix**

EFC was purchased from The Scientific Group (Gauteng) as part of the CYP2B6/EFC High Throughput Inhibitor Screening Kit (Corning, USA). A 25 mM stock solution was prepared by dissolving 0.39 mg per 60 µL acetonitrile and stored at -20°C. An EFC-CYP2B6 mix was prepared by diluting 24 µL EFC, 600 µL CYP2B6 and 24 mL buffer solution per 95 mL deionized water (37°C).

#### **4.3.3. 3-[2-(N,N-diethyl-N-methylamino)ethyl]-7-methoxy-4-methylcoumarin-CYP2D6 mix**

AMMC was purchased from The Scientific Group (Gauteng) as part of the CYP2D6/AMMC High Throughput Inhibitor Screening Kit (Corning, USA). A 10 mM stock solution was prepared by dissolving 0.30 mg per 70  $\mu$ L acetonitrile and stored at -20°C. An AMMC-CYP2D6 mix was prepared by diluting 36  $\mu$ L AMMC, 900  $\mu$ L CYP2D6 and 24 mL buffer solution per 95 mL deionized water (37°C).

#### **4.3.4. 7-Benzyloxy-trifluoromethylcoumarin-CYP3A4 mix**

BFC was purchased from The Scientific Group (Gauteng) as part of the CYP3A4/BFC High Throughput Inhibitor Screening Kit (Corning, USA). A 50 mM stock solution was prepared by dissolving 4.3 mg per 270  $\mu$ L acetonitrile and stored at -20°C. A BFC-CYP3A4 mix was prepared by diluting 240  $\mu$ L BFC, 600  $\mu$ L CYP3A4 and 96 mL buffer solution per 23 mL deionized water (37°C).

#### **4.3.5. Positive controls**

##### **4.3.5.1. Ketoconazole**

Ketoconazole was purchased from The Scientific Group (Gauteng) as part of the CYP3A4/BFC High Throughput Inhibitor Screening Kit (Corning, USA). A 250  $\mu$ M stock solution was prepared by dissolving 80 ng per 60  $\mu$ L acetonitrile and stored at -20°C.

##### **4.3.5.2. Quinidine**

Quinidine was purchased from The Scientific Group (Gauteng) as part of the CYP2D6/AMMC High Throughput Inhibitor Screening Kit (Corning, USA). A 25  $\mu$ M stock solution was prepared by dissolving 0.6 ng per 60  $\mu$ L acetonitrile and stored at -20°C.

##### **4.3.5.3. Tranylcypromine**

Tranylcypromine was purchased from The Scientific Group (Gauteng) as part of the CYP2B6/EFC High Throughput Inhibitor Screening Kit (Corning, USA). A 25 mM stock

solution was prepared by dissolving 0.25 mg per 60  $\mu$ L acetonitrile and stored at -20°C.

#### **4.3.6. Stop solution**

A 0.5 M Tris-base solution was purchased from The Scientific Group (Gauteng) as part of the CYP2B6/EFC, CYP2D6/AMMC and CYP3A4/BFC High Throughput Inhibitor Screening Kits (Corning, USA). The stop solution was diluted with 72 mL acetonitrile per 18 mL and stored at room temperature.

## Appendix IV: Additional cellular experiments

### Materials and Methods

MCF-7 breast carcinoma (ATCC HTB-22), MDA-MB-231 breast carcinoma (ATCC HTB-26) and Sk-Br-3 breast carcinoma (ATCC HTB-30) cells were grown identical to the HepG2 and Caco-2 cell lines in Chapter 3, however Dulbecco's Modified Eagle's Medium (MCF-7 [5 000 cells/well] and MDA-MBA-231 [5 000 cells/well]) and Roswell Park Memorial Institute-1640 (Sk-Br-3 [5 000 cells/well]) medium was used. The SRB assay was performed as described in Chapter 3.

### Results

Plant	Extract	IC <sub>50</sub> ± SEM (µg/mL)		
		MCF-7	MDA-MB-231	SK-Br-3
<i>A. oppositifolia</i>	Hot water	1.29 ± 1.13	3.83 ± 1.04	7.01 ± 1.12
	Methanol	2.72 ± 1.11	8.88 ± 1.21	15.76 ± 1.12
<i>B. disticha</i>	Hot water	7.29 ± 1.11	21.14 ± 1.10	23.87 ± 1.19
	Methanol	9.49 ± 1.05	15.36 ± 1.09	36.44 ± 1.13
<i>M. oleifera</i>	Hot water	>100	>100	>100
	Methanol	>100	>100	>100
<i>M. sericea</i>	Hot water	64.34 ± 1.14	>100	36.44 ± 1.25
	Methanol	2.39 ± 1.16	9.25 ± 1.07	19.28 ± 1.16
<i>S. aculeastrum</i>	Hot water	59.12 ± 1.14	31.67 ± 1.03	50.26 ± 1.09
	Methanol	18.13 ± 1.07	16.88 ± 1.24	21.3 ± 1.28
<i>S. puniceus</i>	Hot water	>100	>100	>100
	Methanol	56.78 ± 1.06	13.27 ± 1.06	23.95 ± 1.07
<i>T. elegans</i>	Hot water	50.17 ± 1.09	65.28 ± 1.18	52.67 ± 1.04
	Methanol	0.35 ± 1.06	1.92 ± 1.10	3.35 ± 1.07
<i>Z. mucronata</i>	Hot water	98.81 ± 1.09	>100	>100
	Methanol	70.98 ± 1.11	>100	>100
Tamoxifen		3.02 ± 1.10	4.06 ± 1.06	4.24 ± 1.50